

Universiteit
Leiden
The Netherlands

Like me, or else: Nature, nurture and neural mechanisms of social emotion regulation in childhood

Achterberg, M.

Citation

Achterberg, M. (2020, March 12). *Like me, or else: Nature, nurture and neural mechanisms of social emotion regulation in childhood*. Retrieved from https://hdl.handle.net/1887/86283

Version:	Publisher's Version
License:	Licence agreement concerning inclusion of doctoral thesis in the Institutional Repository of the University of Leiden
Downloaded from:	https://hdl.handle.net/1887/86283

Note: To cite this publication please use the final published version (if applicable).

Cover Page



Universiteit Leiden



The handle http://hdl.handle.net/1887/86283 holds various files of this Leiden University dissertation.

Author: Achterberg, M.
Title: Like me, or else: Nature, nurture and neural mechanisms of social emotion regulation in childhood
Issue Date: 2020-03-12

LIKE ME OR ELSE ...



Nature, nurture and neural mechanisms of social emotion regulation in childhood

Michelle Achterberg

Like me, or else...

Nature, nurture and neural mechanisms of social emotion regulation in childhood

Michelle Achterberg

Copyright © 2020 by Michelle Achterberg

ISBN: 978-94-6332-584-4
Cover design: Made & Adore Design
Lay-out: Ferdinand van Nispen | Citroenvlinder DTP & Vormgeving
Printed by: GVO drukkers & vormgevers B.V. | Ede, The Netherlands

Proefschrift

ter verkrijging van
de graad van Doctor aan de Universiteit Leiden,
op gezag van Rector Magnificus prof.mr. C.J.J.M. Stolker,
volgens besluit van het College voor Promoties

te verdedigen op donderdag 12 maart 2020
klokke 16:15 uur

door
Michelle Achterberg
geboren te Gouda
in 1991

Promotores

Prof. dr. E A. Crone (Universiteit Leiden)
Prof. dr. M.J. Bakermans-Kranenburg (Vrije Universiteit Amsterdam)

Co-promotor

Dr. A.C.K. van Duijvenvoorde (Universiteit Leiden)

Promotiecommissie

Prof. dr. A.W.M. Evers (Universiteit Leiden)
Prof. dr. A. Popma (Universiteit Leiden-Vrije Universiteit Amsterdam)
Prof. dr. L. Krabbendam (Vrije Universiteit Amsterdam)

Any fool can know. The point is to understand.

- Albert Einstein

Table of contents

Chapter 1	General introduction	9
Chapter 2	The neural and behavioral correlates of social evaluation in childhood	25
Chapter 3	Control your anger! The neural basis of aggression regulation in response to negative social feedback	59
Chapter 4	Heritability of aggression following social evaluation in middle childhood: An fMRI study	83
Chapter 5	Longitudinal changes in DLPFC activation within childhood are related to decreased aggression following social rejection	119
Chapter 6	Distinctive heritability patterns of subcortical-prefrontal cortex resting state connectivity in childhood: A twin study	155
Chapter 7	Genetic and environmental influences on MRI scan quantity and quality	195
Chapter 8	Fronto-striatal white matter integrity predicts development of delay of gratification: A longitudinal study	223
Chapter 9	Summary and general discussion	243
Addendum	Nederlandse samenvatting	263
	Dankwoord	277
	References	281
	List of publications	309
	Curriculum vitae	314

CHAPTER ONE

General introduction

We literally bend over backwards to make a perfect picture, combine it with an inspiring quote, post it on social media and … wait for the likes! Why do we invest so much effort in being recognized and accepted by others? And how come that being rejected can fill us with rage? What are the underlying neural mechanisms of these emotions and behaviors? And how do these mechanisms develop? In this dissertation, I seek out to shed light on the nature, nurture and neural mechanisms of social emotion regulation in childhood.

Social is Salient

The current generation of youth is the first to grow up with smartphones and tablets from birth on. These children are constantly connected to each other through multiplayer video gaming and social media. A 2015 survey amongst over 1200 eight-to-twelve-year-old children revealed that they spend on average six hours on (social) media each day (Common Sense Media Inc., 2015). These statistics show that children deal with social media and social connectedness from an early age on. However, relatively little is known about the influence of this intense form of social connectedness. Some studies have pointed to the potentially addictive aspects of social media (Blackwell *et al.*, 2017), and popular media are warning for a society of social junkies always on the lookout for social confirmation. However, the desire to belong to a social group is not something new: Social acceptance is, and always has been, of key importance in life (Baumeister and Leary, 1995). Receiving positive social feedback increases our self-esteem and gives us a sense of belonging (Leary and Baumeister, 2000; DeWall *et al.*, 2011). Negative social feedback, in contrast, is related to feelings of sadness and depression (Nolan *et al.*, 2003) and can lead to frustration and rage (Twenge *et al.*, 2001). The current dissertation examines how children deal with social evaluation, and what underlying mechanisms come into play. This thesis aims to answer questions such as: How is it that some children are more sensitive to social rejection than others? What are the neural mechanisms of social evaluation and subsequent behavior? And what is a feasible method to examine social evaluation and social emotion regulation in children?

Studying social interactions can be challenging as it is a complex form of behavior that is strongly intertwined with our day-to-day lives. In order to decompose these processes, researchers have often worked with experiments. The advantage of an experiment is that you examine participants in a controlled setting, making it possible to study unique aspects of complex behaviors. Experimental paradigms are also very suitable to use in combination with psychophysiological measures, which enables to additionally study covert

aspects of information processing. Social acceptance and rejection have been studied in a variety of experimental settings, for example by manipulating Instagram likes (Sherman *et al.*, 2018b), by mimicking chat room conversations (Silk *et al.*, 2012) or by simulating peer feedback on the participant's profile (Somerville *et al.*, 2006; Gunther Moor *et al.*, 2010b; Dalgleish *et al.*, 2017; Rodman *et al.*, 2017). These studies showed that social rejection can be quite literally heartbreaking, as negative social feedback can result in cardiac slowing (Gunther Moor *et al.*, 2010a), which was most pronounced in young adolescents compared to adults (Gunther Moor *et al.*, 2014). Other studies found that social rejection resulted in increased pupil dilation (Silk *et al.*, 2012). The pupil becomes more dilated in response to stimuli with a greater emotional intensity (Siegle *et al.*, 2003), and is suggested to reflect increased activity in cognitive and affective processing regions of the brain.

Indeed, a wealth of neuroimaging research has shown that the significance of social evaluation is deeply rooted in our brain. Social acceptance, for example, has been associated with increased activity in striatal regions (Guyer *et al.*, 2009; Davey *et al.*, 2010; Gunther Moor *et al.*, 2010b; Sherman *et al.*, 2018b), specifically in the ventral striatum (VS, **Figure 1**). Numerous studies have shown that the VS is associated with reward processing (Sescousse *et al.*, 2013) and this heightened activation could reflect the rewarding value of positive feedback. Social rejection, in contrast, has been related to increased activation in midline regions of the brain, such as the dorsal and subgenual anterior cingulate cortex (ACC) and medial prefrontal cortex (MPFC) (Cacioppo *et al.*, 2013; Apps *et al.*, 2016), see **Figure 1**. The dorsal ACC, together with the anterior insula (AI, **Figure 1**), have been suggested to signal social pain, as activity in these regions largely overlapped with brain activity after physical pain (Eisenberger and Lieberman, 2004; Kross *et al.*, 2011; Rotge *et al.*, 2015). However, other studies found the dorsal ACC and AI to be sensitive to expectancy violation (Somerville *et al.*, 2006; Cheng *et al.*, 2019) and have suggested that these regions might be important for evaluating social feedback in general, irrespective of its valence (Dalgleish *et al.*, 2017).

Previous experimental studies have thus indicated that different neural processes can be distinguished for social acceptance and rejection in adults and adolescents, but there remain many unanswered questions. Until now the paradigms to study social acceptance and rejections have not been consistently applied to children and young adolescents and there has been little emphasis on behavioral outcomes. To really understand the effects of social acceptance and rejection on children and their development we need a new approach, with a targeted experimental paradigm. Prior studies have provided a solid foundation for studying social evaluation, but an important next step is to disentangle between neural activation that is related to general social saliency and neural activation that is specific for negative social feedback. Understanding the latter

is especially important, as social rejection is often related to negative behavioral outcomes such as anger and frustration.

Regulate or Retaliate?

In some individuals, negative social feedback triggers feelings of anger and frustration, which can lead to reactive aggression (Twenge *et al.*, 2001; Dodge *et al.*, 2003; Leary *et al.*, 2006; Nesdale and Lambert, 2007; Nesdale and Duffy, 2011; Chester *et al.*, 2014). A tragic example of how socially excluded youth can turn violent are school shootings, of which almost all perpetrators have a long history of peer rejection and social exclusion (Leary *et al.*, 2003). But even incidental social rejection can lead to aggression. Reactive aggression after social rejection has been examined experimentally by providing participants with the opportunity to blast a loud noise towards the peer that had just socially excluded them (Bushman and Baumeister, 1998; Twenge *et al.*, 2001; Reijntjes *et al.*, 2010). The participants can set the intensity and duration of the noise blast heard by the other person, providing them with a way to retaliate (Bushman and Baumeister, 1998). These studies consistently showed that rejected participants were considerably more aggressive than accepted participants (Twenge *et al.*, 2001; Leary *et al.*, 2006; Reijntjes *et al.*, 2010; DeWall and Bushman, 2011; Chester *et al.*, 2014; Riva *et al.*, 2015).

The effects of social rejection in terms of behavioral aggression might be associated with a lack of impulse control or inadequate emotion regulation (Chester *et al.*, 2014; Riva *et al.*, 2015). For example, in adults it was found that the extent to which individuals responded aggressively after social rejection was dependent on whether the participant showed high or low executive control (Chester *et al.*, 2014). Participants with high executive control were less aggressive after social rejection, indicating that executive control might down-regulate aggression tendencies. It has been suggested that this form of self-control is dependent on top-down control of the dorsolateral prefrontal cortex (DLPFC, **Figure 1**) over subcortical-limbic regions (such as the VS), to inhibit responses that lead to impulsive actions (Casey, 2015). Evidence for this hypothesis was provided by a study using transcranial direct current stimulation (tDCS), a method to increase neural activation in specific brain regions. Riva and colleagues showed that increased neural activation in the lateral prefrontal cortex during social rejection was related to decreased behavioral aggression, compared to participants that did not receive active tDCS (Riva *et al.*, 2015). Moreover, stronger functional connectivity between the lateral prefrontal cortex and limbic regions was related to less retaliatory aggression (Chester and DeWall, 2016). Similar associations have been found for structural connectivity: stronger connections between subcortical and prefrontal brain regions were related to less

trait aggression (Peper *et al.*, 2015). These studies in adults thus indicate that the lateral prefrontal cortex - and specifically the DLPFC - might serve as a regulating mechanism for aggression after social evaluation. However, relatively few studies have investigated aggression following social rejection in childhood, despite the fact that children deal with social evaluations from an early age. Moreover, as the prefrontal cortex and executive functioning are still developing throughout childhood, children may be more sensitive to aggressive behavior after social rejection, as they might experience more difficulty with social emotion regulation.

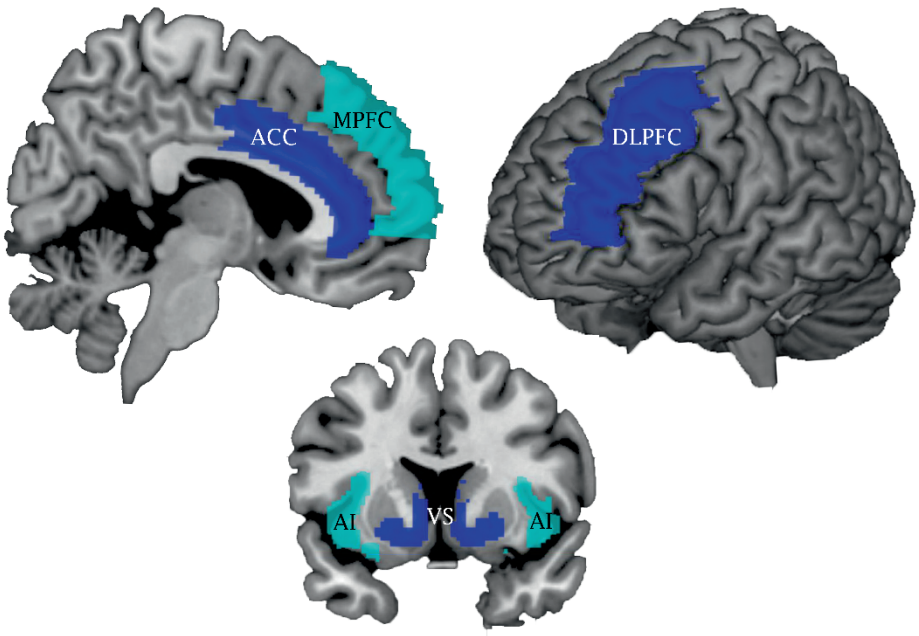


Figure 1. *Brain regions implicated in social evaluation processing and social emotion regulation. ACC- anterior cingulate cortex, MPFF- medial prefrontal cortex, DLPFC- dorsolateral prefrontal cortex, AI- anterior insula, VS- ventral striatum.*

Neurodevelopmental models

When it comes to social evaluation processing, studies in adults have shown that a network of ACC-AI, together with subcortical regions such as the VS, are involved in the direct effects of social rejection and acceptance. With regards to controlling social rejection related aggression, it seems that the DLPFC is involved. Exactly these networks are central to neurodevelopmental models such

as the Social Information Processing Network (Nelson *et al.*, 2005; Nelson *et al.*, 2016) and the Imbalance Model (Casey *et al.*, 2008; Somerville *et al.*, 2010). The Social Information Processing Network (SIPN, Nelson *et al.* (2005); Nelson *et al.* (2016)) states that social information is processed through bi-directional communication between three nodes: the detection node, the affective node, and the cognitive-regulation node (**Figure 2**). The detection node includes regions that have been found to be important to categorize stimuli as being socially relevant, such as the fusiform face area. Once a stimulus has been recognized as a social stimulus, it is further processed by the affective node, which includes - amongst others - the amygdala and the VS (nucleus accumbens). Finally, social stimuli are processed in a network dedicated to complex cognitive operations that is referred to as the cognitive-regulatory node, which includes prefrontal cortical regions. The SIPN model states that goal directed behavior relies on interactions between different (dorsal and ventral) regions within the prefrontal cortex, that process social-emotional information from the affective node (Nelson *et al.*, 2005). Complementary, the Imbalance Model (Casey *et al.*, 2008; Somerville *et al.*, 2010) describes the mismatch in developmental trajectories of subcortical brain regions and the prefrontal cortex. Specifically, the gradual linear increase of prefrontal cortex maturation is slower than the non-linear increase of affective-limbic regions such as the VS. This induces an imbalance between bottom-up limbic regions and top-down control regions, which is most pronounced during adolescence (**Figure 2**). The imbalance model suggests that this imbalance between subcortical and cortical maturation hinders social emotion regulation and can results in risky, reward driven behavior.

Previous studies and theoretical models have shown that social emotion regulation is not solely dependent on isolated brain regions, but relies on a network of integrated connections between subcortical and cortical brain regions (Olson *et al.*, 2009; Chester *et al.*, 2014; de Water *et al.*, 2014; Peper *et al.*, 2015; Silvers *et al.*, 2016b; van Duijvenvoorde *et al.*, 2016a). Most of these studies have focused on adolescence or only included small samples of children. It therefore remains a question whether these integrated subcortical-cortical brain networks are already in place during childhood. The developmental phase towards the teenage years, in which the first friendships are formed, is an underexposed phase in experimental research. Theoretical perspectives have suggested that the increase of executive functions and maturation of DLPFC during childhood are important underlying mechanisms for developing a variety of self-regulation functions in childhood (Bunge and Zelazo, 2006; Diamond, 2013). Few studies have investigated the development of social emotion regulation during childhood, despite empirical findings showing that middle-to-late childhood marks the most rapid changes in executive functions (Luna *et al.*, 2004; Zelazo and Carlson, 2012; Peters *et al.*, 2016). This is a gap in the literature that needs to be investigated. This dissertation takes an important step by focusing precisely on the age of seven to eleven, the pre- to early pubertal years.

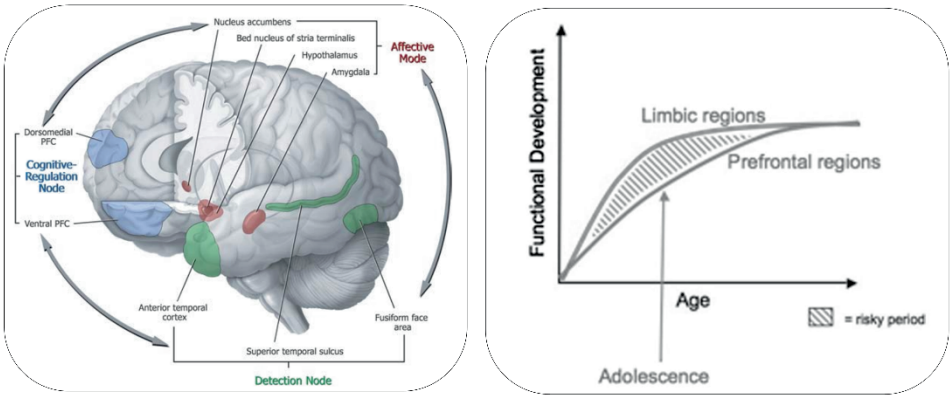


***Figure 2**. Neurodevelopmental models of social emotion regulation. Left: a schematic depiction of the Social Information Processing Network (SIPN), adapted from Nelson, Pine and Tone (2005). Right: the Imbalance model, adapted from Casey, Jones and Hare (2008).*

Hot *vs.* Cool Control

In line with the neurodevelopmental models, previous experimental neuroimaging studies have shown that children become better at regulating their emotions with increasing age (Silvers *et al.*, 2012), which has been suggested to be related to the development of cognitive control (Diamond, 2013; Casey, 2015). The DLPFC has been specifically pointed out as an important region for cognitive control development (Luna *et al.*, 2004; Luna *et al.*, 2010; Crone and Steinbeis, 2017). Most of these studies have focused on *'cool'* cognitive control, that is to say self-control in a non-emotional setting (Welsh and Peterson, 2014). However, whether the same *'cool'* regulatory control functions are also important for regulation of *'hot'* emotions in social contexts is currently unknown (Zelazo and Carlson, 2012; Welsh and Peterson, 2014). Previous studies on '*hot'* emotional control have worked with the now famous delay discounting paradigm (Mischel *et al.*, 1989), which estimates an individual's preference for a smaller immediate reward over larger, delayed rewards (Eigsti *et al.*, 2006; Olson *et al.*, 2007; Scheres *et al.*, 2014). This classic paradigm has been used extensively, as it is suitable for participants in all age ranges, and has shown to be predictive of long-term life outcomes (i.e., Mischel *et al.* (1989); Casey *et al.* (2011); but see Watts *et al.* (2018) for more nuanced findings using a replication design). These studies showed that the ability to delay gratification is very difficult for young children and improves with increasing age (Mischel *et al.*, 1989; Olson *et al.*, 2009; Casey *et al.*, 2011; de Water *et al.*, 2014). Studies in adults and adolescents additionally showed that stronger structural brain connectivity between subcortical (VS)

regions and the prefrontal cortex was related to better delay of gratification abilities (Peper *et al.*, 2013; van den Bos *et al.*, 2015).

Regulating aggression in the case of negative social feedback can been seen as a similar delay of gratification: For some individuals it might feel good to retaliate on the short term (Chester and DeWall, 2016), but on the long term this could result in even more social rejection (Lansford *et al.*, 2010). In fact, examining aggression following social rejection can provide an excellent case to study '*hot'* emotion regulation in an ecological valid social context. This requires a new social evaluation paradigm that exposes the mechanisms through experimental design, ideally combined with neuroimaging measures to inform about brain functions and connections. Such a paradigm can shed light on the underlying neural mechanisms of social acceptance and rejection, and can provide information on why some children are more sensitive to social evaluation than others.

Social Network Aggression Task

In order to gain a better understanding of the mechanisms of social acceptance and rejection, an innovative experimental paradigm is needed that is suitable to combine with neuroimaging. Task-based functional magnetic resonance imaging (fMRI) is based on contrasts between different conditions (for a concise overview of fMRI methodology see Glover (2011)). Most social evaluation studies till date have included only two conditions: participants receive either positive or negative social feedback from unknown, same-aged peers (Somerville *et al.*, 2006; Gunther Moor *et al.*, 2010b; Silk *et al.*, 2014; Rodman *et al.*, 2017). However, such paradigms are unable to investigate brain regions that are active after both positive and negative feedback, as these regions are washed out when both conditions are contrasted against each other. In order to understand the neural mechanisms of social evaluation, it is important to disentangle if regions are specifically sensitive to social rejection, or whether they are sensitive to social evaluation in general, and might signal for social salience (see also Dalgleish *et al.* (2017)). Therefore, we developed a new social evaluation paradigm that included a neutral feedback condition: the Social Network Aggression Task (SNAT), see **Figure 3**. This paradigm enables to study regions that signal for general social salience, by contrasting both positive and negative feedback to a neutral social feedback condition.

Few studies have investigated the neural mechanisms of *'hot'* social emotion regulation during childhood, however, today's youth is constantly connected to each other and they find themselves in an inexhaustible and unceasing pool of social information and subsequent emotions. It is therefore important that we understand how mechanisms of social emotion regulation

develop during childhood. In order to experimentally examine developmental changes in social emotion regulation, we included a retaliation aspect to the Social Network Aggression Task (SNAT, **Figure 3**). After the participants viewed the positive, neutral or negative social feedback, participants got the opportunity to blast a loud noise towards the peer, allowing us to directly examine aggression following social evaluation. By examining differences in aggression regulation after social evaluation within and across individuals, we can examine why some children might be more sensitive for social rejection. By combining this new experimental paradigm with neuroimaging, important insights in the underlying mechanisms of social emotion regulation can be gathered.

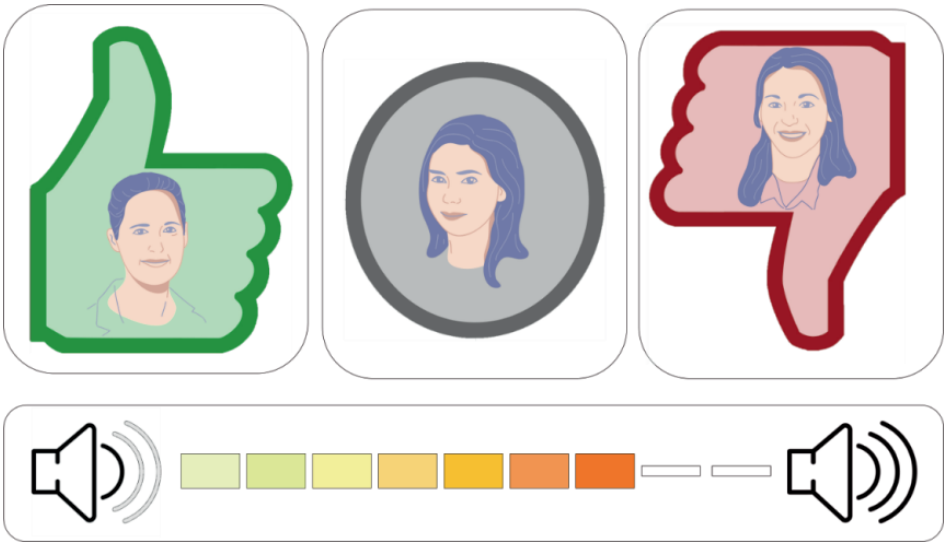


Figure 3. *Social network aggression task (SNAT), a newly developed social evaluation paradigm that includes positive, neutral and negative social feedback from unknown, same-aged peers. In response to the peer feedback, participants are able to blast a loud noise towards the peer, which is used as an index of aggression. The faces used in this figure are cartoon approximations of the photo stimuli used in Achterberg et al. (2016b).*

Nature and Nurture

In a rapid changing digital world with dense social connectedness, it is important to understand why some children are more sensitive to social evaluation than others. Perhaps some children are more sensitive through genetic predisposition. On the other hand, it is possible that specific environments stimulate certain social behavior. An important scientific question is to what extent development

is biologically based or environmentally driven. The caption of this section specifically states nature *and* nurture, as a broad range of literature has shown that these two are strongly intertwined (Polderman *et al.*, 2015). But to what extent nature and nurture contribute to (brain) development has received relatively little attention in developmental neuroscience. One particularly elegant way to study this is using a twin design: Monozygotic (MZ) twins share 100% of their genes, whereas dizygotic (DZ) twins share, on average, 50% of their genes. Therefore, within-twin correlations that are stronger in MZ twins compared to DZ twins indicate heritability (**Figure 4**). Behavioral genetic modeling, a specific structural equation model based on twin similarities, can provide estimates for this heritability (Neale *et al.*, 2016). The 'ACE' model divides similarities among twin pairs into similarities due to additive genetic factors (A) and common environmental factors (C), while dissimilarities are ascribed to unique non-shared environmental influences and measurement error (E), see **Figure 4**. High estimates of A indicate that genetic factors play an important role, whilst C estimates indicate influences of the shared environment. If the E estimate is the highest, the variance is mostly accounted for by unique environmental factors and measurement error (Neale *et al.*, 2016).

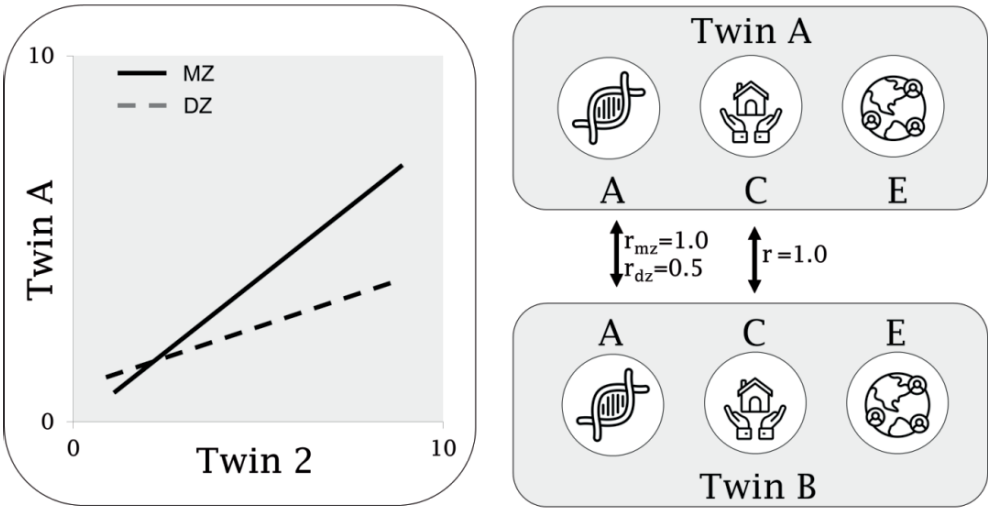


Figure 4. *Twin design: Within-twin correlations that are stronger in monozygotic (MZ) twins compared to dizygotic (DZ) twins indicate heritability (NB: figure is based on hypothetical data). Behavioral genetic modeling can provide heritability estimates by assessing the proportion of variance explained by additive genes (A), common, shared environment (C) and unique environment and measurement error (E). In this ACE model, the correlation between factor A is set to r=1 for MZ twins and to r=0.5 for DZ twins, based on the percentage of overlapping genes. As both MZ and DZ twins share the same environment, the correlation of factor C is set to 1 for all twins. The E factor is freely estimated.*

Previous studies using behavioral data showed high reliability of trait aggression (Miles and Carey, 1997; Rhee and Waldman, 2002; Ferguson, 2010; Tuvblad and Baker, 2011; Porsch *et al.*, 2016). However, the majority of these studies have relied on questionnaire data and very few have used experiments. Also, the number of studies that have investigated heritability of neural mechanisms is scarce. The few studies that investigated genetic and environmental influences on brain function in adults reported significant influences of genetics on functional connectivity, with little shared environmental influences (for an overview, see Richmond *et al.* (2016)). It is important to note that heritability estimates for brain anatomy and connectivity differ across development such that heritability estimates are stronger in adulthood than in childhood (Lenroot *et al.*, 2009; van den Heuvel *et al.*, 2013). Unraveling the extent to which brain development in childhood is influenced by genetics and environment can provide important insights in which neural mechanisms might be more sensitive to environmental influences (Euser *et al.*, 2016). Specifically, using a behavioral genetic approach can provide insights in the etiology of aggression following social evaluation and might offer a starting point for interventions aimed to improve social emotion regulation.

Imaging the Childhood Brain

The majority of previous experimental neuroimaging studies in youth were aimed at adolescence. Some also included children younger than ten years of age, but the sample sizes were often very small. Why has there been so little emphasis on imaging pre-pubertal youth? One possible reason for this could be because scanning children can be very challenging: The MRI scanner is quite imposing and can induce anxiety in children (Tyc *et al.*, 1995; Durston *et al.*, 2009). Such scanner related distress makes it less likely for children to successfully finish an MRI scan, resulting in reduced scan quantity and quality in children compared to older samples (Poldrack *et al.*, 2002; Satterthwaite *et al.*, 2013). However, in order to investigate individual differences (i.e., why are some children more sensitive to social evaluation than others), large sample sizes are required. Not only do we need large sample sizes to investigate inter-individual (between-person) differences in social behavior, multiple waves of that same large sample are needed to capture intra-individual (within-person) differences across development (Telzer *et al.*, 2018). That is to say, to truly capture development we need longitudinal studies. Although more and more studies are using longitudinal methods, these are still not the norm, despite the overall notion that longitudinal research is the golden standard to study changes across development (Pfeifer *et al.*, 2018).

An additional difficulty when it comes to neuroimaging studies in childhood is that different studies seldom used the same experimental paradigm. This makes it difficult to study reproducibility of behavioral and neural findings. Indeed, the (lack of) reproducible results in psychological studies has received a lot of attention (Ioannidis, 2005; Schmidt, 2009; Open Science, 2015). Moreover, findings that show no evidence of significance when analyzed individually (i.e., due to small sample size and/or low statistical power) might provide stronger evidence when collapsed across samples (Scheibehenne *et al.*, 2016). One particularly elegant way to examine a new paradigm is to use a pilot, test and replication design within the same project and combine results meta-analytically. However, to be able to divide a childhood sample into subsamples - again - requires a large sample size.

All of these factors were taken into account when we designed the longitudinal twin study of the Leiden Consortium on Individual Development (L-CID), *Samen Uniek* in Dutch. The L-CID study consists of two cohorts (early childhood and middle childhood) that are being followed for six constructive years, with annual home or lab visits (Euser *et al.*, 2016). The majority of studies in the current thesis (**Chapters 2**, **4**, **5**, **6**, and **7**) are based on data from the middle childhood cohort. Specifically, I made use of the data of the first wave, and a follow up measure two years later. The study included 512 children (256 families) between the ages 7 and 9 at time point 1 (mean age: 7.94±0.67; 49% boys, 55% MZ). This large sample size provides sufficient statistical power to examine childhood brain development, specifically when taken into account that neuroimaging data in developmental samples are more prone to data loss and artifacts due to movement (O'Shaughnessy *et al.*, 2008).

Dissertation Outline

The large sample size of the L-CID study allowed me to test for within-sample replication, thereby contributing to the debate about reproducibility of neuroscientific patterns (Open Science, 2015). In doing so, I first examined the SNAT paradigm using a design with built-in replication and meta-analysis. In **chapter 2**, I tested the SNAT paradigm in separate pilot, test and replication samples and combined the results meta-analytically. The aim of this study was to detect robust behavioral patterns and neural signals related to social feedback, a crucial first step in examining social evaluation processing in childhood. Next, in **chapter 3**, I investigated neural processes of social evaluation in adults, were I additionally investigated brain-behavior associations to shed light on individual differences in the neural mechanisms for social emotion regulation. Unraveling these neural patterns in adults provided an index to compare the results in middle childhood with.

After validating the experimental paradigm in children and adults, the next step was to examine to what extend individual variation in social evaluation were explained by genetics and environmental influences. That is, why are some children more sensitive to social evaluation than others, and how do nature and nurture contribute to this? To examine this, in **chapter 4** I conducted behavioral genetic analyses on neural activation during social evaluation using a large developmental sample. Ultimately, in **chapter 5**, I examined individual differences in longitudinal changes of aggression regulation within childhood. Within-person changes provide a better indication of brain-behavior associations over time and can provide an actual reflection of development. In order to test within-person changes, I examined how neural mechanisms changed within individuals from middle (seven-to-nine-year-old) to late (nine-to-eleven-year-old) childhood, and to what extent these neural changes were related to changes in behavioral aggression.

Taken together, the first four chapters are devoted to an in-depth examination of social emotion regulation using the innovative SNAT paradigm. This paradigm allows to test neural mechanisms of social acceptance and rejection, as well as behavioral aggression in response to social feedback. Previous studies have suggested that social emotion regulation relies on a network of integrated connections between subcortical and cortical prefrontal brain regions (Olson *et al.*, 2009; Chester *et al.*, 2014; de Water *et al.*, 2014; Peper *et al.*, 2015; Silvers *et al.*, 2016b; van Duijvenvoorde *et al.*, 2016a). To date it remains an open question whether these networks are already in place during childhood, as previous studies often used older samples or only included a small sample of children. As L-CID compromises a large and statistically strong sample, I was able to investigate functional brain connectivity specifically in childhood. In **chapter 6**, I investigated the heritability of subcortical-PFC functional connectivity in childhood. The aim of this study was to test whether the subcortical-cortical connections that are central in neurodevelopmental models are already in place in childhood. Here I again made use of the large sample by including an in-sample replication approach to examine the robustness of the findings. Additionally, in **chapter 7**, I provide a comprehensive overview of pitfalls and possibilities in neuroimaging young children, which provides important methodological insights. Specifically, I examined what environmental as well as genetic factors contribute to scan quantity and quality. Here I explicitly compared different MRI modalities, including task-based fMRI, anatomical MRI, and structural and functional brain connectivity measures.

The ultimate goal of developmental neuroscience is to examine brain development from childhood, throughout adolescence, into adulthood and relate neural development to behavioral outcomes. A first step in that direction for social emotion regulation has been taken by relating structural brain connectivity to the ability to delay gratification (Olson *et al.*, 2009; de Water *et al.*, 2014; Peper *et al.*, 2015). In **chapter 8** I investigated the development of structural

subcortical-PFC connectivity and how maturation of this track across development was predictive for delay discounting skills. For this chapter, I used the Braintime data set (van Duijvenvoorde *et al.*, 2016b), a cohort-sequential design including participants aged 8-28, which enabled me to investigate both linear and non-linear brain maturation (see also Braams *et al.* (2015); Peters and Crone (2017). Lastly, in **chapter 9** the findings of the separate chapters are summarized and implications that arise from these findings are discussed in detail.

All empirical chapters are published in, or submitted to international journals. For this, valuable contributions of my co-authors should be acknowledged:

Prof. Dr. Eveline Crone (chapters 2-6, 8)
Prof. Dr. Marian Bakermans-Kranenburg (chapters 2-6)
Prof. Dr. Marinus van IJzendoorn (chapters 5, 6)
Prof. Dr. Nim Tottenham (chapter 6)
Dr. Anna van Duijvenvoorde (chapters 2-5, 8)
Dr. Mara van der Meulen (chapters 2, 4, 6, 7)
Dr. Jiska Peper (chapter 8)
Dr. René Mandl (chapter 8)
Dr. Saskia Euser (chapter 2)

CHAPTER TWO

The neural and behavioral correlates of social evaluation in childhood

This chapter is published as: Achterberg M., Van Duijvenvoorde A.C.K., Van der Meulen M., Euser S., Bakermans-Kranenburg M.J. & Crone E.A. (2017), The neural and behavioral correlates of social evaluation in childhood, *Developmental Cognitive Neuroscience 24*: 107-117.

Abstract

Being accepted or rejected by peers is highly salient for developing social relations in childhood. We investigated the behavioral and neural correlates of social feedback and subsequent aggression in 7-10-year-old children, using the Social Network Aggression Task (SNAT). Participants viewed pictures of peers that gave positive, neutral or negative feedback to the participant's profile. Next, participants could blast a loud noise towards the peer, as an index of aggression. We included three groups (*N*=19, *N*=28 and *N*=27) and combined the results meta-analytically. Negative social feedback resulted in the most behavioral aggression, with large combined effect-sizes. Whole brain condition effects for each separate sample failed to show robust effects, possibly due to the small samples. Exploratory analyses over the combined test and replication samples confirmed heightened activation in the medial prefrontal cortex (mPFC) after negative social feedback. Moreover, meta-analyses of activity in predefined regions of interest showed that negative social feedback resulted in more neural activation in the amygdala, anterior insula and the mPFC/anterior cingulate cortex. Together, the results show that social motivation is already highly salient in middle childhood, and indicate that the SNAT is a valid paradigm for assessing the neural and behavioral correlates of social evaluation in children.

Keywords: Social feedback; Social rejection; Aggression; Childhood; Amygdala; Meta-analysis

Introduction

Social acceptance is of key importance in life. Receiving positive social feedback increases our self-esteem and gives us a sense of belonging (Thomaes *et al.*, 2011). Receiving negative social feedback, in contrast, can induce feelings of depression, and rejected people often react with withdrawal (Nolan *et al.*, 2003). Social rejection can, however, also trigger feelings of anger and frustration, and can lead to reactive aggressive behavior (Dodge *et al.*, 2003; Nesdale and Lambert, 2007; Chester *et al.*, 2014; Riva *et al.*, 2015; Achterberg *et al.*, 2016b). Most developmental studies have focused on the withdrawal reaction after social rejection, while relatively few have examined reactive aggression. The few studies that examined rejection-related aggression showed that early peer rejection was associated with an increase in aggression in children aged 6-8 (Dodge *et al.*, 2003; Lansford *et al.*, 2010). Several prior studies have also shown that rejection can lead to immediate aggression (Chester *et al.*, 2014; Riva *et al.*, 2015; Achterberg *et al.*, 2016b). These immediate effects may be associated with emotional responses to rejection and a lack of impulse control. Although several studies have focused on neural processes involved in negative versus positive social feedback processing, the neural processes involved in dealing with negative or positive social feedback versus a neutral baseline in middle childhood are currently unknown.

Experimental research in adults has examined social evaluation and aggression using a peer acceptance and rejection task. Initially developed as a social feedback task (Somerville *et al.*, 2006), a recent adaptation allowed participants to deliver noise blasts to peers who had rejected them based on a personal profile (Achterberg *et al.*, 2016b), testing the potential expression of reactive aggression. Negative social feedback signaling rejection was associated with louder noise blasts and increased activity in bilateral anterior insula and medial prefrontal cortex (mPFC)/ anterior cingulate cortex (ACC) relative to neutral feedback (Achterberg *et al.*, 2016b). This latter region is suggested to play an important role in evaluating others' behaviors and in estimating others' level of motivation (Flagan and Beer, 2013; Apps *et al.*, 2016). Interestingly, these regions were also more active after positive feedback (compared to neutral feedback), suggesting that both negative and positive feedback leads to social evaluative processes in adults. Other studies also reported the involvement of subcortical regions in processing social feedback. Positive social feedback was found to result in greater activity in striatal regions (Gunther Moor *et al.*, 2010b; Achterberg *et al.*, 2016b), which possibly reflects the rewarding value of this type of feedback (Guyer *et al.*, 2014). Furthermore, peer interactions have been associated with increased amygdala activity, indicating their affective salience (Guyer *et al.*, 2008; Masten *et al.*, 2009; Silk *et al.*, 2014).

Several studies examined the neural correlates of social evaluation in children and adolescents. These studies reported increased neural activity to

positive relative to negative feedback in older adolescents and adults (16-25) as indicated by increased activity in the ventral mPFC, the subcallosal cortex, and the ACC (Gunther Moor *et al.*, 2010b). Another study found increased pupil dilation in response to social rejection (compared to acceptance) in children aged 9-17 (Silk *et al.*, 2012). Pupil dilation is an index of increased activity in cognitive and affective processing regions of the brain, such as the ACC and amygdala (Silk *et al.*, 2012), and the pupil becomes more dilated in response to stimuli with a greater emotional intensity (Siegle *et al.*, 2003). Interestingly, the pupil dilation effect was larger for older participants, indicating that adolescents reacted more strongly to rejection than children. The current study examined the neural correlates of social evaluation in middle childhood, prior to adolescence, because the first long-lasting friendships gradually emerge around this time (Berndt, 2004). Furthermore, we tested whether peer rejection in children results in behavioral aggression, in a similar way as was previously observed in adults (Chester *et al.*, 2014; Riva *et al.*, 2015; Achterberg *et al.*, 2016b).

Thus, our aim was to investigate 7-10-year-old children's responses to social evaluation in terms of neural activity and reactive behavioral aggression. For this purpose, we used the Social Network Aggression Task (SNAT), that elicited robust neural and behavioral responses in adults (Achterberg *et al.*, 2016b), but has not yet been used with children. During the SNAT, participants viewed pictures of peers who gave positive, neutral or negative feedback to the participant's profile. Next, participants could deliver an imagined noise blast towards the peer, as an index of (imagined) aggression or frustration. Since recent studies have reported concerns about the replicability of psychological science (for example see Open Science (2015)), we used three samples to validate the paradigm: a pilot sample, a test sample, and a replication sample. Moreover, findings that may show no evidence of significance when analyzed individually might provide stronger evidence when collapsed across experiments, as was recently shown (Scheibehenne *et al.*, 2016). Therefore we also include a meta-analytic combination of the results across the three samples.

On the behavioral level we expected that the pattern of aggression after positive, neutral, and negative feedback would be similar across the pilot, test and replication samples, with negative feedback resulting in the highest levels of aggressive behavior. On the neural level we examined both the general contrast of social evaluation (all feedback conditions vs. baseline; see Supplementary Materials) and the condition-specific contrasts. To further investigate condition effects, that is the effect of negative *vs.* neutral *vs.* positive feedback, we used regions of interest (ROI) analyses. The individual ROI analyses were meta-analytically combined in order to test for robust condition effects across our samples. Based on studies in adults, the predictions were that negative social feedback would be associated with increased activity in the amygdala (Masten *et al.*, 2009), bilateral insula, and mPFC/Anterior Cingulate Cortex' gyrus ACCg (Somerville *et al.*, 2006; Achterberg *et al.*, 2016b). While prior studies tested only

adults and adolescents, this study tested for the first time if the same regions are engaged in children, including not only positive and negative social feedback but also a neutral social feedback baseline (see Achterberg *et al.*, 2016), and examined the relations with subsequent aggression.

Methods

Participants

Participants in this study were part of the larger, longitudinal twin study of the Leiden Consortium on Individual Development (L-CID). Families with a twin born between 2006 – 2009, living within two hours travel time from Leiden, were recruited through the Dutch municipal registry and received an invitation to participate by post. Parents could show their interest in participation using a reply card. For the larger L-CID study, only same-sex twins were included. Opposite-sex twins were included only in the pilot study. The pilot sample consisted of 20 children between the ages of 7 and 10 (11 boys, *M*=8.16 years, *SD*=0.95), including 9 opposite-sex twin pairs. Two additional participants were recruited from a participant data base at Leiden University. Two months after the pilot sample, the test and replication samples were recruited. The test and replication sample consisted of 30 same-sex twin pairs (16 boys, *M*=8.22 years, *SD*=0.67), including 7 monozygotic pairs. After data collection, but prior to data analyses, first and second born children (within the twin pair) were randomly assigned to the test and replication sample. For a schematic overview of sample selection see Figure S.1 (2.Supplementary Materials). The Dutch Central Committee on Human Research (CCMO) approved the study and its procedures. Written informed consent was obtained from both parents. All participants were fluent in Dutch, had normal or corrected-to-normal vision, and were screened for MRI contra indications. All anatomical MRI scans were reviewed and cleared by a radiologist from the radiology department of the Leiden University Medical Center (LUMC). No anomalous findings were reported.

Six participants were excluded due to excessive head motion, which was defined as >1 mm movement in >20% of the volumes (one from the pilot sample, two from the test sample and three from the replication sample). The final pilot sample consisted of 19 participants, including 8 twin pairs (10 boys, *M*=8.18 years, *SD*=0.97), the final test sample consisted of 28 participants (12 boys, *M*=8.23 years, *SD*=0.67) and the final replication sample consisted of 27 participants (12 boys, *M*=8.28 years, *SD*=0.65). Demographics of the final samples are listed in Table 1. Participants' intelligence (IQ) was estimated with the subsets 'similarities' and 'block design' of the Wechsler Intelligence Scale for Children, third edition (WISC-III; Wechsler, 1997). For all three samples, estimated IQs were in the normal to high range (see Table 1). In all three samples, IQ scores were

unrelated to behavioral outcomes of the SNAT (noise blast duration after positive, neutral, negative feedback, all *p*'s > .214).

Table 1. Demographic characteristics of the sample.

	Pilot	Test	Replication
N	19	28	27
% boys	53%	43%	44%
Left handed	none	3	6
AXIS-I disorder	none	none	1 (ADHD)
Mean Age (SD)	8.18 (0.97)	8.23 (0.67)	8.28 (0.65)
Age Range	7.20 -10.99	7.03 - 8.97	7.03 - 8.97
Mean IQ (SD)	102.76 (11.54)	101.57 (12.33)	104.54 (10.58)
IQ range	85.00 - 127.50	77.50 - 125.00	85.00 - 132.50

Social Network Aggression Task

The Social Network Aggression Task (SNAT) as described in Achterberg *et al.* (2016b) was used to measure (imagined) aggression after social evaluation. The task was programmed in Eprime (version 2.0.10.356). Prior to the fMRI session, the children filled in a personal profile at home, which was handed in at least one week before the actual fMRI session. The profile page consisted of questions such as: *'What is your favorite movie?'*, *'What is your favorite sport?'*, and *'What is your biggest wish?'*. Children were informed that their profiles were reviewed by other, unfamiliar, children. During the SNAT the children were presented with pictures and feedback from same-aged peers in response to their personal profile. Every trial consisted of feedback from a new unfamiliar child. This feedback could either be positive ('I like your profile', or 'I like the same movies and the same sports', visualized by a green thumb up); negative ('I do not like your profile', or 'I hate your sport and don't like that movie'; red thumb down) or neutral ('I don't know what to think of your profile', or 'I like your sport, but hate that movie', grey circle). Following each peer feedback, the children were instructed to imagine that they could send a loud noise blast to this peer. We specifically instructed the children to imagine this to reduce deception, and studies showed that imagined play also leads to aggression (Konijn *et al.*, 2007). The longer they pressed the button the more intense the noise would be, which was visually represented by a volume bar (Figure 1). To keep task demands as similar as possible between the conditions, participants were instructed to always press the button, but they could choose whether they wanted a short noise at low intensity or a long noise at high intensity.

Unbeknownst to the participants, others did not judge the profile, and the photos were created by morphing two children of an existing data base (matching the age range) into a new, non-existing child. Peer pictures were randomly coupled to feedback, ensuring equal gender proportions for each type of feedback. Deception was assessed using an exit interview with open questions, such as 'what did you think of the game', and 'what did you think of the noises that you could delivered'. None of the participants expressed doubts about the cover story. Participants were familiarized with the MRI scanner with a practice session in a mock scanner. Then participants received instructions on how to perform the SNAT and the children were exposed to the noise blast twice during a practice session: once with stepwise build-up of intensity and once at maximum intensity. Participants did not hear the noise during the fMRI session, to prevent that pressing the button would punish the participants themselves. To familiarize participants with the task, participants performed six practice trials. After the practice session, one of the twins continued with the actual scanning session, while the other twin performed the WISC-III and other behavioral tasks. First-born and second-born children were randomly assigned to the scan session or behavioral session as their first task. When the first child completed the scanning session, he/she continued with the WISC-III and behavioral tasks while the other child participated in the scanning session.

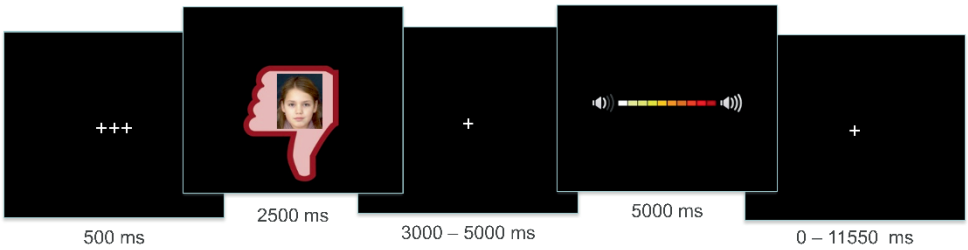


Figure 1. *Display of one trial of the Social Network Aggression Task (SNAT).*

The SNAT consisted of 60 trials, three blocks of 20 trials for each social feedback condition (positive, neutral, negative), that were presented semi-randomized to ensure that no condition was presented more than three times in a row. The first block consisted of 7 positive, 6 neutral, and 7 negative feedback trials; the second block consisted of 8 positive, 6 neutral, 6 negative feedback trials; and the third block consisted of 5 positive, 8 neutral, and 7 negative feedback trials. The optimal jitter timing and order of events were calculated with Optseq 2 (Dale, 1999). Each trial started with a fixation screen (500 ms), followed by the social feedback (2500 ms). After another jittered fixation screen (3000-5000 ms), the noise screen with the volume bar appeared, which was presented for a total of 5000 ms. Children were instructed to deliver the noise blast by pressing one of the buttons on the button box attached to their legs, with their right index finger.

As soon as the participant started the button press, the volume bar started to fill up with a newly colored block appearing every 350 ms. After releasing the button, or at maximum intensity (after 3500 ms), the volume bar stopped increasing and stayed on the screen for the remainder of the 5000 ms. Before the start of the next trial, another jittered fixation cross was presented (0 -11550 ms) (Figure 1). The length of the noise blast duration (i.e., length of button press) was used as a measure of aggression.

MRI data acquisition

MRI scans were acquired with a standard whole-head coil on a Philips 3.0 Tesla scanner. The data of the pilot sample were collected on a Philips Achieva TX MR system, the data of the test and replication sample were collected on a Philips Ingenia MR system. To prevent head motion, foam inserts surrounded the children's heads. The SNAT was projected on a screen that was viewed through a mirror on the head coil. Functional scans were collected during three runs T2*-weighted echo planar images (EPI). The first two volumes were discarded to allow for equilibration of T1 saturation effect. Volumes covered the whole brain with a field of view (FOV) = 220 (ap) x 220 (rl) x 111.65 (fh) mm; repetition time (TR) of 2.2 seconds; echo time (TE) = 30 ms; flip angle (FA) = 80°; sequential acquisition, 37 slices; and voxel size = 2.75 x 2.75 x 2.75 mm. In the pilot sample the FOV was 220 (ap) x 220 (rl) x 114.68 (fh) mm, with a sequential acquisition of 38 slices. All other parameters were equal. Subsequently, a high-resolution 3D T1scan was obtained as anatomical reference (FOV= 224 (ap) x 177 (rl) x 168 (fh); TR = 9.72 ms; TE = 4.95 ms; FA = 8°; 140 slices; voxel size 0.875 x 0.875 x 0.875 mm). In the pilot sample the TR = 9.79 and the TE = 4.60, all other parameters were equal.

MRI data analyses

Preprocessing

MRI data were analyzed with SPM8 (Wellcome Trust Centre for Neuroimaging, London). Images were corrected for slice timing acquisition and rigid body motion. Functional scans were spatially normalized to T1 templates. Volumes of all children were resampled to 3x3x3 mm voxels. Data were spatially smoothed with a 6 mm full width at half maximum (FWHM) isotropic Gaussian kernel. SPM8's ARTrepair toolbox (Mazaika *et al.*, 2009) was used to detect and fix bad slices in preprocessed functional data. Slices with >1 mm scan to scan motion were detected and repaired. Children with >20% repaired slices were excluded from further analyses.

First-level analyses

Statistical analyses were performed on individual subjects' data using a general linear model. The fMRI time series were modeled as a series of two events

convolved with the hemodynamic response function (HRF). The onset of social feedback was modeled as the first event with a zero duration and with separate regressors for the positive, negative, and neutral peer feedback. The start of the noise blast was modeled for the length of the noise blast duration (i.e., length of button press) and with separate regressors for noise blast after positive, negative, and neutral feedback. Trials on which the participants failed to respond in time were modeled separately as covariate of no interest and were excluded from further analyses. On average 7.3% of the trials were invalid (pilot: 7.8%, test: 7.3%, replication: 6.5%), with similar proportions of positive (6.9%), neutral (7.2%) and negative (7.3%) invalid trials. All participants had at least 10 trials for each feedback type. To account for possible motion induced error that had not been solved by realignment and ARTrepair, we included six additional motion regressors (corresponding to the three translational and rotational directions) as covariates of no interest. The least squares parameter estimates of height of the best-fitting canonical HRF for each condition were used in pairwise contrasts. The pairwise comparisons resulted in subject-specific contrast images.

Higher-level group analyses

Subject-specific contrast images were used for the group analyses. Given that the all feedback > fixation baseline generally results in strong and robust activity, we validated our replication approach using this contrast (for results see Supplementary Material). Our main analyses focus on the condition specific contrasts (e.g. 'positive vs. negative' feedback), using t-tests. Results were False Discovery Rate (FDR) cluster corrected ($pFDR<.05$), with a primary voxel-wise threshold of $p<.005$ (uncorrected) (Woo *et al.*, 2014). Cluster-extend based thresholding has relatively high sensitivity (Smith and Nichols, 2009) and takes into account that individual voxel activations are not independent of the activations of voxels nearby (Heller *et al.*, 2006). We set the primary p-value at $p<.005$ to strike the balance between too liberal cluster defining primary thresholds (e.g. $p<.01$; which can induce Type I errors) and more conservative primary thresholds (e.g. $p<.001$; which can induce Type II errors). Recently, cluster corrections have been debated for potential high Type I errors (Eklund *et al.*, 2016), but the current three-sample design should reduce the risk for coincidental findings. Coordinates for local maxima are reported in MNI space.

Region of Interest analyses

To extract patterns of activation in functionally defined clusters, SPM8's MarsBaR toolbox (Brett *et al.*, 2002) was used. Besides ROIs derived from whole brain comparisons, we also performed analyses on three predefined ROIs based on adult social evaluation literature. These were the amygdala (from the Automated Anatomical Labeling (AAL) atlas (Tzourio-Mazoyer *et al.*, 2002), left and right combined, center of mass (x,y,z) right: 27,-1, -19; left: -24, -2, -19), the anterior

insula (from the conjunction contrast of Achterberg *et al.* (2016b); left and right combined, center of mass (x,y,z) right: 34, 21, 0; left: -32, 20, -6) and the mPFC/ACCg (from the conjunction contrast of (Achterberg *et al.*, 2016b)), see Figure 4a. Parameter estimates (PE, average Beta values) were extracted for the ROI analyses.

Statistical analyses

For noise blast duration, we first computed split-half reliability analyses. Positive, neutral and negative trials were randomly split in half and Pearson's correlation coefficients were calculated between both halves for each condition in all three samples. Split-half reliability analyses showed that the SNAT displayed excellent reliability in all three conditions: noise blast duration after positive (pilot: r=.85, test: r=.96, replication: r=.96; all p's<.001), neutral (pilot: r=.83, test: r=.90, replication: r=.89; all p's<.001) and negative social feedback (pilot: r=.89, test: r=.94, replication: r=.84; all p's<.001). Next, we used repeated measures ANOVA to investigate the noise blast duration after positive, neutral, and negative feedback in the three samples. Greenhouse-Geisser corrections were applied when the assumption of sphericitiy was violated. Pairwise comparisons were Bonferroni corrected. When outliers were detected (Z-value <-3.29 or >3.29), scores were winsorized (Tabachnick and Fidell, 2013). To compare the behavioral and neural effects over the different samples, we computed combined effect sizes using the Comprehensive Meta-Analysis (CMA) program (Borenstein *et al.*, 2005).

Results

Behavioral results: Noise blast duration

For each of the three samples (pilot, test, and replication) we performed a repeated measures ANOVA on noise blast duration after positive, negative, and neutral feedback. Results of the pilot sample showed a significant main effect of type of social feedback on noise blast duration, $F(2, 36)=29.55$, $p<.001$, $\omega^2 = 0.46$), see Figure 2. Pairwise comparisons revealed that noise blast duration after negative feedback (M=2718 msec, SD=629) in the pilot sample was significantly longer than noise blast duration after neutral feedback (M=1725 msec; SD=470, $p<.001$, d= 1.78), and after positive feedback (M=1274 msec; SD=782, $p<.001$, d= 2.04). Noise blast duration after neutral feedback was significantly longer than after positive feedback (p=.007, d= 0.62). These results were confirmed in the test sample ($F(2, 54)=29.72$, $p<.001$, $\omega^2 = 0.30$). Participants in the test sample also gave significant longer noise blasts after negative feedback (M=2882 msec;

SD=790), compared to neutral feedback (*M*=2024 msec; *SD*=775, *p*<.001, *d*= 1.10), and positive feedback (*M*=1501 msec; *SD*=966, *p*<.001, *d*= 1.57). Noise blast duration after neutral feedback was also significantly longer than after positive feedback (*p*<.001, *d*= 0.57), see Figure 2. A similar pattern was found in the replication sample (*F*(2, 52)=34.18, *p*<.001, ω^2=0.39). Participants in the replication sample also gave significant longer noise blast after negative feedback (*M*=2967 msec; *SD*=573) compared to neutral feedback (*M*=1967 msec; *SD*=636, *p*<.001, *d*= 1.65) and positive feedback (*M*=1537 msec; *SD*=942, *p*<.001, *d*= 1.86). Noise blast duration after neutral feedback was also significantly longer than after positive feedback (*p*=.007, *d*= 0.50), see Figure 2.

To combine the results of the three different samples, we performed a meta-analysis. The difference between neutral and negative feedback showed a large combined effect size (*d*=1.41, 95% confidence interval (CI): 0.97-1.84, *p*<.001). The difference between positive and negative feedback also showed a large combined effect size (*d*=1.74, 95% CI: 1.19-2.29, *p*<.001). The combined effect for the difference between positive and neutral was medium in size (*d*=0.55, 95% CI: 0.39 - 0.723, *p*<.001). Study outcomes were homogeneous; there was no heterogeneity in the results.

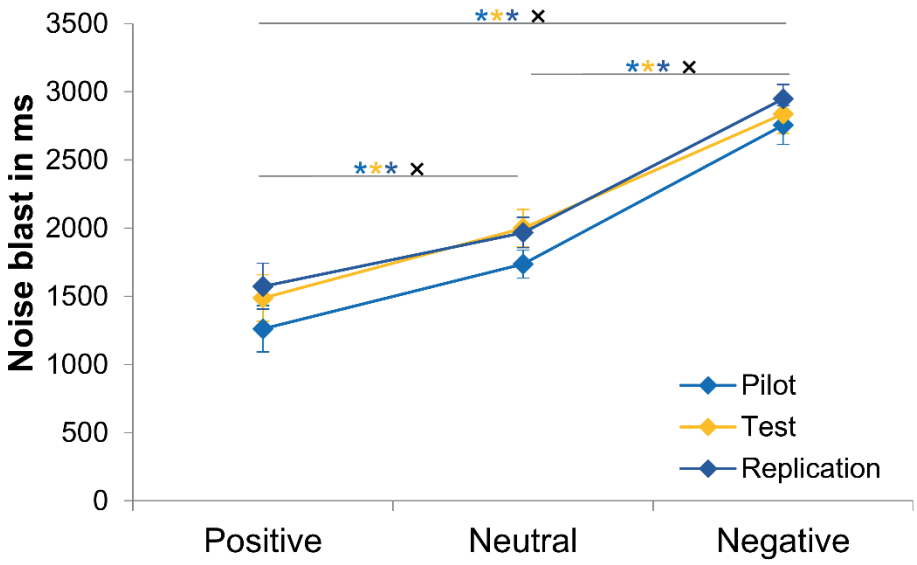


Figure 2. *Noise blast duration across the different social feedback conditions for the pilot, test, and replication sample. Error bars display standard error of mean. * significant differences for sample with matching color. × significant combined effect sizes in the meta-analysis.*

Neural activity: Whole brain and ROI analyses

The general contrast (all feedback conditions vs. baseline) showed a robust pattern of activation. Most regions that were active in the pilot sample could be confirmed in the test sample, and all regions that were active in the test sample were replicated in the replication sample (see Supplementary Materials). To test for differences between conditions, full factorial ANOVA's were performed that were then decomposed by pair-wise comparisons. Moreover, we performed exploratory whole brain analyses in the combined test and replication groups (N=55), for which data were collected using the same MR scanner. Lastly, we performed ROI analyses in the three separate samples on three predefined ROIs: the amygdala (anatomically defined), the anterior insula and the mPFC/ACCg (based on Achterberg *et al.* (2016b)). To combine the results, we performed meta-analyses across the three samples for each of these ROIs.

Whole brain condition effects per sample

Pilot sample

All significant pairwise comparisons are displayed in Table 2. The contrasts positive>negative and positive>neutral feedback both resulted in one cluster of heightened activation in the lateral occipital cortex. The contrast negative > neutral feedback resulted in two significant clusters: one in the left lateral occipital cortex and one in the left orbitofrontal cortex, extending into the left insula.

Test sample

All significant pairwise comparisons are displayed in Table 2. The contrasts positive>negative and positive>neutral feedback in the test sample also resulted clusters of heightened activation in the (lateral) occipital cortex. The contrast negative>neutral feedback resulted in two significant clusters, both in the lateral occipital cortex, extending into the fusiform gyrus.

Replication sample

All significant pairwise comparisons are displayed in Table 2. The contrasts positive>negative and positive>neutral feedback did not result in significant activation in the replication sample. Negative>positive feedback resulted in increased activation in the left inferior frontal gyrus, the left amygdala, and left lateral occipital cortex. Last, negative>neutral feedback resulted in increased activation of the left and right lateral occipital cortex, extending into the fusiform gyrus.

Whole brain condition effects in the combined test and replication samples

A full factorial ANOVA was computed based on the combined test and replication groups (*N*=55). All significant pairwise comparisons are displayed in Table 3. The contrast negative>neutral and positive>neutral feedback resulted in heightened activation in the lateral occipital cortex. The contrast negative>positive feedback resulted in significant heightened activation in the right and left orbitofrontal cortex, the medial prefrontal cortex, the paracingulate gyrus, the left insula and the left superior temporal cortex (see Figure 3a, Table 3). Figure 3b presents a visual representation of mPFC activation after positive and negative social feedback for the combined test and replication group, as well as for the test and replication sample separately. The reversed contrast, positive>negative feedback did not resulted in any significant clusters.

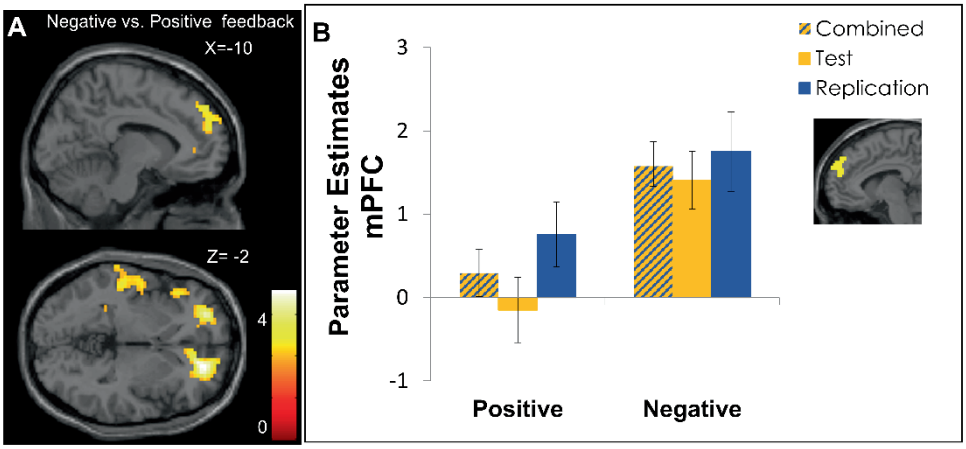


Figure 3. *a) whole brain results of the contrast negative vs. positive feedback in the test and replication samples combined (N=55, p<.005, FDR cluster corrected). b) Mean parameter estimates for negative > positive feedback activation in the medial PFC cluster in the test and replication samples combined (N=55, as displayed in Figure 3A), as well as for the samples separately (center of mass (x,y,z): -1, 55, 31). Note that this graph is purely for visual representation and is not used for statistical inferences. Error bars indicate standard error of mean.*

Table 2. Whole brain condition effects per sample.

Area of Activation	Volume	x	y	z	T	pFDR
Pilot: positive > negative						
Lateral occipital cortex	649	3	-70	7	5.75	<.001
Cuneal cortex		3	-76	25	5.03	
Supracalcarine cortex		0	-67	16	5.01	
Pilot: positive > neutral						
Lateral occipital cortex	2560	-45	-82	7	6.83	<.001
Lingual gyrus		6	-67	4	6.43	
Lingual gyrus		18	-64	-2	6.22	
Pilot: negative > neutral						
Left lateral occipital cortex	348	-45	-82	7	5.04	<.001
Left middle temporal gyrus		-51	-58	10	3.82	
Left lateral occipital gyrus		-39	-64	13	3.77	
Left orbitofrontal cortex	271	-36	23	-14	4.00	.009
Left orbitofrontal cortex		-42	17	-14	3.90	
Left insula		-36	8	-5	3.86	
Test: positive > negative						
Lingual gyrus	337	-15	-88	-5	5.24	.016
Lingual gyrus		9	-76	-5	4.30	
Occipital pole		-21	-94	-17	3.79	
Test: positive > neutral						
Occipital pole	1031	-15	-91	-5	6.17	<.001
Occipital fusiform gyrus		24	-73	-5	5.96	
Lingual gyrus		9	-79	-5	5.36	
Test: negative > neutral						
Occipital pole	348	-6	-97	7	5.13	.008
Lateral occipital cortex		-45	-85	4	4.13	
Lateral occipital cortex		-54	-79	4	3.84	
Lateral occipital cortex	274	48	-70	-5	3.86	.013
Occipital fusiform gyrus		27	-73	-2	3.54	
Occipital fusiform gyrus		21	-82	-2	3.51	

Table 2. (continued)

Area of Activation	Volume	x	y	z	T	pFDR
Replication: negative > positive						
Left inferior frontal gyrus	325	-54	29	4	4.86	.012
Left amygdala		-24	-1	-26	4.15	
Left frontal operculum cortex		-45	23	1	3.99	
Left lateral occipical cortex	402	-42	-79	4	4.38	.008
Left lateral occipical cortex		-42	-76	22	3.71	
Lingual gyrus		-12	-57	-5	3.61	
Replication: neutral > positive						
Left precentral gyrus	1318	-15	-19	70	5.25	<.001
Right precentral gyrus		27	-16	70	5.17	
Right precentral gyrus		9	-25	70	5.03	
Replication: neutral > negative						
Right precentral gyrus	293	30	-16	70	4.11	.018
Left precentral gyrus		-9	-16	73	3.78	
Left precentral gyrus		-15	-22	79	3.37	
Replication: negative > neutral						
Left lateral occipital cortex	707	-42	-82	4	6.55	<.001
Left lateral occipital cortex		-48	-73	-5	4.71	
Left occipital fusiform cortex		-39	-49	-14	4.36	
Left occipital pole	193	-12	-94	22	6.28	.027
Left occipital pole		-6	-97	13	5.18	
Left lateral occipital cortex		-15	-85	40	3.53	
Right lateral occipital cortex	844	36	-76	-2	5.01	<.001
Right lateral occipital cortex		48	-67	-2	4.97	
Right lateral occipital cortex		48	-76	4	4.85	

Table 3. Whole brain condition effects combined test and replication sample.

Area of Activation	Volume	*x*	*y*	*z*	*T*	*pFDR*
Negative > neutral						
Left lateral occipital cortex	1080	-45	-82	4	6.90	<.001
Left lateral occipital cortex		-6	-97	10	6.82	
Left occipital pole		-15	-94	22	5.93	
Right lateral occipital cortex	1053	48	-67	-5	6.10	<.001
Right lateral occipital cortex		33	-76	-2	5.98	
Right occipital fusiform gyrus		18	-82	-2	5.60	
Positive > neutral						
Right occipital fusiform gyrus	1478	24	-73	-5	6.60	<.001
Left occipital pole		-15	-91	-2	5.97	
Left occipital fusiform gyrus		-24	-76	-5	5.86	
Neutral > negative						
Right precentral gyrus	475	30	-13	67	4.21	.002
Right middle frontal gyrus		33	14	43	4.19	
Right middle frontal gyrus		33	11	67	4.04	
Negative > positive						
Right orbitofrontal cortex	207	21	47	-2	4.94	.039
Left orbitofrontal cortex	225	-27	50	-2	4.45	.038
Left inferior frontal gyrus		-51	26	4	4.18	
Medial prefrontal cortex		-18	59	4	3.49	
Medial prefrontal cortex	259	-15	47	40	4.11	.032
Medial prefrontal cortex		-6	62	31	4.07	
Paracingulate gyrus		-6	53	22	3.65	
Left insula	836	-45	-10	7	4.05	<.001
Left parietal operculum cortex		-30	-34	22	3.99	
left superior temporal cortex		-54	-4	7	3.85	

ROI analyses in the three samples and combined effect sizes

Amygdala

Results for each of the three samples separately and the meta-analytic combination of results are displayed in Figure 4b and Table 3. The pilot and replication samples showed significantly more amygdala activation after negative compared to positive feedback, but the test sample did not show an effect. The meta-analysis revealed that the difference in amygdala activation between negative and neutral feedback was not significant (d=0.21, 95% CI: -0.12-0.54, p=.204). The combined effect size for the difference in amygdala activation between positive and neutral was also not significant (d=0.16, 95% CI: -0.15-0.48, p=.299). However, the difference in amygdala activation between positive and negative feedback showed a significant combined effect size (d=0.47, 95% CI: 0.09-0.84, p=.015), being larger for negative feedback. The study outcomes were homogeneous; there was no heterogeneity in the results.

Anterior Insula

Results are displayed in Figure 4c and Table 3. All samples showed increased anterior insula activation after negative *vs* neutral feedback, but the difference was only significant in the replication sample. The meta-analysis showed that the difference in anterior insula activation between negative and neutral feedback showed a significant combined effect size (d=0.40, 95% CI: 0.11-0.69, p=.007), being larger for negative feedback. The combined effect size for the difference in anterior insula activation between positive and neutral was not significant (d=0.15, 95% CI: -0.12-0.42, p=.282). Furthermore, the combined effect size for the difference in anterior insula activation between positive and negative feedback was not significant (d=0.24, 95% CI: -0.06-0.53, p=.123). The study outcomes were homogeneous; there was no heterogeneity in the results.

Medial PFC/ ACC gyrus

Results for each of the three samples separately are displayed in Figure 4d and Table 3. Although the pattern of neural activation across conditions was similar to that of the anterior insula, there were no significant condition effects in the separate samples. However, the meta-analysis showed a significant combined effect size for the difference in mPFC/ACCg activation between negative and neutral feedback (d=0.33, 95% CI: 0.01-0.66, p=.045), with more mPFC/ACCg activation after negative feedback. The combined effect size for the difference in mPFC/ACCg activation between positive and neutral feedback was in the expected direction (being larger for positive feedback) but not significant (d=0.22, 95% CI: -0.03-0.46, p=.080). Furthermore, the combined effect size for the difference in mPFC/ACCg activation between positive and negative feedback was not

significant (*d*=0.09, 95% CI: -0.19-0.36, *p*=.539). The study outcomes were homogeneous; there was no heterogeneity in the results.

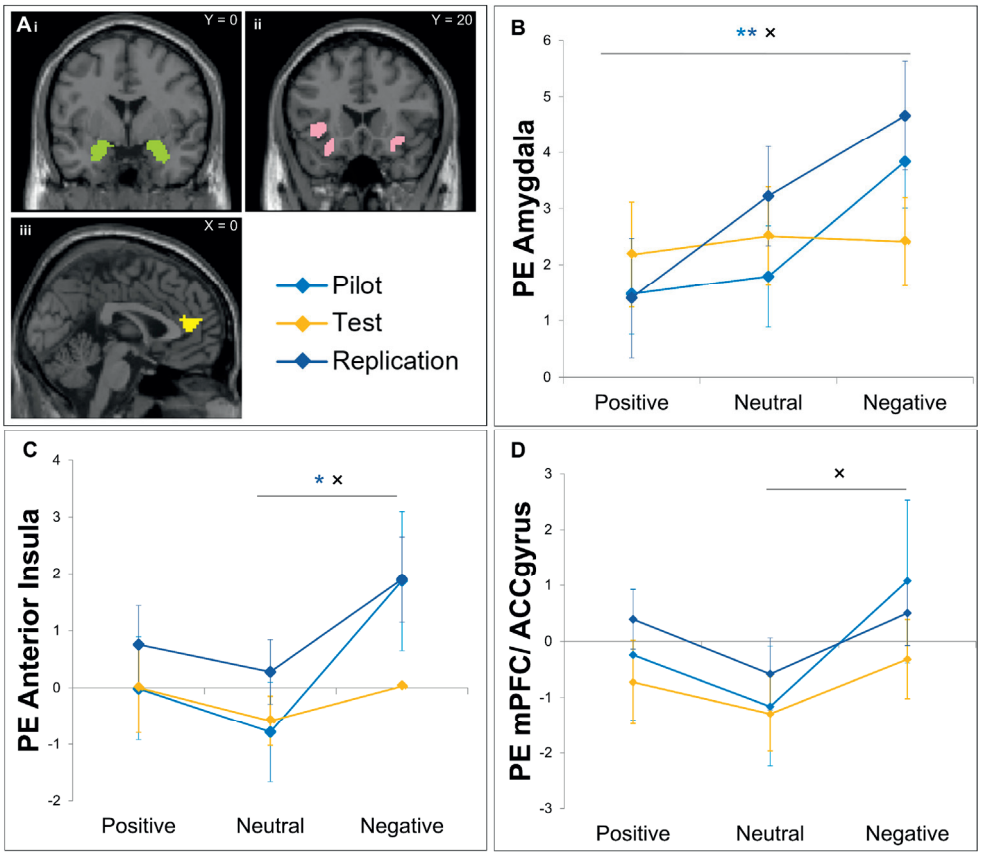


Figure 4. *a) visual representation of the ROIs: i) amygdala, ii) anterior insula and iii) medial PFC/ACC gyrus. b) Amygdala activation across the different social feedback conditions for the pilot, test, and replication sample. c) Anterior insula activation across the different social feedback conditions for the pilot, test, and replication sample. d) Medial PFC/ ACC gyrus activation across the different social feedback conditions for the pilot, test, and replication sample. *significant difference for sample with matching color. ˣsignificant combined effect size in the meta-analysis. Error bars indicate standard error of mean.*

Brain-behavior correlations

Finally, we tested for brain-behavior correlations. Specifically, we correlated the meta-analytically significant brain results with noise blast duration. There were no significant results for negative>positive amygdala activation and aggressive behavior; nor for negative>neutral insula activation and aggression; nor for negative > neutral mPFC activation and aggression. Thus, we did not found

significant brain-behavior relations, not in the samples separately, nor with a meta-analytical approach (see Supplementary Materials).

Table 4. Comprehensive Meta-Analyses of the condition effects.

		d	95% CI lower limit	95% CI upper limit
Amygdala				
Negative > Positive	Pilot	0.70 *	0.06	1.34
	Test	0.05	-0.52	0.62
	Replica	0.61 **	0.20	1.02
	Meta	*0.47 **	*0.09*	*0.84*
Negative > Neutral	Pilot	0.54	-0.05	1.14
	Test	-0.02	-0.41	0.36
	Replica	0.30	-0.22	0.81
	Meta	*0.21*	*-0.12*	*0.54*
Neutral > Positive	Pilot	0.09	-0.52	0.69
	Test	0.07	-0.42	0.55
	Replica	0.36	-0.20	0.91
	Meta	*0.17*	*-0.15*	*0.48*
Anterior Insula				
Negative > Positive	Pilot	0.40	-0.29	1.09
	Test	0.06	-0.44	0.55
	Replica	0.31	-0.14	0.75
	Meta	*0.24*	*-0.06*	*0.53*
Negative > Neutral	Pilot	0.57	-0.08	1.21
	Test	0.22	-0.28	0.72
	Replica	0.46 *	0.03	0.90
	Meta	*0.40 **	*0.11*	*0.69*
Positive > Neutral	Pilot	0.20	-0.30	0.07
	Test	0.11	-0.32	0.55
	Replica	0.14	-0.34	0.62
	Meta	*0.15*	*-0.12*	*0.42*

* p<.05, ** p<.01

Table 4. (continued)

		d	95% CI lower limit	95% CI upper limit
Dorsal Anterior Cingulate Cortex				
Negative > Positive	Pilot	0.23	-0.45	0.90
	Test	0.11	-0.46	0.67
	Replica	0.04	-0.32	0.40
	Meta	*0.09*	*-0.19*	*0.36*
Negative > Neutral	Pilot	0.40	-0.30	1.10
	Test	0.27	-0.32	0.86
	Replica	0.34	-0.12	0.81
	Meta	*0.33* *	*0.01*	*0.66*
Neutral > Positive	Pilot	0.19	-0.31	0.68
	Test	0.15	-0.22	0.52
	Replica	0.32	-0.10	0.73
	Meta	*0.22*	*-0.03*	*0.46*

* $p<.05$, ** $p<.01$

Discussion

This study investigated the behavioral and neural correlates of social evaluation in middle childhood, using a new experimental paradigm: the Social Network Aggression Task (SNAT, Achterberg *et al.* (2016b)). With the combination of a replication design and a meta-analytical approach we thoroughly tested this new experimental paradigm in 7-to-10-year-old children. Overall, we found consistent findings over the pilot, test and replication samples for behavioral aggression following negative social feedback, showing significantly more aggression after negative social feedback compared to positive or neutral social feedback The neural effects indicated increased activity in the amygdala, insula and mPFC/ACCg after negative feedback, but these effects were only significant in part of the samples and in the meta-analyses. The specific social evaluation effects and methodological considerations for future research are described in more detail below.

Social evaluation in childhood

The SNAT showed reliable and consistent behavioral results, with stronger behavioral aggression (noise blast duration) after social rejection. The meta-analysis showed medium to (very) large combined effect sizes over the three samples. This study complements the large number of prior studies that focused mainly on withdrawal, as we showed that social rejection feedback also elicits aggression in children. This is in line with previous results in adults (Achterberg *et al.*, 2016b), suggesting that children make similar distinctions between social evaluation as adults do. Moreover, these results are consistent with questionnaire studies that show more (teacher reported) aggression after social rejection in children (Dodge *et al.*, 2003; Nesdale and Lambert, 2007; Lansford *et al.*, 2010).

The next question concerned whether neural activation differed depending on whether the participant received positive, neutral or negative social feedback. The separate samples did show the same significant condition effects. In the pilot sample, we found significant heightened activation in the insula after negative vs. neutral social feedback, similar to the effects reported in adults (Achterberg *et al.*, 2016b). However, whole brain analyses did not reveal this effect in the test or replication samples. Moreover, although heightened activation in the visual cortex (including the fusiform gyrus) after positive compared to negative and neutral feedback was consistent over the pilot and test sample, we could not confirm this in the replication sample. Our relatively small samples (with sample sizes ranging between n=19 and n=28) might not have had sufficient power to detect robust condition effects in whole brain analyses.

In the larger combined sample (including twin siblings, N=55) rejection feedback was associated with increased activity in mPFC. This region borders the mPFC/ACCg region observed in adults, with increased activity in response to

negative and positive feedback (Achterberg *et al.*, 2016b). Indeed, an ROI analysis of this mPFC/ACCg region based on the adult study (Achterberg *et al.*, 2016) confirmed elevated activity after rejection in children. A recent review on the ACC and social cognition (Apps *et al.*, 2016) describes an anatomical and function subdivision between the anterior cingulate cortex' sulcus and gyrus. The region described as the ACC gyrus (ACCg; located adjacent and dorsal to the genu of the corpus callosum in humans) shows overlap with the region that showed increased activation after negative social feedback in children (this study) and for general social evaluation in adults (Achterberg *et al.*, 2016b). The ACCg region has been suggested to be sensitive to factors determining the others' motivation (see Apps *et al.* (2016)). Moreover, the meta-analysis showed that the anterior insula was more active after negative compared to neutral feedback, which is in line with the results reported in adults (Achterberg *et al.*, 2016b). The anterior insula has been shown to have strong connections (both structurally as functionally) with this ACCg region (Apps *et al.*, 2016) and several neuroimaging studies have pointed towards the anterior insula and midline areas of the brain as important brain regions responding to social rejection (for meta-analysis see Cacioppo *et al.* (2013); Rotge *et al.* (2015)).

In addition, the meta-analysis showed significantly more activation in the amygdala after negative feedback compared to positive feedback. A recent cross-sectional study of 112 participants with ages ranging from 6-23 years showed decreased amygdala reactivity over age, suggesting a shift from bottom-up amygdala based processing to a more top-down processing in adolescence and adulthood (Silvers *et al.*, 2016a). That study focused on the processing of negative and positive scenes and showed strongest reactivity for emotional scenes in general (independent of valence) in younger participants. This may indicate that the amygdala serves as an important region for processing affectively salient stimuli in childhood in particular. An interesting question for future research is to examine how amygdala response to social feedback relates to social behavior in childhood and how it unfolds over time during childhood and adolescence.

Interestingly, in the meta-analyses, we did not find significantly more activation in any of the regions after positive feedback (compared to neutral feedback), which is not in line with previous adult findings (Achterberg *et al.*, 2016b) or with prior studies that focused on adolescents using similar paradigms (Gunther Moor *et al.*, 2010b; Silk *et al.*, 2012). Positivity biases are thought to be larger in childhood than in adolescence or adulthood (Mezulis *et al.*, 2004), possibly indicating that children have a stronger belief that they will be positively evaluated by others. This may result in more salience of neutral or negative feedback relative to positive feedback. Thus, although we found that behaviorally children reacted in a similar way to social evaluation as adults do, the similarities in neural findings between children and adults are more mixed. The neural signature of social rejection in terms of anterior insula and mPFC/ACCg activation was found to be present in middle childhood, but it was less pronounced than in

adults (only detectable in larger samples and meta-analysis). This was the first study to test whether children engage similar brain regions in processing social evaluation as adults. By using various approaches (whole brain analyses, three different samples, meta-analysis) we had the opportunity to investigate these regions in detail. However, there are several methodological considerations that follow from the current study.

Methodological considerations

First, whole brain analyses in this age range may need larger samples, since the use of fMRI in children is more affected by motion (O'Shaughnessy *et al.*, 2008), but also because there is substantial individual variation in the timing of brain maturation (Pfeifer and Allen, 2016). Some of our independent (one sample) ROI analyses did not show significant effects, while meta-analytically combining the results did reveal significant effects (see for similar results Scheibehenne *et al.* (2016)). This highlights the importance not only of internal replication but also of incorporating a meta-analytical approach. By applying meta-analysis in the context of one study testing a paradigm in different subsamples, we can minimize the risk that meta-analytic results in the (broader) field of neuroimaging studies are distorted due to publication bias (i.e., the bias resulting from selective publication of significant results (Franco *et al.*, 2014)).

The current study is the first neuroimaging study to use both a replication and meta-analytical approach to test a new experimental paradigm in children. Our test and replication sample consisted of same-sex twin pairs of which the first and second born twin were randomly assigned to one of the two samples. Therefore these samples are not independent, which could result in more equivalent results. However, additional meta-analyses in which we treated the test and replication samples as if they consisted of the same participants (which is too conservative), and then combined the effect size with the effect size of the pilot sample, showed similar combined effect-sizes, with somewhat larger confidence intervals due to the lower N. Moreover, for an exact replication this can be considered an advantage as it reduces the influence of third variables (for example when the replication sample is older or more intelligent), and methodologically this type of replicability is considered one of the important cornerstones of science (Van IJzendoorn, 1994; Gabrieli *et al.*, 2015). Nevertheless, this does have implications for the whole brain analyses with the test and replication samples combined. These are exploratory, and the results need to be confirmed in future larger and independent samples.

Ultimately, results of different, but comparable, social evaluation paradigms in children should be combined to unravel the neural underpinnings of social evaluation in a developmental perspective. Moreover, although the current study shows increased aggression and increased neural activation after rejection, we could not identify significant brain-behavior correlations, probably

due to our limited sample sizes. Nevertheless, these individual differences in brain activation during social evaluation in children could be informative, as we recently showed that individual differences in dorsal lateral PFC activation during social evaluation in adults was related to individual differences in behavioral aggression (Achterberg *et al.*, 2016b). Future studies should include larger developmental samples to investigate these associations, and explore why some children react with more aggression after negative social feedback than others.

Limitations

In addition to the methodological considerations, some limitation regarding the social evaluation paradigm used in this study need to be acknowledged. First, although the noise blast is often used as a measure of aggression, our cover story explicitly stated that the peers would not hear the noise blast. That is to say, the aggression measure reflects hypothetical aggression or frustration. This decision was based on previous studies using a similar design (Konijn *et al.*, 2007), but future studies may separate real aggression from hypothetical aggression to test the neural differences in these two types of aggression. Secondly, our social evaluation paradigm included a neutral condition. However, our neutral feedback was not purely neutral, but more mixed (not specifically positive and not specifically negative). Nevertheless, the neutral condition was in between positive and negative feedback, therefore making this condition a solid baseline comparison condition.

Conclusion

Using both a replication and a meta-analytical approach, we showed that the Social Network Aggression Task reveals robust and reliable behavioral results. Negative social feedback resulted in the highest levels of behavioral aggression. Moreover, meta-analyses on predefined ROIs revealed that negative social feedback resulted in more neural activation in the amygdala (compared to positive feedback) and in the anterior insula and mPFC/ACCg (compared to neutral feedback). Exploratory whole brain analyses confirmed heightened activation in the medial prefrontal cortex (mPFC) after negative relative to neutral social feedback. Future research should examine how neural responses to social feedback and subsequent aggression are related, using larger samples that allow for testing correlates of individual differences in aggression after negative social feedback. The current findings show that the Social Network Aggression Task is a reliable paradigm for the investigation of social evaluation and aggression in children, and indicate that this paradigm is feasible for use in larger and longitudinal developmental studies.

Acknowledgments

The Leiden Consortium on Individual Development is funded through the Gravitation program of the Dutch Ministry of Education, Culture, and Science and the Netherlands Organization for Scientific Research (NWO grant number 024.001.003).

Supplementary Materials

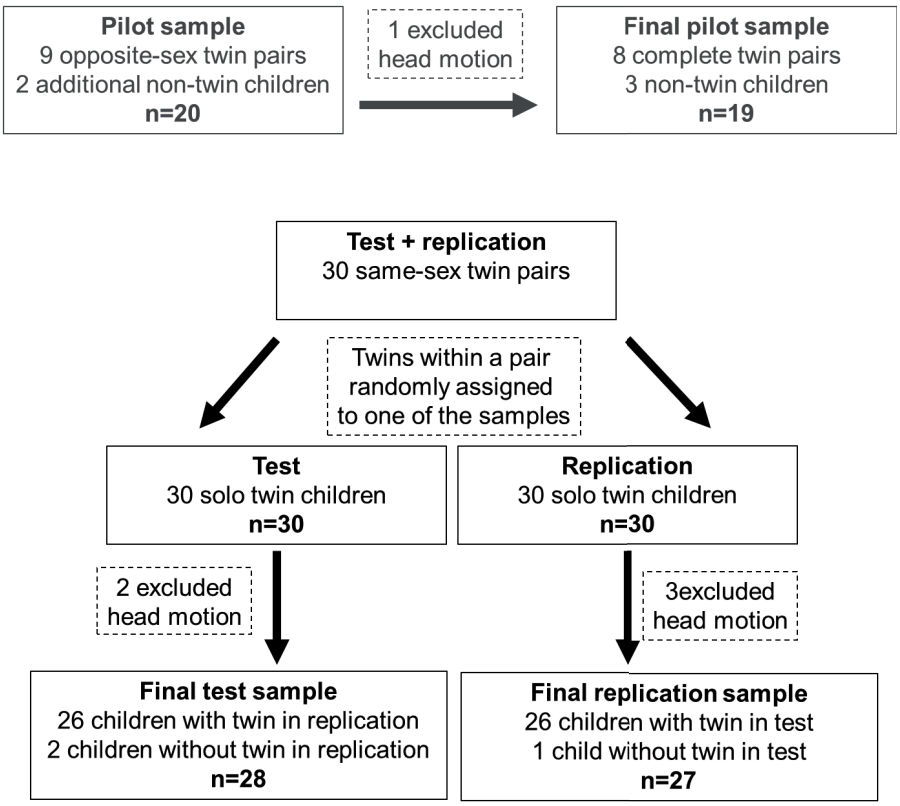


Figure S1*. Schematic overview of sample selection. Head motion exclusion was defined as >1 mm movement in >20% of the volumes.*

All feedback conditions vs. baseline

To investigate the consistency in neural activation in the general contrast of social evaluation (positive, neutral and negative feedback vs. fixation) across the three samples we conducted the analyses in two steps. First, patterns of activations found in the pilot sample were masked with anatomical masks and these ROIs were then used to extract PE values from the test sample. Secondly, we repeated this procedure with the test sample as starting point. The ROIs from the test sample were used to extract PE values from the replication sample. This was done because some regions might not show up in samples as small as our pilot sample.

Functional clusters from the general contrast of social evaluation were masked with anatomical regions. That is to say, we overlapped all functional clusters from the whole brain contrast with anatomical regions from the

Automated Anatomical Labeling (AAL) atlas (Tzourio-Mazoyer *et al.*, 2002). The overlap between functional activation and anatomical regions were then used as regions of interest. All regions from the whole brain contrast were investigated. To mask the medial orbitofrontal cortex (mOFC) we combined the medial OFC left and right. The subcallosal cortex was masked with the subcallosal mask from the Harvard/Oxford atlas (Desikan *et al.*, 2006).

One sample t-tests (one-sided) were used to test whether the activation was significantly different from 0. We specifically chose one sided t-tests (α=0.1), because replication is tested in the same direction as in the hypothesis-generating sample. Alpha level was Bonferroni corrected depending on the number of extracted ROIs (i.e., 0.1 divided by the number of ROIs).

Examination of pilot results in the test sample

The contrast 'all feedback vs. fixation' in the pilot sample resulted in activation with local maxima in the bilateral lateral occipital lobes, the bilateral fusiform cortex, the bilateral amygdala, the bilateral thalamus, the medial prefrontal cortex (PFC), and the posterior cingulate cortex (PCC), see Figure S2a and Table S1. From this whole brain contrast, we selected 8 ROIs: the right and left amygdala, the right and left fusiform cortex, the right and left thalamus, the mPFC and the PCC (Figure S2b). These ROIs were used to extract PE values from the test sample. Bonferroni corrected alpha was set at α=0.013 (0.1/8 ROIs). As Figure S2c shows, activation of the left and right amygdala, the left and right fusiform cortex, and the mPFC was significantly different from 0 in the test sample, and thus the pilot results were confirmed in the test sample (all p's<.013, see Table S2). The test sample showed no significant activation in the left and right thalamus, nor in the PCC.

Examination of test results in the replication sample

The contrast 'all feedback vs. fixation' in the test sample resulted in activation with local maxima in the bilateral occipital lobes, the bilateral fusiform cortex, the bilateral amygdala, the cerebellum, the mPFC, the bilateral inferior orbitofrontal cortex (OFC), the medial OFC and the subcallosal cortex, see Figure S2d and Table S1. We selected five ROIs concerning anatomical regions that were also found and confirmed in step 1: the left and right amygdala, the left and right fusiform cortex and the mPFC. Activation in four addition regions were observed and masked as ROI: the subcallosal cortex, the medial OFC and the left and right inferior OFC (Figure S2e). In total 9 ROIs were used to extract PE values from the replication sample, therefore Bonferonni corrected alpha was set at α=0.011 (0.1/9 ROIs). Activation in all regions was statistically significantly different from 0 in the replication sample, indicating that the test results were replicated in the replication sample (all p's<.011, see Figure S2f and Table S2). Whole brain results

from the 'all feedback vs. fixation' contrast in the replication sample are shown in Figure S3 and Table S1.

Consistency in neural activation in the general contrast

The whole brain analyses resulted in robust activity in the extended face processing network (Scherf *et al.*, 2012), including the FFA and amygdala. Interestingly, these findings were consistent across pilot, test, and replication samples, showing that the task elicits reliable responses in 7-10-year-old children. Even though most activated regions in the pilot sample could be confirmed in the test sample (i.e., bilateral amygdala, bilateral fusiform cortex, and the mPFC), not all regions were confirmed: the PCC and bilateral thalamus were not significantly activated in the test sample. The smaller pilot sample has a reduced chance of detecting a true effect, but a small sample also reduces the likelihood that a significant result reflects a true effect (Button *et al.*, 2013), which shows the need to replicate findings in small samples. This is especially important in developmental neuroimaging studies, since the use of fMRI in children remains a challenging undertaking due to both practical and methodological issues such as more biological noise and motion (Kotsoni *et al.*, 2006; O'Shaughnessy *et al.*, 2008; Thomason, 2009). We therefore repeated the procedure with the test and replication sample and showed that all activated brain regions that were found in the test sample - which was somewhat larger than the pilot sample - could be replicated in the replication sample. Taken together, these findings indicate that the SNAT elicits reliable and consistent neural activation for the general contrast all feedback > fixation.

Brain-behavior correlations

To test for brain-behavior correlations, we correlated the significant meta-analytical brain results with the subsequent behavior. Negative>positive amygdala activation and negative>positive noise blast duration were not significantly correlation in the separate samples (pilot: r=-.02, p=.921; test: r=.28, p=.152; replication: r=-.03, p=.892), nor when tested in a meta-analyses (d=0.14, 95% CI: -0.48-0.76, p=.664). Negative>neutral insula activation and negative>neutral noise blast duration were not significantly correlation in the separate samples (pilot: r=.05, p=.848; test: r=.32, p=.096; replication: r=.04, p=.856), nor when tested in a meta-analyses (d=0.27, 95% CI: -0.35-0.90, p =.394). Lastly, Negative>neutral mPFC/ACCgyrus activation and negative>neutral noise blast duration were not significantly correlation in the separate samples (pilot: r=.17, p=.485; test: r=-.10, p=.600; replication: r=.13, p=.530), nor when tested in a meta-analyses (d=0.14, 95% CI: -0.48-0.76, p =.659). Thus, no significant brain-behavior correlations were found.

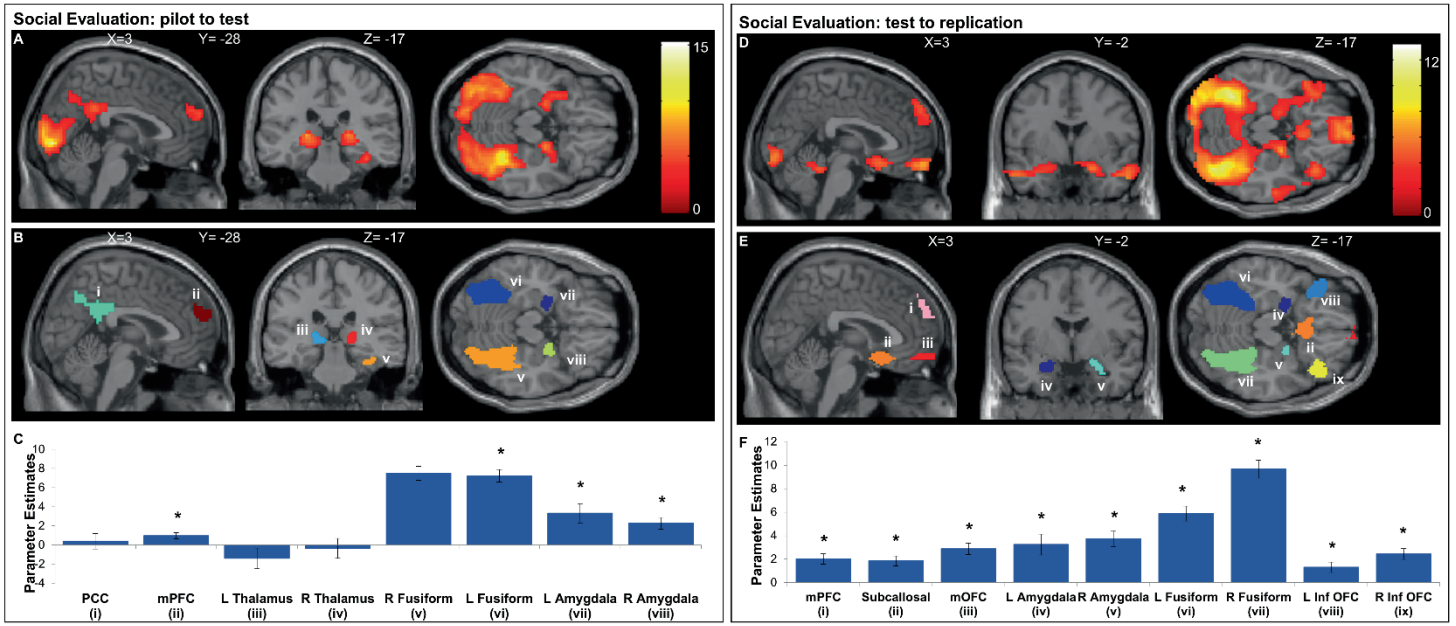


Figure S2. *a) whole brain contrast of all feedback vs. fixation in the pilot sample. b) 8 activation based ROIs chosen from the whole brain contrast: Posterior Cingulate Cortex (PCC, i), medial Prefrontal Cortex (mPFC, ii), left Thalamus (iii), right Thalamus (iv), right Fusiform Cortex (v), left Fusiform Cortex (vi), left Amygdala (vii), and right Amygdala (viii). c) Parameter estimates from the 'all feedback vs. fixation' contrast of the test sample for each of the pilot ROIs. d) whole brain contrast of all feedback vs. fixation in the test sample. e) 9 activation based ROIs chosen from the whole brain contrast: mPFC (i), Subcallosal Cortex (ii), medial orbitofrontal cortex (mOFC, iii), left Amygdala (iv), right Amygdala (v), left Fusiform Cortex (vi), right Fusiform Cortex (vii), left inferior OFC (viii), right inferior OFC (ix). f) Parameter estimates from the 'all feedback vs. fixation' contrast of the replication sample for each of the test ROIs. * indicate significant activation.*

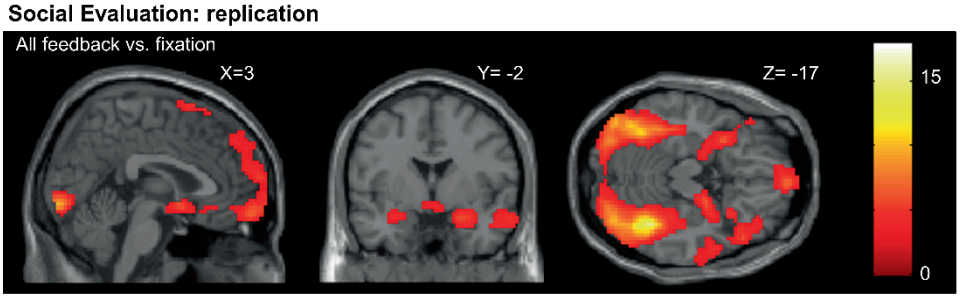


Figure S3. *Whole brain results of the replication sample for the all feedback vs. fixation contrast.*

Table S1. MNI coordinates for local maxima of the general contrasts in the three samples. The results were FDR cluster corrected (*pFDR*<.05), with a primary voxel-wise threshold of *p*<.005.

Area of Activation	*x*	*y*	*z*	Voxels	*T*
all feedback vs. fixation (pilot sample)					
Right Occipital Fusiform Gyrus	18	-79	-8	4260	15.23
Left Lateral Occipital Cortex	-21	-94	10		14.28
Left Lateral Occipital Cortex	-45	-82	-11		13.74
Left Thalamus	-21	-28	4	128	7.77
Right Thalamus	21	-28	4	90	6.99
Right Amygdala	21	-4	-17	67	6.69
Medial Prefrontal Gyrus	9	53	25	100	5.87
Medial Prefrontal Gyrus	-3	53	31		3.77
Posterior Cingulate Cortex	6	-46	31	270	5.75
Right Parietal Cortex	27	-55	40		4.93
Posterior Cingulate Cortex	-6	-37	31		3.64
Left Amygdala	-21	-4	-17	100	5.70
Left Orbitofrontal Cortex	-30	11	-20		4.80
Left Amygdala	-27	2	-20		4.70
Right Precentral Gyrus	42	-13	70	71	5.05
Right Precentral Gyrus	51	-13	64		4.90
Right Precentral Gyrus	42	-4	67		4.02
Right Middle Frontal Gyrus	30	11	28	136	4.70
Right Middle Frontal Gyrus	48	23	28		4.13
Right Inferior Frontal Gyrus	57	32	16		4.07
all feedback vs. fixation (test sample)					
Right Lateral Occipital Cortex	39	-73	-14	4757	13.14
Left Occipital Fusiform Cortex	-33	-52	-20		12.54

Table S1. (continued)

Area of Activation	*x*	*y*	*z*	Voxels	*T*
all feedback vs. fixation (test sample)					
Right Lateral Occipital Cortex	27	-97	7		11.39
medial Orbitofrontal Cortex	3	62	-14	225	6.66
medial Orbitofrontal Cortex	-9	65	-17		5.83
medial Prefrontal Cortex	-6	59	34	336	5.33
medial Prefrontal Cortex	-9	50	49		5.17
medial Prefrontal Cortex	6	65	31		4.59
all feedback vs. fixation (replica sample)					
Right Lateral Occipital Cortex	39	-82	-11	3884	17.88
Right Occipital Fusiform Cortex	39	-52	-17		15.42
Left Lateral Occipital Cortex	-15	-97	4		12.76
medial Orbitofrontal Cortex	6	62	-14	1209	7.34
medial Orbitofrontal Cortex	-3	74	-8		5.70
medial Prefrontal Cortex	6	50	43		5.49
Right Amygdala	21	-4	-17	860	6.24
Right Middle Temporal gyrus	57	8	-26		5.97
Right Orbitofrontal Cortex	51	26	-17		5.90
Left Orbitofrontal Cortex	-30	11	-17	369	6.13
Left Amygdala	-18	-7	-14		4.31
Left Orbitofrontal Cortex	-45	32	-11		4.24
Right Inferior Frontal Gyrus	48	20	31	417	6.11
Right Inferior Frontal Gyrus	57	29	16		4.14

Table S2. One Sample T-tests on the social evaluation contrast.

ROIs	*Mean*	*SD*	*T*	*p*	*d*
Pilot ROIs tested in Test sample					
Amygdala (L)	3.02	4.41	3.62	.001	0.69
Amygdala (R)	2.27	3.20	3.75	.001	0.71
Fusiform Cortex (L)	7.23	3.52	10.87	<.001	2.05
Fusiform Cortex (R)	7.50	3.87	10.26	<.001	1.94
Medial PFC	0.96	1.70	2.97	.006	0.57
Thalamus (L)	-1.40	5.72	-1.30	.205	0.25
Thalamus (R)	-0.36	5.49	-0.34	.733	0.07
Posterior Cingulate Cortex	0.38	4.27	0.47	.640	0.09
Test ROIs tested in Replication sample					
Amygdala (L)	3.24	4.63	3.63	.001	0.70
Amygdala (R)	3.72	3.56	5.44	<.001	1.05
Fusiform Cortex (L)	5.87	3.30	9.23	<.001	1.78
Fusiform Cortex (R)	9.67	3.99	12.59	<.001	2.42
medial Prefrontal Cortex	2.01	2.33	4.50	<.001	0.86
inferior Orbitofrontal Cortex (L)	1.30	2.31	2.93	.007	0.56
inferior Orbitofrontal Cortex (R)	2.43	2.41	5.23	<.001	1.01
medial Orbitofrontal Cortex	2.87	2.49	6.00	<.001	1.15
Subcallosal Cortex	1.84	2.19	4.36	<.001	0.84

CHAPTER THREE

Control your anger! The neural basis of aggression regulation in response to negative social feedback

This chapter is published as: Achterberg M., Van Duijvenvoorde A.C.K., Bakermans-Kranenburg M.J. & Crone E.A. (2016), Control your anger! The neural basis of aggression regulation in response to negative social feedback., *Social cognitive and affective neuroscience 11*(5): 712-720.

Abstract

Negative social feedback often generates aggressive feelings and behavior. Prior studies have investigated the neural basis of negative social feedback, but the underlying neural mechanisms of aggression regulation following negative social feedback remain largely undiscovered. In the current study participants viewed pictures of peers with feedback (positive, neutral, or negative) to the participant's personal profile. Next, participants responded to the peer feedback by pressing a button, thereby producing a loud noise towards the peer, as an index of aggression. Behavioral analyses showed that negative feedback led to more aggression (longer noise blasts). Conjunction neuroimaging analyses revealed that both positive and negative feedback were associated with increased activity in the medial prefrontal cortex (mPFC) and bilateral insula. In addition, more activation in the right dorsal lateral PFC (dlPFC) during negative feedback versus neutral feedback was associated with shorter noise blasts in response to negative social feedback, suggesting a potential role of dlPFC in aggression regulation, or top-down control over affective impulsive actions. This study demonstrates a role of the dlPFC in the regulation of aggressive social behavior.

Keywords: social evaluation; social rejection; social acceptance; emotion regulation; functional magnetic resonance imaging (fMRI)

Introduction

People are strongly motivated to be accepted by others and to establish a sense of belonging. Receiving negative social feedback, therefore, is a distressing experience, related to serious negative consequences such as feelings of depression and anxiety (Nolan *et al.*, 2003). For some individuals, receiving negative social feedback can result in aggression towards people who have negatively evaluated or rejected them (Twenge *et al.*, 2001; Leary *et al.*, 2006; DeWall and Bushman, 2011; Chester *et al.*, 2014; Riva *et al.*, 2015; Chester and DeWall, 2016). However, the relation between negative social feedback and subsequent aggression is not well understood. In the current study we investigated the relation between receiving negative social feedback and subsequent aggression using neuroimaging, which allowed us to 1) examine the neural correlates of negative social feedback relative to neutral or positive feedback, 2) examine aggressive responses towards the person signaling negative social feedback, and 3) examine the association between the neural correlates of negative social feedback and behavioral aggression.

Social rejection and negative social feedback have previously been studied using a variety of experimental paradigms that manipulate social contexts. For example, the negative feelings associated with social rejection have been extensively studied using Cyberball, an online ball tossing game in which three players toss balls to each other, until at some point in the game, one of the players is excluded. It is consistently found that this type of social exclusion leads to feelings of distress, negative mood, and a decreased satisfaction of the need for a meaningful existence (Williams *et al.*, 2000; Williams, 2007). Neuroimaging studies point to a role of the midline areas of the brain, specifically the dorsal and subgenual anterior cingulate cortex (ACC), as well as the anterior insula, as important brain regions responding to social exclusion (Cacioppo *et al.*, 2013; Rotge *et al.*, 2015). Other studies have used a peer feedback social evaluation paradigm to study responses to both positive and negative social feedback. In such paradigms, participants believe they are socially evaluated by same-aged peers, based on first impressions of their profile picture (Somerville *et al.*, 2006; Gunther Moor *et al.*, 2010b; Hughes and Beer, 2013). These studies showed that dorsal ACC (dACC) activation was particularly activated in response to unexpected social feedback, irrespective of whether this was positive or negative (Somerville et al., 2006), whereas ventral mPFC and ventral striatum activation was larger for positive feedback compared to negative feedback (Guyer *et al.*, 2009; Davey *et al.*, 2010; Gunther Moor *et al.*, 2010b).

More insight into the neural and behavioral correlates of social evaluation and rejection has been derived from studies testing the relation between social rejection and subsequent aggression. One study combined the Cyberball task in the scanner with a subsequent aggression index using a noise blast task outside of the scanner (Chester *et al.*, 2014). Individuals responded more aggressively

following the experience of social rejection, but intriguingly, these effects were dependent on whether the participant showed low or high executive control. Participants who scored high on executive control displayed lower aggression after social rejection, suggesting that executive control abilities may down-regulate aggression tendencies. It has been suggested that self-control relies strongly on the lateral prefrontal cortex (PFC), which is thought to exert top-down control over subcortical, affective, brain regions (such as the striatum) to suppress outputs that otherwise lead to impulsive response and actions (Casey, 2015). Transcranial magnetic stimulant (TMS) studies have indeed implicated a causal role for the lateral PFC in executing self-control when choosing long-term rewards (Figner *et al.*, 2010). Similarly, lateral PFC may have an important role in down-regulating aggression following rejection or negative social feedback. This hypothesis finds support in a study where participants had the opportunity to aggress to peers who had excluded them during Cyberball while undergoing transcranial direct current stimulation (tDCS) (Riva *et al.*, 2015). TDCS of the right ventrolateral (vl) PFC reduced participants' behavioral aggression to the excluders.

Taken together, prior studies suggested an important role of dorsal and ventral mPFC regions in processing negative and positive social feedback, but the exact contributions of these regions are not consistent across studies and may depend on the experimental paradigm. The first goal of this study was to disentangle effects of positive and negative feedback in a social evaluation paradigm (Somerville *et al.*, 2006). A novel component of this study relative to prior studies is that we included a neutral baseline condition, in which participants received neutral feedback on a subset of the trials. Based on prior research, we expected that positive social feedback would result in increased activation in the subgenual ACC (Somerville *et al.*, 2006) and the ventral striatum (Guyer *et al.*, 2009; Davey *et al.*, 2010; Gunther Moor *et al.*, 2010b). In contrast, we expected that negative social feedback would be associated with increased activity in the dACC/ dorsal medial PFC (dmPFC) and the insula. Prior studies remained elusive about whether dACC/mPFC and insula activity were associated with salient events per se (Somerville *et al.*, 2006) or social rejection specifically (Eisenberger *et al.*, 2003; Kross *et al.*, 2011). Therefore, we conducted conjunction analyses for both positive and negative feedback versus neutral baseline, as well as direct contrasts testing for differences between positive and negative social feedback.

Importantly, there may be individual differences in how participants respond to negative social feedback, which may be associated with increased neural activity in lateral PFC, as has been found in social rejection studies (Chester and DeWall, 2016). The second goal of this study was therefore to examine how individuals respond to negative social feedback, and if lateral PFC activity is related to aggression regulation following negative social feedback. Therefore, the paradigm included a second event where participants could

directly retaliate to the peer who judged them, by sending a loud noise blast (Twenge *et al.*, 2001; Chester *et al.*, 2014). Noise blast duration was measured after each trial within the fMRI task and therefore we could examine how neural activity related to individual differences in noise blast duration. On a behavioral level, we hypothesized that negative social feedback would trigger reactive aggression, i.e. longer noise blasts (Twenge *et al.*, 2001; Reijntjes *et al.*, 2011; Riva *et al.*, 2015). In addition, we hypothesized that less aggression (i.e., more aggression regulation, shorter noise blasts) would be related to increased activation in lateral PFC (Casey, 2015; Riva *et al.*, 2015) particularly during negative feedback.

Methods

Participants

Thirty participants between the ages of 18 and 27 participated in this study (15 females, *M*=22.63 years, *SD*=2.62). They were either contacted from a participant database or they responded to an advert placed online. The institutional review board of the Leiden University Medical Center (LUMC) approved the study and its procedures. Written informed consent was obtained from all participants. All participants were fluent in Dutch, right-handed, and had normal or corrected-to-normal vision. Participants were screened for MRI contra indications and had no history of neurological or psychiatric disorders. All anatomical MRI scans were reviewed and cleared by a radiologist from the radiology department of the LUMC. No anomalous findings were reported.

Participants' intelligence quotient (IQ) was estimated with the subsets 'similarities' and 'block design' of the Wechsler Intelligence Scale for Adults, third edition (WAIS-III; Wechsler (1997)). All estimated IQs were in the normal to high range (95 to 135; *M*=113.92, *SD*=9.23). IQ scores were not correlated to behavioral outcomes of the Social Network Aggression Task (noise blast duration after positive, neutral, negative feedback and noise blast difference scores, all *p*'s > .244)

Social Network Aggression Task

The Social Network Aggression Task (SNAT) was based on the social evaluation paradigm of Somerville *et al.* (2006) and Gunther Moor *et al.* (2010b). Prior to the fMRI session, participants filled in a profile page at home, which was handed in at least one week before the actual fMRI session. The profile page consisted of personal statements such as: "*My favorite sport is...*", "*This makes me happy:...*", "*My biggest wish is...*". Participants were informed that their profiles were viewed by other individuals. During the SNAT participants were presented with pictures and feedback from same-aged peers in response to the participants' personal profile. This feedback could either be positive ('*I like your profile'*, visualized by

a green thumb up); negative (*'I do not like your profile'*; red thumb down) or neutral (*'I don't know what to think of your profile'*, grey circle), see Figure 1a.

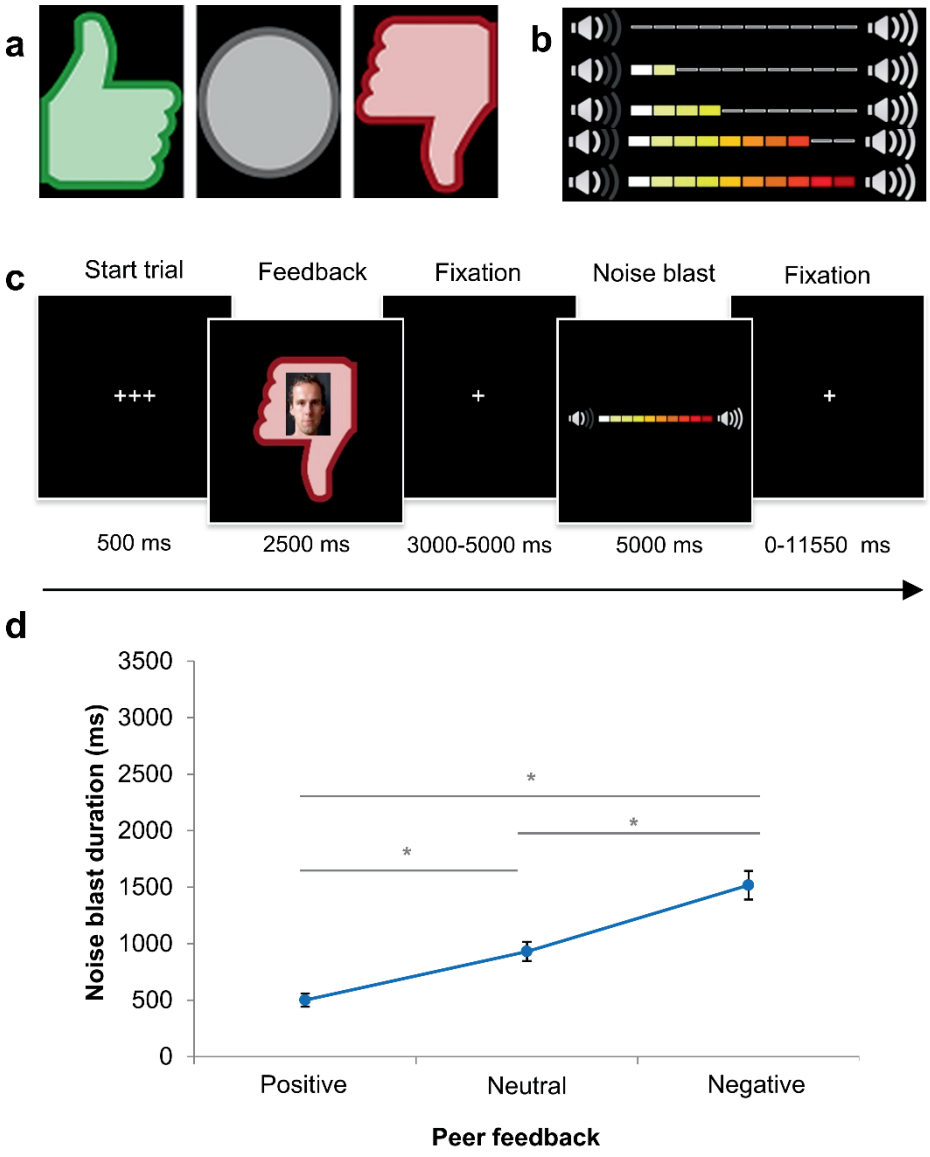


Figure 1. *Social Network Aggression Task. (a) The different feedback types: positive, neutral and negative. (b) Visual representation of intensity buildup of the volume bar. (c) Display of one trial and timing of the SNAT. (d) Noise blast duration across the different social feedback conditions. Asterisks indicate significant differences with p<.05.*

Following each peer feedback (positive, neutral, negative), participants were instructed to send a loud noise blast to this peer. The longer they would press a button the more intense the noise would be, which was visually represented by a volume bar (Figure 1b). Participants were specifically instructed that the noise was not really sent to the peer, but that they had to imagine that they could send a noise blast to the peer, with the volume intensity of the participants' choice. This was done to reduce deception, and prior studies showed that imagined play also leads to aggression (Konijn *et al.*, 2007). Unbeknownst to the participants, the profile was not judged by others, and the photos were taken from an existing data base with pictures matching participants' age range (Gunther Moor *et al.*, 2010b). Peer pictures were randomly coupled to feedback, ensuring equal gender proportions for each condition. None of the participants expressed doubts about the cover story.

Prior to the scan session, the noise blast was presented to the participants twice during a practice session: once with stepwise buildup of intensity and once at maximum intensity. Two evaluation questions were asked after hearing the maximum intensity: '*How much do you like the sound?*' and '*How much do you dislike the sound?*'. Participants rated the sound on a 7-point scale, with 1 representing *very little* and 7 representing *very much*. In order to prevent that pressing the button during the experimental task would punish the participants themselves, they only heard the intensity of the noise blast during the practice session and not during the fMRI session. To familiarize participants with the task, participants performed six practice trials.

The SNAT consists of two blocks of 30 trials (60 trials in total), with 20 trials for each social feedback condition (positive, neutral, negative), that are presented semi randomized to ensure that no condition is presented more than three times in a row. Figure 1c displays an overview of one SNAT trial. Each trial starts with a fixation screen (500 ms), followed by the social feedback (2500 ms). After another fixation screen (jittered between 3000 and 5000 ms), the noise screen with the volume bar appears, which is presented for a total of 5000 ms. As soon as the participants starts the button press, the volume bar starts to fill up with a newly colored block appearing every 350 ms. After releasing the button, or at maximum intensity (after 3500 ms), the volume bar stops increasing and stays on the screen for the remaining of the 5000 ms. Before the start of the next trial, a fixation cross was presented (jittered between 0 and 11550 ms). The optimal jitter timing and order of events were calculated with Optseq 2 (Dale, 1999).

Exit questions

Following the MRI session, three exit questions were asked: *'How much did you like reactions with a thumb up?'*, *'How much did you like reactions with a circle?'*, and *'How much did you like reactions with a thumb down?'*. Participants rated the

reactions on a 7-point scale, with 1 representing *very little* and 7 representing *very much*.

MRI data acquisition

MRI scans were acquired with a standard whole-head coil on a Philips 3.0 Tesla scanner (Philips Achieva TX). The SNAT was projected on a screen that was viewed through a mirror on the head coil. Functional scans were collected during two runs T2*-weighted echo planar images (EPI). The first two volumes were discarded to allow for equilibration of T1 saturation effect. Volumes covered the whole brain with a field of view (FOV)= 220 (ap) x 220 (rl) x 114.68 (fh) mm; repetition time (TR) of 2.2 seconds; echo time (TE) = 30 ms; sequential acquisition, 38 slices; and voxel size= 2.75 x 2.75 x 2.75 mm. Subsequently, a high-resolution 3D T1scan was obtained as anatomical reference (FOV= 224 (ap) x 177 (rl) x 168 (fh); TR=9.76 ms; TE=4.95 ms; 140 slices; voxel size 0.875 x 0.875 x 0.875 mm).

MRI data analyses

Preprocessing

MRI data were analyzed with SPM8 (Wellcome Trust Centre for Neuroimaging, London). Images were corrected for slice timing acquisition and rigid body motion. Functional scans were spatially normalized to T1 templates. Due to T1 misregistration, one participant was normalized to an EPI template. Volumes of all participants were resampled to 3x3x3 mm voxels. Data were spatially smoothed with a 6 mm full width at half maximum (FWHM) isotropic Gaussian kernel. Translational movement parameters never exceeded 1 voxel (<3 mm) in any direction for any participant or scan (movement range: 0.001-1.22 mm, M=0.055, SD=0.036).

First-level analyses

Statistical analyses were performed on individual subjects' data using a general linear model. The fMRI time series were modeled as a series of two events convolved with the hemodynamic response function (HRF). The onset of social feedback was modeled as the first event with a zero duration and with separate regressors for the positive, negative, and neutral peer feedback. The start of the noise blast was modeled for the length of the noise blast duration (i.e., length of button press) and with separate regressors for noise blast after positive, negative, and neutral feedback. Trials on which the participants failed to respond in time were marked as invalid. Note that his happened rarely, on average 3.78% of the trials were invalid. The least squares parameter estimates of height of the best-fitting canonical HRF for each condition were used in pairwise contrasts. The pairwise comparisons resulted in subject-specific contrast images.

Higher-level group analyses

Subject-specific contrast images were used for the group analyses. A full factorial ANOVA with three levels (positive, negative, and neutral feedback) was used to investigate the neural response to the social feedback event. We calculated the contrasts 'Positive versus Negative feedback', 'Positive versus Neutral feedback' and 'Negative versus Neutral feedback'. To investigate regions that were activated both after negative social feedback and after positive social feedback, we conducted a conjunction analysis to explore the main effect of social evaluation. Based on Nichols *et al.* (2005), we used the 'logical AND' strategy. The 'logical AND' strategy requires that all the comparisons in the conjunction are individually significant (Nichols *et al.*, 2005).

All results were False Discovery Rate (FDR) cluster corrected ($p_{FDR}<.05$), with a primary voxel-wise threshold of $p<.005$ (uncorrected) (Woo *et al.*, 2014). Coordinates for local maxima are reported in MNI space. To further visualize patterns of activation in the clusters identified in the whole brain regression analysis, we used the MarsBaR toolbox (Brett *et al.*, 2002) (http://marsbar.sourceforge.net).

In all behavioral repeated measures analyses, Greenhouse-Geisser (GG) corrections were applied when the assumption of sphericitiy was violated. When outliers were detected (Z-value <-3.29 or >3.29), scores were winsorized (Tabachnick and Fidell, 2013).

Results

Behavioral analyses

Noise blast manipulation check

The ratings of how much participants liked the maximum intensity noise blast indicated that overall the noise blast was not liked (M=1.47, SD=0.78; range 1-4) and much disliked (M=5.67, SD=1.30; range 1-7). These results show that the noise blast was indeed perceived as a negative event by the participants.

Social feedback manipulation check

To verify whether participants differentially liked the social feedback conditions (positive, negative, neutral), , we analyzed the exit questions with a repeated measures ANOVA. Analyses showed a significant main effect of type of feedback on feedback liking, $F(2, 58)=53.63$, $p<.001$ (GG corrected), with a large effect size ($\omega^2 = 0.53$). Pairwise comparisons (Bonferroni corrected) showed that participants liked negative feedback (M=3.13, SD=0.14) significantly less than neutral feedback (M=4.23, SD=0.14, $p<.001$) and positive feedback (M=5.23, SD=0.16, $p<.001$). Participants also liked neutral feedback significantly less than that positive feedback ($p<.001$).

Noise blast duration

A repeated measures ANOVA was performed on noise blast duration after positive, negative, and neutral feedback. Results showed a significant main effect of type of social feedback on noise blast duration, $F(2, 58)=75.57$, $p<.001$ (GG corrected), with a large effect size ($\omega^2 = 0.41$), see Figure 1d. Pairwise comparisons (Bonferroni corrected) revealed that noise blast duration after negative feedback (M=1517.08, SD=126.94) was significantly longer than noise blast duration after neutral feedback (M=930.41; SD=84.77, $p<.001$), and after positive feedback (M=483.62; SD=47.19, $p<.001$). Noise blast duration after neutral feedback was significantly longer than after positive feedback ($p<.001$).

To derive a measure indicative of individual differences in aggression we calculated the differences in noise blast duration between negative *versus* neutral feedback and positive *versus* neutral feedback. The noise blast difference for positive-neutral was significantly negatively correlated to the noise blast difference for negative-neutral (r= -.48, p=.008), indicating that shorter noise blasts after positive feedback (compared to neutral feedback) were related to longer noise blasts after negative feedback (compared to neutral feedback). Next, noise blast differences were correlated with the exit questions. The difference of negative-neutral was positively correlated to the feedback liking of positive feedback (r= .39, p=.032) and negatively correlated to the feedback liking of negative feedback (r= -.57, p=.001), indicating that longer noise blasts after negative feedback were related to a stronger preference for positive social feedback and a stronger disfavor of negative social feedback see Figures S1a and S1b. Similarly, the noise blast difference of positive-neutral was negatively correlated to the feedback liking of positive feedback (r= -.42, p=.021) and positively correlated to the feedback liking of negative feedback (r= .73, $p<.001$), indicating that a stronger preference for positive social feedback and a stronger disfavor of negative social feedback were related to shorter noise blasts after positive feedback (see Figures S1c and S1d).

fMRI whole brain analyses

Social evaluation

The first goal was to examine neural activity in the contrast positive versus negative feedback at the moment of peer feedback. The contrast Positive > Negative feedback resulted in activation with local maxima in the bilateral lateral occipital lobes, left postcentral, and activation in the right and left striatum, extending into subgenual ACC (see Figure 2a, Table S1). The contrast Negative > Positive feedback did not result in any significant clusters of activation. Next, we tested how neural activity to positive and negative social feedback related to a neutral baseline condition. The contrast Negative > Neutral feedback resulted in activity in the bilateral insula and mPFC, see Figure 2b (Table S2). The reversed contrast (Neutral > Negative feedback) did not result in any significant clusters

of activation. The contrast Positive > Neutral feedback also revealed widespread activation in the bilateral insula and mPFC. In addition, the contrast resulted in increased activity in the ventral striatum, the subgenual ACC, as well as regions such as the occipital lobe, as shown in Figure 2c (Table S2). The reversed contrast (Neutral > Positive feedback) resulted in activity in the right insula and right postcentral gyrus (Table S2).

Social evaluation conjunction

The analyses above suggested partially overlapping activation patterns for positive and negative social feedback, relative to a neutral baseline. To formally investigate the regions that were activated both after negative social feedback and after positive social feedback, we conducted a conjunction analyses to explore a main effect of social evaluation. Common activation across both positive and negative social feedback were observed in the insula and the mPFC, as well as the bilateral occipital lobes, including left Fusiform Face Area (FFA), see Figure 2d (Table S3).

Brain-Behavior associations

Noise blast duration

To test the association between brain activity and behavior in response to negative social feedback, we conducted a whole brain regression analysis at the moment of receiving negative social feedback (relative to neutral feedback; Negative > Neutral), with the difference in noise blast duration after negative and neutral feedback as a regressor. This way, we tested how initial neural responses to feedback were related to subsequent aggression. The analyses revealed that increased activation in the right dorsal lateral PFC (dlPFC) was associated with smaller increases in noise blast duration after negative social feedback compared to neutral feedback, see Figure 3. A similar relation was observed for the left amygdala, left hippocampus, and bilateral superior parietal cortex (Table S4). The reversed contrast (positive relation between Negative> Neutral feedback and noise blast length difference) did not result in any significant activation.

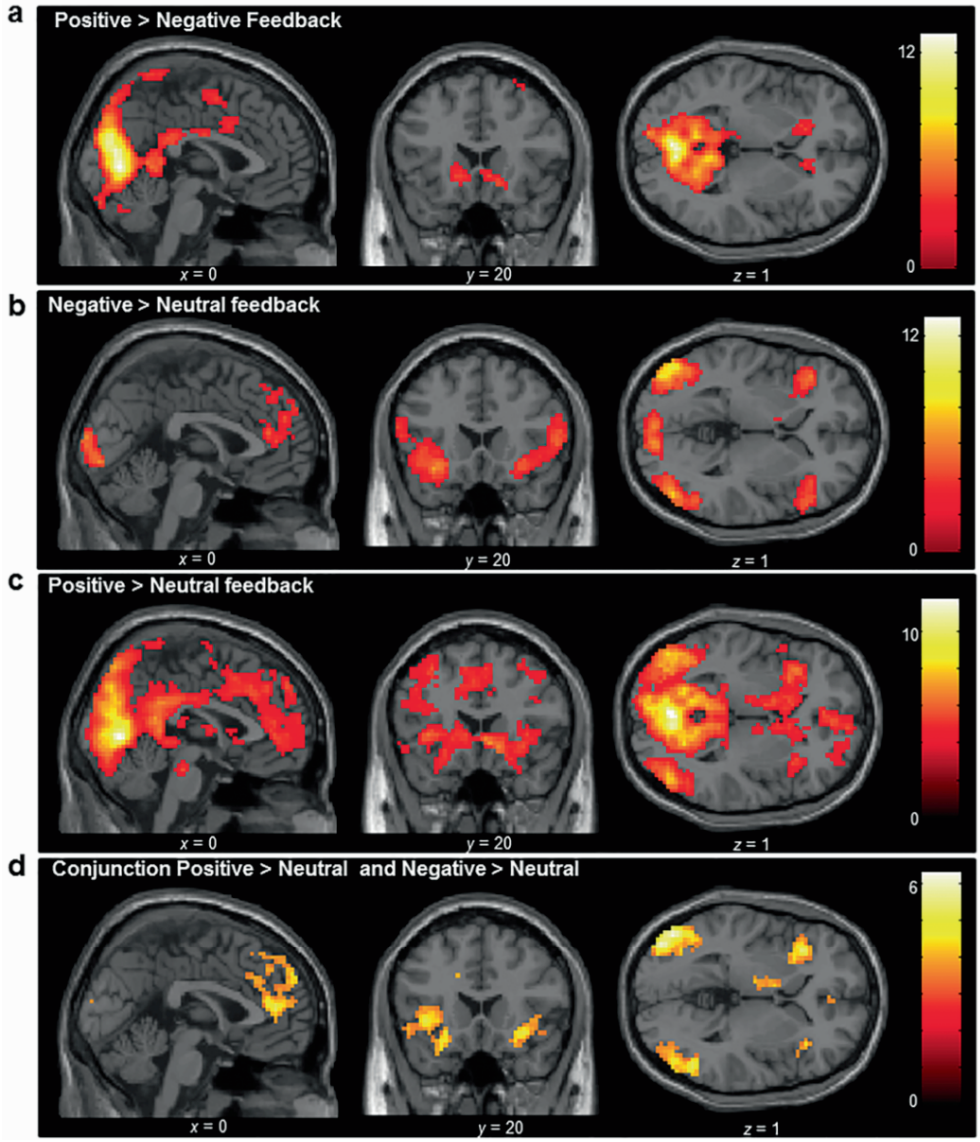


Figure. 2. *Whole brain full factorial ANOVA conducted at group level for the contrasts (a) Positive>Negative feedback, (b) Negative>Neutral feedback, (c) Positive>Neutral feedback and (d) the conjunction of the Positive>Neutral and Negative>Neutral feedback contrasts. Results were FDR cluster corrected (PFDR<0.05), with a primary voxel-wise threshold of P<0.005 (uncorrected).*

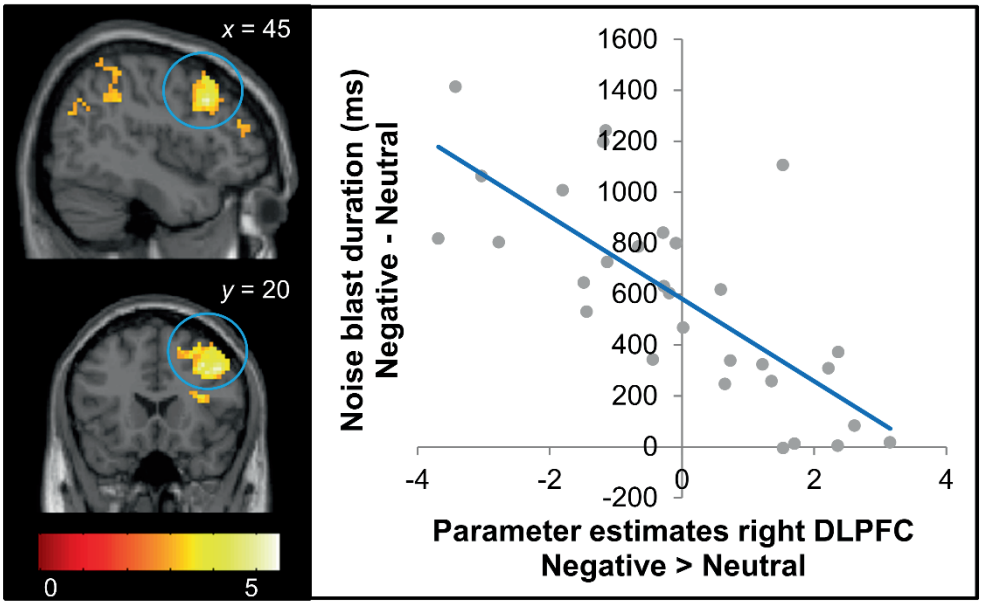


Figure 3. *Brain regions in the contrast Negative>Neutral feedback that were significantly negatively correlated with the difference in noise blast duration after negative vs neutral feedback trials. Results were FDR cluster corrected (PFDR<0.05), with a primary voxel-wise threshold of P<0.005 (uncorrected). The right panel shows the negative relationship between difference in noise blast duration and right dlPFC (for visual illustration only, no statistical tests were carried out on the region of interest).*

Discussion

This study investigated the relation between negative social feedback and subsequent aggression, using neuroimaging. The goals of this study were threefold: 1) to disentangle neural signals of positive and negative social feedback, 2) to examine aggressive responses towards the person signaling negative social feedback, and 3) to test whether lateral PFC activity is related to aggression regulation after experiencing negative social feedback. To these ends, we developed a new social peer evaluation paradigm that included neutral feedback (to be able to compare positive and negative feedback to a neutral baseline) and the possibility to retaliate to the peer that gave the feedback (to be able to study aggression related to social feedback). In line with prior behavioral studies we found that negative social feedback was related to applying a longer noise blast towards the peer (Chester *et al.*, 2014). At the neural level, conjunction analyses showed that both negative and positive social feedback resulted in increased activity in the mPFC and the bilateral insula. Comparing the

conjunction analyses with the separate contrasts of negative and positive versus neutral feedback showed that positive feedback resulted in increased activity in the striatum and the ventral mPFC, whereas negative feedback activation merely overlapped with dorsal mPFC and insula activation observed following both positive and negative feedback. Finally, we found that increased lateral PFC activity after negative social feedback was associated with relative shorter noise blast durations after negative feedback, indicative of more aggression regulation.

Results of prior studies left undecided whether there is a unique neural coding for negative social feedback compared to positive social feedback. In this study we found that, consistent with prior studies (Guyer *et al.*, 2009; Davey *et al.*, 2010; Gunther Moor *et al.*, 2010b) there was increased activity in the ventral mPFC and the striatum after positive feedback. Numerous studies have shown that the striatum is involved in reward processing (for a review, see Sescousse *et al.* (2013)) and this fits well with theories suggesting that positive evaluations and social acceptance activates brain regions overlapping with those that are activated by the primary feelings of reward (Lieberman and Eisenberger, 2009). Notably, there was no neural activation that was specific for negative social feedback. In Cyberball paradigms, a number of studies observed specific heightened activity in insula and ACC in response to social rejection, which was interpreted as the feeling of social pain (Eisenberger and Lieberman, 2004; Lieberman and Eisenberger, 2009). There are several differences in the experimental paradigms, however, that may explain the divergent results. That is to say, in Cyberball paradigms social rejection is unexpected (for example, exclusion after a period of inclusion) and is therefore likely to violate social expectations. In contrast, in social evaluation paradigms such as used in the current study, equal proportions of negative, positive, and neutral feedback are presented, which may result in more equal saliency of negative and positive feedback. The current findings, which show enhanced insula and mPFC activity following both positive and negative feedback (relative to neutral feedback), suggest that the insula and mPFC in social evaluation paradigms might work as a salience network, and signal events that are socially relevant (Guroglu *et al.*, 2010; van den Bos *et al.*, 2011). Resting-state fMRI studies confirm that these regions are often active in concert, and have referred to this network as a salience network (Damoiseaux *et al.*, 2006; Jolles *et al.*, 2011; van Duijvenvoorde *et al.*, 2016a). Future research may disentangle the role of expectation violation in more detail by asking participants to make predictions about whether they expect to be liked (Somerville et al., 2006; Gunther Moor et al. 2010), in combination with positive, negative, and neutral feedback.

An additional goal of this study was to examine the association between brain activation and behavioral responses to negative social feedback. A vast line of research has already shown that social rejection can result in retaliation (Twenge *et al.*, 2001; Leary *et al.*, 2006; DeWall and Bushman, 2011; Chester *et al.*, 2014; Riva *et al.*, 2015). Our study shows that receiving negative social

feedback is also followed by more aggressive behavior (i.e., by a longer noise blast towards the peer). In addition, we show that more activity in the right dlPFC is related to *less* aggression after negative social feedback (compared to neutral feedback), indicating that the lateral PFC is an important neural regulator of social aggression. Several studies on structural brain development have shown that the quality of brain connectivity between the PFC and the striatum is related to impulse control (Peper *et al.*, 2013; van den Bos *et al.*, 2014). That is to say, a large study on structural brain connectivity in typically developing individuals (258 participants, aged 8-25) revealed that less white matter integrity between subcortical and prefrontal brain regions was associated with more trait aggression (Peper *et al.*, 2015). Moreover, Chester and DeWall (2016) recently demonstrated that more functional connectivity between the nucleus accumbens and the lateral PFC during decisions about aggressive acts was related to less behavioral aggression. This study is the first study to investigate aggressive responses after positive, neutral, and negative feedback, and shows a role of the dlPFC in individual differences in the regulation of aggressive behavior.

Some limitations regarding this study need to be acknowledged. First, although the noise blast is often used as a measure of aggression (e.g., Bushman (2002); Chester *et al.* (2014); Riva *et al.* (2015)), our cover story stated that the peers would not hear the noise blast. That is to say, the aggression measure may reflect frustration and anger, and hypothetical aggression. Future research should further test the ecological validity of the noise blast as a measure of aggression by including additional measures of aggression or information on participants' histories of aggressive behavior. Secondly, our paradigm did not include an 'opt out' option, that is, we told participants to always push the noise blast button, even after positive feedback. This was done to keep task demands as similar as possible between the conditions. We explained that the noise would be very short and at very low intensity if the button was released as quickly as possible. However, participants may have wanted to refrain from any noise blast after positive feedback. Future research could take this into account by implementing options to respond either positive, neutral, or negative towards the peer, as can for example be implemented by using symbols (Jarcho *et al.*, 2013).

Conclusion

In conclusion, we found evidence that the insula and mPFC generally respond to socially salient feedback, with no significant differentiation between negative and positive feedback. Positive social feedback received less attention in prior research and it has often been used as a baseline, but our findings show activation in the ventral mPFC and the striatum that is stronger for positive feedback. Additionally, the lateral PFC emerged as an important modulator for individual differences in aggression regulation. This may imply that individuals who show strong activation in the lateral PFC after negative social feedback may be better able to regulate behavioral impulses, and speculatively, impulsive responses in general (Casey *et al.*, 2011). This hypothesis that should be addressed in longitudinal research, including more general measures of impulsivity. An interesting direction for future research is to examine the neural mechanisms underlying social evaluation and aggression regulation processes in populations that are known for difficulties with response control and affect regulation, such as ADHD (Evans *et al.*, 2015), externalizing problems (Prinstein and La Greca, 2004), and depression (Nolan *et al.*, 2003; Silk *et al.*, 2014).

Acknowledgments

The Consortium on Individual Development is funded through the Gravitation program of the Dutch Ministry of Education, Culture, and Science and the Netherlands Organization for Scientific Research (NWO grant number 024.001.003). MJBK was funded by the Netherlands Organization for Scientific Research (VICI) and the European Research Council (AdG 669249).

Supplementary materials

Table S1. MNI coordinates for local maxima activated for the contrasts Positive > Negative feedback. The results were FDR cluster corrected (*p*FDR<.05), with a primary voxel-wise threshold of *p*<.005 (uncorrected).

Area of Activation	*x*	*y*	*z*	Voxels	*T*
Positive > Negative feedback					
Lingual Gyrus	0	-73	4	5491	12.99
R Intracalcarine Cortex	3	-76	13		12.91
Cuneal Cortex	0	-79	22		11.17
L Supramarginal Gyrus	-39	-37	40	951	6.61
L Supramarginal Gyrus	-48	-34	43		5.53
L Postcentral Gyrus	-54	-28	46		5.19
L Caudate	-12	23	-5	76	4.72
L Caudate	-21	29	-2		4.17
L Supplementary Motor Cortex	-12	2	52	206	4.43
L Supplementary Motor Cortex	-9	-10	55		3.95
R Supplementary Motor Cortex	3	-1	55		3.89
R Orbito Frontal Cortex	15	23	-8	90	4.34
R Orbito Frontal Cortex	18	17	-14		4.04
R Orbito Frontal Cortex	27	26	-8		2.84
R Superior Frontal Gyrus	18	11	46	102	4.30
R Middle Frontal Gyrus	30	8	52		4.27
R Middle Frontal Gyrus	33	14	64		3.48
L Precentral Gyrus	-60	5	28	82	4.08
L Precentral Gyrus	-54	-1	37		3.79

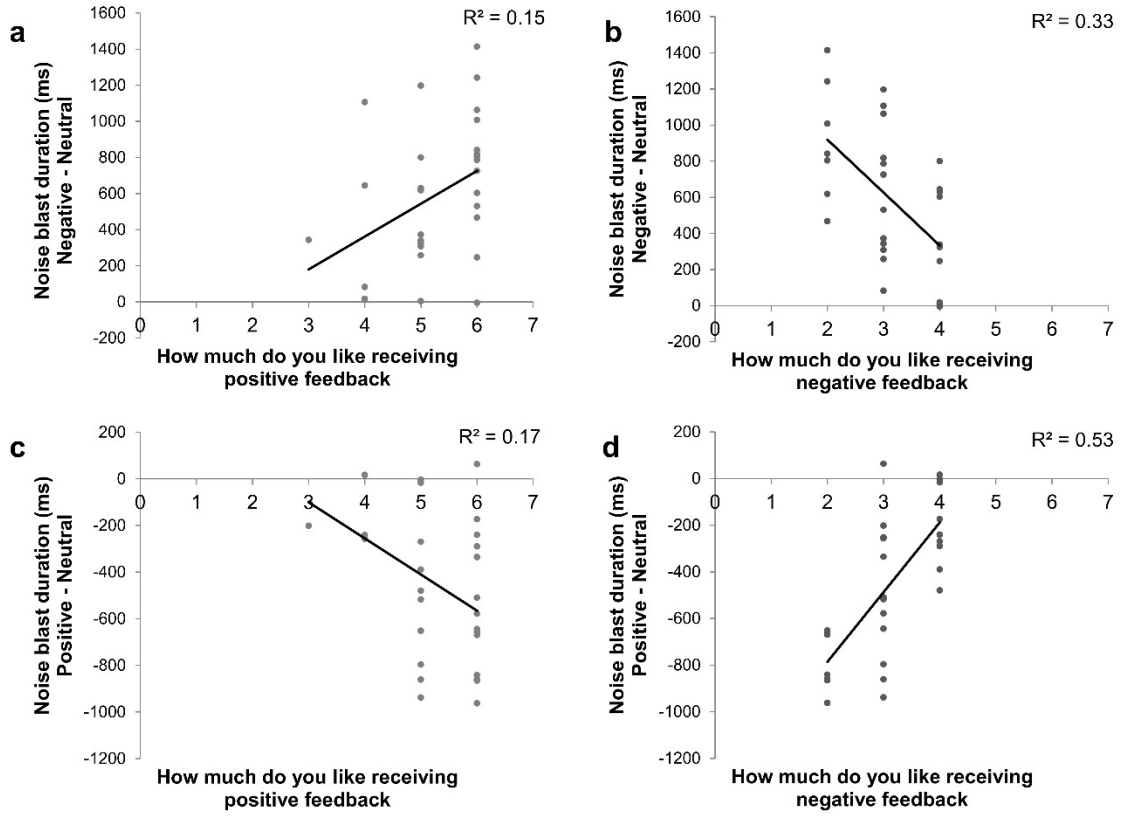


Figure S1 *Relation between noise blast duration difference scores and sensitivity to social evaluation. The y-axis displays the noise blast duration difference between different feedback types as measured by the exit questions. The x-axis displays the liking of the different feedback types. Participants sensitive to social feedback (i.e., liked receiving positive feedback and dislike receiving negative feedback) used a larger noise blast after negative feedback (a and b) and a shorter noise blast after positive feedback (c and d).*

Table S2. MNI coordinates for local maxima activated for the contrasts Negative > Neutral feedback, Positive > Neutral feedback and Neutral > Positive feedback. Results were FDR cluster corrected (p_{FDR}<.05), with a primary voxel-wise threshold of p<.005 (uncorrected).

Area of Activation	*x*	*y*	*z*	Voxels	*T*
Negative> Neutral feedback					
L Lateral Occipital Cortex	-48	-76	-2	3122	12.89
L Occipital Pole	-15	-97	22		8.82
L Occipital Pole	-9	-94	28		8.71
L Orbital Frontal Cortex	-33	20	-14	500	6.48
L Frontal Operculum Cortex	-36	29	4		5.51
L Insular Cortex	-33	23	-2		5.02
R Inferior Frontal Gyrus	57	26	7	346	6.12
R Orbital Frontal Cortex	45	29	-2		4.98
R Insular Cortex	36	17	-11		4.94
L Frontal Pole	-12	41	49	379	4.89
R Anterior Cingulate Cortex	6	35	16		4.65
L Frontal Pole	-12	50	46		4.56
Positive > Neutral feedback					
L Lingual Gyrus	-3	-76	1	14183	14.39
R Lingual Gyrus	6	-73	1		12.87
R Lingual Gyrus	18	-73	-8		11.25
R Precentral Gyrus	45	-1	49	62	4.71
R Middle Frontal Gyrus	33	8	43		3.14

Table S2. (continued)

Area of Activation	*x*	*y*	*z*	Voxels	*T*
Positive> Neutral feedback					
R Middle Frontal Gyrus	30	23	52	107	4.07
R Superior Frontal Gyrus	21	35	49		4.03
R Middle Frontal Gyrus	39	23	46		3.65
R Middle Frontal Gyrus	45	26	25	79	4.03
R Precentral Gyrus	36	5	31		3.47
R Middle Frontal Gyrus	39	32	31		3.35
L Superior Frontal Gyrus	-12	-4	67	110	3.98
L Superior Frontal Gyrus	-12	5	73		3.88
L Superior Frontal Gyrus	-18	-7	73		3.81
Neutral > Positive feedback					
R Insular Cortex	36	-22	4	289	5.72
R Insular Cortex	30	-22	16		4.88
R Superior Temporal Gyrus	63	-16	4		4.75
R Postcentral Gyrus	33	-25	58	236	5.39
R Precentral Gyrus	33	-25	67		5.11
R Precentral Gyrus	33	-22	49		4.61

Table S3. MNI coordinates for local maxima activated for the conjunction of Positive > Neutral and Negative > Neutral. Results were FDR cluster corrected (p_{FDR}<.05), with a primary voxel-wise threshold of p<.005 (uncorrected).

Area of Activation	*x*	*y*	*z*	Voxels	*T*
Conjunction of Positive > Neutral & Negative > Neutral					
L Lateral Occipital Cortex	-48	-76	-2	965	6.23
L Lateral Occipital Cortex	-48	-79	7		5.99
L Lateral Occipital Cortex	-51	-67	7		5.85
L Insular Cortex	-36	23	-2	320	5.06
L Insular Cortex	-30	14	-14		4.46
L Insular Cortex	-30	17	1		3.81
R Lateral Occipital Cortex	51	-61	-2	518	4.99
R Lateral Occipital Cortex	51	-79	7		4.62
R Lateral Occipital Cortex	42	-79	7		4.41
Cingulate Gyrus	0	44	10	367	4.79
Anterior Cingulate Gyrus	0	38	16		4.35
R Frontal Pole	3	56	13		3.95
R Insular Cortex	33	20	-11	94	4.58
R Orbito Frontal Cortex	36	26	1		3.81

Table S4. MNI coordinates for local maxima activated for the whole brain regression analyses. The contrast Negative > Neutral feedback with Negative - Neutral noise blast duration difference as negative regressor. Results were FDR cluster corrected (p_{FDR}<.05), with a primary voxel-wise threshold of p<.005 (uncorrected). dlPFC = dorsolateral prefrontal cortex.

Area of Activation	*x*	*y*	*z*	Voxels	*T*
Negative > Neutral feedback, Noise blast duration difference score as negative regressor					
L Amygdala	-21	-7	-17	173	5.57
L Amygdala	-15	-10	-11		4.21
L Hippocampus	-36	-13	-17		4.01
R Middle Frontal Gyrus (dlPFC)	48	17	37	1144	5.17
R Middle Frontal Gyrus (dlPFC)	36	20	40		5.01
R Middle Frontal Gyrus (dlPFC)	39	14	34		4.57
L Superior Parietal Lobule	-24	-46	37	315	4.95
L Superior Parietal Lobule	-33	-43	52		4.87
L Supramarginal Gyrus	-39	-46	43		4.53
Thalamus	0	-7	16	105	4.62
L Thalamus	-15	-7	10		4.04
L Caudate	-12	-4	19		3.97
R Superior Parietal Lobule	30	-52	40	697	4.61
R Postcentral Gyrus	30	-31	37		4.29
R Lateral Occipital Cortex	15	-70	67		4.26

CHAPTER FOUR

Heritability of aggression following social evaluation in middle childhood: An fMRI study

This chapter is published as: Achterberg M., Van Duijvenvoorde A.C.K., Van der Meulen M., Bakermans M.J. & Crone E.A.M. (2018), Heritability of aggression following social evaluation in middle childhood: An fMRI study, *Human Brain Mapping 39*(7): 2828-2841.

Abstract

Middle childhood marks an important phase for developing and maintaining social relations. At the same time this phase is marked by a gap in our knowledge of the genetic and environmental influences on brain responses to social feedback and their relation to behavioral aggression. In a large developmental twin sample (509 7-9-year-olds) the heritability and neural underpinnings of behavioral aggression following social evaluation were investigated, using the Social Network Aggression Task (SNAT). Participants viewed pictures of peers that gave positive, neutral or negative feedback to the participant's profile. Next, participants could blast a loud noise towards the peer as an index of aggression. Genetic modeling revealed that aggression following negative feedback was influenced by both genetics and environmental (shared as well as unique environment). On a neural level (n=385), the anterior insula and anterior cingulate cortex gyrus responded to both positive and negative feedback, suggesting they signal for social salience cues. The medial prefrontal cortex and inferior frontal gyrus were specifically activated during negative feedback, whereas positive feedback resulted in increased activation in caudate, supplementary motor cortex (SMA) and dorsolateral prefrontal cortex (DLPFC). Decreased SMA and DLPFC activation during negative feedback was associated with more aggressive behavior after negative feedback. Moreover, genetic modeling showed that 13-14% of the variance in dorsolateral PFC activity was explained by genetics. Our results suggest that the processing of social feedback is partly explained by genetic factors, whereas shared environmental influences play a role in behavioral aggression following feedback.

Keywords: Behavioral genetics; Dorsolateral prefrontal cortex; Peer feedback; Twin study

Introduction

Dealing with social evaluations and regulating emotions in the case of negative social feedback are important prerequisites for developing social relations. Several prior studies have shown that negative social feedback can lead to aggressive behavior (Chester *et al.*, 2014; Achterberg *et al.*, 2016b; Achterberg *et al.*, 2017). This type of retaliation may be associated with emotional responses to negative feedback and a lack of impulse control. The capacity to regulate impulsive behavior increases from childhood to adulthood, which has been linked to the increased regulatory control of the prefrontal cortex (PFC) (Somerville *et al.*, 2010; Casey, 2015). Indeed, prior studies in adults showed that stronger brain connectivity between nucleus accumbens and the lateral PFC was related to lower retaliatory aggression (Chester and DeWall, 2016). Moreover, increased dorsolateral PFC (DLPFC) activity after negative social feedback has been associated to less subsequent aggression (Riva *et al.*, 2015; Achterberg *et al.*, 2016b). Therefore, the prefrontal cortex may be important for regulation of neural responses to social emotions and may signal which children are better able to regulate emotions than others. Middle childhood, ranging from approximately 7/8 years until the start of puberty, marks an important phase for regulating (social) emotions and developing social relations. Previous studies have mainly focused on the developmental trajectories of social rejection and acceptance (Guyer *et al.*, 2008; Gunther Moor *et al.*, 2010b; Silk *et al.*, 2014; Guyer *et al.*, 2016). At the same time there is a gap in our understanding of the genetic and environmental influences of brain responses to social feedback and regulatory responses. In this study, we therefore investigated the neural underpinnings and heritability of social feedback processing and subsequent aggression in middle childhood.

The way children respond to social feedback and show aggression in response to negative feedback has only recently been examined using experimental designs. Studies including children, adolescents and adults have used social feedback tasks in chat room settings to unravel neural responses to social feedback, namely social acceptance and rejection (Guyer *et al.*, 2016). These studies point to the anterior cingulate cortex gyrus (ACCg), the medial prefrontal cortex (mPFC), and the anterior insula as important brain regions related to social evaluation and social motivation (Cacioppo *et al.*, 2013; Rotge *et al.*, 2015; Apps *et al.*, 2016). The dorsal ACC / ACCg was found to be activated in response to unexpected social feedback, irrespective of whether it was positive or negative (Somerville *et al.*, 2006). Recently, we developed a social network aggression task (SNAT) to study neural responses to social feedback, both in adults and 7-10-year-old children (Achterberg *et al.*, 2016b; Achterberg *et al.*, 2017). Consistent with prior studies, the ACCg and the anterior insula were active during both positive and negative feedback in adults, indicating that these regions signal social salient cues (Achterberg *et al.*, 2016b). These effects were

also present in middle childhood, but less pronounced (Achterberg *et al.*, 2017). However, prior studies in children used relatively small samples, which might have been underpowered, specifically since neuroimaging data in developmental samples are more prone to data loss and artifacts due to movement (O'Shaughnessy *et al.*, 2008). The current study therefore set out to include over 500 participants, thereby asserting sufficient sample size and statistical power, even after data loss due to excessive motion (Euser *et al.*, 2016).

Prior studies in adults showed that the DLPFC was negatively related to aggression following social evaluation, suggesting that this region is important for regulating aggression (Achterberg *et al.* (2016b), see also Riva *et al.* (2015)). Since the PFC gradually develops until early adulthood (Lenroot and Giedd, 2006; van Duijvenvoorde *et al.*, 2016a), there is ample opportunity for environmental influences. An important question therefore concerns to what extent behavioral and neural responses to social feedback, and subsequent aggression, are influenced by genetic and/or shared environmental factors. Twin models have been particularly important in unraveling to what extent genetic and environmental factors account for the variance in aggression. These studies have shown that trait aggression has both genetic and environmental components (Porsch *et al.*, 2016). Heritability estimates for behavioral aggression are high for both children and adults, explaining up to 48% of the variance (for meta-analyses, see Rhee and Waldman (2002); Ferguson (2010); Tuvblad and Baker (2011)). We aimed to explore whether neural reactions to social feedback that could elicit aggression show similar heritability estimates. Studies of the genetics of functional neuroimaging are currently limited to studies using resting state fMRI (Richmond *et al.*, 2016) or cognitive working memory tasks (Jansen *et al.*, 2015). These studies mostly point to (moderate) genetic influences, with few studies showing significant shared environmental components. It should be noted that these findings are largely based on adult twin studies, whereas previous research showed that heritability estimates of brain measures are stronger in adulthood than in childhood (Lenroot *et al.*, 2009; Lenroot and Giedd, 2011; van den Heuvel *et al.*, 2013). In this study we therefore used a large developmental twin sample (N=509 7-9-year-olds), to investigate i) the heritability of behavioral aggression following social evaluation; ii) the neural underpinnings of social evaluation and their relation to behavioral aggression; and iii) the heritability of these neural underpinnings.

We hypothesized that negative social feedback would result in behavioral aggression (Chester *et al.*, 2014; Achterberg *et al.*, 2016b; Achterberg *et al.*, 2017). Prior studies have shown that trait aggression has a relatively strong genetic component (Porsch *et al.*, 2016), however the influences of genetics and environment on state aggression such as measured with the SNAT are not yet known. On a neural level, we predicted to find a network of regions that process social feedback irrespective of valence, as prior research showed in adults (Achterberg *et al.*, 2016b), including the ACCg and the (anterior) insula. In

addition, we will investigate possible brain-behavior relations between activation of these regions and the aggression measure. Based on prior studies (Riva *et al.*, 2015; Achterberg *et al.*, 2016b), we predicted that the lateral prefrontal cortex would be most strongly correlated to aggression regulation. Since the literature on the heritability of task-based fMRI is limited, and the current study is the first to study such heritability in middle childhood, no a priori hypotheses were formed for the exploratory analyses on heritability of neural activation.

Methods

Participants

Participants in this study took part in the longitudinal twin study of the Leiden Consortium on Individual Development (L-CID). The Dutch Central Committee Human Research (CCMO) approved the study and its procedures. Families with a twin born between 2006 – 2009, living within two hours travel time from Leiden, were recruited through municipal registries and received an invitation to participate by post. Parents could show their interest in participation using a reply card. 512 children (256 families) between the ages 7 and 9 were included in the L-CID study. Written informed consent was obtained from both parents. All twin-pairs had a shared home environment, were fluent in Dutch, and had normal or corrected-to-normal vision. The majority of the sample was Caucasian (91%) and right-handed (87%). Since the sample represents a population sample, we did not exclude children with a psychiatric disorder. Ten participants (2%) were diagnosed with an Axis-I disorder: eight with attention deficit hyperactivity disorder (ADHD); one with generalized anxiety disorder (GAD), and one with pervasive developmental disorder- not otherwise specific (PDD-NOS). Three participants did not have data from the SNAT due to technical problems. Therefore, our final behavioral sample consisted of 509 participants with a mean age of 7.95 ± 0.67 (age range: 7.02-9.68, 49% boys, see Table 1), with 253 complete twin pairs (55% MZ; based on DNA, see section 2.5). Data from 30 twin pairs were previously reported (Achterberg et al., 2017).

Twenty-seven participants did not perform the SNAT in the MRI scanner: 13 due to anxiety, 6 due to MRI contra-indications, 4 participants did not have parental consent for MRI participation, and 4 participants could not be scanned due to technical system failure. For all participants who underwent the MRI scan, anatomical MRI scans were reviewed and cleared by a radiologist from the radiology department of the Leiden University Medical Center (LUMC). Four anomalous findings were reported. To prevent registration errors due to anomalous brain anatomy, these participants were excluded. An additional 89 participants were excluded due to excessive head motion, which was defined as >3 mm motion (1 voxel) in any direction (x, y, z) in more than 2 blocks of the SNAT task (3 blocks in total). Finally, four participants were excluded due to

preprocessing errors. Our final MRI sample consisted of 385 participants with a mean age of 7.99 ± 0.68 (age range: 7.02-9.68, 47% boys, see Table 1), with 158 complete twin pairs (55% MZ; based on DNA, see section 2.5). Participants' intelligence (IQ) was estimated with the subsets 'similarities' and 'block design' of the Wechsler Intelligence Scale for Children, third edition (WISC-III; Wechsler, 1997). Estimated IQs were in the normal range (72.50 - 137.50), with an average IQ of 104 (see Table 1). There were no significant differences in IQ between children in the final sample (n=385) and those who could not be included in the MRI analyses (n=124) ($t(507)=1.36$, $p=.175$), nor were there significant gender differences ($\chi(1, N=512)=2.80$, $p=.092$). Children that could not be included in the MRI analyses were, however, significantly younger ($M=7.80$, $SD=0.64$) than children in the final sample ($M=7.99$, $SD=0.67$, $t(507)=2.72$, $p=.007$), but this effect was small ($d=0.29$).

Table 1. Demographic characteristics.

	Behavioral sample	**MRI sample**
N	509	385
Boys	49%	47%
Left handed	13.0%	12.0%
Caucasian	91.0%	93.0%
AXIS-I disorder	10 (2%)[1]	8 (2%)[2]
Age (SD)	7.94 (.67)	7.99 (.68)
Range	7.02 - 9.68	7.02 - 9.68
Mean IQ (SD)	103.62 (11.77)	104.03 (11.84)
IQ range	72.50 - 137.50	72.50 - 137.50
Complete twin pairs	253	158
Monozygotic	138 (55%)	87 (55%)
Caucasian	230 (91%)	150 (95)%

[1] 8 ADHD; 1 PDD-NOS; 1 Generalized Anxiety Disorder

[2] 6 ADHD; 1 PDD-NOS; 1 Generalized Anxiety Disorder

Social Network Aggression Task

Experimental design

The Social Network Aggression Task (SNAT) as described in Achterberg et al. (2016b; 2017) was used to measure (imagined) aggression after social evaluation. Prior to the fMRI session, the children filled in a personal profile at home, which was handed in at least one week before the actual fMRI session. The profile page

consisted of questions such as: 'What is your favorite movie?', 'What is your favorite sport?', and 'What is your biggest wish?'. Children were informed that their profiles were reviewed by other, unfamiliar, children. During the SNAT the children were presented with pictures and feedback from same-aged peers in response to their personal profile. Every trial consisted of feedback from a new unfamiliar child. This feedback could either be positive ('I like your profile', visualized by a green thumb up); negative ('I do not like your profile', red thumb down) or neutral ('I don't know what to think of your profile', grey circle). Following each peer feedback, the children were instructed to imagine that they could send a loud noise blast to this peer. We specifically instructed the children to imagine this to reduce deception, because it has been shown that imagined play also leads to aggression (Konijn et al., 2007). The longer they pressed the button the more intense the noise would be, which was visually represented by a volume bar (Figure 1). To keep task demands as similar as possible between the conditions, participants were instructed to always press the button, but they could choose whether they wanted a short noise at low intensity or a long noise at high intensity. Unbeknownst to the participants, others did not judge the profile, and the photos were created by morphing two children of an existing data base (matching the age range) into a new, non-existing child. Peer pictures were randomly coupled to feedback, ensuring equal gender proportions for each type of feedback.

Participants were familiarized with the MRI scanner during a practice session in a mock scanner. Then participants received instructions on how to perform the SNAT and the children were exposed to the noise blast twice during a practice session: once with stepwise build-up of intensity and once at maximum intensity. Participants did not hear the noise during the fMRI session, to prevent that they would punish themselves by pressing the button. To familiarize participants with the task, participants performed six practice trials. After the mock scanner session, one of the twins continued with the actual scan, while the other twin performed the WISC-III and other behavioral tasks. First-born and second-born children were randomly assigned to the scan session or behavioral tasks as their first task. When the first child completed the scan, he/she continued with the WISC-III and behavioral tasks while the other child participated in the scanning session.

The SNAT consisted of 60 trials, three blocks of 20 trials for each social feedback condition (positive, neutral, negative), that were presented semi-randomized to ensure that no condition was presented more than three times in a row. The optimal jitter timing and order of events were calculated with Optseq 2 (Dale, 1999). Each trial started with a fixation screen (500 ms), followed by social feedback (2500 ms). After another jittered fixation screen (3000-5000 ms), the noise screen with the volume bar appeared, which was presented for a total of 5000 ms. Children were instructed to deliver the noise blast by pressing one of the buttons on the button box attached to their legs, with their right index

finger. As soon as the participant started the button press, the volume bar started to fill up with a new colored block appearing every 350 ms. After releasing the button, or at maximum intensity (after 3500 ms), the volume bar stopped increasing and stayed on the screen for the remainder of the 5000 ms. Before the start of the next trial, another jittered fixation cross was presented (0 -11550 ms) (Figure 1). The length of the noise blast duration (i.e., length of button press) in milliseconds was used as a measure of imagined aggression.

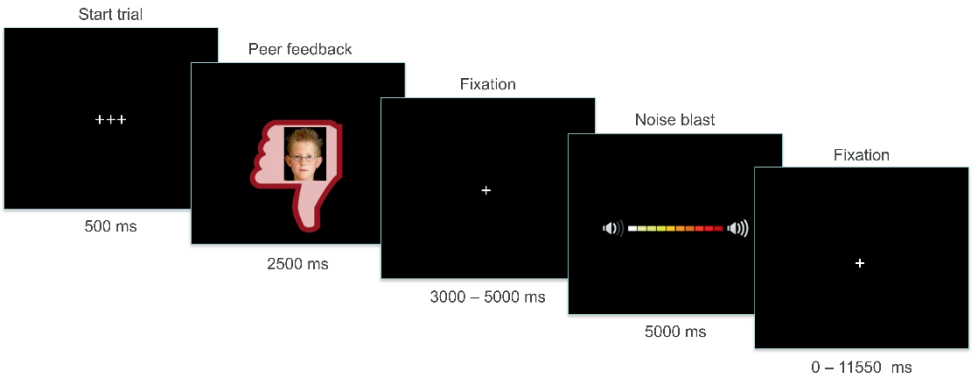


***Figure 1**. Example of one trial of the social network aggression task.*

Social feedback manipulation check

The social feedback manipulation was checked using an exit interview with questions on how much they liked the feedback (*'How much did you like reactions with a thumb up?'*, *'How much did you like reactions with a circle?'*, and *'How much did you like reactions with a thumb down?')*. Participants rated the reactions on a 6-point scale, with 1 representing *very little* and 6 representing *very much*. In addition, we asked two open questions: *'what did you think of the game?'*, and '*what did you think of the noises that you could deliver'*. None of the participants expressed doubts about the cover story.

To verify whether children differentially evaluated the social feedback conditions (positive, negative, neutral), we analyzed answers to the exit questions with a repeated measures ANOVA. Data from the exit questions were missing for 5 participants. Results (Greenhouse-Geisser corrected) showed a significant main effect of type of feedback on the subjective evaluation of social feedback with a large effect size ($F(2, 1002)= 19.16$, $p<.001$, $\omega^2=0.62$). Pairwise comparisons showed that participants liked negative feedback ($M=2.27$, $SD=1.18$) significantly less than neutral feedback ($M=4.14$, $SD=0.87$, $p<.001$, $d= 1.80$) and positive feedback ($M=5.33$, $SD=0.88$, $p<.001$, $d= 2.94$). Participants also liked neutral feedback significantly less than positive feedback ($p<.001$, $d= 1.37$).

MRI data acquisition

MRI scans were acquired with a standard whole-head coil on a Philips Ingenia 3.0 Tesla MR system. To prevent head motion, foam inserts surrounded the children's heads. The total scan protocol lasted 56 minutes, including two fMRI tasks, high resolution T2 and T1 scans, diffusion tensor imaging scans and a resting state fMRI scan. The order of the scans was the same for all participants and always started with the SNAT. The SNAT was projected on a screen that was viewed through a mirror on the head coil. Functional scans were collected during three runs T2*-weighted echo planar images (EPI). The first two volumes were discarded to allow for equilibration of T1 saturation effect. Volumes covered the whole brain with a field of view (FOV) = 220 (ap) x 220 (rl) x 111.65 (fh) mm; repetition time (TR) of 2.2 seconds; echo time (TE) = 30 ms; flip angle (FA) = 80°; sequential acquisition, 37 slices; and voxel size = 2.75 x 2.75 x 2.75 mm. Subsequently, a high-resolution 3D T1scan was obtained as anatomical reference (FOV= 224 (ap) x 177 (rl) x 168 (fh); TR = 9.72 ms; TE = 4.95 ms; FA = 8°; 140 slices; voxel size 0.875 x 0.875 x 0.875 mm).

MRI data analyses

Preprocessing

MRI data were analyzed with SPM 8 (Wellcome Trust Centre for Neuroimaging, London). Images were corrected for slice timing acquisition and rigid body motion. Functional scans were spatially normalized to T1 templates. Due to T1 misregistrations, five participants were normalized to an EPI template. Volumes of all participants were resampled to 3x3x3 mm voxels. Data were spatially smoothed with a 6 mm full width at half maximum (FWHM) isotropic Gaussian kernel. Translational movement parameters were calculated for all participants. Participants that had at least two blocks of fMRI data with <3 mm (1 voxel) motion in any direction were included (*N*=385).

First-level analyses

Statistical analyses were performed on individual subjects' data using a general linear model. The fMRI time series were modeled as a series of two events convolved with the hemodynamic response function (HRF). The onset of social feedback was modeled as the first event, with a zero duration and with separate regressors for the positive, negative, and neutral peer feedback. The start of the noise blast (second event) was modeled for the length of the noise blast duration (i.e., length of button press) and with separate regressors for noise blast after positive, negative, and neutral judgments. Trials on which the participants failed to respond in time were modeled separately as covariate of no interest and were excluded from further analyses. All participants had at least 10 trials for each feedback type. To account for possible motion induced error that had not been

solved by realignment, we included six additional motion regressors (corresponding to the three translational and rotational directions) as covariates of no interest. The least squares parameter estimates of height of the best-fitting canonical HRF for each condition were used in pairwise contrasts. The pairwise comparisons resulted in subject-specific contrast images.

Higher-level group analyses

Subject-specific contrast images were used for the group analyses. A full factorial ANOVA with three levels (positive, negative and neutral judgment) was used to investigate the neural response to the social feedback event. To investigate regions that were activated during both negative and positive feedback, we conducted a conjunction analysis to explore the general valence effects of social evaluation (conjunction negative > neutral and positive > neutral). Based on Nichols *et al.* (2005), we used the 'logical AND' strategy. The 'logical AND' strategy requires that all the comparisons in the conjunction are individually significant (Nichols *et al.*, 2005). Next, we calculated the contrasts negative > positive and positive > negative to investigate brain regions that were specifically activated for social rejection or social acceptance. All results were family wise error (FWE) voxel level corrected, with $p_{FWE}<.05$. Coordinates for local maxima are reported in MNI space.

Region of Interest analyses

SPM8's MarsBaR toolbox (Brett *et al.*, 2002) was used to extract patterns of activation from the whole brain group analyses in order to investigate possible brain-behavior associations and as input for the genetic modeling. Parameter estimates (PE, average Beta values) were extracted from regions that were significantly activated in the whole brain analyses. Specifically, the following ten regions were extracted: the left and right insula and ACCg (from the conjunction contrast); the mPFC and left and right IFG (contrast negative>positive); and the left and right DLPFC, SMA, and caudate (contrast positive>negative). For the brain-behavior relations we focused on associations with noise-blast difference scores following negative social feedback (negative-positive and negative-neutral, corrected for age and IQ).

Genetic modeling

Zygosity was determined using DNA analyses. DNA was tested with buccal cell samples collected via a mouth swab (Whatman Sterile Omni Swab). Buccal samples were collected directly after the MRI session, thereby ensuring that the children did not have anything to eat or drink for at least one hour prior to DNA collection. The results of the DNA analyses indicated that 55% of the twin pairs was MZ.

Phenotypic similarities among twin pairs can be divided into similarities due to shared genetic factors (A) and shared environmental factors (C), while dissimilarities are ascribed to unique environmental influences and measurement error (E). We used behavioral genetic modeling with the OpenMX package (Neale *et al.*, 2016) in R (R Core Team, 2015) to get an estimate of these A, C, and E components. Comparisons of the ACE model with more parsimonious models (AE model; CE model; or E model) are described in the Supplementary Materials. When ACE models show the best fit, both heritability, shared and unique environment are important contributors to explain the variance in the outcome variable. AE models indicate that genetic and unique environmental factors play a role; whilst CE models indicate influences of the shared environment and unique environment. If the E model has no worse fit than AE or CE models, variance in the outcome variable is accounted for by unique environmental factors and measurement error.

Statistical Analysis

In order to detect outliers in the data, we transformed the raw data to z-values. Based on the Z-distribution, 99.9% of z-scores lie between -3.29 and +3.29. Z-values outside this range (<-3.29 or >3.29) were defined as outliers. Outlying scores were winsorized (Tabachnick and Fidell, 2013). To assess effects of condition (positive, neutral, negative) on noise blast duration (in ms) we used a linear mixed-effect model approach using the lme4 package in R (Bates *et al.*, 2015) in R (R Core Team, 2015). Data was fitted on the average response times after positive, neutral and negative trials. Random intercepts per participants and per family allows to account for the nesting of condition within participant (ChildID) and the nesting of twin-pairs within families (FamilyID). Additionally, a random slope of condition was included per participant. Fixed effects included condition (factor with 3 levels), as well as participant's age and IQ as covariates, which were grand mean centered. All main effects and two-way interactions between age ^{x} condition and age ^{x} IQ were included. P-values were determined using Kenward-Rogers approximation as implemented in the mixed function in the afex package (Singmann, 2013). The fitted mixed-effect model is specified in R as:

$$noiseblast \sim condition * age_meancentered + condition * IQ_meancentered + (condition|childID) + (1|familyID).$$

To derive a measure of individual differences in aggression we calculated the differences in noise blast duration between conditions (negative-positive; negative-neutral; neutral-positive). Brain-behavior associations were investigated by least square regressions with ROI activation predicting noise blast difference scores. Due to the nested nature of twin data, the data violates the assumption

of homoscedasticity. Although the estimator of the regression parameters is not influenced when this assumption is violated, the estimator of the covariance matrix can be biased, resulting in too liberal or too conservative significance tests (Hayes & Chai, 2007). Therefore, we used heteroscedasticity-consistent standard error (HCSE) estimators, by using the HCSE macro of Hayes and Cai (2007). As recommended by Long and Ervin (2000), we used the HC3 method. Moreover, we performed genetic modeling of behavioral responses (noise blast difference scores) and neural responses (ROI activation) to social feedback using the OpenMX package (Neale *et al.*, 2016) in R (R Core Team, 2015).

Results

Behavioral analyses

Social feedback retaliation

The linear mixed-effect model showed a significant main effect of type of social feedback on noise blast duration, $F(2, 505) = 300.8754$, $p<.001$. Pairwise comparisons revealed that noise blast duration after negative feedback (M=2688, SD=736) was significantly longer than noise blast duration after neutral feedback (M=1906, SD=648, $p<.001$), and after positive feedback (M=1459, SD=852, $p<.001$). Noise blast duration was significantly longer after neutral feedback than after positive feedback ($p<.001$). There were also significant noise blast ^{x} age $F(2, 505) = 10.57$, $p<.001$) and noise blast ^{x} IQ interaction effects $F(2, 505) = 12.27$, $p<.001$), showing larger condition effects for older children and for children with higher IQ. To control for possible confounding effects of age and IQ, we included these variables as regressors in further models. There were no significant gender differences in noise blast duration after positive, neutral or negative feedback (independent sample T-tests, all p's>.05). Results did not change after exclusion of children with an Axis-I disorder.

Twin analyses

To investigate twin-effects in (imagined) aggression after social feedback we calculated the differences in noise blast duration between negative versus positive feedback, negative versus neutral feedback; and neutral versus positive feedback. Next, we performed Pearson's correlations between these differences scores within MZ (n=138) and DZ (n=115) twin pairs (Table 2). Behavioral genetic analyses revealed that aggression following negative relative to positive social feedback was moderately influenced by genetics (A= 20%, 95% CI: 0-37%), and to a lesser extent influenced by shared environment (C=6%, 95% CI: 0-34%). Unique environment and measurement error explained the largest part of the variance in aggression after negative feedback (E=74%, 95% CI:0.63-0.90), see Table 2. The best fitting model was an ACE-model, see Table S1. Aggression following negative

relative to neutral feedback showed similar influences of shared environment (C=8%) and relatively less influence of genetics (A=10%, Table 2), and was best described by a CE-model (Table S1). Aggression following neutral relative to positive social feedback showed no influence of shared environment (C=0%) and was most influenced by unique environment (90%, see Table 2 and Table S1).

Table 2. Noise blast twin analyses. Pearson's correlations and ACE models for noise blast difference scores.

Noise blast difference		**MZ**	**DZ**		**A²**	**C²**	**E²**
Negative - Positive	*r*	.21	.24	*ACE*	0.20	0.06	0.74
	p	.016	.010	*95% CI*	0.00 - 0.37	0.00 - 0.34	0.63 - 0.90
Negative - Neutral	*r*	.19	.25	*ACE*	0.10	0.08	0.82
	p	.025	.007	*95% CI*	0.00 - 0.40	0.00 - 0.32	0.60 - 0.98
Neutral - Positive	*r*	.10	.04	*ACE*	0.10	0.00	0.90
	p	.260	.67	*95% CI*	0.00 - 0.26	0.00 - 0.13	0.74 - 1.00

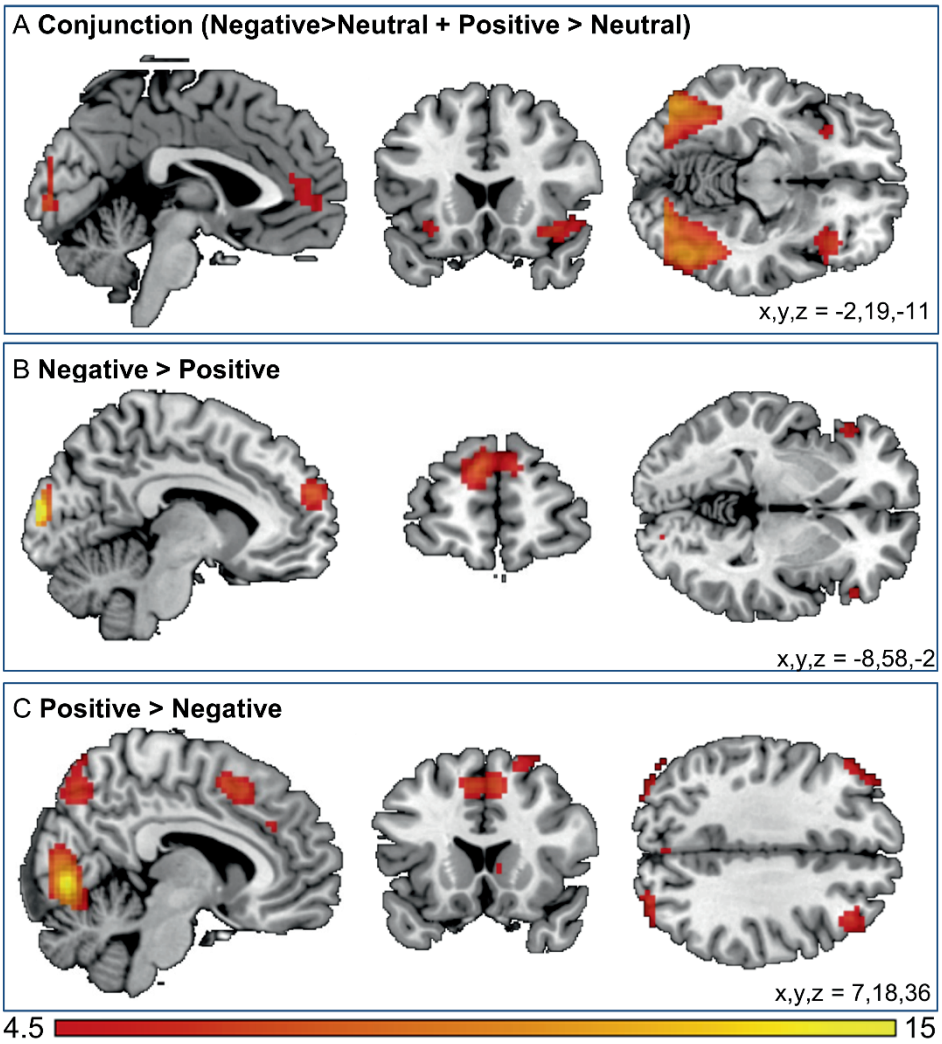


Figure 2. *Whole brain results for A) the conjunction negative>neutral and positive>neutral; B) the contrast negative>positive; and C) the contrast positive>negative. Results were family wise error corrected (p_{FWE}<.05).*

Neural analyses

Whole brain analyses

To investigate the general valence effects of social feedback, we examined neural activity for positive versus neutral *and* negative versus neutral feedback using a conjunction analysis. We found common activation across positive and negative feedback in a wide network of regions including left and right insula, the ACCg, and the lateral occipital cortex (Figure 2a and Table 3).

To investigate effects of negative versus positive social feedback, we investigated the contrasts negative>positive and positive>negative. The contrast negative>positive feedback resulted in activation with local maxima in the medial PFC, the left and right inferior frontal gyrus (IFG), and the occipital pole (Figure 2b and Table 3). The reversed contrast positive>negative resulted in increased activation in the left and right orbitofrontal cortex (OFC), the precuneus, the supplementary motor cortex (SMA), the right caudate, the left and right DLPFC, and the lingual gyrus (Figure 2c and Table 3). Results did not change after exclusion of children with an Axis-I disorder (Table S3).

Brain-behavior analyses

To investigate possible brain-behavior associations in the clusters from the whole brain contrasts 10 ROIs were selected based on a priori hypotheses to predict behavioral aggression using least square regressions with HCSE. We chose 3 ROIs from the conjunction (the ACCg, the left insula, and the right insula), 3 ROIs from the contrast negative>positive (the mPFC, the left IFG, and the right IFG) and 4 ROIs from the contrast positive>negative (the SMA, the right caudate, the left DLPFC, and the right DLPFC) (Table 3). We focused on associations with noise-blast difference scores following negative social feedback (negative-positive and negative-neutral, corrected for age and IQ). We observed a significant association between noise blast differences and activity in left DLPFC, right DLPFC activation, and SMA activation (Table 4, Figure 3). These associations showed that greater activation during positive (versus negative) social evaluation was associated with more aggression after negative social feedback, see Figure 3a-d. To visualize this effect in more detail, we plotted the PE's of the right DLPFC for participants with low aggression after negative feedback and participants with high aggression after negative feedback (Figure 3e). Groups were based on a median split of the noise-blast difference scores following negative social feedback (negative-positive, corrected for age and IQ). Participants who differentiated more in aggression (larger noise blast difference positive versus negative feedback) also differentiated more on a neural level (brain activation after positive versus negative feedback), see Figure 3e. In other words, participants who showed less DLPFC activity during negative feedback relative to positive feedback, were more aggressive after negative feedback. These associations did, however, not survive Bonferroni correction ($p's > 0.025$).

All other ROIs showed no behavioral-brain associations (all *p*'s>.05, see Table 4). Results did not change after exclusion of children with an Axis-I disorder (Table S4). Note that we did not observe any significant clusters of activation scaling with behavior when we performed exploratory whole brain regression analyses with the consecutive noise blast difference scores as covariates of interest (on the contrasts positive>negative, negative>positive, positive>neutral and negative>neutral).

Twin analyses

To investigate twin-effects we calculated Pearson's correlations for neural activation during social feedback in the 10 ROIs for MZ (*n*=87) and DZ (*n*=71) twins, see Table 5. Behavioral genetic analyses revealed that only variance in activation in regions following positive feedback was influenced by genetic factors. Specifically, genetics accounted for 13% (95% CI: 0-32%) of the variance in left DLPFC activation and for 14% (95% CI: 0 - 34%) of the variance in right DLPFC (Table 5). Ten percent of the variance in SMA (95% CI: 0-31%) and right caudate (95% CI: 0-29%) activation was explained by genetics (see Table 5). Estimates for the shared environment were zero, and all of the residuary variance was explained by E (unique environment and measurement error). Genetic modeling for neural activation in the other ROIs revealed minimal or no influence of either genetics or shared environment (estimates 0-4%), and were best explained by unique environment and/or measurement error (Table 5). Variance in neural activation in all ROIs was best explained by an E-model (Table S2).

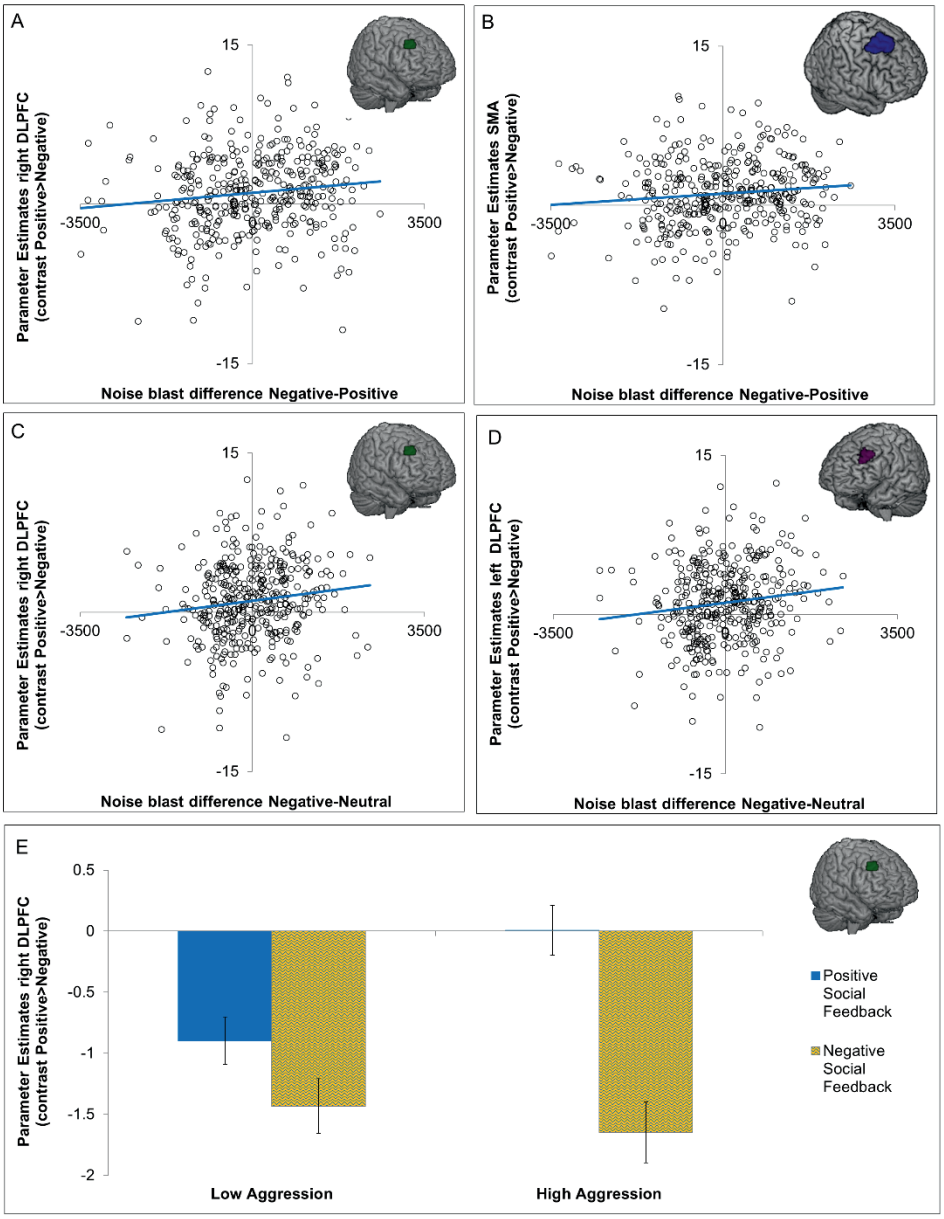


Figure 3. *Visual representation of the brain-behavior associations. (A) right dorsolateral prefrontal cortex (DLPFC) and noise blast difference negative-positive; (B) supplementary motor cortex (SMA) and noise blast difference negative-positive; (C) right DLPFC and noise blast difference negative-neutral; (D) left DLPFC and noise blast difference negative-neutral; and (E) right DLPFC activity after positive and negative social feedback for children with low and high aggression.*

Table 3. MNI coordinates for local maxima activated for the whole brain contrasts.

	Anatomical Region	Voxels	pFWE	T	x	y	z
Conjunction Negative>Neutral and Positive>Neutral							
	Lateral Occipital Cortex	3550	<.001	14.03	-42	-85	4
			<.001	13.79	-48	-76	-5
			<.001	12.72	48	-70	-5
	Lateral Occipital Cortex	124	<.001	6.74	-24	-64	61
*	Right insula	101	<.001	6.35	39	23	-11
*	Left insula	30	.001	5.26	-33	26	-5
			.005	4.98	-30	20	-11
			.026	4.61	-30	11	-17
*	Rostral ACC	108	.002	5.19	0	47	10
			.002	5.18	-6	53	1
			.004	5.02	12	47	13
	Left insula (posterior)	4	.007	4.93	-45	14	-5
	Right IFG	7	.010	4.84	51	23	13
	Supplementary Motor Cortex	4	.035	4.54	6	11	64
Negative > Positive							
	Occipital pole	118	<.001	13.45	-9	-97	13
*	Medial PFC	153	<.001	7.16	-9	59	25
			<.001	5.54	9	59	25
	Occipital pole	51	<.001	6.25	27	-91	16
			0.003	5.10	18	-94	13
*	Left IFG	66	<.001	6.11	-54	29	4
			.001	5.28	-45	26	-8
*	Right IFG	19	.002	5.23	51	32	-2
			.018	4.70	57	32	7
	Left Central Opercular Cortex	3	.017	4.72	-36	-16	25
	Left vlPFC	1	.042	4.49	-21	50	7
	Right vlPFC	1	.048	4.45	30	50	-2

Table 3. (continued)

	Anatomical Region	Voxels	pFWE	T	x	y	z
Positive > Negative							
	Lingual gyrus	762	<.001	13.76	3	-76	-2
			<.001	11.43	-18	-85	-8
			<.001	9.63	-24	-79	-11
	Right OFC	52	<.001	7.58	42	59	-8
			<.001	5.68	36	56	-14
*	Supplementary Motor Cortex	463	<.001	7.43	-6	14	49
			<.001	7.40	24	5	55
			<.001	6.80	6	14	49
	Precuneous	174	<.001	6.19	6	-70	49
			.001	5.27	9	-73	64
	Left OFC	26	<.001	6.16	-45	56	1
			.002	5.19	-48	50	-5
			.023	4.65	-36	62	-2
	Left superior frontal gyrus	125	<.001	6.04	-24	5	64
	Lateral Occipital Cortex	193	<.001	6.01	42	-76	46
			<.001	5.72	27	-82	31
			<.001	5.54	39	-85	34
*	Right dorsolateral PFC	90	<.001	5.87	39	32	37
	Lateral Occipital Cortex	91	<.001	5.83	-42	-82	40
			<.001	5.50	-33	-67	64
			<.001	5.49	-51	-70	46
*	Left dorsolateral PFC	88	<.001	5.58	-45	41	34
			.001	5.32	-48	32	37
			.006	4.95	-39	38	43
	Left middle OFC	5	.003	5.10	-18	56	-17
*	Right Caudate	12	.004	5.07	12	20	4
	Left Supermarginal gyrus	9	.004	5.07	-57	-46	55
	Dorsal ACC	5	.008	4.89	6	35	31
	Right Middle temporal gyrus	3	.015	4.74	63	-22	-17
	Left OFC	1	.022	4.66	-42	53	-11

* Cluster used as region of interest in subsequent analyses

Table 4. Brain-behavior associations. Least square regressions with heteroskedasticity corrected standard error estimations with brain activation in the regions of interest predicting behavioral aggression.

		Conjunction			Negative>Positive			Positive>Neutral			
Noise blast difference		ACC gyrus	left insula	right insula	medial PFC	left IFG	right IFG	SMA	right caudate	left DLPFC	right DLPFC
Negative - Positive	*r*	.07	.08	.07	.02	-0.01	.05	.11	-.04	.10	.13
	p	.152	.105	.169	.674	.845	.401	.027	.460	.074	.017
Negative - Neutral	*r*	.06	.09	.04	.02	.02	.05	.09	-.00	.13	.13
	p	.256	.081	.441	.711	.675	.349	.087	.936	.009	.013

ACC: Anterior Cingulate Cortex; DLPFC: dorsolateral prefrontal cortex IFG: inferior frontal gyrus; PFC: prefrontal cortex; SMA: supplementary motor area

Table 5. Region Of Interest twin analyses. Pearson's correlations and ACE models for brain activation in the regions of interest (ACC: Anterior Cingulate Cortex; AI: Anterior Insula; IFG: inferior frontal gyrus; SMA: supplementary motor area; DLPFC: dorsolateral prefrontal cortex).

ROI		MZ	DZ		A^2	C^2	E^2
Conjunction Negative>Neutral and Positive>Neutral							
ACC gyrus	*r*	-0.04	0.14	*ACE*	0	0.06	0.94
	p	0.739	0.249	*95% CI*	0.00 - 0.20	0.00 - 0.21	0.80-1.00
Left AI	*r*	-0.07	-0.14	*ACE*	0	0	1
	p	0.493	0.252	*95% CI*	0.00 - 0.11	0.00 - 0.09	0.89 - 1.00
Right AI	*r*	0.06	-0.11	*ACE*	0	0	1
	p	0.611	0.377	*95% CI*	0.00 - 0.19	0.00 - 0.12	0.81 - 1.00
Negative > Positive							
Medial PFC	*r*	0.12	-0.2	*ACE*	0.01	0	0.99
	p	0.274	0.091	*95% CI*	0.00 - 0.21	0.00 - 0.12	0.79 - 1.00
Left IFG	*r*	0	-0.06	*ACE*	0	0	1
	p	0.987	0.607	*95% CI*	0.00 - 0.19	0.00 - 0.13	0.81- 1.00
Right IFG	*r*	0.02	0.06	*ACE*	0	0.04	0.96
	p	0.853	0.628	*95% CI*	0.00 - 0.22	0.00 - 0.19	0.81 - 1.00
Positive > Negative							
SMA	*r*	0.23	-0.21	*ACE*	0.1	0	0.9
	p	0.031	0.087	*95% CI*	0.00 - 0.31	0.00 - 0.14	0.69 - 1.00
Right caudate	*r*	0.12	0.02	*ACE*	0.1	0	0.9
	p	0.289	0.855	*95% CI*	0.00 - 0.29	0.00 - 0.22	0.71 - 1.00
Left DLPFC	*r*	0.18	-0.05	*ACE*	0.13	0	0.87
	p	0.09	0.652	*95% CI*	0.00 - 0.32	0.00 - 0.20	0.68 - 1.00
Right DLPFC	*r*	0.27	-0.22	*ACE*	0.14	0	0.86
	p	0.01	0.06	*95% CI*	0.00-0.34	0.00 - 0.14	0.66-1.00

Discussion

This study aimed to investigate genetic and shared environmental influences on neural activity and aggression following social feedback in children. Consistent with prior studies, negative social feedback resulted in behavioral aggression (Achterberg *et al.*, 2016b; Achterberg *et al.*, 2017). Behavioral genetic modeling revealed that aggression following negative feedback (negative-positive and negative-neutral) was influenced by genetic as well as shared and unique environmental influences. Genetic influences ranged from 10-20%, whereas approximately 7% of the variance was explained by shared environmental influences. Although previous studies have also found influences of shared environment, with similar (Ferguson, 2010) or higher estimates (Rhee and Waldman, 2002; Porsch *et al.*, 2016), most studies have suggested stronger genetic influences (around 50%) on behavioral aggression (Rhee and Waldman, 2002; Ferguson, 2010). These differences can be partly attributed to the way the aggression was assessed. Indeed, a review of Tuvblad and Baker (2011) showed that twin correlations of aggression based on parent/ teacher reports were twice as high as twin correlations of observed aggressive behavior. Using single raters for multiple children might result in inflated genetic influences (Tuvblad and Baker, 2011), and an experimental design can overcome such rater bias. This study is the first to use an experimental task to test genetic influences on reactive social aggression in a developmental twin-sample. It shows that environmental factors are important predictors of reactive aggressive behaviors. In line with our results, longitudinal stability in reactive aggression has been shown to be influenced by environmental effects (Tuvblad *et al.*, 2009).

Our analyses of neural responses to negative, positive, and neutral social feedback showed that brain activation in the ACCg and anterior insula was related to general valiance/ social saliency. The ACCg has been suggested to be sensitive to determining others' motivation (Apps *et al.*, 2016), which is important in the processing of social feedback, irrespective of whether it is positive or negative. Moreover, the ACCg has been shown to have strong structural and functional connectivity with the anterior insula (Apps *et al.*, 2016), and together these regions have been indicated as the salience network (Damoiseaux *et al.*, 2006; van Duijvenvoorde *et al.*, 2016a). Our results show that activation of regions coding social saliency is present already in childhood, indicating this might be a core social motivational mechanism in humans. Previous social evaluation studies did not report heightened activation that was specific for negative social feedback (Gunther Moor *et al.*, 2010b; Guyer *et al.*, 2012; Achterberg *et al.*, 2016b; Achterberg *et al.*, 2017), which might be due to the smaller samples in previous studies (n=30-60) as compared to the current study (N=385). In the current study, medial PFC and IFG were activated during negative feedback. Interestingly, the ACCg is connected to the portions of the mPFC that signal other-oriented

information (Apps *et al.*, 2016; Lee and Seo, 2016), and both play important roles in social cognition and behavior (Blakemore, 2008). Our results suggest that whereas the ACCg signals for social salient cues, the mPFC might signal for social threatening cues. Positive feedback, on the other hand, resulted in heightened activation in the caudate, SMA and bilateral DLPFC, which is consistent with previous social evaluation paradigms that reported increased activation in striatum (Davey *et al.*, 2010; Gunther Moor *et al.*, 2010b; Guyer *et al.*, 2012), superior frontal gyrus/SMA (Gunther Moor *et al.*, 2010b; Guyer *et al.*, 2012), and middle frontal gyrus /DLPFC (Gunther Moor *et al.*, 2010b).

Interestingly, SMA and DLPFC activity were also associated with aggressive behavior on the task. SMA and DLPFC activations were related to aggression after negative (relative to neutral and/or positive) feedback. Post hoc visualization of PE values showed that children who were *more* aggressive after negative feedback showed relatively *less* activation of the DLPFC during negative feedback compared to positive social feedback. This is in line with prior studies in adults which showed that *more* DLPFC activity after negative social feedback was related to *less* subsequent aggression (Riva *et al.*, 2015; Achterberg *et al.*, 2016b). It should be noted, however, that we did not observe brain-behavior associations when we performed whole brain regression analyses, in contrast to earlier studies in adults (Achterberg *et al.*, 2016b). Moreover, our brain-behavior associations on ROIs did not survive Bonferroni correction. The DLPFC is one of the brain regions that take longest to mature (Sowell *et al.*, 2001; Gogtay *et al.*, 2004), leaving ample room for individual, developmental differences. Although our sample size was fairly large compared to previous fMRI studies, individual developmental differences are best captured with longitudinal designs, due to individual variation in the timing of brain maturation.

We did not find significant brain-behavior associations in other ROIs (caudate, IFG, insula, mPFC, ACCg) that responded to social peer feedback. The lack of brain-behavior associations might indicate that these regions signal for social cues, but are not sensitive to retaliation behaviors. Indeed previous studies have indicated the IFG, insula, mPFC and ACCg as important regions of the "social brain" (for reviews, see Blakemore (2008) and Adolphs (2009)). The social brain is defined as a network of brain regions that is activated when we evaluate others and think about others' intentions and feelings (Brothers, 1990; Blakemore, 2008). Activation in these regions during peer feedback evaluation could indicate that children evaluate the intentions of the peers, but might not be specifically related to the actions they intent towards that peer. Regions that did show a relation with aggression, namely the SMA and DLPFC, have indeed been shown to be associated with behavioral motor planning (SMA) and behavioral control (DLPFC) in previous research (Riva *et al.*, 2015; Achterberg *et al.*, 2016b).

Genetic modeling showed that genetics played a role in activation in the DLPFC, the SMA and the right caudate, with 10-14% of the variance explained by genetics. Previous heritability studies on structural brain measures have focused

on rather large anatomical regions (i.e., the whole frontal cortex) and also report genetic influences (Jansen *et al.*, 2015). One developmental study that specifically investigated heritability of the DLPFC showed heritability estimates of around 40% for cortical thickness (age range 5-19, Lenroot *et al.* (2009)). Only a handful of studies have addressed heritability in task-based fMRI (for an overview, see Jansen *et al.* (2015)). Blokland and colleagues (2011) investigated brain activation during a working memory task in young adults (aged 20-30) and showed heritability of brain function in (amongst others) DLPFC, ranging from 20-65%. To our best knowledge, our study is the first to investigate the heritability of task-based fMRI in middle childhood, so direct comparisons to previous studies cannot be made. However, test-retest reliability studies on task-based fMRI in developmental samples have shown higher interclass correlation coefficients (ICCs) for lateral PFC regions than for subcortical regions (van den Bulk *et al.*, 2013; Peters *et al.*, 2016), indicating that the DLPFC might indeed reflect trait-like genetic influences. An important next step would be to reveal *which* environmental and genetic factors play a role in explaining the variance in brain activation and aggression following social evaluation, and test whether specific environmental influences (e.g. supportive parenting) might moderate the influence of specific genetic factors (for example, see the study protocol of Euser *et al.* (2016).

Several limitations of the current study may be addressed in future research. First, the cover story of the SNAT task explicitly stated that the peers would not hear the noise blast. This decision was based on previous studies using a similar design (Konijn *et al.*, 2007). Therefore the aggression measure reflects imagined aggression. Future studies may separate real aggression from imagined aggression to test any neural differences between these two types of aggression. Second, although our sample size can be considered large with regards to fMRI, it is rather small for behavioral genetic modeling. The statistical power of genetic studies is influenced by, amongst others, the sample size and the ratio MZ:DZ (Visscher, 2004; Verhulst, 2017). Our genetic analyses of neural responses resulted in high estimates for the E component (and specifically E- models, see supplementary materials), reflecting influences from the unique environment and measurement error. However, our sample size may have been insufficient to detect significant contributions of A (genetics) and C (shared environment). Fortunately, our sample did have an approximately equal numbers of MZ and DZ twins, which is considered optimal (Visscher, 2004). Moreover, prior studies have showed that the E component was also the primary determinant of variance in structural brain measures (Lenroot *et al.*, 2009), highlighting the urgent need to disentangle unique environmental influences from measurement error. Last, we used several ROIs to investigate brain-behavior associations and twin correlations. Significant results did not survive Bonferroni correction for multiple

testing, and therefore need to be interpreted with caution. Nevertheless, our results provide important hypotheses which can be further examined in future (meta-) analyses.

Conclusion

Taken together, our results suggest that the processing of social feedback is partly explained by genetic factors, and the level of behavioral aggression following these evaluations are related to genetics and shared environmental influences. The regulatory role of DLPFC in aggression regulation fits with prior research in adults (Riva *et al.*, 2015; Chester and DeWall, 2016) and may be sensitive to developmental changes (Somerville *et al.*, 2010; Casey, 2015). Our findings underscore that the way children react to positive and negative social feedback is influenced by environmental factors. This stresses the important role of environmental inputs on observed behavior, such as parents and teachers, and point to an important role for parenting programs and interventions.

Acknowledgments

The Leiden Consortium on Individual Development is funded through the Gravitation program of the Dutch Ministry of Education, Culture, and Science and the Netherlands Organization for Scientific Research (NWO grant number 024.001.003). The authors declare no conflict of interests.

Supplementary Materials

Genetic modeling - comparison of parsimonious models

Similarities among twin pairs are divided into similarities due to shared genetic factors (A) and shared environmental factors (C), while dissimilarities are ascribed to unique environmental influences and measurement error (E). Behavioral genetic modeling with the OpenMX package (Neale *et al.*, 2016) in R (R Core Team, 2015) provides estimates of these A, C, and E components. To investigate whether the more parsimonious AE model (with C fixed to zero), CE model (with A fixed to zero) or E model (with both A and C fixed to zero) showed a better fit to the data, we subtracted the log-likelihood of the AE and CE models from the log-likelihood of the ACE model and the fit of the E model from the fit of the AE or CE models to get an estimate of the Log-likelihood Ratio Test (LRT). In most circumstances LRT follows the X^2 distribution, with 3.84 as a critical value at p=.05, thus a LRT>3.84 indicates a significantly worse fit of the data. In addition, we used the Akaike Information Criterion (AIC; Akaike (1974)) a standardized model-fit metric, to compare the different models. Lower AIC values indicate a better model fit. When ACE models show the best fit, both heritability, shared and unique environment are important contributors to explain the variance in the outcome variable. AE models indicate that genetic and unique environmental factors play a role; whilst CE models indicate influences of the shared environment and unique environment. If the E model has no worse fit than AE or CE models, variance in the outcome variable is accounted for by unique environmental factors and measurement error.

Table S1. Twin analyses on noise blast difference scores. ACE models compared to parsimonious AE, CE and E models.

Noise blast difference	model	A[2]	C[2]	E[2]	LTR	AIC
Negative - Positive	* ACE	0.20	0.06	0.74		7542.16
	AE	0.24	-	0.76	4.17	7544.33
	CE	-	0.14	0.86	38.67	7578.84
	E	-	-	1.00	>22.18	7599.02
Negative - Neutral	ACE	0.10	0.08	0.82		7173.47
	AE	0.09	-	0.91	-0.33	7171.13
	* CE	-	0.20	0.80	-.5.58	7165.88
	E	-	-	1.00	>23.81	7192.95
Neutral - Positive	ACE	0.10	0.00	0.90		6888.43
	AE	0.10	-	0.90	<.001	6886.43
	CE	-	0.07	0.93	0.19	6886.63
	* E	-	-	1.00	<1.39	6885.83

[1] LTR < 3.85 equals a significant better fit of the model (p<.05)

[2] Lower AIC values indicate a better model fit

* asterics indicate the best model fit

Table S2. Twin analyses on brain activation in the regions of interest (ACC: Anterior Cingulate Cortex; PFC: prefrontal cortex; IFG: inferior frontal gyrus; SMA: supplementary motor area; DLPFC: dorsolateral prefrontal cortex). ACE models compared to parsimonious AE, CE and E models

ROI	model	A[2]	C[2]	E[2]	LTR[1]	AIC[2]
Conjunction Negative>Neutral and Positive>Neutral						
ACC gyrus	ACE	0.00	0.04	0.96		944.02
	AE	0.02	-	0.98	0.38	942.41
	CE	-	0.04	0.96	<0.001	942.02
	* E	-	-	1.00	<0.50	940.53
Left Insula	ACE	0.00	0.00	1.00		1130.48
	AE	0.00	-	1.00	<0.001	1128.48
	CE	-	0.00	1.00	<0.001	1128.48
	* E	-	-	1.00	<0.001	1126.48
Right Insula	ACE	0.01	0.00	0.99		1072.13
	AE	0.01	-	0.99	<0.001	1070.13
	CE	-	0.00	1.00	<0.001	1070.13
	* E	-	-	1.00	<0.001	1068.13
Negative > Positive						
Medial PFC	ACE	0.01	0.00	0.99		950.65
	AE	0.01	-	0.99	<0.001	948.65
	CE	-	0.00	1.00	0.01	948.66
	* E	-	-	1.00	<0.01	946.66
Left IFG	ACE	0.00	0.00	1.00		1141.15
	AE	0.00	-	1.00	<0.001	1139.15
	CE	-	0.00	1.00	<0.001	1139.15
	* E	-	-	1.00	<0.001	1137.15
Right IFG	ACE	0.00	0.04	0.96		1160.12
	AE	0.04	-	0.96	0.07	1158.19
	CE	-	0.04	0.96	<0.001	1158.12
	* E	-	-	1.00	<0.021	1156.32

[1] LTR < 3.85 equals a significant better fit of the model (p<.05)

[2] Lower AIC values indicate a better model fit

* asterics indicate the best model fit

Table S2. (continued)

ROI	model	A²	C²	E²	LTR¹	AIC²
Positive > Negative						
SMA	ACE	0.10	0.00	0.90		1003.64
	AE	0.10	-	0.90	<0.001	1001.64
	CE	-	0.00	1.00	0.87	1002.52
	* E	-	-	1.00	<0,87	1000.52
Right caudate	ACE	0.10	0.00	0.90		1308.21
	AE	0.10	-	0.90	<0.001	1306.21
	CE	-	0.08	0.92	0.24	1306.45
	* E	-	-	1.00	<1.48	1305.36
Left DLPFC	ACE	0.13	0.00	0.87		1064.97
	AE	0.13	-	0.87	<0.001	1062.97
	CE	-	0.07	0.93	0.96	1063.93
	* E	-	-	1.00	<1,64	1062.61
Right DLPFC	ACE	0.14	0.00	0.86		1108.45
	AE	0.14	-	0.86	<0.001	1106.45
	CE	-	0.03	0.97	1.83	1108.29
	* E	-	-	1.00	<1.97	1106.42

¹ LTR < 3.85 equals a significant better fit of the model (p<.05)

² Lower AIC values indicate a better model fit

* asterics indicate the best model fit

Table S3. MNI coordinates for local maxima activated for the whole brain contrasts without participants with pathology (N=377). ACC: Anterior Cingulate Cortex; IFG: Inferior Frontal Gyrus; SMA: Supplementary motor cortex; OFC: Orbitofrontal Cortex; PFC: Prefrontal Cortex

Anatomical Region	Voxels	pFWE	T	x	y	z
Conjunction Negative>Neutral and Positive>Neutral						
Lateral Occipital Cortex	3379	<.001	13.74	-45	-82	1
			13.57	-48	-76	-5
			12.52	48	-70	-5
Occipital Cortex	113	<.001	6.81	-24	-64	61
Right insula	80	<.001	6.31	39	23	-11
			6.07	33	17	-14
Left insula	28	.001	5.15	-33	26	-5
			4.95	-30	20	-11
Medial PFC	5	.013	5.03	-6	53	-2
Right IFG	7	.009	4.93	51	23	13
Rostral ACC	31	<.001	4.91	12	47	13
			4.85	3	56	19
			4.81	0	47	10
Left insula	2	.024	4.67	-45	14	-5
SMA	1	.032	4.61	6	5	67
SMA	1	.032	4.57	6	11	64
ACC	1	.032	4.52	0	47	1
Negative > Positive						
Occipital pole	132	<.001	16.55	-9	-97	13
Occipital pole	118	<.001	8.39	27	-91	13
			8.19	18	-94	13
Medial PFC	138	<.001	6.95	-9	56	25
			5.46	9	62	25
Left IFG	57	<.001	6.35	-54	29	4
			5.24	-45	26	-8
Right IFG	16	.003	5.15	51	32	-2
			4.86	57	32	7
Right Occipital Fusiform Gyrus	3	.021	4.83	18	-85	-5

Table S3. (continued)

Anatomical Region	Voxels	pFWE	T	x	y	z
Negative > Positive						
Left Lateral Occipital Cortex	9	.008	4.72	-48	-82	1
Left Central Opercular Cortex	1	.033	4.63	-36	-16	25
Positive > Negative						
Lingual gyrus	844	<.001	14.75	6	-76	-2
			13.96	-18	-85	-8
			10.93	18	-73	-11
Right superior frontal gyrus	353	<.001	7.27	24	5	55
			7.07	-6	14	49
			6.41	9	11	52
Right Lateral Occipital Cortex	133	<.001	6.90	30	-82	31
			5.74	42	-76	46
			5.62	39	-73	55
Precuneous	151	<.001	6.14	0	-70	49
			5.20	9	-73	64
Left Superior Frontal Gyrus	98	<.001	6.05	-24	2	58
Right OFC	32	.001	6.03	42	59	-8
			5.62	48	53	-2
			4.89	36	56	-14
Left Lateral Occipital Cortex	58	<.001	5.69	-36	-85	40
			5.36	-39	-70	58
			5.23	-51	-67	49
Left OFC	15	.004	5.68	-45	56	4
Right dorsolateral PFC	47	<.001	5.51	39	32	37
			4.89	39	32	46

Table S3. (continued)

Anatomical Region	Voxels	pFWE	T	x	y	z
Positive > Negative						
Left dorsolateral PFC	41	<.001	5.43	-45	41	34
			5.06	-48	32	37
			4.82	-36	47	40
Right Caudate	6	.012	4.95	9	20	4
Left middle OFC	2	.026	4.88	-18	56	-17
Right Supermarginal gyrus	13	.005	4.82	60	-43	49
			4.62	57	-40	58
Left Supermarginal gyrus	2	.026	4.73	-48	-58	58
Dorsal ACC	3	.021	4.73	6	35	31
Left OFC	2	.026	4.69	-48	50	-5
Left Supermarginal gyrus	1	.033	4.54	-57	-46	55

Table S4. Brain-behavior associations without participants with pathology (N=377). Least square regressions with heteroskedasticity corrected standard error estimations with brain activation in the regions of interest predicting behavioral aggression.

		Conjunction			Negative>Positive			Positive>Neutral			
Noise blast difference		ACC gyrus	left insula	right insula	medial PFC	left IFG	right IFG	SMA	right caudate	left DLPFC	right DLPFC
Negative - Positive	*r*	.08	.08	.07	.01	.03	.05	.11	.04	.09	.13
	p	.146	.125	.186	.832	.548	.407	.032	.433	.083	.019
Negative - Neutral	*r*	.06	.09	.03	.01	.00	.05	.09	.00	.13	.13
	p	.263	.096	.504	.817	.896	.346	.089	.914	.011	.014

ACC: Anterior Cingulate Cortex; DLPFC: dorsolateral Prefrontal Cortex IFG: Inferior Frontal Gyrus; OFC: Orbitofrontal Cortex; PFC: Prefrontal Cortex; SMA: Supplementary Motor Cortex

CHAPTER FIVE

Longitudinal changes in DLPFC activation within childhood are related to decreased aggression following social rejection

This chapter is based on: Achterberg M., Van Duijvenvoorde A.C.K., IJzendoorn, M.H., Bakermans M.J. & Crone E.A.M. Longitudinal changes in DLPFC activation within childhood are related to decreased aggression following social rejection (in revision, 2019)

Abstract

Regulating aggression in the case of negative social feedback is an important prerequisite for developing and maintaining social relations. Prior studies in adults highlighted the role of the dorsolateral prefrontal cortex (DLPFC) as a regulating mechanism for behavioral control. Despite the fact that middle-to-late childhood is an important period for both brain maturation and social relations, no prior study examined development of aggression regulation following social feedback within childhood. The current study investigated this using a longitudinal fMRI study, with 456 same-sex twins undergoing two fMRI sessions, across the transition from middle childhood (7-9 years) to late childhood (9-11 years). Aggression regulation was studied using the Social Network Aggression Task: Participants viewed pictures of peers that gave positive, neutral or negative feedback to the participant's profile. Next, participants could blast a loud noise towards the peer as an index of aggression. Confirmatory analyses revealed that behavioral aggression after social evaluation decreased over time, whereas neural activation in anterior insula, medial PFC and DLPFC increased over time. Exploratory whole brain-behavior analyses in late childhood showed a negative association between aggression and bilateral DLPFC, with increased DLPFC activity resulting in decreased aggression. Change analyses further revealed that children who showed larger increases in DLPFC activity from middle to late childhood showed stronger decreases in aggression over time. These findings highlight the importance of the development of social emotion regulation mechanisms within childhood.

Keywords: Social evaluation processing; Social emotion regulation; Dorsolateral prefrontal cortex; development; childhood;

Introduction

Regulating emotions in social interactions is one of the most important requirements for developing social relations in childhood. With increasing age, children become better at regulating their emotions (Silvers *et al.*, 2012), which has been suggested to be related to the development of cognitive and behavioral control functions between early childhood and adolescence (Diamond, 2013; Casey, 2015). Few studies have investigated the development of social emotion regulation within childhood, despite empirical findings showing that middle-to-late childhood marks the most rapid changes in cognitive control (Luna *et al.*, 2004; Zelazo and Carlson, 2012; Peters *et al.*, 2016). Although neuroimaging studies have shed light on the underlying neurobiological changes that sub serve childhood development in cognitive control, most studies have relied on cross-sectional comparisons which hinders the possibility to examine within-person change. The current study builds upon new insights in the neural processing of social emotion regulation by examining within childhood change in neural and behavioral social control in a longitudinal fMRI study.

Emotion regulation is of upmost importance when social interactions result in rejection. It is well documented that social rejection can lead to aggression and retaliation (Dodge *et al.*, 2003; Nesdale and Lambert, 2007; Chester *et al.*, 2014; Novin *et al.*, 2018). Social evaluation, including social acceptance and rejection, has previously been studied using ecologically valid social judgment paradigms, in which participants' profiles are evaluated by same-aged peers (Somerville *et al.*, 2006; Gunther Moor *et al.*, 2010b; Hughes and Beer, 2013; Silk *et al.*, 2014). Developmental neuroimaging studies including adolescent participants showed that receiving positive (acceptance) relative to negative (rejection) social feedback was associated with increased neural activity in the ventral medial prefrontal cortex (MPFC), the anterior insula (AI), and the anterior cingulate cortex (ACC) (Gunther Moor *et al.*, 2010a; Guyer *et al.*, 2016). The Social Network Aggression Task is an extended social evaluation paradigm that includes also a neutral feedback condition, and that provides participants with the opportunity to blast a loud noise towards the peer that evaluated them (Achterberg *et al.*, 2016b; Achterberg *et al.*, 2017; Achterberg *et al.*, 2018b). Consistent with prior studies (Dalgleish *et al.*, 2017), it was found that both adults and children showed stronger ACC and AI activity in this task after receiving both positive and negative feedback (relative to neutral feedback), indicating that these regions signal social salient cues (Achterberg *et al.*, 2018b). How neural responses to social evaluation feedback influence behavioral aggression in childhood, and how these neural regions change over time, remains currently unknown.

Controlling emotions elicited by social evaluation feedback relies on cognitive control, that is: individuals with better cognitive control functions show less subsequent aggression following rejection (Chester *et al.*, 2014). Moreover,

increased activation in the dACC and AI was related to less aggression in adults with high executive functioning, whereas adults with low executive functioning showed increased aggression with increasing neural activation (Chester *et al.*, 2014). Prior studies in adults further showed that the dorsolateral prefrontal cortex (DLPFC) might serve as a regulating mechanism for aggression after social evaluation, such that increased DLPFC activity after social rejection was related to less behavioral aggression (Riva *et al.*, 2015; Achterberg *et al.*, 2016b). Moreover, stronger functional connectivity between the lateral PFC and limbic regions was related to less retaliatory aggression (Chester and DeWall, 2016). Interestingly, prior theoretical perspectives have suggested that DLPFC maturation is an important underlying mechanism for developing a variety of control functions in childhood (Bunge and Zelazo, 2006; Diamond, 2013). Prior research revealed that in 7-8 year old children there were indications for associations between DLPFC and behavioral aggression(Achterberg *et al.*, 2018b), although these were less pronounced than in adults. Taken together, studies in adults showed a link between cognitive control and regulation of emotions after rejection in the ACC/insula (Chester *et al.*, 2014) and DLPFC (Achterberg *et al.*, 2016b), but no study to date examined longitudinal developmental changes in these brain regions in childhood in the context of social evaluation. These prior studies led us to hypothesize that within-person maturation of the ACC/AI and DLPFC may be associated with better aggression regulation in childhood.

The current study makes use of a unique developmental twin sample of the Leiden Consortium for Individual Development (L-CID; Euser *et al.* (2016)). The design is based on recent insights showing that home environment is an important factor that impacts children's behavioral control (Sektnan *et al.*, 2010; Vrijhof *et al.*, 2018). The L-CID study makes use of the video feedback intervention to promote positive parenting and sensitive discipline (VIPP-SD), an attachment based intervention that aims to enhance parental sensitivity and sensitive discipline (Juffer *et al.*, 2017a). The VIPP-SD has proven to diminish externalizing behavior problems such as aggression in younger age groups (0-6 years (Van Zeijl *et al.*, 2006; Juffer *et al.*, 2017b)). The L-CID study tests whether the VIPP-SD is also effective in parents with older children and possibly likewise beneficial for behavioral outcomes of older children. Therefore, this study design allows us to not only examine the development of aggression regulation within individuals over time, but also the effect of genetics and variations in the social environment.

Using this unique study design, we address the following research questions: i) How does aggression regulation following social evaluation changes longitudinally within childhood? And ii) to what extent are these changes dependent on heritability and changes in the social environment? In doing so, 492 same-sex twins (246 families) underwent two fMRI sessions across the transition from middle childhood (7-9 years) to late childhood (9-11 years). In between fMRI sessions, families received either the VIPP-Twins or a dummy

intervention (Euser *et al.*, 2016). Using linear mixed effects modeling, we first investigated how behavioral aggression after positive, negative and neutral social feedback changed over time, and whether variation in the environment influenced these changes. Next, we investigated changes in brain responses related to positive, negative and neutral social feedback longitudinally within childhood and examined brain-behavior associations. Based on previous studies, we selected the AI, the IFG, the MPFC, and DLPFC as regions of interest (Gunther Moor *et al.*, 2010b; Vijayakumar *et al.*, 2017; Achterberg *et al.*, 2018b). To test individual differences in aggression regulation we additionally performed exploratory whole brain-behavior MRI analyses to test for relations between prefrontal cortex activation and aggression regulation.

Methods

Participants

Participants in this study took part in the longitudinal twin study of the Leiden Consortium on Individual Development (L-CID (Euser *et al.*, 2016)). The procedures were approved by the Dutch Central Committee Human Research (CCMO) and written informed consent was obtained from both parents. 512 children (256 families) between the ages 7 and 9 were included at the first wave (previously described in Achterberg *et al.* (2018b), van der Meulen *et al.* (2018)), with a mean age of 7.94 ± 0.67 (49% boys, 55% monozygotic). The majority of the sample was Caucasian (91%) and right-handed (87%). Ten participants (2%) were diagnosed with an Axis-I disorder: eight with attention deficit hyperactivity disorder (ADHD); one with generalized anxiety disorder (GAD), and one with pervasive developmental disorder- not otherwise specific (PDD-NOS). Intelligence (IQ) was estimated at W1 with the subtests 'similarities' and 'block design' of the Wechsler Intelligence Scale for Children, third edition (WISC-III; Wechsler, 1997). Estimated IQs were in the normal range (72.50 - 137.50). 456 children participated in a second lab two years later (for details regarding participant dropout see **Figure S1** and *supplementary materials*). **Table 1** provides an overview of demographic characteristics of the sample at wave 1 (W1) and wave 2 (W2). Participants underwent an MRI scan as part of the lab visits. At W1, 385 participants were included in the MRI analyses (mean age 7.99 ± 0.68, 47% boys, see also Achterberg *et al.* (2018b)). At W2 360 participants were included in the MRI analyses (mean age 10.01 ± 0.67, 48% boys). A total of 293 participants were included on the MRI analyses at both waves (mean age W1: 7.99 ± 0.66, 47% boys).

Parenting intervention

Families were contacted 1.5 year after W1 to inform them on a parenting support program for parents of twins (VIPP-Twins (Euser *et al.*, 2016)). We then explained that we were unable to personally visit all families within the L-CID to offer the training. Therefore, families would be randomly assigned to either receiving the training in person, through six home visits (see Juffer and Bakermans-Kranenburg (2018)), or to alternatively discuss the development of your twin through six phone meetings (dummy intervention - control group). Detailed sample selection is described in the *supplementary materials*. The VIPP-Twins group consisted of n=164 children, of which 133 had sufficient quality MRI data (**Figure S1**). The control group consisted of n=244 children, of which n=186 had sufficient quality MRI data (**Figure S1**). Twenty-seven families (n=54 children) did not comply with random assignment to one of the conditions. These families received the (non-randomly assigned) dummy intervention in order to keep this group comparable to the control group for future analyses within the longitudinal L-CID study. Given that the participants in the non-randomly assigned control group could not be included in the analyses, these participants' MRI data were used as a reference group, and used to create task-relevant independent regions of interest (ROI) (see **section 2.4.4**).

Social Network Aggression Task

The Social Network Aggression Task (SNAT) as described in Achterberg et al. (2016b; 2017; 2018b) was used to measure aggression after social feedback. Participants viewed pictures of peers that gave positive, neutral or negative feedback to the participant's profile. Next, participants could blast a loud noise towards the peer as an index of aggression. To keep task demands as similar as possible between the conditions, participants were instructed to always press the button. The longer they pressed the button the more intense the noise would be, which was visually represented by a volume bar. Participants received instructions on how to perform the SNAT and the children were exposed to the noise blast during a practice session. Thereafter, participants practiced six trials of the task. The time line of a SNAT trial was as follows: start screen (500 ms), social feedback (2500 ms), fixation screen (3000-5000 ms), noise screen (5000 ms), intra-trial interval fixation screen (0-11550 ms), see **Figure 1a**. The optimal jitter timing and order of events were calculated with Optseq 2 (Dale, 1999). The SNAT consisted of 60 trials, three runs of 20 trials for each feedback condition (positive, neutral, negative). Intra class coefficient (ICC) analyses (modeled with a two-way mixed model using the consistency definition) showed poor (ICC<0.40, (Cicchetti, 1994)) consistency in noise blast duration after positive (ICC=0.32 [95%CI= 0.24-0.41]), neutral (ICC=0.26 [95%CI=0.17-0.35]) and negative feedback (ICC=0.17 [95%CI=0.08 - 0.26)] between W1 and W2.

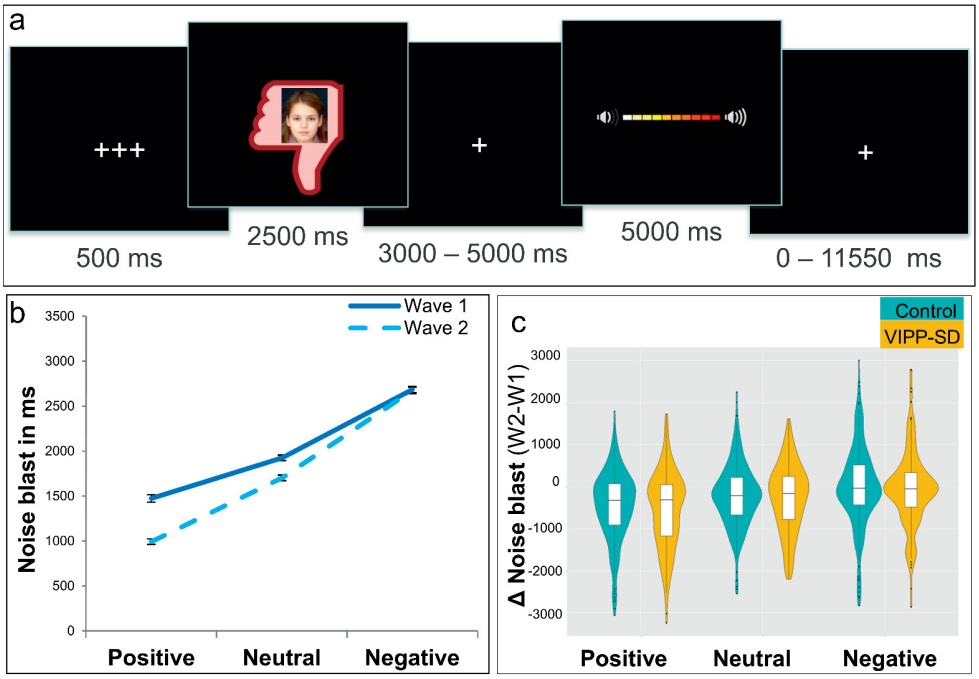


Figure 1. *Social Network Aggression Task (SNAT). a) Visualization of one trial with negative social feedback. b) Noise blast duration is influenced by condition, wave, and condition × wave. c) Individual differences in change for noise blast after positive, neutral and negative social feedback did not differ between the VIPP-Twin and control group.*

MRI data

Acquisition

MRI scans were acquired with a standard whole-head coil on a Philips Ingenia 3.0 Tesla MR system. To prevent head motion, foam inserts surrounded the children's' heads (see also Achterberg and van der Meulen (2019)). The SNAT was projected on a screen that was viewed through a mirror on the head coil. Functional scans were collected during three runs T2*-weighted echo planar images (EPI). The first two volumes were discarded to allow for equilibration of T1 saturation effect. Volumes covered the whole brain with a field of view (FOV) = 220 (ap) x 220 (rl) x 111.65 (fh) mm; repetition time (TR) of 2.2 seconds; echo time (TE) = 30 ms; flip angle (FA) = 80°; sequential acquisition, 37 slices; and voxel size = 2.75 x 2.75 x 2.75 mm. Subsequently, a high-resolution 3D T1scan was obtained as anatomical reference (FOV= 224 (ap) x 177 (rl) x 168 (fh); TR = 9.72 ms; TE = 4.95 ms; FA = 8°; 140 slices; voxel size 0.875 x 0.875 x 0.875 mm).

Preprocessing
MRI data were analyzed with SPM8 (Wellcome Trust Centre for Neuroimaging, London). The exact same preprocessing steps were used in preprocessing MRI data from W1 and W2. Images were corrected for slice timing acquisition and rigid body motion. Functional scans were spatially normalized to T1 templates. Some participants did not finish the T1 scan and were normalized to an EPI template (W1: n=5 at W1; n=10 at W2). Volumes of all participants were resampled to 3x3x3 mm voxels. Data were spatially smoothed with a 6 mm full width at half maximum (FWHM) isotropic Gaussian kernel. Translational movement parameters were calculated for all participants. Participants that had at least two out of three runs of fMRI data with <3 mm (1 voxel) motion in all directions were included in subject-specific analyses (W1: n=385; W2: n=358).

Subject-specific analyses
Statistical analyses were performed on individual subjects' data using a general linear model, previously described in Achterberg *et al.* (2018b). The fMRI time series were modeled as a series of two events convolved with the hemodynamic response function (HRF). The onset of social feedback was modeled as the first event, with a zero duration and with separate regressors for the positive, negative, and neutral peer feedback. The start of the noise blast was modeled as the second event, with the HRF modeled for the length of the noise blast and with separate regressors for noise blast after positive, negative, and neutral judgments. Trials on which the participants failed to respond in time were modeled separately as covariate of no interest and were excluded from further analyses. Additionally, six motion regressors (corresponding to the three translational and rotational directions) were included as covariates of no interest. The least squares parameter estimates of height of the best-fitting canonical HRF for each condition were used in pairwise contrasts. The pairwise comparisons resulted in subject-specific contrast images.

Confirmatory ROI analyses

ROI selection
Regions of interest were based on higher-level group analyses of W2 in an independent reference group (the non-randomized dummy control group, n=41, **Table S1**). The advantage of this approach is that the participants were in exactly the same study protocol, but were not included in the subsequent analyses, leading to an independent selection of ROIs (Poldrack, 2007). Using comparable sample sizes, we previously reported replicable results of main effects of the social network aggression task (Achterberg *et al.*, 2017). We first investigated social feedback (positive, neutral, negative) versus fixation (see *supplementary materials*, **Figure S2a** and **Table S1**). SPM8's MarsBaR toolbox (Brett *et al.*, 2002)

was used to construct ROIs based on the whole brain contrast by masking significant activation with regions from the Automated Anatomical Labeling (AAL) atlas (Tzourio-Mazoyer *et al.*, 2002). Based on a-priori hypotheses, we selected the bilateral anterior insula, inferior frontal gyrus (IFG), and medial prefrontal cortex (MPFC) from the *social feedback vs fixation* contrast, see **Figure 2**. In addition to the *social feedback vs fixation* contrast, we also investigated the specific conditions. From the contrast *positive vs negative social feedback* (see **Figure S2b** and **Table S1**), we selected the left dorsolateral prefrontal cortex (DLPFC) as additional ROI (**Figure 2**). The contrasts *negative vs positive social feedback* did not result in clusters of significant activation. The contrasts *positive vs neutral social feedback*; and *negative vs neutral social feedback* resulted in increased activation in occipital (visual) cortex (**Table S1**), but given that this was not an a priori hypothesized area, this region was not included in ROI selection.

Thus, in total, four ROIs were used in further analyses: the bilateral AI, bilateral IFG, MPFC, and the left DLPFC (see **Figure 2**). Parameter estimates (PE, average Beta values) were extracted from the subject-specific contrasts (*positive vs fixation*, *neutral vs fixation*, and *negative vs fixation*) for the entire sample minus the reference group with available MRI data on W1 (n=343) and W2 (n=317). ICC analyses (two-way mixed model using consistency) showed low consistency (ICC's<0.40, (Cicchetti, 1994)) in brain activation for the contrasts negative>neutral, negative>positive, and positive>neutral feedback between W1 and W2 (see **Table S2**).

Linear mixed effects models

To test time-related changes in participant's behavior (noise blast length) and ROI brain activation (parameter estimates) we used linear mixed effects models using the lme4 package (Bates *et al.*, 2015) in R (R Core Team, 2015). For these analyses we included the whole sample minus the reference group (n=458). Data was fitted on the average response times (for behavior) and average parameter estimates (for ROIs) after positive, neutral and negative social feedback. Two random effects were included to account for the nesting of condition and waves within participant (ChildID) and the nesting of twin-pairs within families (FamilyID). Fixed effects included feedback condition (3 levels: positive, neutral, and negative), wave (2 levels: wave 1 and wave 2), and intervention group (2 levels: VIPP-SD and control) and all 2-way and 3-way interactions. Participant's gender and estimated IQ (grand mean centered) were included as covariates and all main effects and two-way interactions between covariates and condition were included (gender ^{x} condition and condition ^{x} IQ). The fitted mixed-effect model was specified in R as:

$$Noise/ROI \sim condition * wave * intervention + condition * gender + condition * IQ + (1|childID) + (1|familyID).$$

In addition, we examined associations between brain and behavioral responses, in which we were specifically interest to what extent behavior was associated with neural activation. To this end, we added noise blast to the model including all 2 and 3-way interactions with condition and wave. Results were inspected with type III ANOVA's using Satterthwaite's method. Significant main effects of condition were further inspected using least-square means, with Kenward-Roger corrected degrees of freedom and Bonferroni adjusted p-values.

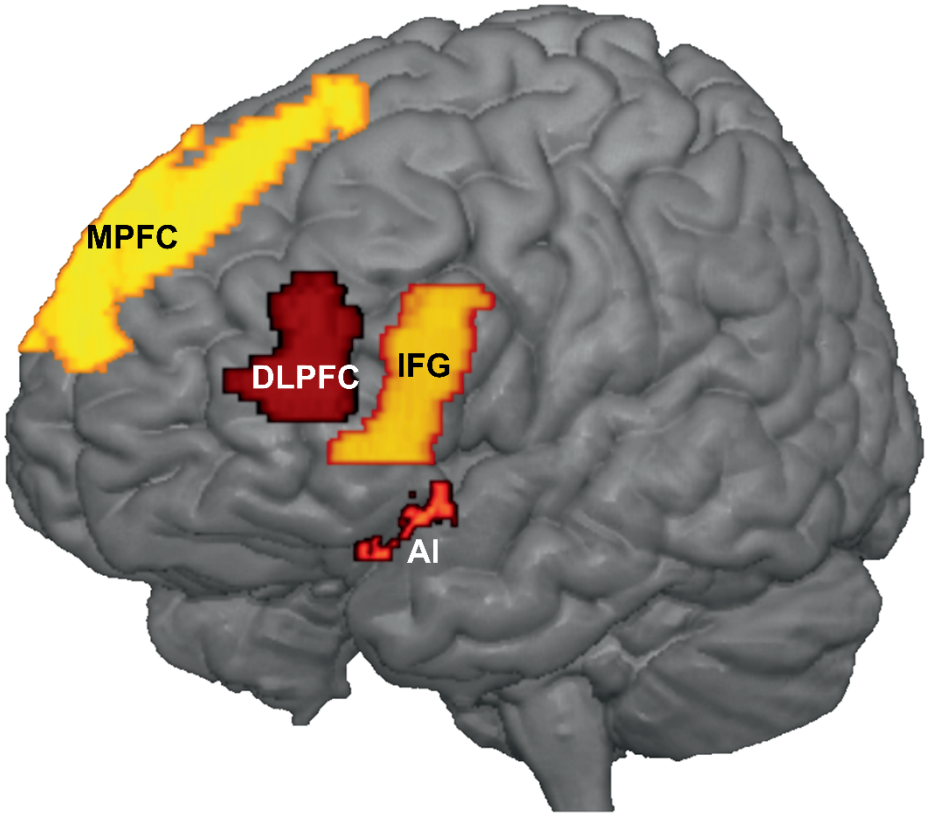


Figure 2. *Regions of interest in the left hemisphere. mPFC= medial prefrontal cortex, dlPFC = dorsolateral prefrontal cortex, IFG = inferior frontal gyrus, AI= anterior insula. IFG and AI ROIs are bilateral.*

Exploratory analyses

Whole brain analyses at wave 2

In order to prevent that specific effects were overlooked due to a smaller sample size in the reference group, we performed exploratory whole brain analyses at

wave 2 including the VIPP-SD group, the control group and the reference group (n=360). Results were False Discovery Rate (FDR) cluster corrected (*p*FDRcc<0.05), with a primary voxel-wise threshold of $p<.005$ (uncorrected) (Woo *et al.*, 2014). We computed a full factorial ANOVA with three levels (positive, negative and neutral feedback) to investigate the neural response to the social feedback. Similarly to the whole brain analyses at wave 1 (reported in Achterberg *et al.* (2018b)), we first explored the general valence effects of social evaluation, by calculating a conjunction (using the "logical AND" strategy, see Nichols *et al.* (2005)) of *positive vs neutral* and *negative vs neutral* social feedback. Next, we calculated the contrasts *negative vs positive* and *positive vs negative* to investigate brain regions that were specifically activated for social rejection or social acceptance.

Brain-behavior analyses

In addition to neural responses to social feedback, we also examined whole brain-behavior relations in late childhood (wave 2). Similar to previous brain-behavior analyses in adults (Achterberg *et al.*, 2016b) we conducted a whole brain regression analysis at the moment of receiving negative social feedback (*negative vs neutral*), with the difference in noise blast duration after negative and neutral feedback as a regressor. In this way, we tested how initial neural responses to feedback were related to subsequent aggression. The difference in noise blast was computed by:

$$\Delta NegNeut\ W2 = \ Negative\ noise\ blast\ W2 - \ Neutral\ noise\ blast\ W2.$$

To investigate brain-behavior associations across time, we computed the difference over time in noise blasts duration for the contrast negative-neutral and for brain activation in this contrast. A total of 293 participants had behavioral and brain data available at two waves and were included in the analyses regarding brain-behavior associations over time. Difference scores over time for behavior and brain were computed as follows:

$$\begin{aligned}\Delta NegNeut\ behavior \\ &= (Noise\ blast\ negative\ W2\ - Noise\ blast\ neutral\ W2) \\ &- \ (Noise\ blast\ negative\ W1\ - Noise\ blast\ neutral\ W1)\end{aligned}$$

$$\begin{aligned}\Delta NegNeut\ brain\ &= (Neural\ activity\ negative\ W2\ - Neural\ activity\ neutral\ W2) \\ &- (Neural\ activity\ negative\ W1\ - Neural\ activity\ neutral\ W1)\end{aligned}$$

Behavioral genetic analyses

To examine genetic and environmental influences on brain and behavior, we calculated Pearson within-twin correlations for mono- and dizygotic twin pairs. Similarities among twin pairs can be due to additive genetic variance (A) and

common (shared) environmental factors (C), while dissimilarities are ascribed to unique environmental influences and measurement error (E) (see **Figure S3**). We used behavioral genetic modeling with the OpenMX package (Neale *et al.*, 2016) in R (R Core Team, 2015) to calculate these A, C, and E estimates (see *supplementary materials*).

Results

Behavioral aggression following social evaluation

To test whether behavioral aggression decreased with increasing age, we performed a linear mixed-effect model on noise blast duration after feedback across two waves. The linear mixed effect model for noise blast duration showed the expected main effect of type of social feedback (**Table S3**). Noise blast duration was longer after negative feedback compared to neutral feedback, and shortest after positive feedback (all pairwise comparisons $p<.001$). We also found the expected main effect of wave (**Table S3**), with shorter noise blast durations at wave 2 compared to wave 1, indicating a decrease of behavioral aggression over time. Moreover, there was a significant condition × wave interaction effect (**Table S3**). As can be seen in **Figure 1b**, noise blast duration decreased more strongly between wave 1 and 2 after positive feedback than after negative feedback ($F=23.75$, $p<.001$) and more after positive feedback than after neutral feedback ($F=16.27$, $p<.001$). The same result was observed for neutral feedback: noise blast duration decreased more strongly between wave 1 and 2 after neutral feedback than after negative feedback ($F=5.00$, $p=.025$). That is, over time children showed a decrease in behavioral aggression, and this effect was most pronounced for aggression following positive feedback, see **Figure 1b**. We did not find any main or interaction effects of the parental intervention on behavioral aggression (**Table S3**) and visualization of the data showed large individual differences in aggression regulation in both groups (**Figure 1c**).

Confirmatory ROI analyses

Confirmatory ROI analyses were performed in two steps: First, we examined neural responses patterns after social feedback across two time points. Second, we examined relations between changes in neural activity and noise blast durations.

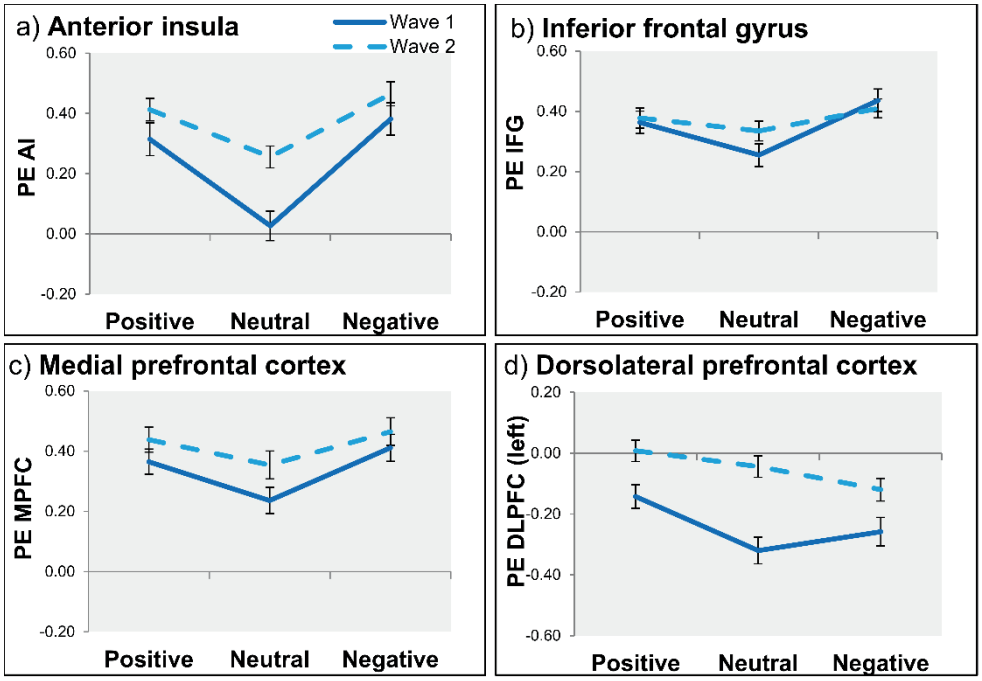


Figure 3. *Neural activation after positive, neutral and negative social feedback at wave 1 (solid lines) and wave 2 (dotted lines) for the anterior insula (a), the inferior frontal gyrus (b), the medial prefrontal cortex (c) and the dorsolateral prefrontal cortex (DLPFC). PE = parameter estimates.*

Neural responses following social evaluation

To test for developmental changes in neural responses to social feedback, we performed linear mixed effect models on four ROIs (AI, IFG, MPFC and dlPFC). As expected, we observed significant main effects of type of social feedback on neural activation in all ROIs (**Table S4**). Patterns of activity differed between the ROIs. For the AI, IFG and MPFC there was significantly more neural activation after negative and positive feedback, relative to neutral feedback (**Figure 3a**, **3b** and **3c**), but the differences between positive and negative social feedback were not significant. For the DLPFC, in contrast, there was more activation after positive social feedback compared to both neutral and negative feedback, but no significant difference between neutral and negative social feedback, see **Figure 3d**. Next, we addressed whether these activity patterns changed over time, by testing for main effects and interactions with wave. We observed a significant effect of wave in the AI, the MPFC and the DLPFC, with generally stronger neural activation at wave 2 compared to wave 1 (**Figure 3a**, **3c** , **3d** and **Table S4**). There were no main or interaction effects of the parental intervention (**Table S4**).

Brain-Behavior associations

To investigate brain-behavior associations we added noise blast duration as a factor to the previously tested models. We found a significant main effect of noise blast duration on AI and DLPFC activation (**Table S5**). These findings indicated that increased AI activation was associated with longer noise blast (B=1.11e-04), whereas increased DLPFC activation was associated with shorter noise blast (B= -3.57e-05). The IFG and MPFC did not show significant brain-behavior associations. The condition × noise blast interaction effects on brain activation in the ROIs were not significant (see **Table S5**).

Exploratory analyses

Whole brain analyses on social evaluation processing

To prevent that specific effects were overlooked by due to a relatively small sample size in the reference group, we performed exploratory whole brain analyses at wave 2 including the VIPP-SD group, the control group and the reference group (n=360). Results from the whole brain contrasts for wave 2 (children ages 9-11-years see **Figure S3, Table S6**) resulted in similar patterns of neural activation as was previously observed at wave 1 (children aged 7-9 years, Achterberg et al., 2018,) and in a different sample of adults (Achterberg et al., 2016). These results are described in more detail in the *supplement materials*.

Brain-behavior analyses on aggression following negative feedback

We conducted a whole brain regression analysis at wave 2 for receiving negative feedback (contrast Negative vs Neutral), with the difference in noise blast duration after negative and neutral feedback as a regressor (ΔNegNeut W2, see section 2.6.2.). Consistent with our hypothesis, we observed a negative association between behavioral aggression and activation in the bilateral DLPFC (**Figure 4a, Table 2**). Visualization of the effect (**Figure 4b**) showed that an increase in DLPFC activation after negative feedback (relative to neutral feedback) resulted in less subsequent behavioral aggression.

To test whether children who showed larger increases in DLPFC activity over time also showed less behavioral aggression over time, we included the data points at wave 1 to the analysis. Note that for this analysis we only included participants who had behavioral and brain data available at two waves (n=293). For these participants, we calculated the relation between the change in DLPFC activation (ΔNegNeut brain, see section 2.6.3.) in whole-brain DLPFC ROI (**Figure 4a**) and the change in noise blast duration (ΔNegNeut behavior, see section 2.6.3). We found a significant negative association (r=-.16, p=.005), indicating that children who showed the largest increase in DLPFC activation across childhood also showed the largest decrease in behavioral aggression across childhood (**Figure 4c**).

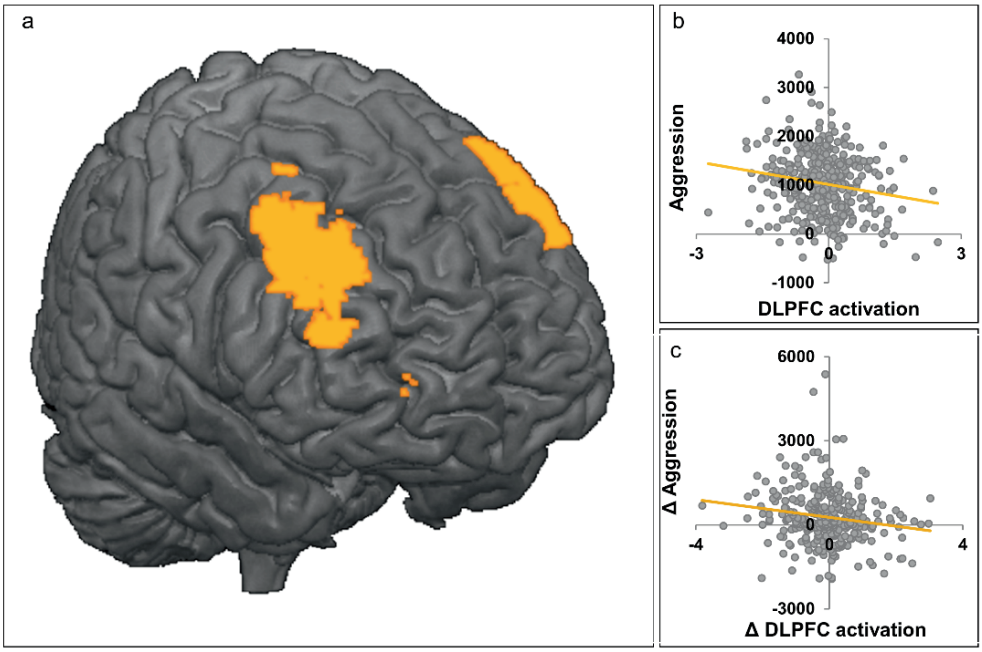


Figure 4. *Whole brain-behavior analyses with all available MRI data at wave 2 (N=360). a) Significant cluster of activation in bilateral DLPFC for negative> neutral social feedback with noise blast (Δ negative-neutral) as regressor. b) Visualization of brain-behavior association at wave 2: increased DLPFC activity after negative feedback is related to decreased aggression. c) Brain-behavior association over time: the change in DLPFC activation is negatively correlated to the change in aggression, with larger increases in DLPFC activity over time being related to larger decreases in aggression.*

Genetic and environmental influences

Given that our sample consists of both mono- and dizygotic twins, we were able to test for effects of genetics, shared environment and unique environments. As can been seen in **Table 3**, behavioral aggression was driven by a combination of genetic, shared and unique environmental factors. Variation in neural activity in the salience ROIs (AI, IFG, MPFC) showed little to no genetic influence, but did show moderate effects of shared environmental effects. Most variation was explained by the unique, non-shared environment (including measurement error). For DLPFC activation, results were inconclusive. There were some indications of heritability (i.e., on individual differences in positive-neutral), whereas individual differences were partly explained by shared environment (negative-neutral). Again, most individual differences were explained by unique non-shared environment (including measurement error).

Discussion

There is a great need to have a better understanding of the mechanisms that drive changes in emotion regulation during social interactions across childhood. The current study tested the neural signature of aggression regulation in childhood in the context of social evaluations, specifically social acceptance and social rejection. For this purpose, we made use of the unique longitudinal L-CID cohort, which allowed us to examine the development of aggression regulation within individuals over time and take into account possible effects of genetics and environmental variations. By using longitudinal behavioral-neural comparisons, we were able to address the question how change in neural activity relates to change in behavioral development. The current study revealed three main findings: 1) behavioral aggression after social evaluation decreased over time, and this decrease was most pronounced for aggression after positive and neutral social feedback; 2) confirmatory ROI analyses showed that increased activity in AI was related to more aggression, whereas increased activity in DLPFC was correlated with less aggression; and 3) bilateral DLPFC was correlated to less subsequent aggression following negative social feedback. Longitudinal comparisons confirmed that a larger increase in DLPFC activity across childhood was related to a larger decrease in behavioral aggression after negative social feedback.

The behavioral results confirmed our initial hypothesis that behavioral aggression decreases over time, consistent with prior reports on age related increases in behavioral control (Diamond, 2013; Casey, 2015). Interestingly, however, these reductions in aggression were most pronounced following positive and neural feedback, suggesting that participants were more motivated to refrain from aggression towards liked others. These findings fit well with research showing that the importance of being liked and accepted by others increases over the course of childhood and into adolescence (Rodman *et al.*, 2017; Sherman *et al.*, 2018a). Thus, with increasing age, children become more focused on refraining punishment towards people with whom they socially connect and they differentiate more between liked (individuals signaling social acceptance) and disliked (individuals signaling social rejection) others (see also Guroglu *et al.* (2014)).

By using functional neuroimaging we were able to address the neural correlates following social evaluation feedback across two time points. Consistent with prior reports (Achterberg *et al.*, 2018b), children activate the same network across two waves, with stronger activity in ACC, AI and IFG after both positive and negative social feedback (relative to neutral feedback). These findings fit well with results from the adult literature, showing that neural activation in ACC, AI, and IFG, is associated with social rejection (Eisenberger *et al.*, 2003; Cacioppo *et al.*, 2013)) and signaling social salient events (Dalgleish *et al.*, 2017). The DLPFC, in contrast, was more active for positive than

negative/neutral feedback, comparable to the behavioral results showing a stronger reduction over time in aggression following positive feedback. Interestingly, AI and DLPFC also showed opposite relations to aggression. Even though both regions increased in activation over time, stronger AI activity was associated with more behavioral aggression and stronger DLFPC activity was associated with less behavioral aggression. The AI results are comparable to a previous finding in adults with low executive control functions, showing that for individuals with low executive control AI activity and aggression were positively correlated (Chester *et al.*, 2014). Even though we did not observe changes in AI activity over time, an interesting direction for future research will be to examine whether this relation is stronger in childhood than adolescence and adulthood, when executive control functions increase.

The positive relation between DLPFC activity and aggression regulation was confirmed in several analyses. First, bilateral DLPFC activity was the only neural predictor in a whole brain regression analysis for aggression control following negative relative to neural feedback. These findings fit well with two decades of research pinpointing the DLPFC as an important regions for cognitive control development (Luna *et al.*, 2004; Luna *et al.*, 2010; Crone and Steinbeis, 2017). The current study extends this finding to the novel domain of social interactions, and demonstrates that the same 'cold' regulatory control functions are also important for regulation 'hot' emotions in social evaluation contexts (Zelazo and Carlson, 2012; Welsh and Peterson, 2014). Moreover, DLPFC activity also explains individual differences in emotion regulation following rejection. A change-change analysis confirmed that those children who showed the largest increase in DLPFC activity after negative social feedback, also showed the largest reductions in behavioral aggression following negative feedback. This study was performed in a relatively small age range, from 7-9-year old to 9-11-year old, to provide a detailed analysis of changes in childhood. The results provide a window for understanding individual differences in these developmental trajectories, showing that some children develop stronger regulation skills already in childhood. Future research should examine these questions in a longer developmental time window (including more time points) using large samples, which allows disentangling general developmental patterns from individual differences in trajectories.

An intriguing question for future research is whether and how social influences impact individual differences in developmental trajectories. In this study, we addressed this question by examining the effects of a randomized control parenting intervention. Behavioral genetic analyses revealed mostly environmental influences on both behavior and brain (moderate effects of shared environment). Therefore, it was unexpected that we did not find effects of the parental intervention on brain and behavioral outcomes. Although previous studies using VIPP-SD in younger children reported transfer effects (i.e., less externalizing problems in children (Juffer *et al.*, 2017a)) the current study did not

reveal effects for the VIPP-Twins on behavioral emotion regulation or neural activity. One possible explanation is that participants were tested in a relatively short period after the parenting interventions was completed (approximately one month), and effects on the child may only be visible after a longer time period (Bakermans-Kranenburg *et al.*, 2008). Alternatively, during the transition from middle childhood to early adolescence, peers become more important (Berndt, 2004). An interesting future direction for interventions is therefore to target the peer-environment. One particularly ecological valid way to study the peer environment is to focus on social media use (Giglietto *et al.*, 2012). Despite the fact that social media are everywhere around us and used by almost everyone on a daily basis, little scientific research has been conducted on the effects of social media on the developing brain (Crone and Konijn, 2018). Social judgment paradigms as the SNAT mimic social rejection and acceptation by peers in a way that is comparable to social media environments where individuals connect based on first impression. Future research could take into account variations of the social environment by additionally monitoring real life social media use (for example using a smartphone app, see Montag *et al.* (2017)).

Conclusion

This study set out to test longitudinal changes in neural systems underlying social evaluation and aggression regulation, and its relation to behavioral outcomes. We found an increase in behavioral control across childhood, as behavioral aggression decreased over time and DLPFC activation was related to decreased behavioral aggression. Notably, children that showed larger increases in DLPFC activity within childhood also displayed the largest longitudinal decrease in behavioral aggression. These results gain in our understanding on how the developing brain processes social feedback and suggest that the DLPFC might serve as emotion regulation mechanisms in terms of negative social feedback. However, it remains unknown how these results relate to actual, real-life social interactions such as social media use. Novel approaches are needed to bring together both real-life social media monitoring, as well as innovative experimental neuroimaging as this will provide cutting edge research and can provide insights through a neuro-mechanistic approach.

Acknowledgements

We are grateful to Dr. Mara van der Meulen for her collaboration on the longitudinal MRI data collection. The Leiden Consortium on Individual Development is funded through the Gravitation program of the Dutch Ministry of Education, Culture, and Science and the Netherlands Organization for Scientific Research (NWO grant number 024.001.003).

Supplementary Materials

Participants and sample selection

Of the initial 256 families, 10 families (3.8%) dropped out of the study directly after W1, whereas one family (n=2) was included in the L-CID study after W1. An additional 19 families (7.4%) dropped out before W2, after randomization of the parental intervention (see **Figure S1**). The remaining 456 children participated in a second lab visit at W2 (time between waves 2.06±0.10, time range: 1.86-2.53). Participants underwent an MRI scan as part of the lab visits. All anatomical MRI scans were reviewed and cleared by a radiologist from the radiology department of the Leiden University Medical Center (LUMC). Four anomalous findings were reported. To prevent registration errors due to anomalous brain anatomy, these participants were excluded. At W1, 27 participants did not start the scan due to anxiety (n=13), contraindications (n=6), or lack of parental consent for MRI participation (n=4), or technical issues with the MR system (n=4) (Achterberg and van der Meulen, 2019). Eighty-nine participants were excluded at W1 due to excessive head motion, which was defined as >3 mm motion (1 voxel) in any direction (x, y, z) in more than 2 runs of the SNAT task (3 runs in total). An additional seven participants were excluded due to data export failures. At W1, 385 participants were included in the MRI analyses (mean age 7.99 ± 0.68, 47% boys, see also Achterberg *et al.* (2018b)). At W2 48 participants did not start the scan due to anxiety (n=26), contraindications (n=10), or due to lack of parental consent for MRI participation (n=10). 46 participants were excluded at W2 due to excessive head motion and two participants were excluded due to data export failures. At W2 360 participants were included in the MRI analyses (mean age 10.01 ± 0.67, 48% boys).

Of the initial sample that participated at W1, 246 families were contacted 1.5 year after W1 to inform them on a parenting support program for parents of twins (VIPP-Twins (Euser *et al.*, 2016)). 91 families (37%) were assigned to the parental intervention group and received the VIPP-Twins, of which 9 families (9.9%) dropped out before the second MRI visit (final VIPP-Twins group: n=164, of which n=133 with sufficient quality MRI (**Figure S1**)). 129 families (52%) were assigned to the control group and received the dummy intervention, of which 7 families (5.5%) dropped out before the second MRI visit (final control group: n=244, of which n=186 with sufficient quality MRI (**Figure S1**)). Twenty-seven (11%) families did not want to be randomly assigned to one of the conditions. These families received the (non-randomly assigned) dummy intervention in order to keep this group comparable to the control group for future analyses within the longitudinal L-CID study. Given that the participants in the non-randomly assigned control group could not be included in the analyses, these participants were used as a reference group for regions of interest (ROI) selection (see section 2.4.4). Of the 27 families in the reference group, 3 dropped out before

W2. Of the remaining 48 children (**Figure S1**), 43 participated in the MRI session. Two participants were excluded due to excessive head motion. The final reference group therefore consisted of 41 participants, with a mean age of 10.13 ± 0.71 (age range: 9.09-11.28, 63% boys).

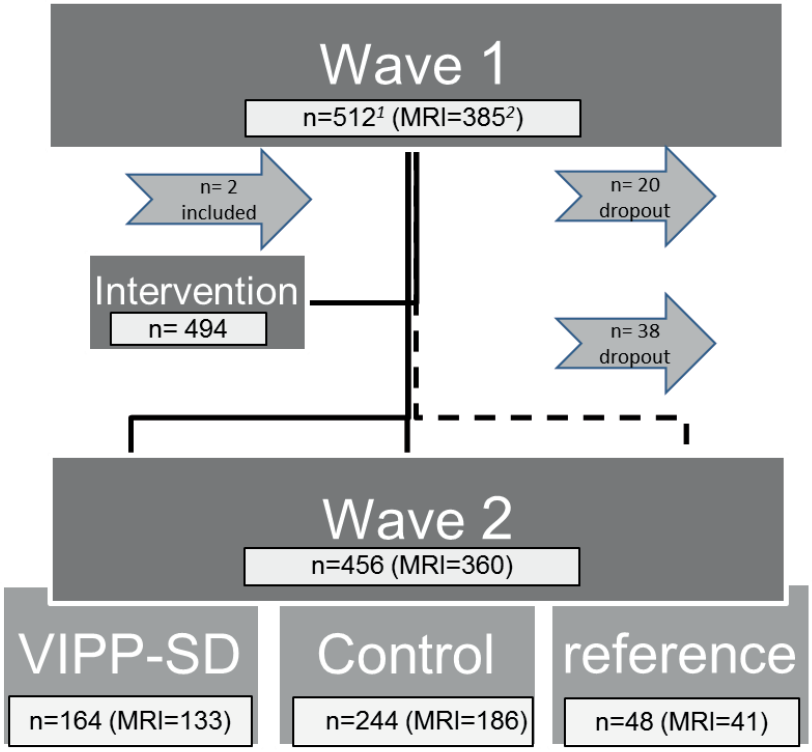


Figure S1. *Participant flowchart. minus reference group: [1] n=458, [2] n=343*

Whole brain analyses reference group

Regions of interest were based on higher level group analyses of W2 in an independent reference group (the non-randomized dummy control group, n=41, **Table S1**). A full-factorial ANOVA with three levels (positive, negative and neutral feedback) was used to investigate the neural response to the social feedback event in the reference group. Results were False Discovery Rate (FDR) cluster corrected (pFDRcc<0.05), with a primary voxel-wise threshold of p<.005 (uncorrected) (Woo *et al.*, 2014). We first investigated social feedback (positive, neutral, negative) versus fixation. This contrast resulted in activation in amongst others the fusiform gyrus, the inferior frontal gyrus, and the superior frontal gyrus (see **Figure S2a** and **Table S1**). In addition to the *social feedback vs fixation* contrast, we also investigated the specific conditions. The contrast *Positive vs*

Negative feedback resulted in activation in the right lingual gyrus, the left middle frontal gyrus, and the right inferior parietal lobule (see **Table S1**, **Figure S2**). The contrasts *positive vs neutral social feedback*; and *negative vs neutral social feedback* resulted in increased activation in occipital (visual) cortex (**Table S1**).

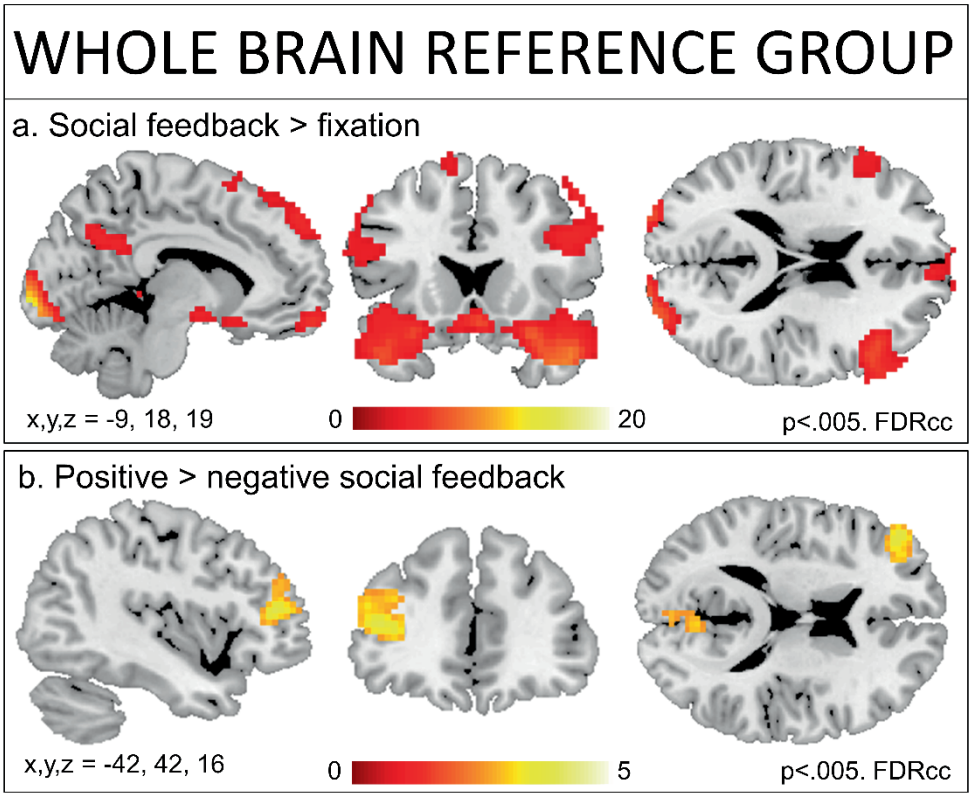


Figure S2. *Whole brain analyses for reference group (n=41).*

Behavioral genetic analyses

Similarities among twin pairs are divided into similarities due to additive genetic factors (A) and common (shared) environmental factors (C), while dissimilarities are ascribed to unique non-shared environmental influences and measurement error (E). Behavioral genetic modeling with the OpenMX package (Neale *et al.*, 2016) in R (R Core Team, 2015) was used to provide estimates of these A, C, and E components. The correlation of the shared environment (factor C) was set to 1 for both MZ and DZ twins, while the correlation of the genetic factor (A) was set to 1 for monozygotic twins and to 0.5 for dizygotic twins. The last factor, unique environmental influences and measurement error, was freely estimated (**Figure S4**). We calculated the ACE models for noise blast duration and brain activation

in the contrasts negative-neutral, negative-positive and positive-neutral. High estimates of A indicate that genetic factors play an important role, whilst C estimates indicate influences of the shared environment. If the E estimate is the highest, variance in motion is mostly accounted for by unique environmental factors and measurement error.

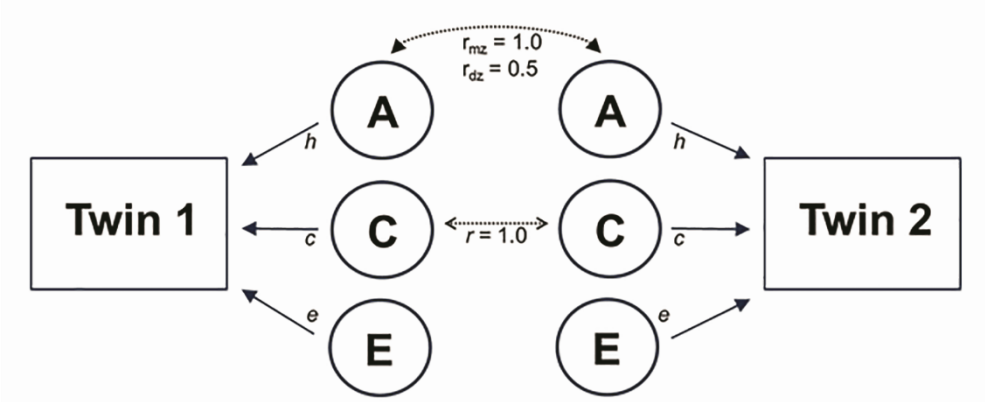


Figure S3. *ACE model. The correlation between the additive genetic factor (A) of twin 1 and 2 is set to 1.0 for monozygotic (MZ) twins and to 0.5 for dizygotic (DZ) twins. The correlation between common, shared environmental factors (C) is set to 1.0 for both MZ and DZ twins. The correlation between the unique, non-shared environmental factors (including measurement error, (E)) is freely estimated within the model.*

Exploratory whole brain analyses

To prevent that specific developmental effects were overlooked, we performed exploratory whole brain analyses at wave 2 including the VIPP-SD group, the control group and the reference group (n=360). We first investigated the general valence effects of social evaluation, that is to say, regions in the brain that were active after positive and negative feedback, relative to neutral social feedback. In doing so, we calculated a conjunction of *positive vs neutral* and *negative vs neutral* social feedback. We found common activation across positive and negative feedback in three clusters of activation: in the left AI; in the right AI extending into the right IFG; and in the occipital lobe, extending into the fusiform gyrus (**Figure S4a, Table S6**). To test for specific effects of positive versus negative social feedback, we examined pair-wise contrasts on social rejection and social acceptance. The contrast of social rejection (*negative vs positive* social feedback) resulted in significant activation in -amongst others- the right putamen/thalamus, the bilateral IFG, and the MPFC (**Figure S4b,Table S6**). The contrast of social acceptance (*positive vs negative* social feedback) resulted in two large clusters of significant activation, one cluster in the prefrontal cortex (including the superior frontal gyrus and the left and right DLPFC) and one cluster

with local maxima in the occipital lobe (including the right and left lingual gyrus extending to more parietal regions and the precuneus) see **Figure S4c** and **Table S6**.

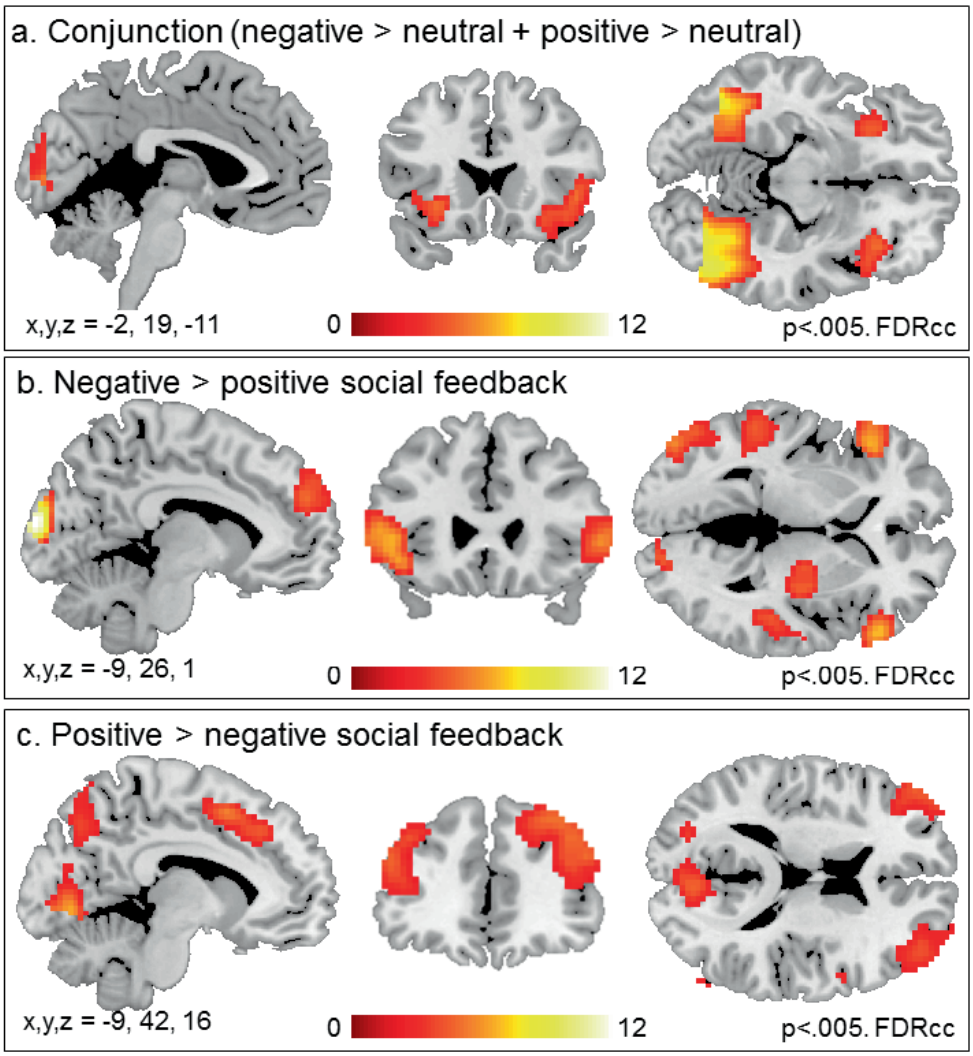


Figure S4. *Whole brain analyses for all available MRI data at wave 2 (N=360). A) Neural activation for the general valence effects of social evaluation (Conjunction of negative>neutral and positive > neutral). B) Neural activation after social rejection. C) neural activation after social acceptance.*

Table S1. MNI coordinates for local maxima activated for the whole-brain contrasts in the reference group (N=41).

Anatomical Region	Voxels	pFDRcc	T	x	y	z
Social feedback > fixation						
Right Fusiform Gyrus	7710	<.001	19.07	39	-52	-17
			18.87	39	-79	-11
			18.61	30	-94	4
Right Posterior Cingulate Cortex	790	<.001	6.53	3	-55	31
			5.03	39	-67	61
			4.87	36	-61	43
Right Inferior Frontal Gyrus	542	<.001	6.11	54	26	22
			6.08	60	29	28
			5.94	45	29	19
left Rectal Gyrus	158	0.009	5.95	0	65	-17
Right Superior Frontal Gyrus	453	<.001	4.87	15	50	49
			4.69	-9	53	46
			4.28	-12	38	55
Left Angular Gyrus	170	0.008	4.06	-48	-61	37
			3.57	-57	-55	52
			3.04	-39	-67	55
Positive > negative social feedback						
Right Lingual Gyrus	908	<.001	5.43	6	-76	-2
			5.25	-18	-85	-8
			4.70	15	-73	-5
Left Inferior/Middle Frontal Gyrus	185	0.037	4.08	-42	41	13
			4.06	-36	47	13
			3.26	-39	44	25
Right Inferior Parietal Lobule	170	0.037	3.89	57	-34	55
			3.39	69	-31	43
			3.30	63	-16	28

Table S1. (continued)

Anatomical Region	Voxels	pFDRcc	T	x	y	z
Positive > neutral social feedback						
Left Fusiform Gyrus	3186	<.001	6.43	-27	-79	-11
			6.41	24	-70	-11
			5.98	12	-76	-8
Negative > neutral social feedback						
Left Middle Occipital Gyrus	1958	<.001	7.05	-48	-79	4
			6.10	-12	-97	16
			5.29	45	-82	7

Table S2. Intra class coefficients between wave 1 and wave 2 brain activation in region of interest.

ROI	contrast	ICC	95% CI lower bound	95% CI upper bound
Insula	negative > positive	-0.05	-0.16	0.07
	negative > neutral	0.05	-0.07	0.16
	positive > neutral	-0.03	-0.14	0.09
IFG	negative > positive	-0.05	-0.16	0.07
	negative > neutral	0.10	-0.02	0.21
	positive > neutral	0.05	-0.06	0.17
mPFC	negative > positive	-0.08	-0.20	0.03
	negative > neutral	0.06	-0.05	0.17
	positive > neutral	0.03	-0.09	0.14
left DLPFC	negative > positive	0.04	-0.08	0.15
	negative > neutral	0.04	-0.07	0.16
	positive > neutral	0.05	-0.06	0.16

Table S3. Linear mixed effect model with noise blast duration as dependent variable. Output is based on type III ANOVA's using Satterthwaite's method. Significant effects are depicted in black fonts, insignificant effects in grey.

Linear Mixed Effect Models	***DF***		***F***	***p***
Condition	2	2181.60	1033.61	<0.001
Wave	1	2185.79	157.17	<0.001
Intervention Group	1	217.81	0.07	0.795
Conditon × Wave	2	2181.60	16.06	<0.001
Conditon × Intervention	2	2181.60	0.65	0.523
Wave × Intervention	1	2185.79	3.18	0.075
Conditon × Wave × Intervention	2	2181.60	0.14	0.874
Estimated IQ	1	406.16	0.01	0.928
Gender	1	217.86	1.21	0.273
Conditon × Estimated IQ	2	2181.60	13.55	<0.001
Conditon × Gender	2	2181.60	2.26	0.104

Table S4. Linear mixed effect model with brain activation in regions of interest as dependent variable. Output is based on type III ANOVA's using Satterthwaite's method. Significant effects are depicted in black fonts, insignificant effects in grey.

Linear Mixed Effect Models		***DF***	***F***	***p***
Anterior Insula				
Condition	2	1526.24	27.79	<0.001
Wave	1	1783.92	10.09	<0.001
Intervention Group	1	181.80	0.00	0.953
Conditon × Wave	2	1526.24	2.06	0.127
Conditon × Intervention	2	1526.24	0.83	0.437
Wave × Intervention	1	1783.75	0.11	0.737
Conditon × Wave × Intervention	2	1526.24	0.93	0.394
Estimated IQ	1	313.02	1.88	0.171
Gender	1	182.36	0.19	0.663
Conditon × Estimated IQ	2	1526.24	0.61	0.544
Conditon × Gender	2	1526.24	0.83	0.435
Inferior Frontal Gyrus				
Condition	2	1531.45	8.22	<0.001
Wave	1	1804.24	0.54	0.461
Intervention Group	1	175.23	0.15	0.696
Conditon × Wave	2	1531.45	1.58	0.205
Conditon × Intervention	2	1531.45	0.60	0.549
Wave × Intervention	1	1804.11	3.17	0.075
Conditon × Wave × Intervention	2	1531.45	0.00	0.997
Estimated IQ	1	278.98	0.52	0.471
Gender	1	175.66	2.53	0.113
Conditon × Estimated IQ	2	1531.45	0.84	0.430
Conditon × Gender	2	1531.45	2.10	0.123

Table S4. (continued)

Linear Mixed Effect Models		***DF***	***F***	***p***
Medial Prefrontal Cortex				
Condition	2	1530.08	6.64	0.001
Wave	1	1790.59	5.61	0.018
Intervention Group	1	161.09	0.69	0.408
Conditon × Wave	2	1530.08	0.61	0.543
Conditon × Intervention	1	1790.41	2.43	0.119
Wave × Intervention	2	1530.08	0.26	0.769
Conditon × Wave × Intervention	1	314.32	0.03	0.853
Estimated IQ	1	161.60	0.93	0.337
Gender	2	1530.08	0.64	0.527
Conditon × Estimated IQ	2	1530.08	1.32	0.267
Conditon × Gender	2	1530.08	0.44	0.646
Dorsolateral Prefrontal Cortex				
Condition	2	1532.09	8.21	0.000
Wave	1	1788.11	34.44	0.000
Intervention Group	1	187.98	0.00	0.993
Conditon × Wave	2	1532.09	2.53	0.080
Conditon × Intervention	2	1532.09	0.95	0.386
Wave × Intervention	1	1787.97	0.10	0.747
Conditon × Wave × Intervention	2	1532.09	0.04	0.958
Estimated IQ	1	300.71	5.67	0.018
Gender	1	188.49	0.05	0.827
Conditon × Estimated IQ	2	1532.09	4.21	0.015
Conditon × Gender	2	1532.09	1.98	0.138

Table S5. Linear mixed effect models with brain activation in regions of interest as dependent variable and noise blast duration added as factor. Output is based on type III ANOVA's using Satterthwaite's method. Significant effects are depicted in black fonts, insignificant effects in grey.

Linear Mixed Effect Models	*DF*		*F*	*p*
Anterior Insula				
Condition	2	1693.46	14.59	<0.001
Noise blast	1	1908.4	5.47	0.019
Wave	1	1808.94	9.26	0.002
Intervention Group	1	181.67	0.01	0.907
Conditon × Wave	2	1659.61	1.18	0.306
Conditon × Intervention	2	1525.39	0.81	0.447
Conditon × Noise blast	2	1728.48	1.09	0.337
Wave × Intervention	1	1785.34	0.13	0.718
Wave × Noise blast	1	1913.4	1.74	0.188
Conditon × Wave × Intervention	2	1525.17	1.03	0.356
Conditon × Wave × Noise blast	2	1676.93	0.45	0.637
Estimated IQ	1	317.03	1.91	0.168
Gender	1	182.85	0.29	0.592
Conditon × Estimated IQ	2	1531.67	0.56	0.569
Conditon × Gender	2	1526.86	0.90	0.406
Inferior Frontal Gyrus				
Condition	2	1709.10	5.45	0.004
Noise blast	1	1872.52	2.57	0.109
Wave	1	1830.86	0.83	0.363
Intervention Group	1	172.89	0.20	0.655
Conditon × Wave	2	1673.03	1.60	0.202
Conditon × Intervention	2	1527.06	0.52	0.592
Conditon × Noise blast	2	1752.47	0.34	0.711
Wave × Intervention	1	1804.98	3.14	0.077
Wave × Noise blast	1	1929.34	1.07	0.302
Conditon × Wave × Intervention	2	1526.81	0.01	0.994
Conditon × Wave × Noise blast	2	1695.95	0.06	0.940
Estimated IQ	1	280.10	0.80	0.373
Gender	1	174.04	2.89	0.091

Table S5. (continued)

Linear Mixed Effect Models	*DF*		*F*	*p*
Conditon × Estimated IQ	2	1533.92	0.70	0.498
Conditon × Gender	2	1528.65	2.22	0.109
Medial Prefrontal Cortex				
Condition	2	1699.33	5.73	0.003
Noise blast	1	1895.96	2.71	0.100
Wave	1	1816.12	8.20	0.004
Intervention Group	1	159.34	0.81	0.370
Conditon × Wave	2	1665.49	1.00	0.369
Conditon × Intervention	2	1529.67	0.52	0.594
Conditon × Noise blast	2	1736.36	0.48	0.621
Wave × Intervention	1	1791.29	2.22	0.136
Wave × Noise blast	1	1910.81	4.59	0.032
Conditon × Wave × Intervention	2	1529.44	0.20	0.815
Conditon × Wave × Noise blast	2	1684.20	1.31	0.271
Estimated IQ	1	316.05	0.00	0.959
Gender	1	160.39	1.17	0.282
Conditon × Estimated IQ	2	1536.06	0.39	0.675
Conditon × Gender	2	1531.15	1.39	0.248
Dorsolateral Prefrontal Cortex				
Condition	2	1697.56	0.93	0.396
Noise blast	1	1911.70	4.32	0.038
Wave	1	1810.80	10.22	0.001
Intervention Group	1	187.45	0.00	0.958
Conditon × Wave	2	1664.25	3.34	0.036
Conditon × Intervention	2	1532.15	1.08	0.339
Conditon × Noise blast	2	1731.91	0.70	0.499
Wave × Intervention	1	1788.91	0.12	0.726
Wave × Noise blast	1	1918.14	0.07	0.797
Conditon × Wave × Intervention	2	1531.93	0.03	0.968
Conditon × Wave × Noise blast	2	1680.74	1.48	0.228
Estimated IQ	1	305.09	5.19	0.023
Gender	1	188.65	0.01	0.912
Conditon × Estimated IQ	2	1538.32	4.88	0.008
Conditon × Gender	2	1533.61	1.96	0.141

Table S6. MNI coordinates for local maxima activated for the whole brain contrast in the whole sample at wave 2 (N=358). Results were FDR cluster corrected (p_{FDR}<0.05), with a primary voxel-wise threshold of p<0.005.

Anatomical Region	Voxels	pFDRcc	T	x	y	z
Conjunction of negative>neutral and positive> neutral social feedback						
Left Middle Occipital Gyrus	3527	<.001	12.45	-48	-79	1
Right Fusiform Gyrus			11.48	27	-76	-8
Right Middle Occipital Gyrus			10.43	48	-73	-2
Left Insula	206	0.024	5.47	-30	26	-8
Left Insula			3.42	-42	17	-2
Left Insula			3.06	-39	23	-17
Right Inferior Frontal Gyrus	266	0.013	4.96	48	20	-2
Right Inferior Frontal Gyrus			4.80	33	26	-14
Right Insula			3.75	39	32	4
Negative > positive social feedback						
Left Calcarine Gyrus	554	<.001	12.21	-6	-97	10
Left Superior Occipital Gyrus			11.78	-12	-94	19
Right Superior Occipital Gyrus			7.56	24	-91	16
Right Inferior Frontal Gyrus	200	0.015	6.62	57	32	1
Left Middle Occipital Gyrus	608	<.001	6.56	-48	26	1
Left Inferior Frontal Gyrus			6.08	-45	26	-8
Left Middle Temporal Gyrus			5.57	-54	8	-23
Left Middle Occipital Gyrus	236	0.009	5.49	-48	-82	1
Left Middle Occipital Gyrus			4.42	-54	-73	1
Left Middle Temporal Gyrus			3.89	-54	-61	4
Left Superior Medial Gyrus	366	0.002	5.20	-6	53	31
Left Superior Frontal Gyrus			4.80	-18	47	31
Left Superior Frontal Gyrus			3.71	-15	62	25
Right Superior Temporal Gyrus	567	<.001	5.00	48	-34	7
Right Putamen			4.90	33	-13	4

Table S6. (continued)

Anatomical Region	Voxels	pFDRcc	T	x	y	z
Negative > positive social feedback						
Right Thalamus			4.40	21	-10	-2
Left Postcentral Gyrus	337	0.003	4.69	-42	-16	40
Left Postcentral Gyrus			4.42	-42	-19	28
Left SupraMarginal Gyrus			3.83	-42	-37	28
Left Middle Temporal Gyrus	178	0.020	4.51	-54	-25	-5
Left Middle Temporal Gyrus			4.34	-57	-37	1
Left Middle Temporal Gyrus			3.84	-48	-40	4
Right Precentral Gyrus	133	0.044	4.14	42	-16	43
Right Precentral Gyrus			4.06	51	-10	43
Right Postcentral Gyrus	313	0.003	3.89	24	-34	61
Right Postcentral Gyrus			3.88	21	-34	76
Right Superior Parietal Cortex			3.19	24	-46	70
Positive > negative social feedback						
Right Lingual Gyrus	3999	<.001	13.80	6	-73	-2
Right Lingual Gyrus			9.61	21	-70	-5
Left Lingual Gyrus			8.94	-18	-85	-2
Right Middle Frontal Gyrus (DLPFC)	4230	<.001	7.72	39	35	43
Right Superior Frontal Gyrus			7.10	27	5	61
Right Middle Frontal Gyrus (DLPFC)			6.69	48	23	40

CHAPTER SIX

Distinctive heritability patterns of subcortical-prefrontal cortex resting state connectivity in childhood: A twin study

This chapter is published as: Achterberg M., Bakermans M.J., Van IJzendoorn M.H., Van der Meulen M., Tottenham N. & Crone E.A.M. (2018), Distinctive heritability patterns of subcortical-prefrontal cortex resting state connectivity in childhood: A twin study, *NeuroImage, 175*: 138-149.

Abstract

Connectivity between limbic/subcortical and prefrontal-cortical brain regions develops considerably across childhood, but less is known about the heritability of these networks at this age. We tested the heritability of limbic/subcortical-cortical and limbic/subcortical-subcortical functional brain connectivity in 7- to 9-year-old twins (N=220), focusing on two key limbic/subcortical structures: the ventral striatum and the amygdala, given their combined influence on changing incentivied behavior during childhood and adolescence. Whole brain analyses with ventral striatum (VS) and amygdala as seeds in genetically independent groups showed replicable functional connectivity patterns. The behavioral genetic analyses revealed that in general VS and amygdala connectivity showed distinct influences of genetics and environment. VS-prefrontal cortex connections were best described by genetic and unique environmental factors (the latter including measurement error), whereas amygdala-prefrontal cortex connectivity was mainly explained by environmental influences. Similarities were also found: connectivity between both the VS and amygdala and ventral anterior cingulate cortex (vACC) showed influences of shared environment, while connectivity with the orbitofrontal cortex (OFC) showed heritability. These findings may inform future interventions that target behavioral control and emotion regulation, by taking into account genetic dispositions as well as shared and unique environmental factors such as child rearing.

Keywords: Amygdala; Behavioral Genetics; Functional Brain Connectivity; Subcortical-Cortical Connectivity; Ventral Striatum

Introduction

The contributions of limbic brain regions and the prefrontal cortex (PFC) to enhanced coordination in affective/motivational behaviors change considerably from childhood to adulthood (van Duijvenvoorde *et al.*, 2016b). Resting State functional MRI (RS-fMRI) studies on limbic/subcortical-cortical functional brain connectivity in adults have provided insights into the connectivity patterns between different limbic/subcortical (sub) regions and the PFC, with positive connectivity between limbic/subcortical regions and affective PFC regions, and negative connectivity between limbic/subcortical regions and dorsal control regions of the PFC (Di Martino *et al.*, 2008; Roy *et al.*, 2009; Choi *et al.*, 2012). Despite the consistent findings in general connectivity patterns in adults, not much is known about the robustness of these effects in children, and the role of genetic and environmental influences on limbic/subcortical- PFC brain connectivity. To date, the size of environmental and genetic contributions to limbic/subcortical-PFC connectivity has not been examined in children. In this study, we therefore investigated the robustness of findings regarding limbic/subcortical-PFC functional brain connectivity in childhood, and the heritability of these connections in 7-to-9-year-old twins (N=220). The current paper is the first to investigate childhood RS connectivity in two independent samples *and additionally* explore genetic and environmental influences on that connectivity, thereby providing important insights in the underlying mechanisms of functional brain connectivity in childhood.

RS-fMRI studies in adults have shown that the striatum is functionally connected to distributed regions throughout the entire brain, including motor, cognitive, and affective systems (Di Martino *et al.*, 2008; Barnes *et al.*, 2010; Choi *et al.*, 2012). Different sub regions within the striatum show distinct functional connectivity patterns (Di Martino *et al.*, 2008; Choi *et al.*, 2012). A pioneering study of Choi *et al.* (2012) revealed distinct cortical-connectivity for five different sub regions in the striatum. For example, a dorsal sub region of the striatum was mainly connected to a network of the dorsolateral PFC (dlPFC), the dorsal medial PFC (dmPFC), and parietal regions, whereas a more ventral sub region of the striatum was primarily connected to medial/orbitofrontal regions of PFC (Di Martino *et al.*, 2008; Choi *et al.*, 2012). In the current study we focused on the ventral striatum, since this striatal sub region is consistently implicated in affective/motivational behavior (Haber and Knutson, 2010). Adult studies revealed that the ventral striatum is positively connected to limbic-affective regions such as the ventral medial PFC (vmPFC), the ventral anterior cingulate cortex (vACC), the orbitofrontal cortex (OFC), and the insula (Di Martino *et al.*, 2008; Choi *et al.*, 2012). In contrast, negative connectivity has been reported between the ventral striatum and cortical regions related to cognitive control, such as the dlPFC, the dorsal anterior cingulate cortex (dACC), the parietal cortex, and the precuneus (Di Martino *et al.*, 2008). The amygdala also shows negative

connectivity with dorsal cortical regions, including the dlPFC, dACC, dmPFC, the parietal cortex, and to the cerebellum (Roy *et al.*, 2009). The positive connectivity patterns from the amygdala are ventrally oriented, including the vmPFC, the rostral ACC, and the OFC, but also more temporally oriented, towards the insula and inferior frontal gyrus (IFG) (Stein *et al.*, 2007; Roy *et al.*, 2009).

The development of limbic/subcortical-prefrontal cortex functional brain connectivity from childhood to adulthood has also been studied with RS-fMRI (e.g., Fareri *et al.* (2015), Gabard-Durnam *et al.* (2014), van Duijvenvoorde *et al.* (2016a)). Developmental studies consistently report an overall shift from local limbic/subcortical-subcortical connectivity in childhood towards more distributed long-range limbic/subcortical-cortical connectivity in adulthood (Fair *et al.*, 2009; Vogel *et al.*, 2010; Menon, 2013; Rubia, 2013). However, this age-related shift from local to distributed connectivity was called into question after several studies had shown that these developmental changes were largely influenced by age-related changes in head-motion (Van Dijk *et al.*, 2010; Power *et al.*, 2012). That is to say, head motion can result in substantial changes in RS-fMRI connectivity (Van Dijk *et al.*, 2010; Power *et al.*, 2012). Specifically, volume-to-volume micro movement (i.e., head motion between two frames) can overestimate short-distance connectivity and underestimate long-distance connectivity (Satterthwaite *et al.*, 2013). Young children usually have more difficulty lying still, resulting in more volume-to-volume micro movement, which may have resulted in an underestimation of subcortical-cortical brain connectivity in childhood. Therefore, there is a need to better understand connectivity patterns in childhood, using large samples and replication designs.

The PFC gradually develops both structurally and functionally until maturation in early adulthood (Lenroot and Giedd, 2006; van Duijvenvoorde *et al.*, 2016a). Both the striatum and the amygdala show plasticity to the environment (for a review, see Tottenham and Galvan (2016)). For example, caregiving adversity during childhood (neglect, institutional care or low parental warmth) has been associated with amygdala hyper reactivity during adolescence (Tottenham *et al.*, 2011; Garrett *et al.*, 2012; Casement *et al.*, 2014). In addition, adults and adolescents with a history of childhood stress show less striatum activity when receiving a monetary reward (Goff *et al.*, 2013; Boecker *et al.*, 2014; Hanson *et al.*, 2016). Given these environmental influences on ventral striatum and amygdala activity, the connectivity between these limbic regions and cortical PFC regions may also be influenced by environmental factors. Alternatively, the high commonality of psychiatric disorders that rely on limbic/subcortical-PFC connections in families may suggest a heritability factor as well (Bouchard and McGue, 2003; Flint and Kendler, 2014). It is important to note that heritability estimates for brain anatomy and connectivity differ across development such that heritability estimates are stronger in adulthood than in childhood (Lenroot *et al.*, 2009; van den Heuvel *et al.*, 2013).

The few studies that examined these contributions in monozygotic (MZ) and dizygotic (DZ) twins in adults reported significant influences of genetics on functional connectivity, with little shared environmental influences (for a review see Richmond *et al.* (2016)), although some studies reported influences of both genetics and shared environment (Yang *et al.*, 2016). Prior findings are mostly based on adult twin studies, whereas limbic/subcortical-PFC connectivity changes considerably during child and adolescent development. That is to say, functional connectivity from the ventral striatum and the amygdala with (medial) prefrontal regions increases substantially during development (Gabard-Durnam *et al.*, 2014; Fareri *et al.*, 2015; van Duijvenvoorde *et al.*, 2016a). This increase in long range interactions between the ventral striatum, the amygdala, and the PFC may contribute to the improved ability of children to regulate behavior and emotions in the transition to adolescence (Somerville *et al.*, 2010; Ernst, 2014; Casey, 2015). Together, these findings underscore the importance of studying heritability of RS brain connectivity in childhood.

Taken together, the aims of the current study were to investigate (1) the robustness of limbic/subcortical-cortical and limbic/subcortical-subcortical brain connectivity in childhood, and (2) the heritability of these connections in 7-to-9-year-old twins (N=220). We included 7- to-9-year-old twins since they are old enough to produce relatively good MRI data, while still representing (middle) childhood as a developmental phase. The study pursued two goals: 1) to investigate subcortical-cortical and subcortical-subcortical brain connectivity in childhood using two key limbic structures: the ventral striatum and the amygdala, and 2) to examine the heritability of these connections comparing MZ and DZ twins. We specifically focused on connectivity between limbic/subcortical regions and six PFC regions: the vmPFC, the vACC, the OFC, the dmPFC, the dACC and the dlPFC. These regions have been shown to be functionally connected to both the ventral striatum and the amygdala in adults (Di Martino *et al.*, 2008; Roy *et al.*, 2009) and display developmental changes related to increased cognitive control and emotion regulation (Somerville *et al.*, 2010; Ernst, 2014; Casey, 2015), making them key targets to study in our sample.

The first question, regarding replicability of childhood RS connectivity, was addressed in two independent samples in order to examine connectivity patterns without genetic components. This allowed us to test for replication, thereby contributing to the debate about reproducibility of neuroscientific patterns (Open Science, 2015). Next, we specifically focused on RS-fMRI connectivity from the ventral striatum and amygdala to the six PFC regions and two additional subcortical regions (thalamus and hippocampus); since prior studies have shown that these regions show important developmental effects (Gabard-Durnam *et al.*, 2014; Fareri *et al.*, 2015). Based on prior studies, we expect to find replicable and robust resting state connectivity in childhood (Misic and Sporns, 2016), with distinctive patterns for ventral striatum and amygdala (Roy *et al.*, 2009; Choi *et al.*, 2012; Porter *et al.*, 2015).

To address the second question, concerning the heritability of limbic connectivity, we compared MZ and DZ twin pairs using ACE modeling. This decomposition model provides an estimate of the proportions of the variance in the data that are attributed to heritable, shared environmental, and unshared/unique environmental factors. Previous studies have shown both influences of genetics (Richmond *et al.*, 2016) and environmental contributions (Tottenham and Galvan, 2016), indicating that there could be an interplay between genetics and environment (Yang *et al.*, 2016).

Methods

Participants

Participants were part of the Leiden Consortium on Individual Development (L-CID) twin study. Families with a same-sex twin pair born between 2006 – 2009, living within two hours travel time from Leiden, were recruited through the Dutch municipal registry and received an invitation by mail to participate. 256 families with a twin pair (512 children) were included in the L-CID study, of which 443 children underwent the RS scan (Table S1). The Dutch Central Committee on Human Research (CCMO) approved the study and its procedures (NL50277.058.14). Written informed consent was obtained from both parents. Families received financial compensation (€80.00) for their participation in the L-CID study. All participants were fluent in Dutch, had normal or corrected-to-normal vision, and were screened for MRI contra indications. All anatomical MRI scans were reviewed and cleared by a radiologist from the radiology department of the Leiden University Medical Center (LUMC). Three anomalous findings were reported and these participants were excluded. Participants' intelligence (IQ) was estimated with a verbal intelligence subtest (Similarities) and a performance intelligence subtest (Block Design) of the Wechsler Intelligence Scale for Children, third edition (WISC-III, Wechsler (1991)).

Since head motion can result in substantial changes in RS-fMRI connectivity (Van Dijk *et al.*, 2010; Power *et al.*, 2012), we investigated micro-movement using the motion outlier tool in FSL version 5.0.9 (FMRIB's Software Library, Smith *et al.* (2004)). Volumes with more than 0.5 mm framewise displacement (FD) were flagged as outliers. In line with recent studies (Couvy-Duchesne *et al.*, 2014; Engelhardt *et al.*, 2017), our twin analyses indicated that motion (amount of FD) was heritable. That is to say, there was a stronger correlation within MZ than DZ twins (r_{mz}=.44, p<.001; r_{dz}=.25, p=.02). Behavioral genetic modeling of the amount of motion in the initial sample pointed towards genetic influences (A=38%, 95 confidence interval (CI): 26-56%, see Table S2). Children with more than 20% of their volumes flagged were excluded from further analyses (Power *et al.*, 2012). In total, 209 participants (47.5%) were

excluded based on excessive head motion. An additional 11 participants were excluded due to registration problems. The final sample consisted of 220 children (41% boys, mean age 8.00±0.67, age range 7.02-9.08), of which 64 complete twin pairs (128 children, 58% MZ). There was no association between age and motion in the final sample (r=.06, p=.35). Moreover, there were no significant influences of heritability for head motion in the final sample (A=0%, 95% CI: 0-35%, see Table S2), implying that only more extreme motion is heritable, and this is not true of more subtle motion. For an overview of sample selection and dropout, see Table S1.

For the first set of analyses (examining replicability of childhood RS connectivity) we divided the sample into two subsamples of genetically independent individuals. Of the 64 complete twin pairs, we randomly chose either the youngest or oldest child within a twin pair. The other half of the twin pair was left out of the replication analyses. The replication sample therefore consisted of 156 (220-64) genetically independent children who were divided over two samples of N=78. Table 1 provides an overview of demographic characteristics, estimated IQ and motion in samples I and II. There were no significant differences in demographic characteristics between the samples (Table 1). Moreover, the distribution of gender did not significantly differ from chance (Sample I - 45% boys, t(77)=0.91, p=.37; Sample II - 44% boys, t(77)=1.13, p=.26).

For the second set of analyses (testing heritability of childhood RS connectivity), we estimated the contributions of genetic and environmental factors to subcortical-cortical and subcortical-subcortical functional brain connectivity using behavioral genetic modelling on seed-ROI connections. The complete twin pairs were therefore divided in monozygotic (N=37) and dizygotic (N=27) twin pairs. Table 2 provides an overview of demographic characteristics, estimated IQ and motion in MZ and DZ twins. There were no significant differences in demographic characteristics between the samples (Table 2). For the twin samples, the distribution of gender significantly differed from chance, with the inclusion of fewer boys than girls in both samples (MZ - 35% boys, t(73)=2.66, p=.01; DZ - 30% boys, t(53)=3.25, p=.002).

Data Acquisition

MRI scans were acquired with a standard 32 channel whole-head coil on a Philips Ingenia 3.0 Tesla MR system. Resting state data was acquired at the end of a fixed imaging protocol. Children were instructed to lie still with their eyes closed for 5 minutes. They were explicitly told not to fall asleep. To prevent head motion, foam inserts surrounded the children's heads. A total of 142 T2 -weighted whole-brain echo planar images (EPIs) were acquired, including 2 dummy volumes preceding the scan to allow for equilibration of T1 saturation effects (scan duration 316.8 sec; repetition time (TR) = 2.2 sec; echo time (TE) = 30 ms; flip

angle = 80°; field of view (FOV, in mm) = 220.000 (rl) x 220.00 (ap) x 111.65 (fh); 37 slices). In addition, a high-resolution EPI scan was obtained for registration purposes (scan duration 46.2 sec; TR = 2.2 sec; TE = 30 ms, flip angle = 80°, FOV= 220.000 (rl) x 220.00 (ap) x 168.00 (fh), 84 slices), as well as a T1-weighted anatomical scan (scan duration 296.6 s; TR = 9.72 sec; TE = 4.59 ms, flip angle = 8°, FOV = 177.333 (rl) x 224.000 (ap) x 168.000 (fh), 140 slices). Since motion causes substantial artifacts within structural scans, we visually inspected the quality of the T1-weighted anatomical scan directly after acquisition. If the scan was affected by motion (blurry T1 image), we repeated the T1 scan. This was the case for 3% of the included participants.

Table 1. Comparison of demographic characteristics of replication samples I and II.

	Sample I	**Sample II**	**Statistics**
n	78	78	
Boys	45%	44%	$\chi(1, N=156)=0.26$, $p=.872$
Left handed	8%	14%	$\chi(1, N=156)=1.65$, $p=.199$
AXIS-I disorder	2 (ADHD, GAD)	1 (ADHD)	$\chi(1, N=156)=0.34$, $p=.560$
Age (SD)	8.01 (0.69)	8.02 (0.69)	$t(154)= -.14$, $p=.887$
Range	7.02 -9.07	7.03 - 9.08	
Mean IQ (SD)	103.75 (11.96)	106.03 (12.26)	$t(154)=-1.17$, $p=.242$
IQ range	80.00-137.50	77.50-137.50	
Frames >0.5 mm FD	7%	7%	$t(154)=.25$, $p=.800$

ADHD: Attention deficit hyperactivity disorder; GAD: Generalized Anxiety Disorder; FD: Framewise Displacement

Data Preprocessing

The preprocessing of resting-state fMRI data was carried out using FMRIB's Expert Analysis Tool (FEAT; version 6.00) as implemented in FSL version 5.09 (Smith *et al.*, 2004). The following preprocessing steps were used: motion correction (MCFLIRT; Jenkinson *et al.* (2002)), slice time correction, removal of non-brain tissue using the Brain Extraction Tool (BET; Smith (2002)), spatial smoothing using a Gaussian kernel of 6 mm full width at half maximum, and high-pass temporal filtering (Gaussian weighted least-squares straight line fitting, with sigma = 100 sec, 0.01 Hz cut-off). To register fMRI scans to standard space, each subject's functional scan was registered to the corresponding high resolution EPI

scan, by using FMRIB's Linear Image Registration Tool (FLIRT, Jenkinson *et al.* (2002)). Next, an integrated version of boundary based registration (BBR; Greve and Fischl (2009)) was performed to improve the accuracy of the registration from high resolution EPI to subjects' structural space. Lastly, FMRIB's Nonlinear Imaging Registration Tool (FNIRT) with a 10 mm warp resolution was used to further refine registration from subjects' structural space to standard MNI-152 space (Jenkinson and Smith, 2001; Jenkinson *et al.*, 2002). To ensure accurate alignment, we visually inspected the summery of the registration for all participants. Examples of correct and incorrect registration can be found in the supplementary materials (Figure S1). In total, 11 participants were excluded due to registration problems (Table S1).

Table 2. Demographic characteristics of the mono- and dizygotic twins.

	Monozygotic	Dizygotic	Statistics
n	74 (37 pairs)	54 (27 pairs)	
% boys	35%	30%	$\chi(1, N=128)=0.43$, $p=.570$
Left handed	11%	6.00%	$\chi(1, N=128)=1.10$, $p=.354$
AXIS-I disorder	none	1 (ADHD)	$\chi(1, N=128)=1.38$, $p=.422$
Age (SD)	8.01 (0.72)	7.88 (0.56)	$t(126)= 1.05$, $p=.294$
Range	7.03-9.05	7.15 - 8.94	
Mean IQ (SD)	106.21 (12.09)	103.52 (10.10)	$t(126)=1.34$, $p=.184$
IQ range	77.50-137.50	77.50-130.00	
Frames >0.5 mm FD	6%	7%	$t(126)=-0.97$, $p=.336$

First-Level Seed Based Analysis

To investigate limbic/subcortical-cortical and limbic/subcortical-subcortical functional brain connectivity we used two subcortical seeds: the ventral striatum (VS) and the amygdala (AMY). The VS seed was based on the "limbic striatum" of the Oxford-GSK-Imanova structural connectivity striatal atlas (Tziortzi *et al.*, 2014). The AMY seed was based on the Harvard-Oxford subcortical structural atlas. Seeds were anatomical, bilateral and thresholded at ≥75% probability, resulting in a VS seed of 197 voxels and an AMY seed of 254 voxels (Fig 1). To extract subject specific time series, seeds were first registered to subject space

by using FLIRT (Jenkinson *et al.*, 2002). The subject-specific seeds were then used to extract time series from preprocessed RS data.

First-level general linear models (GLM) were performed separately on time-series from each seed. The following nuisance signals were included: global signal, white matter (WM), cerebral spine fluid (CSF), 6 motion parameters and FD outliers. The global signal was included to reduce the influence of artifacts caused by physiological processes (i.e., cardiac and respiratory fluctuations) and scanner drifts (Birn *et al.*, 2006; Fox and Raichle, 2007). In order to extract the time series for WM and CSF, we used subject specific WM and CSF masked, which were generated with FMRIB's Automated Segmentation Tool (FAST, Zhang *et al.* (2001)). Additionally, each frame with an FD outlier, (FD>0.5 mm) was represented by a single regressor in the first-level GLM (see also Chai *et al.* (2014)). With this approach the amount of regressors is different between participants (ranging from 0-28). To account for this difference in first-level GLMs, the number of FD outliers (and thus the number of extra regressors) was added to the higher level statistical analyses as an additional covariate.

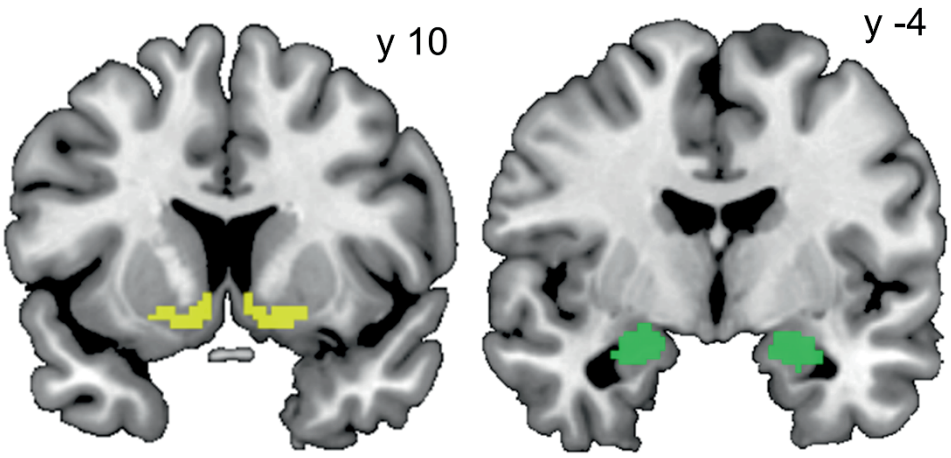


Figure 1. *Subcortical seeds: ventral striatum (left), and amygdala (right).*

Higher-Level Seed Based Analysis

For both seeds, two higher-level group analyses were carried out using FMRIB's Local Analysis of Mixed Effects (FLAME) stage 1; one for sample I and one for sample II. Higher-level analyses were performed using FLAME stage 1 with automatic outlier detection and included the number of extra regressors induced by the FD outlier modeling as covariate of no interest. Corrections for multiple comparisons were thresholded with Gaussian Random Field Theory cluster-wise correction with a minimal Z>3.09 (corresponding to p<.001) and cluster

significance of $p< .05$. Next, we inspected the overlap between whole brain connectivity from sample I and sample II using conjunction analyses. Conjunction analyses were performed using the *easythresh_conj* script in FSL (Nichols *et al.*, 2005), using the same threshold described for the previous analyzes ($Z > 3.09$, $p<0.05$) in order to identify regions commonly connected in both samples.

Region of Interest Analysis

To further investigate limbic/subcortical-cortical and limbic/subcortical-subcortical brain connectivity we examined the zstats in predefined ROIs. Since studies have shown that different regions of the PFC have distinct functions, we investigated six specific subdivisions of the PFC (Fig 4a): the ventral and dorsal medial prefrontal cortex (vmPFC, dmPFC), the orbitofrontal cortex (OFC), the dorsal lateral prefrontal cortex (dlPFC), and the ventral and dorsal anterior cingulate cortex (vACC, dACC). All ROIs were bilateral. Regions were based on the Harvard-Oxford cortical structural atlas and were thresholded on ≥25% probability, resulting in the following sizes of anatomical ROIs: vmPFC 1189 voxels; dmPFC 5378 voxels; OFC 3502 voxels; dlPFC 5741 voxels; vACC 1313 voxels; and dACC1925 voxels. The following regions were used: Frontal Medial Cortex for vmPFC, Superior Frontal Gyrus for dmPFC, Frontal Orbital Cortex for OFC, Middle Frontal Gyrus for dlPFC, and the Cingulate Cortex anterior division for the ACC. The ACC was divided in a dorsal and ventral division with a cutoff at y=30.

Since both the VS and AMY also have shown to be connected the hippocampus (HPC) and the thalamus (TH) (Roy *et al.*, 2009; Gabard-Durnam *et al.*, 2014; Fareri *et al.*, 2015), we included exploratory analyses of limbic/subcortical-subcortical connectivity, with additional subcortical ROIs of the TH and HPC (Fig 4b). Regions were based on the Harvard-Oxford subcortical structural atlas and were thresholded on ≥75% probability, resulting in a bilateral, anatomical TH ROI of 1646 voxels and a HPC ROI of 494 voxels. We used a stricter probability for the subcortical regions in order to prevent subcortical regions would overlap. In addition, we investigated functional connectivity between the VS and AMY. Zstats were extracted from subjects' specific first level for each seed with the different ROIs as a mask using Featquery (as implemented in FSL v5.09). This way we extracted subject-specific connectivity estimates for 12 different subcortical-PFC connections and 5 different subcortical-subcortical connections.

To explore possible outliers, we calculated z-values of the subject specific zstats at the group level. When outliers were detected (Z-value <-3.29 or >3.29), scores were winsorized (Tabachnick and Fidell, 2013). One sample t-tests were used to investigate whether connectivity between a seed and a ROI was significantly different from zero (separately for both samples). Independent sample t-tests were used to test whether there were differences in connectivity

between sample I and II. Paired sample t-tests were used to test whether there were differences in connectivity between ROIs and the VS and AMY seeds.

Genetic Modeling

Within the final sample (N=220), there were 64 complete twin pairs (37 MZ and 27 DZ, Table 2). Zygosity was determined by DNA analyses. DNA was tested with buccal cell samples collected via a mouth swab (Whatman Sterile Omni Swab). Buccal samples were collected directly after the MRI session, thereby ensuring that the children had not eaten for at least one hour prior to DNA collection.

Similarities among twin pairs can be due to shared genetic factors (A) and shared environmental factors (C), while dissimilarities are ascribed to unique environmental influences and measurement error (E), see Fig S2. Behavioral genetic modeling with the OpenMX package (Neale *et al.*, 2016) in R (R Core Team, 2015) provides estimates of these A, C, and E components. Since several heritable psychiatric disorders are associated with limbic/subcortical-PFC connections (Bouchard and McGue, 2003; Flint and Kendler, 2014), VS and AMY connectivity might also be heritable. However, these regions have also shown plasticity to the environment (Tottenham and Galvan (2016), which could indicate influences of (shared or unique) environment. Therefore, we calculated the ACE models for each of the 17 seed-ROI connections and report the point estimates and 95% confidence intervals of A, C and E. High estimates of A indicate that genetics play an important role, whilst C estimates indicate influences of the shared environment. If the E estimate is the highest, variance in connectivity is mostly accounted for by unique environmental factors and measurement error. Comparisons of the ACE models with more parsimonious models (AE model, CE model, and E model) are described in the Supplementary Materials.

Results

Whole Brain Analyses

First, we performed whole brain analyses for the subcortical seeds (VS and AMY) in sample I and II. Next we investigated the overlap between the two samples by using conjunction analyses.

Ventral Striatum

Whole brain functional connectivity with the VS as seed for sample I is displayed in Fig 2a (left top panel) and Table S3. Whole brain results for sample II are displayed in Fig 2a (right top panel) and Table S4. To formally assess which connectivity patterns replicated across samples, conjunction analyses were performed. As visualized in Fig 2a, whole brain VS connectivity in the two

samples showed pronounced consistent positive connectivity with vACC, vmPFC, thalamus, insula, inferior temporal gyrus, parietal operculum cortex, putamen, pallidum, caudate, nucleus accumbens, amygdala, and the OFC (Table 3). Negative connectivity was consistent over two samples between VS and dACC, dlPFC, paracingulate gyrus, para-hippocampus, and hippocampus (Table 3).

Amygdala

Whole brain functional connectivity with the AMY as seed for sample I is displayed in Fig 2b (left top panel) and Table S3. Whole brain results for sample II are displayed in Fig 2b (right top panel) and Table S4. As visualized in Fig 2b, whole brain AMY connectivity patterns showed overlap across the two samples, showing pronounced positive connectivity with the thalamus, pallidum, putamen, caudate, hippocampus, para-hippocampus, brainstem, frontal pole, insula, inferior frontal gyrus (IFG), fusiform cortex, and superior temporal gyrus (STG) (Table 3). Moreover, we found consistent negative connectivity between AMY and dmPFC, dlPFC, paracingulate gyrus, precuneus cortex, parietal cortex, posterior cingulate cortex, and lateral occipital cortex (Table 3).

Post-Hoc Examination of Subcortical-Cortical Connectivity

We investigated limbic/subcortical-cortical brain connectivity in more detail by visualizing connectivity patterns between subcortical seeds (VS and AMY) and prefrontal cortical ROIs of the vmPFC, dmPFC, vACC, dACC, OFC, and dlPFC. Connectivity patterns replicated across sample I and II, with the exception of VS-dmPFC and AMY-vACC connectivity (Fig 3a, Table S5). Overall, subcortical regions exhibited positive connectivity with ventral cortical regions (vmPFC, vACC, OFC) and negative connectivity with dorsal cortical regions (dmPFC, dACC, dlPFC), see Fig 3a. Paired sample t-tests were used to investigate differences in VS-PFC and AMY-PFC connectivity. For the vmPFC and vACC, positive connectivity with the VS was significantly stronger than connectivity with AMY (Table 4). Note that connectivity between AMY and the vmPFC and vACC was not significantly different from zero in one of the samples (Table S6). There were no differences between the VS and the AMY in connectivity with the OFC. The VS and AMY showed pronounced negative connectivity with dorsal cortical regions (Fig 3a). For the dlPFC and dmPFC, negative connectivity with the AMY was significantly stronger than connectivity with the VS (Fig 3a, Table 4). Note that connectivity between VS and the dmPFC was not significantly different from zero in one of the samples (Table S6). Connectivity between dACC and AMY was stronger than connectivity between dACC and VS in sample II, but not in sample I (Table 4). There were no significant gender or age-related differences in subcortical-cortical connectivity (sample I and II combined).

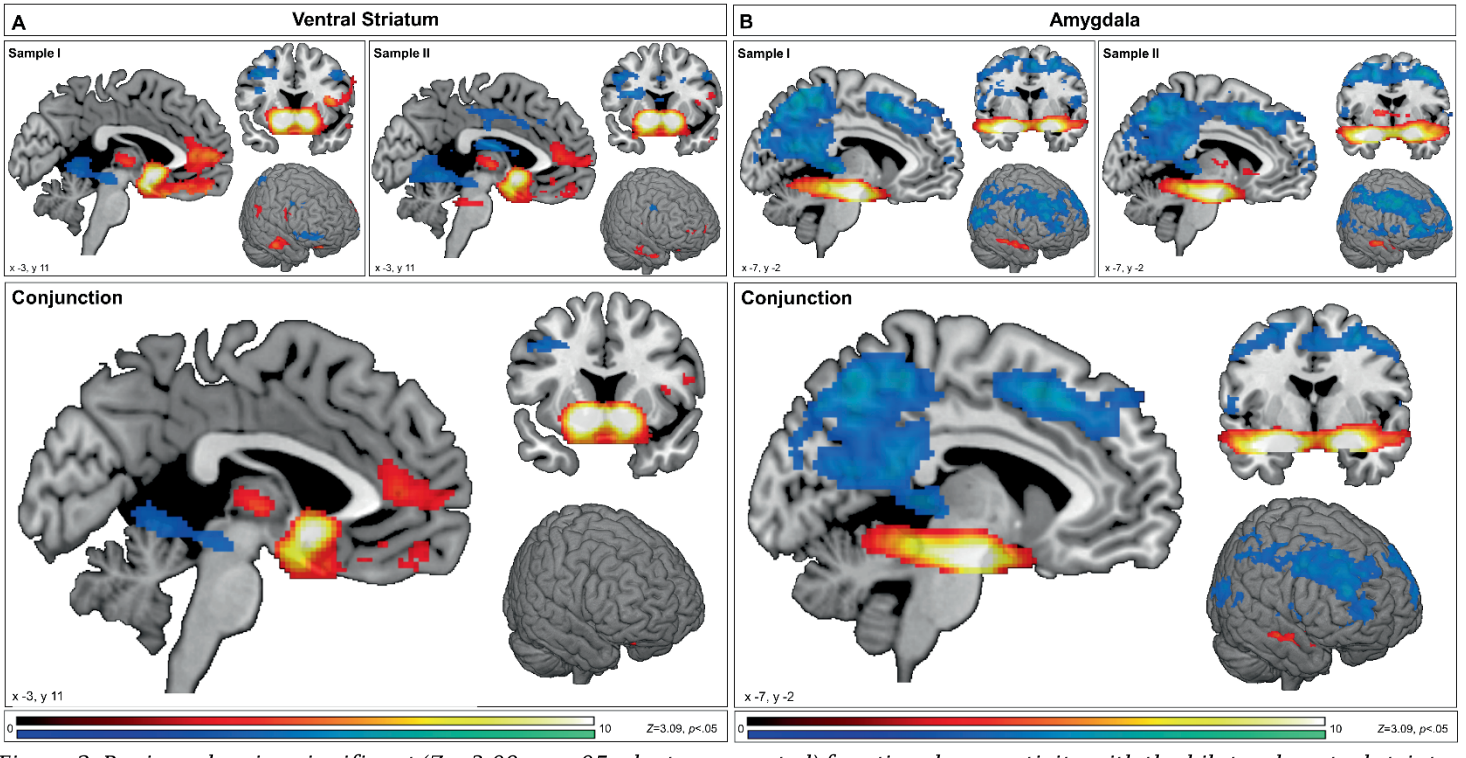


Figure 2. Regions showing significant (Z > 3.09, p < .05; cluster-corrected) functional connectivity with the bilateral ventral striatum seed (A) and the bilateral amygdala seed (B). Positive connectivity is displayed in warm colors and negative connectivity in cool colors.

Table 3. MNI coordinates and local maxima for whole brain connectivity clusters from conjunction analyses (Sample I and Sample II) with Z > 3.09, p < .05 cluster correction. Anatomical regions were derived from the Harvard-Oxford atlas in FSL.

	voxels	max zstat	max x	max y	max X	anatomical regions
VS positive	7607	14.2	10	10	-8	Medial prefrontal cortex, anterior cingulate cortex, superior frontal gyrus, frontal pole, subcallosal cortex, thalamus, orbitofrontal cortex, putamen, pallidum, caudate, nucleus accumbens
	367	4.45	44	-10	16	Right inferior frontal gyrus, right central opercular cortex, right frontal operculum cortex
VS negative	1546	4.42	30	-4	28	Right middle frontal gyrus, right postcentral gyrus, right precentral gyrus, right supplementary cortex
	1188	4.57	-6	-48	-8	Lingual gyrus, parahippocampal gyrus, posterior cingulate cortex, brainstem, thalamus
	569	4.51	-40	8	38	Left middle frontal gyrus, left precentral gyrus, left inferior frontal gyrus
AMY positive	14334	15.2	-20	-4	-20	Hippocampus, parahippocampal gyrus, putamen, pallidum, thalamus, brainstem, Fusiform cortex, insula, temporal pole, subcallosal cortex, orbitofrontal cortex
AMY negative	45194	6.66	0	14	50	supplementary motor cortex, superior frontal gyrus, paracingulate gyrus, anterior cingulate gyrus, middle frontal gyrus, frontal pole, precentral gyrus, precuneous, postcentral gyrus, lateral occipital cortex, left inferior frontal gyrus, left precentral gyrus, left central opercular cortex
	468	4.62	0	-22	12	right inferior frontal gyrus, right precentral gyrus, right central opercular cortex

Post-Hoc Examination of Subcortical-Subcortical Connectivity

To investigate limbic/subcortical-subcortical brain connectivity in more detail, we used two additional ROIs of the HPC, TH. Moreover, we investigated connectivity between the VS and the AMY. Connectivity patterns replicated across sample I and II (Fig 3b, Table S6). The overall pattern showed pronounced positive connectivity between subcortical regions, see Fig 3b. Interestingly, the HPC ROI showed strong positive connectivity with AMY (Fig 3b, Table 4). More stringent thresholded (smaller) HPC ROIs resulted in similarly strong positive connectivity patterns (see supplementary materials, Fig S3), indicating that this strong connectivity was not inflated by cross-boundary blurring. VS-Hippocampus showed negative connectivity (Fig 3b, Table 4), however, note that VS-HPC connectivity was not significantly different from zero in Sample II (Table S6). VS-TH connectivity was significantly stronger than AMY-TH connectivity, which was negative, and not significantly different from zero in sample II (Table S6). The connectivity estimate between the VS and AMY was small and not significantly different from zero in both samples (Fig 3 and Table S6). There were no significant gender differences in limbic/subcortical-subcortical connectivity (sample I and II combined). We found weak negative correlations between age and VS-HPC connectivity in (r=-.20, p=.01), and VS-AMY connectivity (r=-.17, p=.04).

Heritability of Subcortical-Cortical Connectivity

An overview of ACE models for limbic/subcortical-cortical brain connectivity between seed (VS and AMY) and cortical ROIs (vmPFC, vACC, OFC, dmPFC, dACC, dlPFC) is provided in Table 5. Comparisons of the full ACE model with more parsimonious AE, CE and E models are displayed in Table S7 (VS) and Table S8 (Amygdala). Note that the estimates of the different components add up to 1 (100%). The overall pattern showed that the variance in VS-PFC connectivity was best accounted for by genetic and unique environmental factors (including measurement error). That is to say, the A estimate was moderately high for connectivity between VS and vmPFC (A=67%, E=33%), OFC (A=32%, C=9% E=59%), dmPFC (A=37%, C=1%, E=63%), dACC (A=46%, E=54%), and dlPFC (A=19%, E=81%), see Table 5. In addition to genetic influences, VS-vACC connectivity also showed influences of shared environment (A= 12%, C=17%, E=71%). Variance in AMY-dorsalPFC connectivity was less influenced by genetics, with small contributions of the A component for connectivity between AMY and dmPFC (A=8%, C=0%, E=92%), dACC (A=8%, C=0%, E=92%), and dlPFC (A=14%, C=0%, E=86%). AMY-vACC connectivity showed moderately high estimates of the shared environment (C=35%, E=65%), with no influence of genetics (A=0%). AMY-vmPFC connectivity

showed moderate influences of genetics (A=23%, C=0%, E=77%), and AMY-OFC connectivity showed high heritability (A=54%, E=46%), see Table 5.

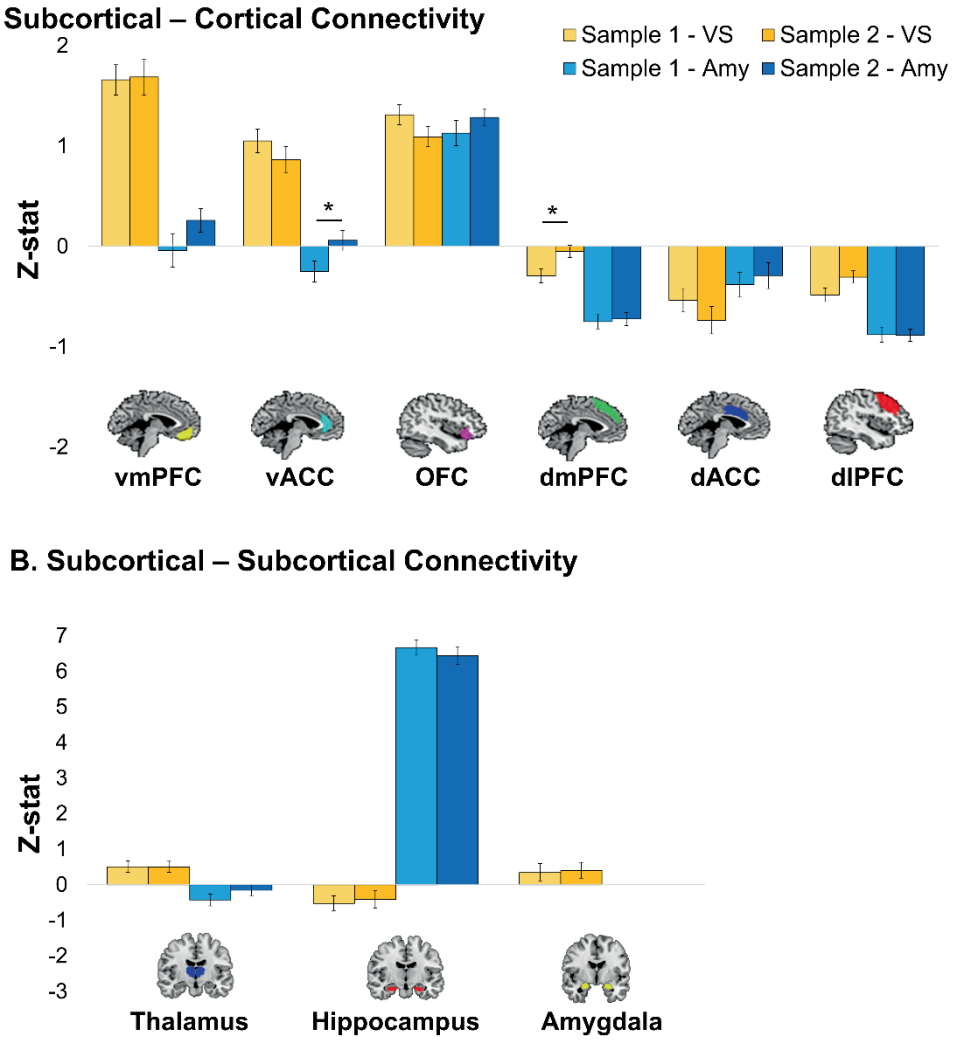


Figure 3. *Subcortical-cortical and subcortical-subcortical brain connectivity. A) Connectivity between subcortical seeds (ventral striatum (VS) and amygdala (AMY)) and prefrontal cortical regions ventral medial prefrontal cortex (vmPFC), ventral anterior cingulate cortex (vACC), orbitofrontal cortex (OFC), dorsal medial PFC (dmPFC), dorsal ACC (dACC) and dorsal lateral PFC (dlPFC). B) Connectivity between VS, AMY, hippocampus and thalamus. Error bars represent standard error of mean. Asterisks indicate significant differences between samples.*

Heritability of Subcortical-Subcortical Connectivity

An overview of ACE models for limbic/subcortical-cortical brain connectivity between seed (VS and AMY) and the subcortical ROIs (HPC, TH, AMY) is provided in in Table 6. Comparisons of the full ACE model with more parsimonious AE, CE and E models are displayed in Table S9. Note that the estimates of the different components add up to 1 (100%). Subcortical-subcortical connectivity was moderately influenced by genetics, with A estimates ranging from 32-42% (VS-HPC A=37%, E=63%; VS-AMY A=42%, E=58%; AMY-HPC A=32%, E=68%; AMY-TH A=35%, E=65%), and no influence of the shared environment (C=0%), with the exception of VS-TH connectivity, which was mostly influenced by environmental factors (A=4%, C=15%, E=81%), see Table 6.

Table 4. Mean and standard deviations of Z-values for all subcortical-cortical and subcortical-subcortical connectivity patterns. Differences in connectivity patterns from ventral striatum and amygdala were tested with paired sample T-tests.

ROI	Sample	VS mean (SD)	AMY mean (SD)	*Statistics*	*p*
vmPFC	Sample I	1.66 (1.34)	-0.04 (1.45)	t(77)= 8.19	<.001
	Sample II	1.69 (1.60)	0.26 (1.03)	t(77)=7,33	<.001
vACC	Sample I	1.05 (1.04)	-0.25 (0.93)	t(77)=7,33	<.001
	Sample II	0.86 (1.14)	0.06 (0.86)	t(77)=5,37	<.001
OFC	Sample I	1.31 (0.88)	1.13 (1.11)	t(77)=1,21	.229
	Sample II	1.09 (0.89)	1.28 (0.76)	t(77)=-1,70	.093
dmPFC	Sample I	-0.29 (0.61)	-0.75 (0.62)	t(77)=4,93	<.001
	Sample II	-0.05 (0.54)	-0.72 (0.59)	t(77)=7,70	<.001
dACC	Sample I	-0.54 (1.03)	-0.38 (1.11)	t(77)=-,89	.379
	Sample II	-0.73 (1.21)	-0.29 (1.14)	t(77)=-2,49	<.001
dlPFC	Sample I	-0.48 (0.59)	-0.88 (0.67)	t(77)=4,05	<.001
	Sample II	-0.31 (0.55)	-0.88 (0.54)	t(77)=7,01	<.001
Thala-	Sample I	0.51 (1.37)	-0.43 (1.47)	t(77)=3,53	.001
mus	Sample II	0.50 (1.37)	-0.15 (1.32)	t(77)=2,92	.005
Hippoc	Sample I	-0.52 (1.87)	6.67 (1.93)	t(77)=-21,87	<.001
ampus	Sample II	-0.41 (2.10)	6.43 (2.17)	t(77)=-18,49	<.001

Table 5. Genetic modeling of Cortical- Subcortical connectivity.

Start Seed	ROI	model	A²	C²	E²	LTR	AIC
VS	vmPFC	ACE	0.67	0.00	0.33		182.29
		AE*	0.67	-	0.33	<0.001	182.29
		CE	-	0.44	0.56	5.68	187.97
		E	-	-	1.00	>14.03	200.00
	vACC	ACE	0.12	0.17	0.71		138.13
		AE	0.32	-	0.68	0.19	136.31
		CE*	-	0.27	0.73	0.07	136.20
		E	-	-	1.00	>4.71	139.03
	OFC	ACE	0.32	0.09	0.59		83.87
		AE*	0.42	-	0.58	0.05	81.92
		CE	-	0.34	0.66	0.58	82.44
		E	-	-	1.00	>8.09	88.54
	dmPFC	ACE	0.36	0.01	0.63		-41.82
		AE*	0.37	-	0.63	0.001	-43.82
		CE	-	0.27	0.73	0.65	-43.17
		E	-	-	1.00	>5.00	-40.17
	dACC	ACE	0.46	0.00	0.54		165.63
		AE*	0.46	-	0.54	<0.001	163.63
		CE	-	0.27	0.73	4.00	167.62
		E	-	-	1.00	>4.97	170.60
	dlPFC	ACE	0.19	0.00	0.81		-50.46
		AE	0.19	-	0.81	<0.001	-52.46
		CE	-	0.12	0.88	0.73	-51.73
		E*	-	-	1.00	<1.74	-52.72

[1] LTR < 3.85 equals a significant better fit of the model (p<.05)

[2] Lower AIC values indicate a better model fit

* Asterics indicate the best model fit

Table 5. (continued)

Start Seed	ROI	model	A²	C²	E²	LRT	AIC
AMY	vmPFC	ACE	0.23	0.00	0.77		184.64
		AE	0.23	-	0.77	<0.001	182.64
		CE	-	0.07	0.93	1.43	184.08
		E*	-	-	1.00	<1.79	182.43
	vACC	ACE	0.00	0.35	0.65		84.01
		AE	0.34	-	0.66	1.12	83.14
		CE*	-	0.35	0.65	<0.001	82.01
		E	-	-	1.00	>7.41	88.55
	OFC	ACE	0.54	0.00	0.46		84.33
		AE*	0.54	-	0.46	<0.001	82.33
		CE	-	0.46	0.54	1.79	84.11
		E	-	-	1.00	>15.30	97.41
	dmPFC	ACE	0.08	0.00	0.92		-14.87
		AE	0.08	-	0.92	<0.001	-16.87
		CE	-	0.00	1.00	0.24	-16.62
		E*	-	-	1.00	<0.24	-18.62
	dACC	ACE	0.08	0.00	0.92		130.54
		AE	0.08	-	0.92	<0.001	128.54
		CE	-	0.03	0.97	0.22	128.77
		E*	-	-	1.00	<0.27	126.82
	dlPFC	ACE	0.14	0.00	0.86		-4.94
		AE	0.14	-	0.86	<0.001	-6.94
		CE	-	0.04	0.96	0.68	-6.26
		E*	-	-	1.00	<0.76	-8.18

[1] LTR < 3.85 equals a significant better fit of the model (p<.05)

[2] Lower AIC values indicate a better model fit

* Asterics indicate the best model fit

Table 6. Genetic modeling of Subcortical- Subcortical connectivity.

Start Seed	ROI	model	A[2]	C[2]	E[2]	LRT	AIC
VS	Hippocampus	ACE	0.37	0.00	0.63		266.12
		AE*	0.37	-	0.63	<0.001	264.12
		CE	-	0.32	0.68	0.74	264.87
		E	-	-	1.00	>6.95	269.81
	Thalamus	ACE	0.04	0.15	0.81		175.08
		AE	0.21	-	0.79	0.13	173.21
		CE*	-	0.18	0.82	0.01	173.08
		E	-	-	1.00	<2.10	173.18
	Amygdala	ACE	0.42	0.00	0.58		281.83
		AE*	0.42	-	0.58	<0.001	279.83
		CE	-	0.36	0.64	0.92	280.75
		E	-	-	1.00	>9.07	287.83
AMY	Hippocampus	ACE	0.32	0.00	0.68		277.93
		AE*	0.32	-	0.68	<0.001	275.93
		CE	-	0.19	0.81	2.24	278.18
		E	-	-	1.00	>2.27	278.44
	Thalamus	ACE	0.35	0.00	0.65		154.42
		AE*	0.35	-	0.65	<0.001	152.42
		CE	-	0.23	0.77	1.98	154.40
		E	-	-	1.00	>3.47	155.87

[1] LTR < 3.85 equals a significant better fit of the model (p<.05)

[2] Lower AIC values indicate a better model fit

* Asterics indicate the best model fit

Discussion

We investigated genetic and environmental influences on limbic/subcortical-cortical and limbic/subcortical-subcortical RS-fMRI in a relatively large sample of 7-to-9-year-old MZ and DZ twins. As a complement to prior studies of genetic and environmental influences in adults (for example, Yang *et al.* (2016)), here we assessed twin concordance in children during a time of rapid development of these connections.

Replicability of childhood resting state connectivity

First we addressed childhood resting state brain connectivity, by studying patterns of connectivity from the ventral striatum and the amygdala, in two genetically independent samples. Reassuringly, and consistent with adult research (Power *et al.*, 2010; Thomason *et al.*, 2011; Misic and Sporns, 2016), we observed strongly replicable brain connectivity patterns over two samples of 7-to-9-year-old children, both in the whole brain seed based analyses and in the post-hoc ROI analyses. The general patterns showed positive connectivity between amygdala and ventral striatum and orbitofrontal cortex; and negative connectivity between these limbic/subcortical regions and dorsal medial and lateral regions. Previous studies showed that orbitofrontal cortex is more strongly involved in affective processes, whereas dorsal medial and lateral prefrontal cortex is more strongly associated with behavioral control, and the current findings fit with the hypothesized top-down control of dorsal lateral prefrontal cortex over the limbic subcortical brain regions (Somerville *et al.*, 2010; Ernst, 2014; Casey, 2015).

In line with adult striatal-cortico connectivity patterns we found positive connectivity between the ventral striatum and vACC, vmPFC, and OFC (Di Martino *et al.*, 2008), suggesting that these connections are already in place during middle childhood. The post-hoc ROI analyses indicated negative connectivity between the VS and the dACC, dlPFC and dmPFC, but these were less pronounced in the whole brain analyses. The difference between the current results and the connectivity patterns in adults could be due to developmental processes, since dorsal medial and lateral PFC regions continue to develop throughout adolescence (Ernst, 2014; Casey, 2015). Moreover, these differences in results might derive from the differences in limbic/subcortical seed regions. To date there is no consensus about the different sub regions of the striatum and different studies have used different approaches. Prior studies have suggested a more detailed subdivision of the striatum with, for example, additional distinctions within the ventral striatum (Di Martino *et al.*, 2008; Choi *et al.*, 2012). For the current paper we specifically chose only the ventral striatum, since this striatal sub region is specifically associated with developmental differences in affective/motivational behaviors. Future research could shed light on

developmental differences in connectivity from different sub regions within the striatum, by directly comparing children and adults, using the same methodology in both samples (as was previously done for the VS by Fareri *et al.* (2015)).

Regarding amygdala-cortico connectivity, our developmental results were generally in line with the findings in adults. That is, we found positive connectivity with the OFC, the insula and the IFG, and negative connectivity with the dlPFC, dACC, dmPFC and parietal cortex (Stein *et al.*, 2007; Roy *et al.*, 2009). This is also in line with previous findings spanning ages from childhood to adulthood, showing that amygdala connectivity over development was largely stable (Gabard-Durnam *et al.*, 2014). We did, however, find differences in amygdala-cerebellum connectivity compared to results in adults (Roy *et al.*, 2009). Our whole brain analyses revealed a band of positive connectivity from the amygdala through the brainstem to the dorsal cerebellum, whereas adult results showed negative connectivity between the amygdala and the dorsal cerebellum (Roy *et al.*, 2009). Interestingly, a recent study on amygdala functional connectivity in 4-to-7-year-old children also showed positive connectivity between amygdala and the cerebellum (Park *et al.*, in press). We submit that this is a developmental effect, reflecting positive connectivity to the dorsal cerebellum in childhood that becomes negative over development. Indeed age dependent changes in amygdala connectivity have been documented, with increasingly negative connectivity between the amygdala and cerebellum with increasing age (Gabard-Durnam *et al.*, 2014). Notably, a recent cross-sectional longitudinal study of Jalbrzikowski *et al.* (2017) reported strong amygdala-mPFC connectivity in childhood, which declined to zero by adulthood (age range 10-19). However, we did not find strong amygdala-vmPFC connectivity in neither of the samples. This could be due to differences in age ranges, differences in the amygdala and vmPFC sub regions that were examined, as well as methodological differences in RS-fMRI analyses. In the current paper, we chose to use the whole amygdala as seed, to strike a balance between completeness and the number of connections and additional genetic analyses. However, it should be noted that the amygdala is not a single unit, but consists of several nuclei (Ball *et al.*, 2007; Roy *et al.*, 2009). Some studies have shown distinct connectivity patterns from different amygdala sub nuclei in adults (Roy *et al.*, 2009), and over development (Gabard-Durnam *et al.*, 2014).

In sum, our results showed robust and replicable whole brain connectivity in children, for the amygdala as well as the ventral striatum. In addition to previous studies that have shown that limbic/subcortical-cortical connectivity increases during adolescence (Fair *et al.*, 2009; Vogel *et al.*, 2010; Menon, 2013; Rubia, 2013; Gabard-Durnam *et al.*, 2014); the findings from this study show that the vast architecture of this connectivity is already present before adolescence.

Heritability of childhood resting state connectivity

The second aim of this study was to examine the heritability of childhood resting state connections, specifically focusing on connections between the ventral striatum and amygdala with prefrontal cortex and other subcortical regions. Variance in the majority of connections from the ventral striatum to the prefrontal cortex was best described by genetics, with moderately strong heritability factors (up to 67%). Weaker ventral striatum-prefrontal cortex connections have been linked to psychiatric disorders such as depression (Russo and Nestler, 2013) and substance abuse (Deadwyler *et al.*, 2004), which are thought to have a genetic component (Bouchard and McGue, 2003; Flint and Kendler, 2014). The association between genotypic characteristics and psychiatric disorders might be mediated by genetically based connectivity in the brain (Hyman, 2000). Interestingly, connectivity from the ventral striatum to the vACC and thalamus was mostly influenced by shared and unique environmental factors, which is in line with previous findings that reported environmental plasticity of the striatum (Tottenham and Galvan, 2016). These results suggest that long-range cortical-striatal connectivity is more strongly influenced by genetic profiles, while short range thalamic and vACC connectivity is more influenced by environmental factors.

With the exception of ventral striatum-thalamic connectivity, limbic/subcortical-subcortical connectivity was notably influenced by genetics, with heritability estimates ranging from 32-42%. For instance, we found heritability for amygdala-hippocampus connectivity (A=32%), indicating that this emotional memory network (Phelps, 2004) is influenced by genetic factors. Interestingly, a broad literature has shown that these two regions independently are affected by environmental influences such as stress and early adversity (Lupien *et al.*, 2009; Tottenham and Sheridan, 2009; Barch *et al.*, 2016). This raises new questions with respect to how the amygdala-hippocampus circuitry is shaped and develops during child development. Moreover, while ventral striatum-prefrontal cortex connective showed large genetic influences, amygdala-prefrontal cortex connectivity showed mostly effects of the environment, with high estimates of the E component (up to 92%). There were two exceptions to this general pattern. First, in line with the ventral striatum, amygdala-vACC connectivity showed influences of the shared environment. The vACC has been shown to signal for socially salient cues such as peer feedback, both in adults as well as in children (Somerville *et al.*, 2006; Achterberg *et al.*, 2016b; Achterberg *et al.*, 2018b). Connectivity between the vACC and limbic/subcortical regions might also be susceptible to social context and social environmental factors, as these connections are significantly influenced by environment (Gee *et al.*, 2014). Secondly, 54% of the variance in amygdala-OFC connectivity was explained by genetic influences. Interestingly, Whittle and colleagues (2014) have reported longitudinal effects of positive parenting on structural development of the amygdala and OFC. Our study is the first to show

that variance in amygdala-OFC functional connectivity in childhood is explained by genetic factors. This finding has important implications for intervention research: Certain genetic profiles might be more susceptible to environmental influences than others, as is proposed by the differential susceptibility theory (Bakermans-Kranenburg and van Ijzendoorn, 2007; Ellis *et al.*, 2011). A next step could be to examine whether children with specific genetic profiles are more susceptible to both the adverse effects of unsupportive environments and the beneficial effects of supportive rearing (see the study protocol of Euser *et al.* (2016)). Important aspects to take into account in those studies are the developmental differences in heritability estimates for brain anatomy and connectivity (Lenroot *et al.*, 2009; van den Heuvel *et al.*, 2013). That is, previous studies have found lower heritability estimates in children than in adults (van den Heuvel *et al.*, 2013). However, the literature on heritability of functional brain connectivity is still relatively sparse, and most studies have examined whole brain RS and/or used different RS methods (Glahn *et al.*, 2010; Richmond *et al.*, 2016; Yang *et al.*, 2016; Colclough *et al.*, 2017; Ge *et al.*, 2017), making comparisons between studies difficult. Studying differences in heritability estimates between children and adults, nevertheless, is an important issue for future studies, providing important insights in the developmental phase during which connections might be most sensitive to environmental influences.

Overall, the patterns of genetic and environmental influences for ventral striatum and amygdala were distinct: Long-range PFC connectivity with the ventral striatum was genetically influenced, whereas long-range amygdala connectivity was mostly environmentally influenced. These results may be the starting point for a better understanding of how brain development is both biologically based and environmentally driven.

Methodological considerations

Some methodological considerations should be noted. First, due to excessive motion, we had to exclude almost half of our initial sample. Nevertheless, due to our large sample size we could still perform analyses on a relatively large group of children, thereby increasing the statistical power of our analyses. It should be noted that the current standard of remaining motion in (adult) RS studies is even stricter, often using a cutoff of 0.3 mm FD. However, in terms of motion, the current results are based on a very clean dataset compared to earlier developmental studies. After exclusion of participants with excessive motion the gender distribution was significantly different from chance in the MZ and DZ twin samples, with more girls than boys included. Although there were no significant differences in gender between the MZ and DZ samples, and therefore this gender distribution is unlikely to have influenced our results, future studies on heritability of brain measures in childhood should opt to oversample young boys, since our results show the highest attrition rate in boys. Secondly, even

after controlling for motion and including additional regressors with CSF and WM signals, our whole brain analyses show minimal but potentially artefactual correlations with non grey matter tissue. Future studies could include additional analytic steps to further minimize these effects, for example by controlling for cortical signal bleeding, i.e., regressing out signal from surrounding voxels (Buckner *et al.*, 2011; Choi *et al.*, 2012).

Third, we included the global signal as nuisance signals to reduce artifacts of cardiac and respiratory fluctuations and scanner drifts (Birn *et al.*, 2006; Fox and Raichle, 2007), however, inclusion of global signal regression can introduce negative correlations between regions (Murphy *et al.*, 2009) and therefore the intepretation of these negative connectivities should be done with caution.

Fourth, some of our genetic analyses of neural responses resulted in high estimates for the E component (up to 92%), reflecting influences from the unique environment and measurement error. The statistical power of genetic studies is influenced by, amongst others, the sample size (Visscher, 2004; Verhulst, 2017). Although our sample size can be considered relatively large for a developmental RS-fMRI study, it is modest for behavioral genetic modeling. Our sample size may have been insufficient to detect significant contributions of A (genetics) and C (shared environment), resulting in inflated estimates of the E component. Future studies should try to discriminate between the influence of unique environment and measurement error, for example by accounting for intra-subject fluctuations using repeated measures, as has recently been described by Ge et al. (2017).

Lastly, the current study made use of post hoc ROI analyses to further investigate limbic/subcortical-cortical connectivity, based on structural brain atlases. Although recent studies have provided functional atlases of the brain (Yeo *et al.*, 2011; Choi *et al.*, 2012), these are based on adults. To our best knowledge, there are no functional atlases based on developmental samples, and the vast majority of developmental studies have used anatomical regions to mask and/or extract functional connectivity (Gabard-Durnam *et al.*, 2014; Fareri *et al.*, 2015; van Duijvenvoorde *et al.*, 2016a). By using these structural ROIs our results can be compared or combined with previously published studies. Nevertheless, we acknowledge that the functional architecture of the brain does not follow structural subdivisions, and this may be considered as a limitation of the current design.

Conclusion

Taken together, this study was the first to investigate twin effects in subcortical-subcortical and subcortical-cortical RS-fMRI in children, providing important insights in genetic and environmental influences on childhood brain connectivity. The behavioral genetic analyses showed moderate to substantial heritability of striatum-prefrontal cortex brain connectivity, and environmental influences on amygdala-orbitofrontal cortex connectivity, with implications for our understanding of the etiology of disorders that are associated with disrupted connectivity, such as drug abuse and depression. Prior studies have mainly estimated heritability for brain connectivity in adults (Yang *et al.*, 2016), whereas child development provides unique possibilities for understanding the role of shared environment (Polderman *et al.*, 2015). Examining how limbic/subcortical brain regions are functionally connected to the prefrontal cortex and whether a positive childrearing environment can foster these connections are important issues to address in future research. The current findings provide the first step in laying the groundwork for understanding genetic and environmental influences in shaping brain connectivity and may be the starting point for a better understanding of how brain development is both biologically based and environmentally driven.

Acknowledgments

The Leiden Consortium on Individual Development is funded through the Gravitation program of the Dutch Ministry of Education, Culture, and Science and the Netherlands Organization for Scientific Research (NWO grant number 024.001.003). MA was additionally funded by the Ter Meulen Grant of the Royal Netherlands Academy of Arts and Sciences (KNAW).

Supplementary materials

Genetic modeling - comparison of parsimonious models

Similarities among twin pairs are divided into similarities due to shared geneti factors (A) and shared environmental factors (C), while dissimilarities ar ascribed to unique environmental influences and measurement error (E) Behavioral genetic modeling with the OpenMX package (Neale *et al.*, 2016) in R (Core Team, 2015) provides estimates of these A, C, and E components. For eac of the 17 connections, four different models (ACE, AE (with C set to zero), C (with A set to zero), and E (with A and C set to zero)) were estimated and a lo likelihood was calculated. Each model was then compared to a mor parsimonious model (e.g. ACE vs. AE; ACE vs. CE; AE vs. E and CE vs. E) b subtracting the log likelihoods, resulting in an estimate of the Log- Likelihoo Ratio Test (LRT). Given that the LRT follows the χ2-distribution, an LRT<3.8 would indicate that the more parsimonious model has no worse fit to the data The Akaike Information Criterion (AIC; Akaike (1974) was used to determine th best model for equally parsimonious non-nested models (i.e. AE and CE), wit better model fit being indicated by a lower AIC. When ACE models show the bes fit, both heritability, shared and unique environment are important contributor to explain the variance in the outcome variable. AE models indicate that geneti and unique environmental factors play a role; whilst CE models indicat influences of the shared environment and unique environment. If the E mode has no worse fit than AE or CE models, variance in the outcome variable i accounted for by unique environmental factors and measurement error.

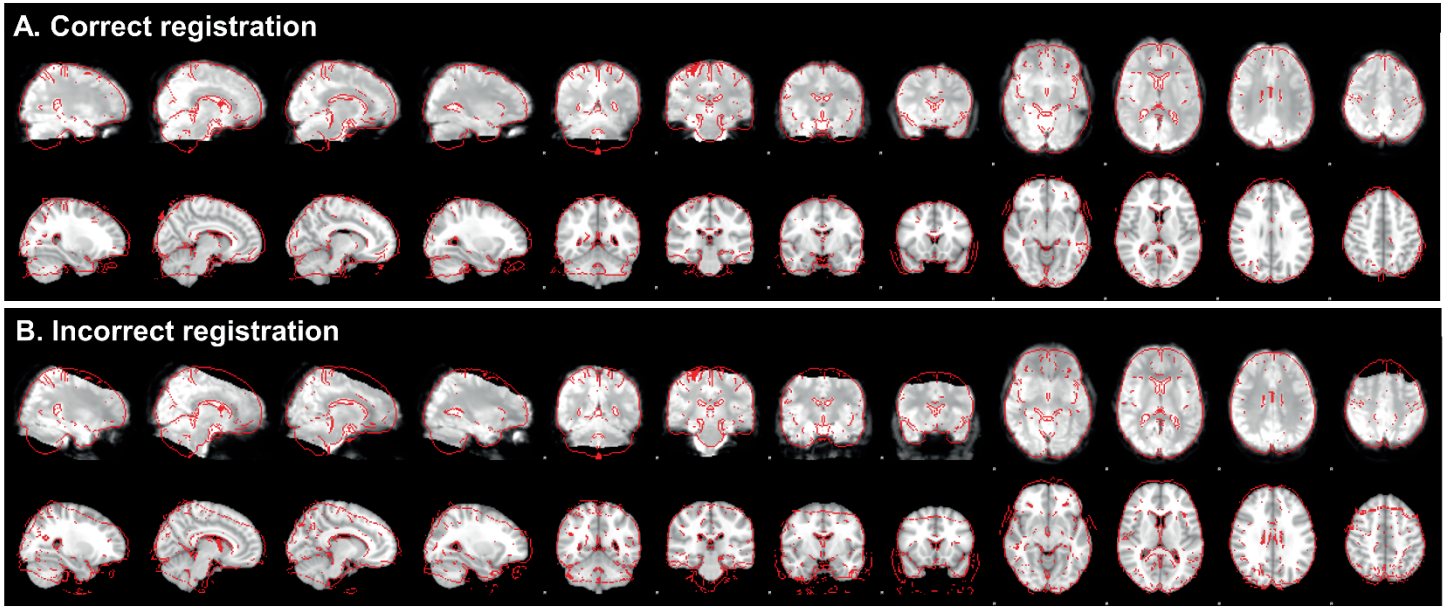


Figure S1. *Example of correct (A) and incorrect (B) registration from subject specific functional data to standard MNI space.*

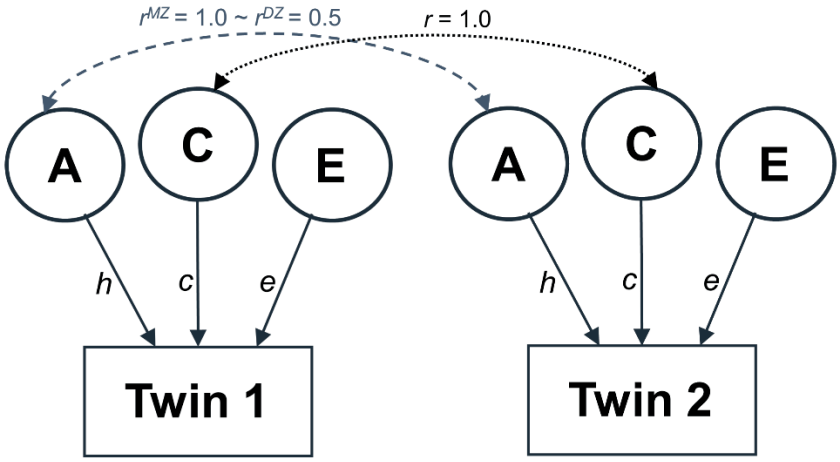


Figure S2. *ACE model. Similarities among twin pairs are divided into similarities due to shared genetic factors (A) and shared environmental factors (C), while dissimilarities are ascribed to unique environmental influences and measurement error (E). The correlation of factor C within twins is 1 for both MZ and DZ twins, while the correlation of factor A is 1 within MZ twins and on average 0.5 within DZ twins.*

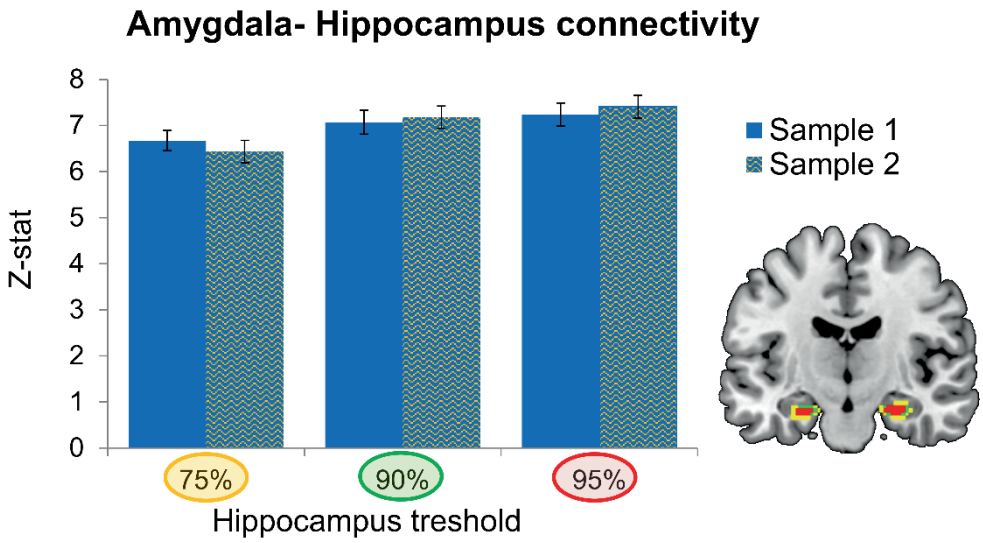


Figure S3*. Amygdala-Hippocampus connectivity for different thresholds of the Harvard/Oxford hippocampus region: 75% (yellow), 90% (green), and 95% (red).*

Table S1. Sample selection

N		age (SD)	age range	% boys
512	Children included	7.94 (0.67)	7.02 - 9.68	48.80
- 69	No RS scan*	7.92 (0.69)	7.02 - 9.26	55.07
-3	Anomalous findings**	8.82 (0.03)	8.80 - 8.85	33.33
-209	Excessieve head motion***	7.90 (0.66)	7.02-9.68	55.02
-11	Registration errors	7.65 (0.64)	7.03 - 8.84	54.54
220	final sample	7.99 (0.67)	7.02 - 9.08	40.91

* due to no parental consent (4); MRI contra-indications (7); anxiety (14) or lack of time (44)

** as indicated by a radiologist

*** defined as 0.5 mm framewise displacement in >20% of the data

Table S2. Genetic modeling of framewise displacement (FD) for the initial sample (prior to motion exclusion, N=398) and the final sample (N=220).

% frames >0.5 mm FD	model	A^2	C^2	E^2	LTR	AIC
Initial sample (prior to motion exclusion)	ACE	0.38	0.06	0.56		3146.62
	95% CI	0.26-0.56	0.00-0.42	0.44-0.72		
	AE*	0.44	-	0.56	0.08	3144.7
	CE	-	0.35	0.65	2.49	3147.11
	E	-	-	1	>26.72	3171.83
Final sample (after motion exclusion)	ACE	0.00	0.15	0.85		670.68
	95% CI	0.00-0.35	0.00-0.38	0.62-1.00		
	AE	0.11	-	0.89	0.93	669.61
	CE	-	0.15	0.85	<.001	668.68
	E*	-	-	1	<1.53	668.21

* Asterics indicate the best model fit

Table S3. MNI coordinates and local maxima for whole brain connectivity clusters from Sample I, with $Z>3.09$, $p<.05$ cluster correction. Anatomical regions were derived from the Harvard-Oxford atlas in FSL.

Sample I	voxels	max zstat	max x	max y	max X	anatomical regions
VS positive	10712	16	12	8	-12	Medial prefrontal cortex, anterior cingulate cortex, paracingulate gyrus, superior frontal gyrus, frontal pole, subcallosal cortex, thalamus, orbitofrontal cortex, putamen, pallidum, caudate, nucleus accumbens
	2128	6.39	38	12	10	Right frontal operculum cortex, right insula, right inferior frontal gyrus, right precentral gyrus, right postcentral gyrus
	374	4.7	50	-34	-22	Right inferior temporal gyrus, right teporal fusiform cortex
	352	5.31	66	-6	-20	Right middle temporal gyrus, right superior temporal gyrus
	271	4.02	-56	-10	-6	Left insula, left Heschl's gyrus
	214	4.75	-44	50	20	Left frontal pole
VS negative	3368	5.38	-38	10	40	Left middle frontal gyrus, left precentral gyrus, left inferior frontal grus, left superior frontal gyrus, left lateral occipital cortex, left superior parietal lobule
	3064	5.59	24	-34	14	Hippocampus, Thalamus, brainstem, parahippocampal gyrus
	2230	5.13	36	-20	42	Right postcentral gyrus, righ precentral gyrus, right supramarginal gyrus

Table S3. (continued)

Sample I	voxels	max zstat	max x	max y	max X	anatomical regions
VS negative	671	6.71	-46	30	-8	Left frontal pole, left orbitofrontal gyrus, left inferior frontal gyrus
	477	5.22	42	50	-8	Right frontal pole, right orbitofrontal gyrus, right inferior frontal gyrus
	461	4.91	50	8	40	Right middle frontal gyrus, right precentral gyrus
	353	4.92	36	-56	60	Right lateral occipital cortex
AMY positive	15999	15.2	-22	-4	-18	Hippocampus, parahippocampal gyrus, putamen, pallidum, thalamus, brainstem, Fusiform cortex, insula, temporal pole, subcallosal cortex, orbitofrontal cortex
AMY negative	66829	7.31	-2	-30	2	supplementary motor cortex, superior frontal gyrus, paracingulate gyrus, anterior cingulate gyrus, middle frontal gyrus, frontal pole, precentral gyrus, precuneous, postcentral gyrus, lateral occipital cortex, inferior frontal gyrus,precentral gyrus, central opercular cortex

Table S4. MNI coordinates and local maxima for whole brain connectivity clusters from Sample II, with $Z>3.09$, $p<.05$ cluster correction. Anatomical regions were derived from the Harvard-Oxford atlas in FSL.

Sample II	voxels	max zstat	max x	max y	max X	anatomical regions
VS positive	9397	14.3	10	10	-8	Medial prefrontal cortex, anterior cingulate cortex, paracingulate gyrus, superior frontal gyrus, frontal pole, subcallosal cortex, thalamus, orbitofrontal cortex, putamen, pallidum, caudate, nucleus accumbens
	1503	5.18	-38	-20	4	Left insula, left middle temporal gyrus, left inferior frontal gyrus
	443	4.58	46	-12	16	Right central opercular cortex, right inferior frontal gyrus
	336	3.95	50	-54	-12	Right inferior temporal gyrus, right temporal gyrus, right temporal fusiform cortex
	204	4.42	46	18	-32	Right temporal pole, right middle temporal gyrus
VS negative	7743	6.23	-10	2	38	Middle frontal gyrus, precentral gyrus, left inferior frontal grus,superior frontal gyrus, lateral occipital cortex, superior parietal lobule, postcentral gyrus
	3191	4.97	-6	-70	2	Hippocampus, Thalamus, brainstem, parahippocampal gyrus
	356	4.7	50	10	40	Right middle frontal gyrus, right precentral gyrus, right inferior frontal gyrus
AMY positive	17843	16.3	-24	-2	-20	Hippocampus, parahippocampal gyrus, putamen, pallidum, thalamus, brainstem, Fusiform cortex, insula, temporal pole, subcallosal cortex, orbitofrontal cortex
AMY negative	61466	7.8	2	16	48	Supplementary motor cortex, superior frontal gyrus, paracingulate gyrus, anterior cingulate gyrus, middle frontal gyrus, frontal pole, precentral gyrus, precuneous, postcentral gyrus, lateral occipital cortex, inferior frontal gyrus,precentral gyrus, central opercular cortex, left inferior frontal gyrus
	884	5.5	58	14	2	Right inferior frontal gyrus, right precentral gyrus, right central opercular cortex

Table S5. Mean and standard deviations of Z-values for all subcortical-cortical and subcortical-subcortical connectivity patterns. Differences in connectivity between different samples were tested with independent sample T-tests. Asterisks indicate significant differences between samples.

Seed	ROI	Sample I mean (SD)	Sample II mean (SD)	*T*	*p*	
VS	vmPFC	1.66 (1.34)	1.69 (1.60)	-0.12	0.905	
	vACC	1.05 (1.04)	0.86 (1.14)	1.07	0.287	
	OFC	1.31 (0.88)	1.09 (0.89)	1.54	0.125	
	dmPFC	-0.29 (0.61)	-0.05 (0.54)	-2.68	0.008	*
	dACC	-0.54 (1.03)	-0.73 (1.21)	1.10	0.274	
	dlPFC	-0.48 (0.59)	-0.31 (0.55)	-1.95	0.053	
	Thalamus	0.51 (1.37)	0.50 (1.37)	0.03	0.980	
	Hippocampus	-0.52 (1.87)	-0.41 (2.10)	-0.36	0.716	
	Amygdala	0.34 (2.17)	0.40 (2.04)	-0.17	0.862	
AMY	vmPFC	-0.04 (1.45)	0.26 (1.03)	-1.51	0.134	
	vACC	-0.25 (0.93)	0.06 (0.86)	-2.16	0.032	*
	OFC	1.13 (1.11)	1.28 (0.76)	-1.02	0.308	
	dmPFC	-0.75 (0.62)	-0.72 (0.59)	-0.28	0.777	
	dACC	-0.38 (1.11)	-0.29 (1.14)	-0.50	0.616	
	dlPFC	-0.88 (0.67)	-0.88 (0.54)	0.04	0.969	
	Thalamus	-0.43 (1.47)	-0.15 (1.32)	-1.24	0.218	
	Hippocampus	6.67 (1.93)	6.43 (2.17)	0.72	0.471	

Table S6. Simple T-tests for all subcortical-cortical and subcortical-subcortical connectivity patterns. Bold statistics indicate connectivity that was not significantly different from zero. For means and standard deviations, see **Table S5**.

Seed	ROI	Sample I	Sample II
VS	vmPFC	t(77)=10.94, *p*<.001	t(77)=9.31, *p*<.001
	vACC	t(77)=8.95, *p*<.001	t(77)=6.71, *p*<.001
	OFC	t(77)=13.09, *p*<.001	t(77)=10.86, *p*<.001
	dmPFC	t(77)=-4.30, *p*<.001	t(77)=-.80, *p*=.428
	dACC	t(77)=-4.59, *p*<.001	t(77)=-5.37, *p*<.001
	dlPFC	t(77)=-7.29, *p*<.001	t(77)=-4.93, *p*<.001
	Thalamus	t(77)=3.29, *p*=.002	t(77)= 3.25, *p*=.002
	Hippocampus	t(77)=-2.47, *p*=.016	t(77)= -1.71, *p*=.091
	Amygdala	t(77)=1.40, *p*=.167	t(77)=1.74, *p*=.085
AMY	vmPFC	t(77)=-.261, *p*=.795	t(77)=2.24, *p*=.028
	vACC	t(77)=-2.37, *p*=.021	t(77)=.63, *p*=.532
	OFC	t(77)=8.95, *p*<.001	t(77)=14.92, *p*<.001
	dmPFC	t(77)=-10.77, *p*<.001	t(77)=-10.90, *p*<.001
	dACC	t(77)=-3.04, *p*=.003	t(77)=-2.25, *p*=.027
	dlPFC	t(77)=-11.59, *p*<.001	t(77)=-14.50, *p*<.001
	Thalamus	t(77)=-11.59, *p*<.001	t(77)= -1.00, *p*=.321
	Hippocampus	t(77)=30.45, *p*<.001	t(77)=26.12, *p*<.001

Table S7. Genetic modeling of Ventral Striatum-Cortical connectivity: full ACE model versus more parsimonious models.

Seed	ROI	model	A²	C²	E²	LRT	AIC
VS	vmPFC	ACE	0.67	0.00	0.33		182.29
		AE*	0.67	-	0.33	<0.001	182.29
		CE	-	0.44	0.56	5.68	187.97
		E	-	-	1.00	>14.03	200.00
	vACC	ACE	0.12	0.17	0.71		138.13
		AE	0.32	-	0.68	0.19	136.31
		CE*	-	0.27	0.73	0.07	136.20
		E	-	-	1.00	>4.71	139.03
	OFC	ACE	0.32	0.09	0.59		83.87
		AE*	0.42	-	0.58	0.05	81.92
		CE	-	0.34	0.66	0.58	82.44
		E	-	-	1.00	>8.09	88.54
	dmPFC	ACE	0.36	0.01	0.63		-41.82
		AE*	0.37	-	0.63	0.001	-43.82
		CE	-	0.27	0.73	0.65	-43.17
		E	-	-	1.00	>5.00	-40.17
	dACC	ACE	0.46	0.00	0.54		165.63
		AE*	0.46	-	0.54	<0.001	163.63
		CE	-	0.27	0.73	4.00	167.62
		E	-	-	1.00	>4.97	170.60
	dlPFC	ACE	0.19	0.00	0.81		-50.46
		AE	0.19	-	0.81	<0.001	-52.46
		CE	-	0.12	0.88	0.73	-51.73
		E*	-	-	1.00	<1.74	-52.72

[1] LRT < 3.85 equals no worse fit of the model (p<.05)

[2] Lower AIC values indicate a better model fit

* Asterisks indicate the best model fit

Table S8. Genetic modeling of Amygdala-Cortical connectivity: full ACE model versus more parsimonious models.

Seed	ROI	model	A²	C²	E²	LRT	AIC
AMY	vmPFC	ACE	0.23	0.00	0.77		184.64
		AE	0.23	-	0.77	<0.001	182.64
		CE	-	0.07	0.93	1.43	184.08
		E*	-	-	1.00	<1.79	182.43
	vACC	ACE	0.00	0.35	0.65		84.01
		AE	0.34	-	0.66	1.12	83.14
		CE*	-	0.35	0.65	<0.001	82.01
		E	-	-	1.00	>7.41	88.55
	OFC	ACE	0.54	0.00	0.46		84.33
		AE*	0.54	-	0.46	<0.001	82.33
		CE	-	0.46	0.54	1.79	84.11
		E	-	-	1.00	>15.30	97.41
	dmPFC	ACE	0.08	0.00	0.92		-14.87
		AE	0.08	-	0.92	<0.001	-16.87
		CE	-	0.00	1.00	0.24	-16.62
		E*	-	-	1.00	<0.24	-18.62
	dACC	ACE	0.08	0.00	0.92		130.54
		AE	0.08	-	0.92	<0.001	128.54
		CE	-	0.03	0.97	0.22	128.77
		* E	-	-	1.00	<0.27	126.82
	dlPFC	ACE	0.14	0.00	0.86		-4.94
		AE	0.14	-	0.86	<0.001	-6.94
		CE	-	0.04	0.96	0.68	-6.26
		* E	-	-	1.00	<0.76	-8.18

[1] LRT < 3.85 equals no worse fit of the model (p<.05)

[2] Lower AIC values indicate a better model fit

* Asterisks indicate the best model fit

Table S9. Genetic modeling of Subcortical-Subcortical connectivity: full ACE model versus more parsimonious models.

Seed	ROI	model	A²	C²	E²	LRT	AIC
VS	Hippocampus	ACE	0.37	0.00	0.63		266.12
		AE*	0.37	-	0.63	<0.001	264.12
		CE	-	0.32	0.68	0.74	264.87
		E	-	-	1.00	>6.95	269.81
	Thalamus	ACE	0.04	0.15	0.81		175.08
		AE	0.21	-	0.79	0.13	173.21
		CE*	-	0.18	0.82	0.01	173.08
		E	-	-	1.00	<2.10	173.18
	Amygdala	ACE	0.42	0.00	0.58		281.83
		AE*	0.42	-	0.58	<0.001	279.83
		CE	-	0.36	0.64	0.92	280.75
		E	-	-	1.00	>9.07	287.83
AMY	Hippocampus	ACE	0.32	0.00	0.68		277.93
		AE*	0.32	-	0.68	<0.001	275.93
		CE	-	0.19	0.81	2.24	278.18
		E	-	-	1.00	>2.27	278.44
	Thalamus	ACE	0.35	0.00	0.65		154.42
		AE*	0.35	-	0.65	<0.001	152.42
		CE	-	0.23	0.77	1.98	154.40
		E	-	-	1.00	>3.47	155.87

[1] LRT < 3.85 equals no worse fit of the model (p<.05)

[2] Lower AIC values indicate a better model fit

* Asterisks indicate the best model fit

CHAPTER SEVEN

Genetic and environmental influences on MRI scan quantity and quality

This chapter is published as: Achterberg M. & Van der Meulen M. (2019). Genetic and environmental influences on MRI scan quantity and quality, *Developmental Cognitive Neuroscience, 38*.

Abstract

The current study provides an overview of quantity and quality of MRI data in a large developmental twin sample (N=512, aged 7-9), and investigated to what extent scan quantity and quality were influenced by genetic and environmental factors. This was examined in a fixed scan protocol consisting of two functional MRI tasks, high resolution structural anatomy (3DT1) and connectivity (DTI) scans, and a resting state scan. Overall, scan quantity was high (88% of participants completed all runs), while scan quality decreased with increasing session length. Scanner related distress was negatively associated with scan quantity (i.e., completed runs), but not with scan quality (i.e., included runs). In line with previous studies, behavioral genetic analyses showed that genetics explained part of the variation in head motion, with heritability estimates of 29% for framewise displacement and 65% for absolute displacement. Additionally, our results revealed that subtle head motion (after exclusion of excessive head motion) showed lower heritability estimates (0-14%), indicating that findings of motion-corrected and quality-controlled MRI data may be less confounded by genetic factors. These findings provide insights in factors contributing to scan quality in children, an issue that is highly relevant for the field of developmental neuroscience.

Keywords: Childhood; Functional MRI; Head motion; Heritability; Scanner related distress; Structural MRI

Introduction

In the first decade of life, extensive changes occur in the structure and function of the brain (Gilmore *et al.*, 2018). With the introduction of Magnetic Resonance Imaging (MRI), these changes in brain characteristics can be studied in vivo, and a growing body of literature has provided insight in the developing brain. Although MRI research is non-invasive, the scanner itself - in particular its noise level and narrow space- and the surrounding procedures are rather imposing and can induce anxiety in children (Tyc *et al.*, 1995; Durston *et al.*, 2009). Such scanner related distress makes it less likely for children to successfully finish an MRI scan, resulting in reduced scan quantity compared to older samples. Moreover, the quality of the scans heavily depends on the amount of (head) motion, which is specifically troublesome in developmental samples, as head movement during MRI is strongly correlated with age (Poldrack *et al.*, 2002; Satterthwaite *et al.*, 2013). Several prior developmental neuroimaging findings have been called into question after studies showed that these findings were largely influenced by age-related differences in head motion (Power *et al.*, 2012; Van Dijk *et al.*, 2012; Savalia *et al.*, 2017), highlighting the need for an in-depth investigation of factors that can influence scan quality in children. In the current study we therefore provide an overview of MRI scan quantity and quality in a large developmental twin sample (N=512, 256 twin pairs, aged 7-9), and investigated the genetic and environmental influences on MRI data quantity and quality.

Scan quality is not only influenced by head motion but can also be influenced by additional sources of noise such as scanner drift and respiratory signals (Kotsoni *et al.*, 2006; Liu, 2017; Power, 2017). However, as excessive head motion is especially pronounced in developmental samples (Satterthwaite *et al.*, 2013), the current study focused on head motion as measure of scan quality. In the last couple of years, the topic of MRI motion artifacts has received increasing attention, and several methods to correct for motion during MRI analyses have been developed (Power *et al.*, 2015; Fassbender *et al.*, 2017b; Power, 2017). Much less research has focused on specific factors that contribute to MR scan quality in children. Recent studies have pointed towards genetics as a possible factor influencing scan quality, with findings suggesting that head motion in adults is a stable and heritable phenotype (Van Dijk *et al.*, 2012; Couvy-Duchesne *et al.*, 2014), with heritability estimates ranging from 37-51% in adults. Exploratory twin-analyses on pediatric MRI data also showed familial similarities in children (Engelhardt *et al.*, 2017), although the small sample size hindered direct estimations of heritability. In the current study we provide direct estimates of heritability by conducting behavioral genetic analyses on a large childhood twin sample.

In addition to trait-like, genetic influences on scan quality, we also investigated the influence of environmentally affected factors, such as emotional

state towards the MR scan and MR protocol length. Previous research has described several child-specific scanner environment adaptations that have been used in (clinical) radiology departments (Galvan *et al.*, 2012; Raschle *et al.*, 2012; Fassbender *et al.*, 2017b). One adaptation that has been shown to be particularly useful is the use of a mock scanner (Rosenberg *et al.*, 1997; Hallowell *et al.*, 2008; Durston *et al.*, 2009), which replicates the MRI environment and can be used to familiarize young subjects with the procedure of an MRI scan. Children who underwent such an MRI simulation were less stressed (as indicated by lower heart rate) than children who were not trained with a simulator (Rosenberg *et al.*, 1997). Moreover, studies showed a linear decrease in (self and parent reported) anxiety levels after MRI simulation (Rosenberg *et al.*, 1997; Durston *et al.*, 2009), indicating that an MRI simulation can make children feel more at ease with MRI research. This is important for the well-being of the participant, and a positive experience with the MRI scan can also increase retention of participants in longitudinal imaging studies, which is important for the validity of developmental MRI studies (Telzer *et al.*, 2018). However, it is currently unknown whether a more positive emotional state towards the MRI scan is related to better outcomes in terms of scan quantity and quality. By using multi-informant estimations of emotional state, we directly tested the relation between scanner related distress and scan quantity and scan quality. We first examined how scanner related distress changed over time at three moments: before the MRI simulation, before the MRI scan, and after the MRI scan. We hypothesized that the emotional state would become more positive over time (Durston *et al.*, 2009). Moreover, we hypothesized that there would be little influence of genetics on scanner related distress, as it is highly influenced by the environment (i.e., the MRI simulation). Next, we evaluated MRI scan quantity by investigating how scan quantity was related to emotional state, and to what extend scan quantity was influenced by genetics. Scan quantity was defined as the number of completed MRI runs within the protocol (ranging from 0-9). It should be noted that completing a run does not necessarily indicate that the MRI data is useable, and therefore scan quantity is essentially different from scan quality.

Similar to scan quantity, we investigated whether scan quality was related to emotional state, and to what extend scan quality was influenced by genetics. As an additional factor of interest, we examined scan quality across the duration of the MR session, as children tend to lose focus faster than adults, which may result in increased motion over time (Van Horn and Pelphrey, 2015; Fassbender *et al.*, 2017b). Scan quality was examined in two ways: 1) the percentage of included MRI runs within the session (defined as the number of scans with sufficient quality relative to the number of runs completed), and 2) the amount of absolute and framewise head displacement in mm in fMRI runs. The first estimate of scan quality provides an overall, relatively simple measure of quality over the whole MRI session. The second measure provides a more sophisticated, quantitative measure of scan quality, but could only be calculated for functional MRI runs

(Power, 2017). By investigating both trait-like genetic influences as well as state-like environmental influences this study can provide insights in factors contributing to scan quantity and quality in developmental samples.

Methods

Participants

Participants in this study took part in the preregistered longitudinal twin study of the Leiden Consortium on Individual Development (L-CID; Euser *et al.* (2016)). The Dutch Central Committee on Human Research (CCMO) approved the study and its procedures (NL50277.058.14). Families with a same-sex twin born between 2006 – 2009, living within two hours travel time from Leiden, were recruited through municipal registries and received an invitation to participate via mail. Parents could show their interest in participation using a reply card. 512 children (256 families) between the ages 7 and 9 were included in the L-CID study (mean age: 7.94±.67; 49% boys). Written informed consent was obtained from both parents. All children were fluent in Dutch or English and had normal or corrected-to-normal vision. The majority of the sample was Caucasian (90%) and right-handed (87%). Since the sample represents a population sample, we did not exclude children with a psychiatric disorder. For information on psychiatric disorders, we asked parents whether the children received a medical diagnosis from a psychologist or medical expert. Eleven participants (2%) were diagnosed with an Axis-I disorder: nine with attention deficit (hyperactivity) disorder (ADD/ADHD); one with generalized anxiety disorder (GAD), and one with pervasive developmental disorder-not otherwise specified (PDD-NOS). Participants' intelligence (IQ) was estimated with the subtests 'Similarities' and 'Block Design' of the Wechsler Intelligence Scale for Children, third edition (WISC-III; Wechsler (1991)). Estimated IQs were in the normal range (72.50 - 137.50, mean: 103.58 ±11.76). Zygosity was determined by DNA analyses, which classified 55% of the twins as monozygotic.

Procedure

Participating twins visited the lab with their primary parent (defined as the parent that spends the most time with the children). Before the visit to the lab families received a step-by-step explanation of the MRI procedure, including a description of the magnetic field, the materials used during the MRI scan (earplugs, headphones, button box, alarm), and the movies that were available to watch. The step-by-step approach was specifically aimed at the young participants, and

consisted of child appropriate texts and illustrative pictures. The lab visit took place at the Leiden University Medical Centre (LUMC) and consisted of four components: the MRI preparation session, the MRI scan session, parent-child interaction tasks, and a child behavioral tasks session. In the current study, data from the MRI preparation session and the MRI scan session were evaluated. During the practice session the whole family was further introduced to the aims of the study, and carefully instructed about safety around the MRI system and the influence of motion on the scans. Next, the children participated in a MRI simulation with the MRI researcher. In the MRI simulation, the exact same steps that were also explained in the step-by-step explanation were followed. A prototype of a Philips scanner (without a working magnet) was used to mimic the MRI environment. Children listened to MRI sounds via a laptop. They were shown the various materials (e.g. headphones, button box, coil with mirror attached) for the MRI procedure. Next, they were asked to practice lying very still on the scanner bed while wearing the headphones and button box. Finally, they practiced looking in the mirror on the coil, while they were slowly slid into the MRI bore. After the MRI simulation, the children were familiarized with the MRI tasks on a laptop. First-born and second-born children of each twin pair were randomly assigned to the MRI scan session or to the parent-child interaction tasks as their first activity. There were no differences in outcome measures (scanner related distress, scan quantity or scan quality) for children that were scanned directly after the MRI simulation or an hour later.

The MRI session lasted 60 minutes, including two fMRI tasks, high resolution T2 and T1 scans, diffusion tensor imaging (DTI) scans and a resting state (RS) fMRI scan. The first fMRI task was the Social Network Aggression Task (SNAT), as described in detail in Achterberg *et al.* (2018b). In short, participants viewed pictures of peers that gave positive, neutral or negative feedback to the participant's personal profile. Next, participants could blast a loud noise towards the peer as an index of aggression. The SNAT consisted of 3 runs of approximately 5 minutes each. The second task was the Prosocial Cyberball Game (PCG), as described in detail in van der Meulen *et al.* (2018). In short, participants were instructed to participate in a virtual ball tossing game with three other players. During the game, two of the other players excluded the third player. The participant could choose to compensate for this exclusion by tossing the ball more often to the excluded participant (prosocial compensating behavior). The PCG consisted of 2 runs of approximately 5 minutes each. After the fMRI tasks participants watched a self-chosen child-friendly movie during the structural anatomical scan (3DT1) and the structural connectivity scans (DTI). The scan session ended with a RS fMRI scan, in which participants were instructed to lay still with their eyes closed and not to fall asleep (for details, see Achterberg *et al.* (2018a)). The order of the scans was the same for all participants and always started with the SNAT fMRI task, followed by the PCG fMRI task, the 3DT1, DTI and the RS fMRI.

Scanner related distress

To get an estimate of the children's scanner related distress we asked the children to indicate how they felt about the scanner by using a visual analogue scale, based on Durston *et al.* (2009). Children's feelings of stress and excitement were assessed at three different moments: before the MRI simulation, before the MRI scan, and after the MRI scan. Participants were asked to indicate how *tensed* and how *excited* they felt about the scan session, by pointing to the cartoon smiley that best represented their feelings (Figure 1a). Since children tend to underreport their tension or anxiety (Durston *et al.*, 2009), the child's emotional state was consecutively also estimated by the researcher and the parent. It should be noted that both the child's and the researcher's estimates were written on the same form with the child reporting first, making them not independent. The parents estimated scanner related distress separately from the child and therefore these estimates were independent. Therefore, multi-informant ratings were based on child and parent reports. Parents, however, did not estimate the children's emotional state after the MRI scan, as they were not present during the MRI scan (being involved in parent-child interaction tasks with the other twin sibling). Therefore, the scores after the MRI scan were based on child report only.

MRI data acquisition

MRI scans were acquired with a standard whole-head coil on a Philips Ingenia 3.0 Tesla MRI system. To prevent head motion, foam inserts surrounded the children's heads. The fMRI tasks and the movie were projected on a screen that was visible through a mirror on the head coil. Functional runs of the fMRI tasks (first task: SNAT (Achterberg *et al.*, 2018b); second task: PCG (van der Meulen *et al.*, 2018)) were acquired using a T2*-weighted echo-planar imaging (EPI). The first two (dummy) volumes were discarded to allow for equilibration of T1 saturation effects. The SNAT consisted of 3 runs in total with 148 volumes (5.43 min), 142 volumes (5.21 min), and 141 volumes (5.17 min) respectively. The PCG consisted of 2 runs in total. The number of volumes was dependent on the reaction time of the participant, with a maximum of 175 volumes. On average, 136 volumes (4.99 min) were acquired for each PCG run. Volumes covered the whole brain with a field of view (FOV) in mm = 220 (ap) x 220 (rl) x 111.65 (fh) mm; repetition time (TR) of 2.2 seconds; echo time (TE) = 30 ms; flip angle (FA) = 80°; sequential acquisition, 37 slices; and voxel size = 2.75 x 2.75 x 2.75 mm. Subsequently, a high-resolution 3D T1scan was obtained as anatomical reference (FOV= 224 (ap) x 177 (rl) x 168 (fh); TR = 9.72 ms; TE = 4.95 ms; FA = 8°; 140 slices; voxel size 0.875 x 0.875 x 0.875 mm). In addition, a high-resolution EPI scan was obtained for RS-fMRI registration purposes (TR = 2.2 sec; TE = 30 ms, flip angle = 80°, FOV= 220.000 (rl) x 220.00 (ap) x 168.00 (fh), 84 slices). Next, two transverse Diffusion Weighted Imaging (DWI) scans were obtained with the following parameter settings (similar to Achterberg *et al.* (2016a)): 30 diffusion-weighted volumes with

different noncollinear diffusion directions with b-factor 1,000 s/mm2 and 5 diffusion-unweighted volumes (b-factor 0 s/mm2); anterior -posterior phase encoding direction; parallel imaging SENSE factor = 3; flip angle = 90°; 75 slices of 2 mm; no slice gap; reconstruction matrix 128 × 128; FOV = 240 × 240 mm; TE = 69 ms; TR = 7,315 ms. The second DWI set had identical parameter settings as used for the first set except that it was acquired with a reversed k-space readout direction (posterior-anterior phase encoding direction) enabling the removal of susceptibility artifacts during post processing (Andersson *et al.*, 2003). Resting state data was acquired at the end of the imaging protocol (for details see Achterberg *et al.* (2018a)). A total of 142 T2 -weighted whole-brain echo planar images (EPIs) were acquired, including 2 dummy volumes preceding the scan to allow for equilibration of T1 saturation effects (TR = 2.2 sec; TE = 30 ms; flip angle = 80°; FOV = 220.000 (rl) x 220.00 (ap) x 111.65 (fh); 37 slices).

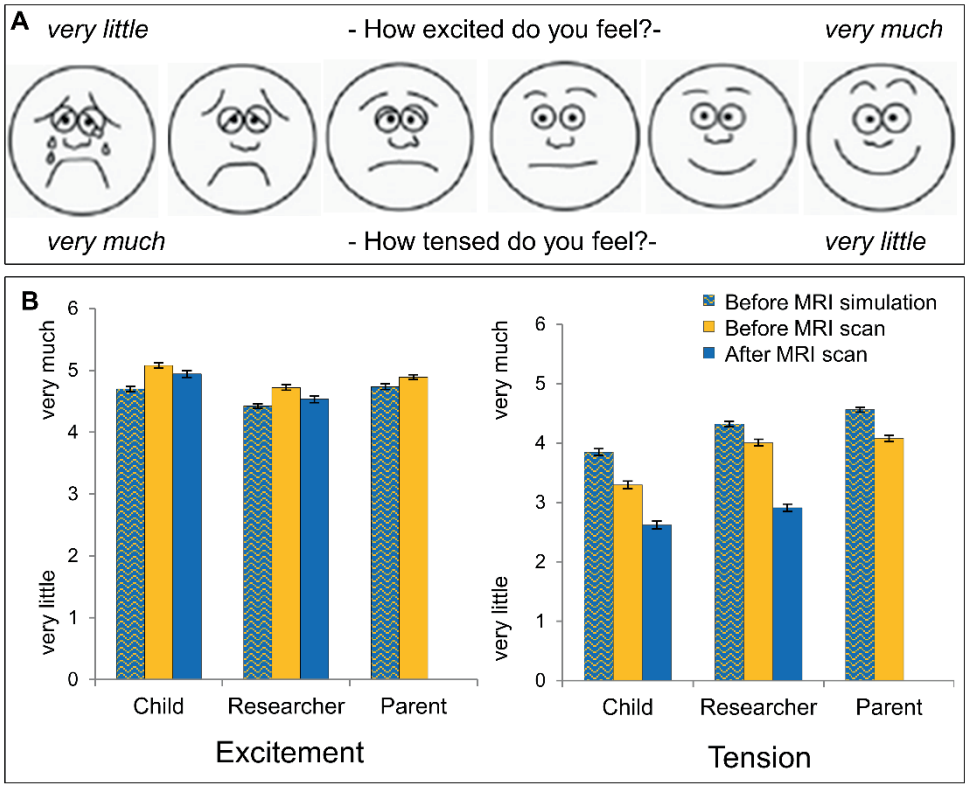


Figure 1. *Emotional state towards the MRI scan. A) Visual analogue scales. B) Estimation of excitement and tension on three moments (before MRI simulation, before MRI scan, and after MRI scan) and by three raters (child, researcher, and parent).*

MRI data quality control

Motion estimation of functional MRI (task-based and resting state) was carried out using Motion Correction FMRIB's Linear Image Registration Tool (MCFLIRT Jenkinson *et al.* (2002), as implemented in the FMRIB Software Library (FSL) version 5.09 (Smith *et al.*, 2004). Absolute displacement (AD) in x, y, and z direction was calculated for all runs, for all participants (Table 1), with the middle volume of the run as a reference. We additionally investigated micro-movement (i.e., motion between two volumes) using the motion outlier tool (*fsl_motion_outliers*). Mean framewise displacement (FD) was calculated for all runs, for all participants (Table 1). Reliability analyses showed consistency in head motion over fMRI runs: mean FD: α=.77; mean AD (mean x-y-z direction): α=.84. For further analyses we computed a mean score over all fMRI runs for framewise displacement (M=.77, SD=1.29, range=.09-17.5) and absolute displacement (M=2.55, SD=3.77, range=.21-37.91). Framewise and absolute displacement were significantly positively correlated: r=.88, p<.001. For task-based fMRI runs, we defined runs with <3 mm (1 voxel) maximum motion in all directions as sufficient quality (Achterberg *et al.*, 2018b; van der Meulen *et al.*, 2018). For the RS fMRI data, volumes with framewise displacement of >0.3 mm (stringent threshold) or >0.5 (lenient threshold) were flagged as outliers (Power *et al.*, 2012). RS fMRI data with < 20% of the volumes flagged as outlier was classified as sufficient quality, see Table 1. Although inclusion criteria for task-based and RS fMRI were different, they resulted in comparable motion estimates for the different fMRI runs of included participants (Table 1).

Structural T1 scans were pre-processed in FreeSurfer (v5.3.0). Anatomical labeling and tissue classification was performed on the basis of the T1- weighted MRI image using various tools of the FreeSurfer software (http://surfer.nmr.mgh.harvard.edu/). The pre-processing pipeline included non-brain tissue removal, cortical surface reconstruction, subcortical segmentation, and cortical parcellation (Dale *et al.*, 1999; Fischl *et al.*, 1999). After pre-processing, each scan was manually checked to assess quality by three trained raters. Scans were rated based on a set of specific criteria (e.g., affection by movement, missing brain areas in reconstruction, inclusion of dura or skull in reconstruction, see Klapwijk *et al.* (2019). 31% of the structural T1 scans were rated as 'Excellent', 43% of the scans were rated as 'Good', 16% of the scans were rated as 'Doubtful', and 10% of the scans were rated as 'Failed' (see Figure 2a). Structural anatomical data rated as 'Failed' and 'Doubtful' were classified as insufficient quality, and data coded as 'Excellent' and 'Good' were classified as sufficient quality. We investigated whether scans with different ratings would show actual differences in estimated brain volume, by comparing the four different ratings on the "Total Gray Volume" variable from the Freesurfer output. We found a significant difference in gray matter volume between the different ratings (F(3, 463) = 5.07, p = .002), with post hoc analyses revealing a significant difference between scans rated as 'Failed' and scans rated as 'Excellent' to

'Doubtful' (all *p's*<.02). Therefore, for analyses using more lenient quality control, we included data that were classified as 'Excellent', 'Good' and 'Doubtful'.

Diffusion weighted images were preprocessed using several FSL analysis tools. Firstly, Top-up was used to estimate and correct susceptibility induced distortions (Andersson *et al.*, 2003). Secondly, the Brain Extraction Tool (BET) was used to delete non-brain tissue from images of the entire head (Smith, 2002). Third, the Eddy tool was used to correct for eddy current-induced distortions and subject movement. Thereafter, a diffusion tensor model was fitted at each voxel by using the analysis-tool DTIFIT. Scans were rated by two independent researchers. 86% of the DTI data were rated as 'Excellent', 8% of the data were rated as 'Good', 4% of the data were rated as 'Doubtful', and 2% of the data were rated as 'Failed' (see Figure 2b). DTI data rated as 'Failed' and 'Doubtful' were classified as insufficient quality, and all other data ('Excellent' and 'Good') were classified as sufficient quality. For analyses using more lenient quality control, we included data that were classified as 'Excellent', 'Good' and 'Doubtful'.

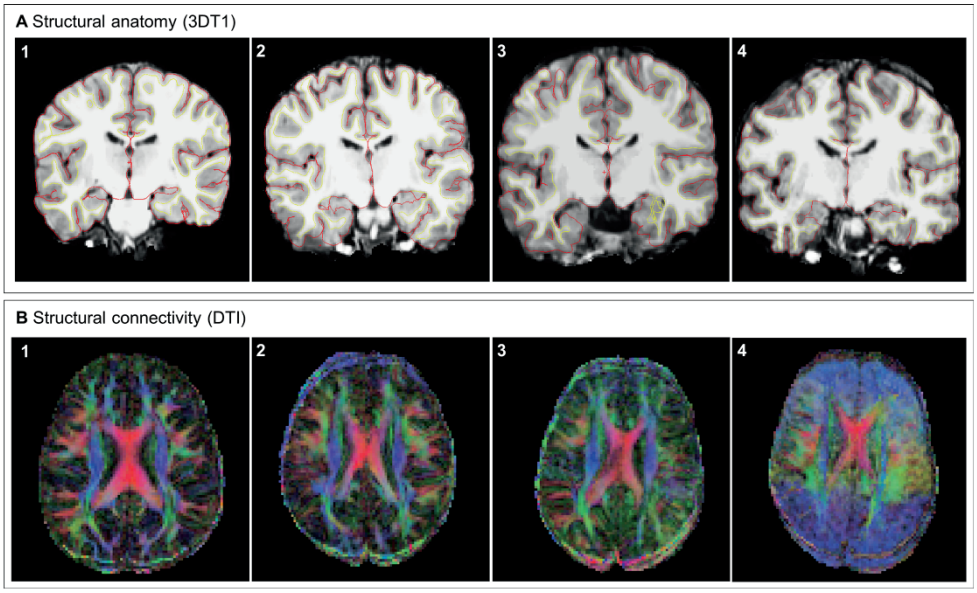


Figure 2. *Examples of quality control classifications with scans rated as (1) Excellent, (2) Good, (3) Doubtful, and (4) Failed. A) Parcellated structural anatomy (T1 weighted) scan with pial surface (red line) and white matter/grey matter division (yellow line). B) Diffusion tensor fitted structural connectivity (DTI) scan with connections in right-left (red), anterior-posterior (green), and dorsal-ventral (blue) direction (For interpretation of the references to colour in this figure legend, the reader is referred to the web version of this article).*

Table 1. Framewise and absolute head displacement.

	N	meanFD (mm)	mean X, Y, Z (mm)	X (mm)	Y (mm)	Z (mm)
all participants						
SNAT run 1	488	.48 (1.12)	1.82 (4.37)	.59 (1.33)	2.27 (6.44)	2.59 (5.90)
SNAT run 2	483	.65 (1.28)	2.11 (4.38)	.71 (1.66)	2.65 (6.82)	3.00 (5.19)
SNAT run 3	481	.68 (1.05)	2.20 (3.64)	.78 (1.37)	2.52 (4.44)	3.30 (5.71)
PCG run 1	480	.69 (1.63)	2.37 (5.10)	.79 (1.83)	2.84 (7.53)	3.46 (6.43)
PCG run 2	478	.98 (3.23)	3.01 (5.50)	1.01 (1.89)	3.53 (8.78)	4.48 (7.26)
RS	442	1.07 (2.4)	3.82 (6.80)	1.16 (2.38)	4.47 (8.73)	5.83 (9.97)
included participants						
SNAT run 1*	385	.32 (.90)	.76 (.42)	.29 (.25)	.87 (.56)	1.11 (.66)
SNAT run 2*	345	.26 (.14)	.74 (.43)	.27 (.26)	.83 (.57)	1.10 (.68)
SNAT run 3*	320	.28 (.18)	.79 (.49)	.30 (.31)	.91 (.65)	1.17 (.76)
PCG run 1*	307	.24 (.14)	.72 (.44)	.25 (.25)	.83 (.58)	1.07 (.71)
PCG run 2*	266	.27 (.15)	.82 (.47)	.29 (.30)	.93 (.59)	1.24 (.79)
RS stringent[1]	151	.18 (.08)	.75 (1.26)	.23 (.24)	.79 (.63)	1.21 (3.35)
RS lenient[2]	230	.25 (.27)	1.04 (1.47)	.30 (.32)	1.15 (1.51)	1.68 (3.14)

* Based on < 3 mm absolute displacement (X, Y and Z)

[1] Based on <20 % frames with >0.3 mm framewise displacement

[2] Based on <20 % frames with >0.5 mm framewise displacement

Statistical Analyses

Statistical analyses were performed in the Statistical Package for Social Sciences (SPSS version 24) and in R version 3.5.0 (R Core Team, 2015). Scanner related distress over time was examined with repeated measures ANOVAs in SPSS. Associations between emotional state, scan quantity, and scan quality were investigated using Pearson's correlations (in SPSS). To estimate familial influences on our outcome measures we calculated Pearson within-twin correlations for monozygotic (MZ) and dizygotic (DZ) twin pairs. Similarities among twin pairs are divided into similarities due to shared genetic factors (A) and shared environmental factors (C), while dissimilarities are ascribed to unique environmental influences and measurement error (E). Behavioral genetic modeling with the OpenMX package (Neale *et al.*, 2016) in R (R Core Team, 2015) was used to provide estimates of these A, C, and E components. The correlation of the shared environment (factor C) was set to 1 for both MZ and DZ twins, while the correlation of the genetic factor (A) was set to 1 for MZ twins and to 0.5 for DZ twins (see Figure S1). The last factor, unique environmental influences and measurement error, was freely estimated. We calculated the ACE models for emotional state towards the MRI scan, scan quantity, and scan quality. High estimates of A indicate that genetic factors play an important role, whilst C estimates indicate influences of the shared environment. If the E estimate is the highest, variance in motion is mostly accounted for by unique environmental factors and measurement error. We first examined genetic influences on mean FD and mean AD for all scanned participants. Next, we examined the influence of genetics on moderate head motion, by excluding participants with excessive head motion (>1 mm mean FD, >3 mm mean AD). To investigate the effects of minimal head motion we only included participants with little head motion (<0.3 mean FD, < 1 mm mean AD).

Results

Scanner Related Distress

Scanner related distress over time

To investigate scanner related distress preceding and following the MRI scan, we measured the emotional state towards the scanner using the visual analogue scales. Over time, children reported more excitement and less tension, see Figure 1b. That is to say, children reported being significantly more excited before the MRI scan (M= 5.10, SD= .93), and after the MRI scan (M= 4.95, SD= 1.23), compared to before the MRI simulation (M= 4.72, SD= .94; F (491) = 23.25, p<.001, all Bonferroni corrected pair-wise comparisons p<.05). Furthermore, children reported significantly less tension before the MRI scan (M= 3.28, SD= 1.44), and

after the MRI scan (*M*= 2.62, *SD*= 1.49), compared to before the MRI simulation (*M*= 3.84, *SD*= 1.28; *F* (491) =124.65, *p*<.001, all Bonferroni corrected pair-wise comparisons *p*<.05). Ratings of tension by the researchers and parents showed a similar pattern (Figure 1b) and were significantly correlated with ratings of children (*r*-range= .23-.80, see Table S1). Scanner related distress (before simulation and before the MRI scan, for excitement and tension) was more strongly correlated between children and researchers (*r*-range: .70-.80, Table S1), than between children and parents (*r*-range .23-.42, Table S1), but it should be noted that the child and researcher filled in the rating at the same form and therefore were not independent. The multi-informant scores (estimated emotional state averaged across child and parent) of tension and excitement were significantly negatively correlated: *r*=-.33, *p*<.001 before MRI simulation, and *r*=-.35, *p*<.001 before the MRI scan.

Genetic influences on scanner related distress

To investigate genetic and environmental influences on scanner related distress, we calculated Pearson's within-twin correlations for MZ and DZ twins and performed behavioral genetic analyses. Within-twin correlations for the multi-informant ratings of scanner related distress (tension and excitement; before MRI simulation and before MRI scan) were similar for MZ and DZ twins (r_{mz} range=.24-.58; r_{dz} range=.22-.48; all *p*'s<.05, see Table 2). Behavioral genetic analyses revealed that scanner related distress was mostly explained by environmental factors, both the shared environment (C-range=23-47%) as well as the unique environment/measurement error (E-range=45-77%), with little to no influence of genetics (A-range= 2-27%) (Table 2).

MRI Quantity

Scan quantity

Of the 512 included participants, 24 children (4.7%) never started with the MRI scan due to MRI contra indications (n=6); lack of parental consent (n=4); technical error (n=1), or substantial anxiety (n=13), see Table S2. As can be seen in Table S2 and Figure 3a, there was a drop in scan quantity (i.e. the number of scans completed) after the structural anatomy scan (from 94% to 88%). Scan quantity decreased because some children reported tiredness (n=18) or due to time constraints (i.e. the reserved time was over; n=12). For some children the DTI scans were skipped and only the RS-fMRI scan was acquired (n=12), as the RS-fMRI run was shorter in duration (5 minutes compared to 2*5 minutes DTI). To investigate age and gender effects on scan quantity we compared participants who completed all scans (age *M*=7.96, *SD=0.*67; 48% boys; n=433), and participants who missed one or more scans (excluding participants who missed scans due to time constraints; age *M*=7.84, *SD=0.*66; 59% boys, n=39). However, we found no effects of age (*t*(470)=-1.08, *p*=.28) or gender (χ(1, N=472)=1.86,

p=.12). We also found no association between age and the number of completed scans (*r*=.02, *p*=.63).

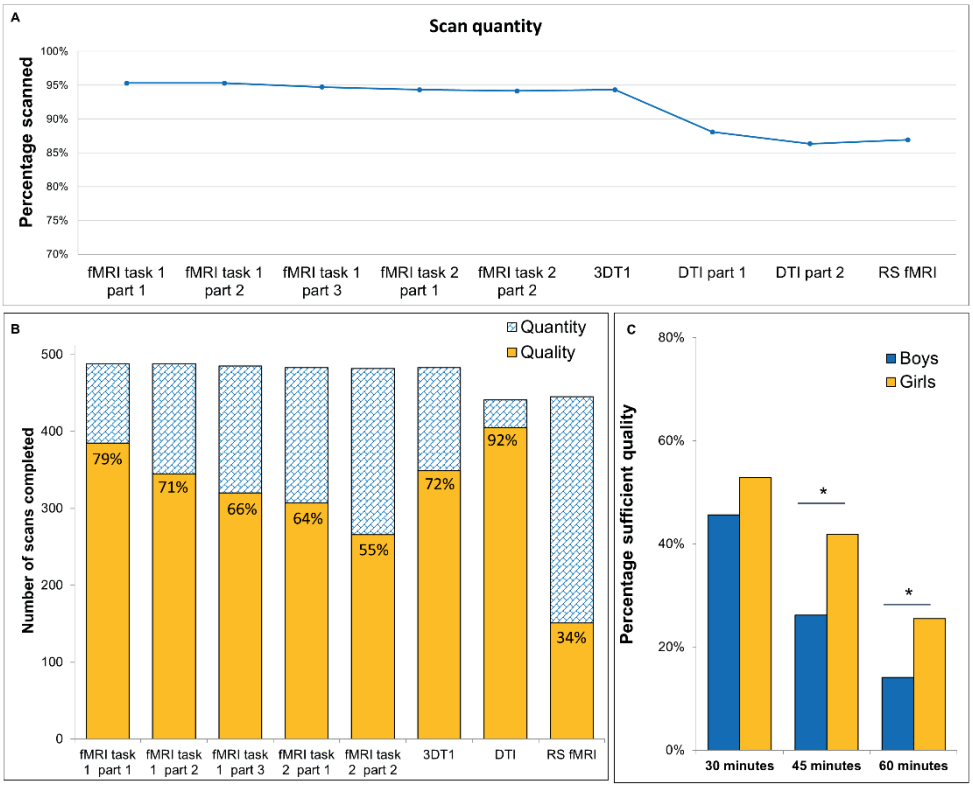


Figure 3. *Scan quantity and quality. A) Scan quantity: the percentage of children that completed the MR run (100%=512 participants). B) The number (and percentage) of scans with sufficient scan quality relatie to the quantity of the scans. C) Scan quality over time: the percentage of participants that were included on all scans in 30, 45 or 60 min, separately for boys and girls.*

Scan quantity in relation to scanner related distress

Pearson's correlations on the number of completed scans (ranging from 0-9, *M*=8.29, *SD*=2.08) showed a positive association between excitement towards the scan and the number of scans completed (before MRI simulation: *r*=.21, *p*<.001; before MRI scan: *r*=.30, *p*<.001; after MRI scan: *r*=.25, *p*<.001), and a negative association between tension towards the scan and the number of scans completed (before MRI simulation: *r*=-.18, *p*<.001; before MRI scan: *r*=-.16, *p*<.001; after MRI scan: *r*=-.17, *p*<.001), see Figure 4. All Pearson correlations were significant at Bonferroni corrected alpha level, adjusted for the number of distress estimates (six in total: excitement and tension before MRI simulation, before MRI scan, after MRI scan; α=0.5/6, Bonferroni corrected α=.008).

Table 2. Genetic modeling of emotional state towards the MRI scan.

Mood estimates		MZ	DZ		A²	C²	E²
Excitement							
Before MRI simulation	*r*	.50**	.48**	*ACE*	0.02	0.47	0.51
	*n*¹	138	114	*95% CI*	0.00-0.38	0.15-0.57	0.40-0.62
Before MRI scan	*r*	.41**	.30**	*ACE*	0.09	0.27	0.63
	*n*¹	135	113	*95% CI*	0.00-0.47	0.00-0.45	0.51-0.76
Tension							
Before MRI simulation	*r*	.58**	.39**	*ACE*	0.27	0.28	0.45
	*n*¹	138	114	*95% CI*	0.00-0.62	0.00-0.55	0.36-0.57
Before MRI scan	*r*	.24**	.22*	*ACE*	0	0.23	0.77
	*n*¹	134	113	*95% CI*	0.00-0.36	0.00-0.34	0.66-0.90

* p<.05, ** p<.001, ¹ Number of complete twin pairs

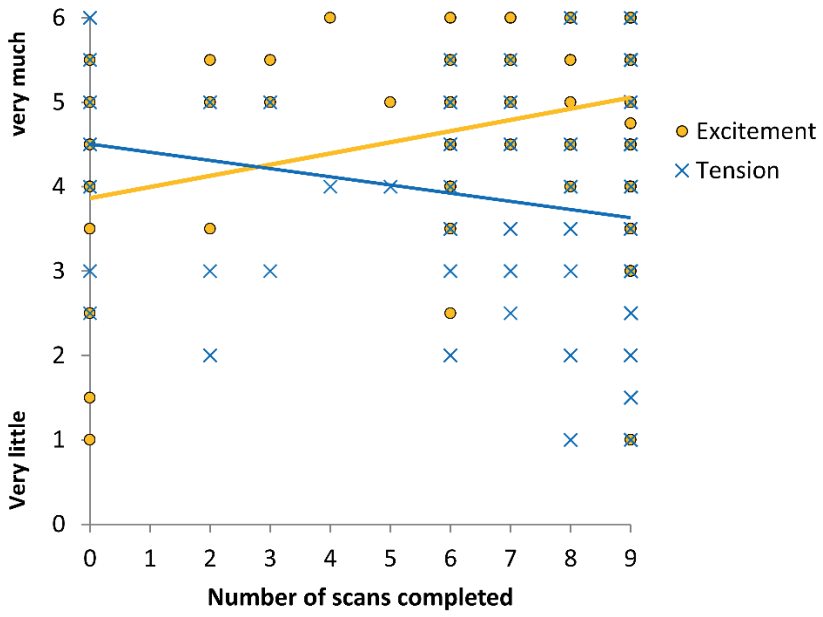


Figure 4. *Number of scans completed plotted against excitement and tension towards the scan. Data visualized is from emotional state before MRI scan, emotional states before MRI simulation and after MRI scan showed similar patterns.*

Genetic influences on scan quantity

To investigate genetic and environmental influences on scan quantity (number of scans completed), we calculated Pearson's within-twin correlations for MZ and DZ twins and performed behavioral genetic analyses. Fisher r-to-z transformations showed that within-twin correlations for scan quantity were significantly stronger for MZ twins (r_{mz}=.50, p<.001) than DZ twins (r_{dz}=.14, p=.14), Z=3.21, p<.001. Behavioral genetic analyses revealed substantial influences of genetics (A=45%, 95% CI [18-56%]) and unique environment/measurement error (E=55%, 95% CI [44-68%]), with no influence of the shared environment (C=0%, CI: 0-22%).

MRI Quality

Scan quality

An overview of the number (and percentage) of scans with sufficient quality relative to the quantity of the scans is provided in Figure 3b. Of the 488 participants that started the MRI protocol, 385 participants (79%) had sufficient data in the first run. Sufficient MRI scan quality for task-based fMRI was defined as <3 mm (1 voxel) motion in all directions. The percentage sufficient data decreased over the first five task-based fMRI runs: 71% in the second run; 66% in the third run; 64% in the fourth run; and 55% in the fifth run. For the 3DT1 structural anatomy scans, 72% of the scans were classified as sufficient quality using a stringent threshold, and 88% was included using a lenient threshold (including scans coded as 'Doubtful'). The percentage of DTI scans classified as sufficient quality was 92% using a stringent threshold and 96% using a lenient threshold (including 'Doubtful'). The RS-fMRI data, which was the final run of the MRI session, showed the lowest scan quality, with 34% of the acquired data being of sufficient quality with a cut-off of <0.3 mm FD in > 20% of the volumes (Figure 3b). Using a more lenient cut-off of <0.5 mm FD in > 20% of the volumes, 52% of the acquired data would have been included. Inclusion based on <3 mm absolute displacement (similar to the threshold used for task-based fMRI data) resulted in 51% of sufficient RS fMRI data. Across all scans, we found a small positive association between percentage of the acquired data being of sufficient quality (using stringent thresholds) and age (r=.10, p=.03).

Scan quality over time

There was an increase in head motion over time, both framewise as well as absolute (x, y, and z-direction) displacement (Table 1). After excluding participants with insufficient data, head motion within the different task based and resting state fMRI runs was comparable (Table 1). To provide an overview of scan quality with respect to time, we calculated the percentage participants with sufficient quality data after 30, 45 and 60 minutes (for participants that completed the full scan protocol, n=433, 48% boys), see Figure 3c. The first 30

minutes consisted of four task-based fMRI runs; the 45 minutes included all task-based fMRI runs and the 3DT1. The 60-minute protocol was the full L-CID scan protocol. 214 participants (49%) had sufficient quality on all scans in the first 30 minutes, with no significant gender differences (p=.149), see Figure 3c. 160 participants (33%) had sufficient quality on all scans in the first 45 minutes, with a larger proportion of girls being included than boys being included (χ^2(1, N=433) =11.70, p=.001), see Figure 3c. 87 participants (20%) had sufficient quality on all eight scans of the full 60-min protocol, with a larger proportion of girls being included than boys being included (χ^2(1, N=433) =8.85, p=.002), see Figure 3c. There were no age differences in scan quality over time.

Scan quality in relation to scanner related distress

Pearson's correlations on the number of included scans (range=0-8, M=5.58, SD=2.47,) showed no association with excitement or tension (neither before the MRI simulation nor before the MRI scan, all $p's$>.05). Children's own estimate of excitement after the MRI scan was significantly correlated to scan quality (r=.13, p=.003), whereas tension after the MRI scan was not related to scan quality (r=.03, p=.52). Pearson's correlations of the quantitative measures of scan quality (i.e. head motion based on the fMRI runs) showed a positive correlation between excitement before the MRI scan and mean FD (r=.12, p=.01), a positive association between absolute displacement and excitement before the MRI simulation (r=.10, p=.03) and before the MRI scan (r=.09, p=.04); and a negative association between absolute displacement and tension before the MRI simulation (r=-.09, p=.04). However, these correlations did not survive Bonferroni correction (Bonferroni corrected α=.008).

Genetic influences on scan quality

Within-twin correlations for general scan quality (percentage of scans included) were significantly stronger for MZ twins (r_{mz}=.47, p<.001) than DZ twins (r_{dz}=.19, p=.05), Z=2.40, p=.016. Behavioral genetic analyses revealed substantial influence of genetic factors (A=46%, 95% CI [33-58%]) and unique environment/measurement error (E=54%, 95% CI [42-67%]), with no influence of shared environment (C=0%, 95% CI [0-26%]).

Next, we investigated genetic influences on head motion, quantified by the mean framewise and mean absolute displacement over all fMRI runs. Within-twin correlations for framewise displacement were significantly stronger for MZ twins than DZ twins (r_{mz}=.51, p<.001; r_{dz}=.19, p=.05, Z=2.81, p=.002), see Table 3. Similar correlations were found for absolute displacement, with a significantly stronger association between MZ twins (r_{mz}=.70, p<.001) than between DZ twins (r_{dz}=.17, p=.09, Z=5.27, p<.001), indicating substantial genetic influences. More detailed behavioral genetic analyses showed that framewise displacement was significantly influenced by genetics, with a heritability estimate of 29% (95% CI:

[23-46%], Table 3). Absolute displacement also showed influence of genetics, with a heritability estimate of 65% (95% CI: [54-73%]), see Table 3.

As is often the case with childhood samples, some participants displayed excessive head motion: up to 18 mm mean framewise displacement (Figure 5a) and 38 mm mean absolute displacement (Figure 5b). To prevent the genetic analyses from being biased by these extremes, we also investigated heritability of "moderate" head motion (Figure 5). For these analyses, we only included participants with mean framewise displacement <1 and <3 mm absolute displacement. Within-twin correlations for moderate framewise displacement were similar for MZ twins (r_{mz}=.29, p=.005) and DZ twins (r_{dz}=.28, p=.02, see Table 3). Similarly, within-twin correlation for moderate absolute displacement were similar for MZ twins (r_{mz}=.29, p=.005) and DZ twins (r_{dz}=.23, p=.06). Behavioral genetic analyses revealed low heritability estimates for moderate head motion (compared to overall head motion), and in addition showed influence of shared environment. That is to say, influence of genetics on moderate framewise displacement was estimated as 12% (95% CI: [0-51%]) and 22% of the variation was explained by shared environment (95% CI: [0-45%]). Influence of genetics on moderate absolute displacement was 14% (95% CI: [0-46]), and 15% of the variation was explained by shared environment (95% CI: [0-39%], Table 3).

As previous studies showed the tremendous effect of motion on fMRI signals in pediatric samples (Poldrack *et al.*, 2002; Satterthwaite *et al.*, 2013), and recent studies advise more stringent quality control (Power *et al.*, 2014; Power *et al.*, 2015) we performed additional analyses on "minimal" head motion (Figure 5). For these analyses, we only included participants with mean framewise displacement <0.3 mm and <1 mm absolute displacement. Within-twin correlations for minimal framewise displacement did not differ for MZ twins (r_{mz}=.26, p=.183) and DZ twins (r_{dz}=.49, p=.04; Z=-0.83, p=.406, see Table 4). Similarly, within-twin correlation for minimal absolute displacement were similar for MZ twins (r_{mz}=.32, p=.123) and DZ twins (r_{dz}=.28, p=.225; Z=0.14, p=.888). Behavioral genetic analyses revealed even lower heritability estimates for minimal head motion (compared to overall and moderate head motion, see Table 3). There was no influence of genetics on minimal framewise displacement (A=0.00, 95% CI: [0-47%]) and 33% of the variation was explained by shared environment (95% CI: [0-54%]). Influence of genetics on minimal absolute displacement was 6% (95% CI: [0-61]), and 29% of the variation was explained by shared environment (95% CI: [0-55%]). Note that the sample size for analyses on minimal head motion was considerably smaller (n=44 twin pairs, 55% MZ) than for analyses on moderate (n=159 twin pairs, 59% MZ) and excessive (n=237 twin pairs, 54%MZ) head motion. Figure 5 provides a visual representation of the within-twin correlation of extreme, moderate and minimal head displacement, split out by zygosity.

Table 3. Genetic modeling of framewise and absolute head displacement for all participants scanned (prior to motion exclusion, including excessive head motion); for participants with moderate head motion (excluding excessive head motion); and for participants with minimal head motion (after stringent quality control).

Max motion		**MZ**	**DZ**		**A²**	**C²**	**E²**
Excessive head motion							
Framewise Displacement	*r*	.51**	0.19	*ACE*	0.29	0.05	0.66
	n[1]	129	108	*95% CI*	0.00-0.46	0.00-0.39	0.54-0.80
Absolute Displacement	*r*	.70**	0.17	*ACE*	0.65	0	0.35
	n[1]	129	108	*95% CI*	0.54-0.73	0.00-0.12	0.27-0.46
Subtle head motion°							
Framewise Displacement	*r*	.29**	.28*	*ACE*	0.12	0.22	0.66
	n[1]	96	72	*95% CI*	0.00-0.52	0.00-0.45	0.48-0.84
Absolute Displacement	*r*	.29**	0.23	*ACE*	0.14	0.15	0.71
	n[1]	92	67	*95% CI*	0.00-0.46	0.00-0.39	0.54-0.90
Minimal head motion×							
Framewise Displacement	*r*	0.26	.49*	*ACE*	0	0.33	0.67
	n[1]	28	18	*95% CI*	0.00-0.47	0.00-0.54	0.46-0.94
Absolute Displacement	*r*	0.32	0.28	*ACE*	0.06	0.29	0.65
	n[1]	24	20	*95% CI*	0.00-0.61	0.00-0.55	0.39-0.95

* p<.05, ** p<.001, [1] Number of complete twin pairs

° mean FD <1 mm; mean AD < 3mm; × mean FD <0.3 mm; mean AD <1 mm

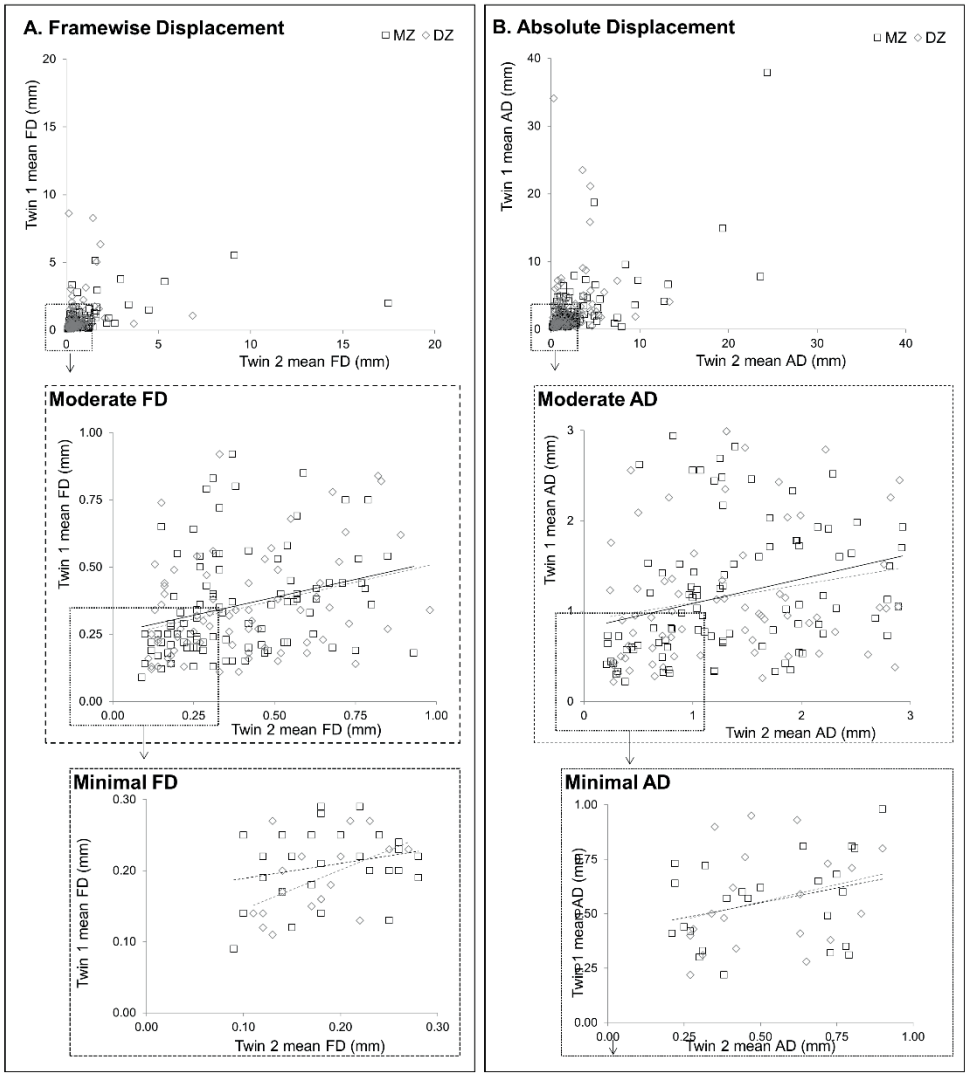


Figure 5. *Visual representation of within-twin correlations of maximum head movement (in mm), split out by zygosity. A) Framewise head displacement in mm. The dashed frameworks are zoomed in on moderate (< 1mm mean FD) and minimal (< 0.3mm mean FD) head motion. B) Absolute head displacement in mm. The dashed frameworks are zoomed in on moderate (< 3mm mean AD) and minimal (< 1mm mean AD) head motion. Solid lines represent significant correlations (p < .001).*

Discussion

To address questions on quality of MRI scans in developmental samples we provided an overview of scan quantity and scan quality in a large developmental twin sample (N=512 7-9-year-olds). Overall, scan quantity was high and 88% of the children completed all runs. We report a drop in the number of runs completed after approximately 45 minutes of scan time, which is comparable with prior findings in this age range (Engelhardt *et al.*, 2017). Scan quality decreased with increasing scan time, consistent with previous studies that reported an increase in head motion over time (Centeno *et al.*, 2016; Engelhardt *et al.*, 2017; Fassbender *et al.*, 2017b).

Genetic influences on scan quantity and quality

As a complement to the growing literature on familial similarities in head motion (Couvy-Duchesne *et al.*, 2014; Engelhardt *et al.*, 2017), we also investigated genetic and environmental influences on scan quantity and scan quality. . Behavioral genetic modeling showed substantial to strong heritability estimates (45-46%) for both scan quantity (number of runs completed) and scan quality (percentage of scans included). Whether or not a scan was included was based on often used, but arbitrary cut-off of head motion (task fMRI: <3 mm absolute head displacement; structural scans: manual ratings; RS-fMRI: <20% volumes with >0.3 mm framewise displacement). Therefore, we additionally estimated genetic influences of MRI scan quality on a more sophisticated and continuous measure of scan quality, i.e., the quantitative measures of head motion for all fMRI runs (framewise and absolute displacement in mm) including all scanned participants. Head motion over fMRI runs was stable (α=.77-84) and within-twin correlations were higher in MZ than DZ twins. Similar findings were previously reported by Engelhardt *et al.* (2017), showing familial similarity of pediatric framewise head displacement in RS-fMRI. To provide direct estimates of the percentage of variation explained by genetics and (shared and unique) environment, we used behavioral genetic analyses. These analyses revealed that head motion in fMRI runs was substantially influenced by genetics, with heritability estimates ranging from 29-65%, consistent with heritability estimates in adults (Couvy-Duchesne *et al.*, 2014). Thus, both the overall measure of scan quality (percentage of scans included), as well as the more sophisticated measure of scan quality in fMRI runs (framewise- and absolute displacement) showed substantial influence of genetics. Together, these findings show evidence for genetic contributions to head motion, highlighting the need for careful control of motion related artifacts (Caballero-Gaudes and Reynolds, 2017; Power, 2017), specifically for studies in domains where genetic effects might play a strong role, such as in the case of psychiatric disorders that have a genetic basis (Hyman, 2000).

Reassuringly, heritability estimates for subtle head motion (after exclusion based on excessive head motion) were considerably smaller, ranging from 0-14%. This is contrary to previous findings of Engelhardt *et al.* (2017) who reported similar within-twin correlations on framewise head displacement before and after scrubbing (i.e., exclusion of frames with excessive motion). Differences might be due to the smaller sample size (N_{mz}=12 and N_{dz}=22) and the differences in exclusion based on head motion, since Engelhardt *et al.* (2017) excluded volumes with excessive head motion, whereas we excluded complete runs of participants with excessive head motion. Thus, in line with previous studies (Van Dijk *et al.*, 2012; Couvy-Duchesne *et al.*, 2014; Engelhardt *et al.*, 2017), we report that excessive head motion is heritable and systematic, but additionally show that, after careful motion correction and exclusion based on excessive head motion, subtle head motion shows little influence of genetics. Possibly, subtle head movement is more strongly dependent on participant instruction and scanner adjustments. Indeed, behavioral genetic analyses on quality controlled head motion not only revealed small heritability estimates (0-14%, compared to 29-65% in overall head motion), but also showed that a similar, or even larger, proportion of the variance was explained by shared environmental influences (15-33%).

Environmental influences on scan quantity and quality

An additional goal of this study was to examine how emotional state towards the scanner was related to scan quality and quantity. Consistent with findings for quality controlled head movement, reports of emotional states showed little to no influence of genetics, but a moderate to strong relation with shared environmental influences. These findings suggest that emotional states can be significantly influenced by preparation of the scanner experiences. It was interesting to note that children's tension was on average rated higher by researchers and parents than by children themselves, which is in line with previous studies suggesting that children may underreport their anxiety (Tyc *et al.*, 1995; Durston *et al.*, 2009). Multi-informant estimates of children's emotional state towards the MRI scan were significantly associated with MRI quantity, as we found that children with higher estimated excitement and lower estimated tension completed more runs during the MRI scan. However, the association between children's emotional state towards the MRI scan and scan quality was less clear, as the correlations did not survive Bonferroni correction. These findings suggest that by decreasing scanner related distress researchers can increase scan quantity, but more detailed future studies are necessary to reveal whether this would also lead to an increase in scan quality.

One aspect that did show influence on scan quality was the length of the MRI scan session. Results showed that a protocol of >30 minutes resulted in less than 50% sufficient quality on all scans in this age range of 7-9-year-olds. This is

in line with other research that also recommends a scanning time of 30-40 minutes for young children (Raschle *et al.*, 2012), whereas a longer scanning protocol of 60 minutes is only recommended for an older population ((Fassbender *et al.*, 2017b). If more scanning time is required to collect all data, a way to ensure scan quality would be to conduct two separate MRI sessions divided over different days (Fassbender *et al.*, 2017b). Moreover, as the field of (developmental) neuroimaging is rapidly evolving, the technology of MRI is progressing. New methods such as simultaneous multi-slice imaging (SMS or 'Multiband', Feinberg and Yacoub (2012); Demetriou *et al.* (2018)) and real-time monitoring of head motion (Framewise Real-time Integrated MRI Motion Monitoring (FIRMM; Dosenbach *et al.* (2017)) have the potential to drastically shorten acquisition time without compromising on the number of scans. The effects on these methods on MRI scan quality should be examined in more detail in future studies. For example, a pioneering study of Greene *et al.* (2018b) reported that real time feedback about motion (using FIRMM) reduced head displacement in 5-10 year old children, but not in children older than 10.

Limitations

The study had several limitations, which should be addressed in future research. First, the current study examined one general aspect of scan quality (head motion), nevertheless, several other factors can influence scan quality, amongst others: thermal noise, respiratory signals, and scanner drifts (Kotsoni *et al.*, 2006; Liu, 2017; Power, 2017). Future studies should also investigate the effects of these other factors, for example by investigating fMRI signal variability in regions of interest. Second, due to ethical considerations all participating children in the current study received the MRI simulation, therefore we were unable to directly test the effects of the MRI simulation and can only conclude that scanner related distress changed over time. Third, we report that children displayed the most head motion in the RS fMRI run, but this might be influenced by different definitions of sufficient quality, as the threshold for RS fMRI data was more conservative than the criteria for task-based fMRI. Nevertheless, Engelhardt et al. (2017) also report that their sample of 7-8-year-olds showed the most movement during rest and the least movement during an inhibition task and they suggested that the inhibition task was more engaging and therefore might have resulted in less head motion than the RS fMRI run. The sequence of MRI runs in our MR session was fixed, hindering direct comparison of task engagement, as the differences in head motion between task-based and RS fMRI might reflect a time effect. Studies in adults have indeed reported less head motion under engaging task conditions than during rest, irrespective of acquisition order (Huijbers *et al.*, 2017) and future studies should investigate the effects of task demands versus time on scan quality in children. Relatedly, we instructed participants to lie still with eyes closed for the RS-fMRI. During the piloting phase of the scan protocol

we experienced that the eyes closed condition was more comfortable for children than eyes open. Although recent studies have shown similar RS networks across different RS conditions (Yan et al., 2009; Zou et al., 2015), differences in connectivity strength (Van Dijk et al., 2010; Yan et al., 2009) and test-retest reliability have also been reported (Patriat et al., 2013; Zou et al., 2015). Moreover, despite the specific instructions to participants to not to fall asleep, sleep was not directly monitored, which is a limitation of our RS design. Last, the behavioral genetic analyses had smaller sample sizes for moderate (N_{mz}=92, N_{dz}=67) and minimal head motion (N_{mz}=24, N_{dz}=20) than the analyses on the full sample (N_{mz}=129, N_{dz}=108). As the statistical power of genetic studies is influenced by the sample size (Verhulst, 2017), differences in results could be influenced by differences in sample sizes.

Conclusion

We report that participants' scanner related distress was associated to scan quantity, but not to scan quality. Overall, scan quantity was high, as 88% of the children that started the protocol also completed it. The percentage of sufficient scans was considerably higher (49%) in the first 30 minutes of the protocol than in the full 60-minute protocol (20%), indicating that shorter scan protocols have less attrition. Consistent with previous studies (Couvy-Duchesne *et al.*, 2014; Engelhardt *et al.*, 2017), the behavioral genetic analyses revealed heritability effects on head motion, with heritability estimates ranging from 29-65%. Importantly, however, our results also show that after exclusion based on excessive head motion, heritability estimates declined to 0-14%, indicating that MRI findings of motion corrected and quality-controlled data are not substantially confounded by genetic factors. Moreover, shared environmental influences played a larger role (15-33%) in the variation in quality controlled head motion, suggesting that head motion can be influenced by participant instruction and scanner adjustments. These results provide insight in the genetic and environmental influences on scan quantity and quality and can inform future studies on developmental neuroimaging.

Acknowledgements

We thank Prof. dr. Eveline Crone, Dr. Anna van Duijvenvoorde, Prof. dr. Marian Bakermans-Kranenburg, and Prof. dr. Marinus van IJzendoorn for providing constructive comments on previous versions of the manuscript and for their helpful discussions on the behavioral genetic modeling. The Leiden Consortium on Individual Development is funded through the Gravitation program of the Dutch Ministry of Education, Culture, and Science and the Netherlands Organization for Scientific Research (NWO grant number 024.001.003).

Supplementary materials

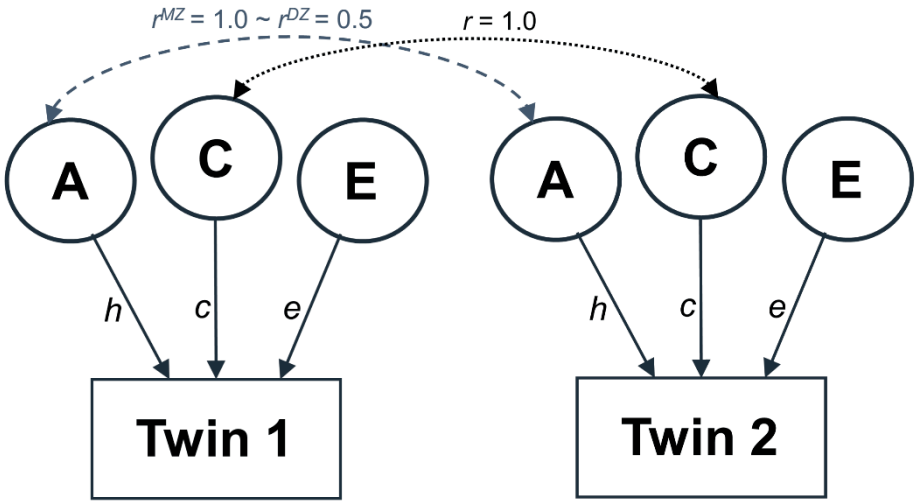


Figure S1. *ACE model. Similarities among twin pairs are divided into similarities due to shared genetic factors (A) and shared environmental factors (C), while dissimilarities are ascribed to unique environmental influences and measurement error (E). The correlation of the shared environment (factor C) was set to 1 for both MZ and DZ twins, while the correlation of the genetic factor (A) was set to 1 for MZ twins and to 0.5 for DZ twins (see Figure S1). The last factor, unique environmental influences and measurement error, was freely estimated.*

Table S1. Correlation matrix of emotional state towards the MR estimated by children, researchers, and parents.

		Children	
		Excitement	Tension
Before MRI simulation	Researchers	.75**	.72**
	Parents	.38**	.23**
Before MRI scan	Researchers	.80**	.70**
	Parents	.42**	.35**
After MRI scan[0]	Researchers	.73**	.74**

[0] Parents did not estimate the emotional state after the real scan

*** p<.001*

Table S2. Scan quantity: percentage included participants and drop out reasons per MR run.

	fMRI task 1 part 1	fMRI task 1 part 2	fMRI task 1 part 3	fMRI task 2 part 1	fMRI task 2 part 2	3DT1 structural	DTI part 1	DTI part 2	RS fMRI	All scans completed
Scan completed	488	488	485	483	482	483	451	442	445	433
% completed	*95%*	*95%*	*95%*	*94%*	*94%*	*94%*	*88%*	*86%*	*87%*	*85%*
Scan missing	24	24	27	29	30	29	61	70	67	79
contra indication	*6*	*6*	*6*	*6*	*6*	*6*	*6*	*6*	*6*	*6*
no parental consent	*4*	*4*	*4*	*4*	*4*	*4*	*4*	*4*	*4*	*4*
technical error	*1*	*1*	*1*	*1*	*1*	*1*	*1*	*1*	*1*	*1*
Anxiety	*13*	*13*	*14*	*14*	*15*	*15*	*17*	*17*	*19*	*19*
child tired	-	-	*2*	*2*	*2*	*2*	*20*	*29*	*23*	*33*
time constraints	-	-	-	*2*	*2*	*1*	*13*	*13*	*14*	*16*

CHAPTER EIGHT

Frontostriatal white matter integrity predicts development of delay of gratification: A longitudinal study

This chapter is published as: Achterberg M.*, Peper J.S.*, Van Duijvenvoorde A.C.K., Mandl R.C.W. & Crone E.A. (2016), Frontostriatal white matter integrity predicts development of delay of gratification: A longitudinal study, *Journal of Neuroscience 36*(6): 1954-1961. * shared first authorship

Abstract

The ability to delay gratification increases considerably across development. Here, we test the hypothesis that this impulse control capacity is driven by increased maturation of frontostriatal circuitry using a fiber-tracking approach combined with longitudinal imaging. In total, 192 healthy volunteers between 8 and 26 years underwent diffusion tensor imaging scanning and completed a delay-discounting task twice, separated by a 2-year interval. We investigated dynamic associations between frontostriatal white matter (WM)integrity and delay of gratification skills. Moreover, we examined the predictive value of frontostriatal WM integrity for future delay of gratification skills. Results showed that delay discounting increases with age in a quadratic fashion, with greatest patience during late adolescence. Data also indicated nonlinear development of frontostriatal WM, with relative fast development during childhood and early adulthood and—on average—little change during mid-adolescence. Furthermore, the positive association between age and delay dis-counting was further increased in individuals with higher WM integrity of the frontostriatal tracts. Predictive analysis showed that frontostriatal WM development explained unique variance in current and future delay of gratification skills. This study adds to a descriptive relation between WM integrity and delay of gratification by showing that maturation of frontostriatal connectivity predicts changes in delay of gratification skills. These findings have implications for studies examining deviances in impulse control by showing that the developmental path between striatum and prefrontal cortex may be an important predictor for when development goes astray.

Keywords: adolescence; development; impulsivity; longitudinal; white matter

Introduction

Between childhood and adulthood, vigorous advancements in the ability to sustain goal-directed cognition in the face of immediate rewards are observed (Eigsti *et al.*, 2006; Olson *et al.*, 2007; de Water *et al.*, 2014). This ability to delay gratification can be captured in delay discounting tasks, estimating an individual's preference for a smaller immediate reward over larger, delayed rewards. A crucial element of these tasks is that the subjective value of a reward decreases when the delay to that reward increases (Critchfield and Kollins, 2001). This capacity has been interpreted as an index of impulse regulation, which changes considerably during adolescence (van den Bos *et al.*, 2015).

A leading hypothesis suggests that maturation of this type of impulse regulation capacity is driven by increased regulatory control of the prefrontal cortex (PFC) over reward-related striatal areas (Figner *et al.*, 2010; Christakou *et al.*, 2011). Several studies showed that the striatum is more activated by decisions involving immediately available rewards, whereas prefrontal and parietal cortices are activated when individuals control the temptation to choose immediate rewards (McClure *et al.*, 2004; Peters and Buchel, 2011). These results lead to the question whether maturation of prefrontal-striatal white matter connections concurs with, and predicts future-oriented choices across development.

The integrity of connections between the striatum and prefrontal cortex can be assessed by using diffusion tensor imaging (DTI). DTI measures the diffusion profile of water molecules *in vivo* allowing us to probe microstructural properties of the connecting white matter (WM) fiber bundles (Jones, 2008). The measurements most commonly derived from DTI are fractional anisotropy (FA), measuring the directional variation of diffusion, and mean diffusivity (MD), measuring the amount of diffusion (Basser and Pierpaoli, 1996). Several DTI studies revealed higher WM integrity across adolescence (Olson *et al.*, 2009; Bava *et al.*, 2010; Simmonds *et al.*, 2014; Peper *et al.*, 2015), although the shape of the trajectory is not yet well understood, some reporting linear and others non-linear changes (for an overview see Schmithorst and Yuan (2010)). Moreover, recent studies in adults (Peper *et al.*, 2013) and adolescents (Van den Bos et al., 2015) reported an association between higher fronto-striatal WM integrity and increased preference for delayed rewards. From these studies, two important issues remain unresolved: 1) whether the relationship between age and discounting is eliminated—or merely diminished—when brain connectivity is taken into account (Steinberg and Chein, 2015) and 2) whether maturation of fronto-striatal white matter connections across development is an important *predictor* of individual development of delay of gratification skills

To address these questions, the current study followed participants with ages ranging from childhood throughout early adulthood (age 8-26) over a two-year period. This longitudinal design enabled us to (1) test whether the association between age and discounting behavior is mediated by WM integrity

between striatum and PFC, and (2) move beyond a descriptive relation between age, WM integrity and behavior, by testing how brain maturation predicts change in behavior over time.

In line with the existing literature, we hypothesized that (i) the ability to delay gratification improves with increasing age (Green *et al.*, 1994; Olson *et al.*, 2007; de Water *et al.*, 2014) and (ii) the integrity of fronto-striatal WM matures with increasing age (Olson *et al.*, 2009; Bava *et al.*, 2010; Schmithorst and Yuan, 2010; Simmonds *et al.*, 2014; Peper *et al.*, 2015). The longitudinal design allowed us to test in more detail the shape of change (Braams *et al.*, 2015). In addition, we hypothesized that (iii) the increasing effect of age on the ability to delay gratification is further increased in individuals with relatively high fronto-striatal WM integrity (Liston et al., 2006) (positive mediation). Ultimately, we hypothesized that (iv) fronto-striatal WM integrity predicts the improvement of delay gratification over time. That is to say, we expect that fronto-striatal WM integrity at timepoint 1 can predict delay of gratification at timepoint 2, and that thereby brain maturation precedes and predicts behavioral change .

Methods

Participants

The current study was part of a large longitudinal study, referred to as Braintime, conducted at Leiden University, the Netherlands. A total number of 299 participants (ages 8-25) were recruited through local schools and advertisements at timepoint 1 (T1). All participants were fluent in Dutch, right-handed, had normal or corrected-to-normal vision, and an absence of neurological or psychiatric impairments. Two years later, at timepoint 2 (T2), 254 participants were included. From the 254 participants that had measurements on both time points, 14 participants had missing delay discounting data at one of the two time points and 13 participants had missing DTI data at one of the two time points. 34 participants were excluded due to erratic discounting behavior at one of the two time points. Consistent discounting behavior was defined as having at least two decreases in subjective value (indifference points) and not more than one increase in subjective value as time increased (Dixon et al. 2003). The excluded participants had similar demographic characteristics as the included participants (excluded participants: 50% male; age range 8.21-24.44; age at T2 M = 16.05, SD= 3.66). Results with the excluded participants remained unchanged.

There were no outliers in delay discounting data (Z-value < -3.29 or > 3.29). Outliers in DTI data were winsorized (Tabachnick and Fidell, 2013).The final longitudinal sample (participants included at T1 and T2) consisted of 192 participants (48.4% males; age range = 8.01 - 26.62; age at T2 M = 16.31, SD=3.61), see **Table 1** for demographic characteristics.Written informed consent was obtained from all participants, or participant's parents in the case of minors. All

anatomical MRI scans were reviewed and cleared by a radiologist from the radiology department of the Leiden University Medical Center (LUMC). No anomalous findings were reported. Participants received a financial reimbursement for their participation in a larger scale study (e.g., Braams *et al.* (2014a); Braams *et al.* (2014b); Peters *et al.* (2014a); Peters *et al.* (2014b); van Duijvenvoorde *et al.* (2016a)). The institutional review board of the LUMC approved the study and its procedures.

Intelligence quotient (IQ) was estimated with the subsets 'similarities' and 'block design' at T1 and the subsets 'vocabulary' and 'picture completion' at T2 of the Wechsler Intelligence Scale for Adults, third edition (WAIS-III) or the Wechsler Intelligence Scale for Children, third edition (WISC-III). Different subsets were used to prevent learning effects. The demographic characteristics of the sample are listed in **Table 1**. There was no significant correlation between estimated IQ and delay of gratification skills at T1 (r=.0195, p=.195) nor at T2 (r=.113, p=.119). Therefore, IQ was not included as covariate in the remaining analyses.

Table 1. Demographic characteristics of the sample (N=192, 48.4% male) at time point 1 and time point 2 [means (SD)]. IQ: intelligence quotient; AUC: area under the discounting curve (normalized); FS-tract: fronto-striatal tract; FA: fractional anisotropy; MD: mean diffusivity (in mm^2/s).

	Timepoint 1	**Timepoint 2**
Age (years)	14.32 (3.59)	16.28 (3.61)
Age range	8.01 - 24.55	9.92 - 26.62
Estimated IQ	110.78 (9.81)	108.23 (10.20)
AUC (normalized)	0.42 (0.28)	0.47 (0.25)
FS-tract FA	0.329 (0.020)	0.333 (0.020)
FS-tract MD	0.00080 (0.00002)	0.00080 (0.00002)

Delay-Discounting Task

A computerized version of a hypothetical delay-discounting task described by Peper *et al.* (2013) was used, based on the paradigm explained by Richards *et al.* (1999). Subjects were asked to make a series of choices, between either a small, immediately available amount of money or €10 available after a delay (i.e., "What would you rather have: €2 right away or €10 in 30 days?"). Discounting was assessed at four delays (2, 30, 180 and 365 days later). Trials with different delays were presented in a mixed fashion. Furthermore, the task was adaptive: after the choice for the immediately available money, this amount was decreased on a next trial, whereas if the delayed money was preferred, the amount of immediately

available money on the next trial was increased (decreasing adjustment algorithm) (Du *et al.*, 2002).

The amount of immediately available money the participant considered to be equivalent to the €10 delayed reward was taken to indicate the subjective value of the delayed rewards. Based on these so called 'indifference points', the area under the discounting curve (AUC) was obtained, an often-used measure of amount of discounting (Myerson *et al.*, 2001). The normalized AUC ranges from 0 (complete discounting) to 1 (no discounting). The smaller the AUC, the faster people discount the delayed reward and the more impulsive (or delay aversive) they are. The task was presented as a hypothetical delay-discounting task. However, several studies have shown that choices on a hypothetical delay-discounting task substantially and significantly correlate (*r*'s up to 0.74) with choices on a delay discounting task with real rewards in adults (Bickel *et al.*, 2009; Scheres *et al.*, 2010).

Imaging acquisition and processing

The same imaging acquisition was used as described in Peper *et al.* (2013). Scans were acquired on a 3-Tesla Philips Achieva MRI system. Two transverse Diffusion Weighted Imaging (DWI) scans were obtained with the following parameter settings: 30 diffusion-weighted volumes with different noncollinear diffusion directions with b-factor 1,000 s/mm2 and 5 diffusion-unweighted volumes (b-factor 0 s/mm2); anterior -posterior phase encoding direction; parallel imaging SENSE factor = 3; flip angle = 90 degrees; 75 slices of 2 mm; no slice gap; reconstruction matrix 128 × 128; Field of view (FOV) = 240 × 240 mm; TE = 69 ms; TR = 7,315 ms; total scan duration = 271 s per DWI set. The second DWI set had identical parameter settings as used for the first set except that it was acquired with a reversed k-space readout direction (posterior-anterior phase encoding direction) enabling the removal of susceptibility artifacts during post processing (Andersson *et al.*, 2003). During scanning, the FOV was angulated according to the anterior commissure-posterior commissure line, and diffusion gradients were adjusted accordingly during data processing. Subsequently, diffusion scans were realigned to the averaged b0 scan and corrected for motion, eddy current, and susceptibility distortions (Andersson and Skare, 2002; Andersson *et al.*, 2003). A tensor was fitted to the diffusion profile in each voxel using a robust tensor fitting method to correct for possible effects of cardiac pulsation and head motion (Chang *et al.*, 2005; Chang *et al.*, 2012). The main diffusion direction was determined as the principal eigenvector of the eigenvalue decomposition of this fitted tensor.

Based on the eigenvalue decomposition, two measures derived from the diffusion tensor were computed: 1) the fractional anisotropy (FA), which measures the *directional variation* of diffusion and ranges from 0 (no preferred diffusion direction) and 1 (highly preferred diffusion direction) and 2) mean

diffusivity (MD), measuring the *amount* of diffusion (Basser and Pierpaoli, 1996). White matter pathways were reconstructed using deterministic streamline tractography, based on the Fiber Assignment by Continuous Tracking (FACT) algorithm (Mori *et al.*, 1999). Within each voxel of the cerebral white matter, 8 streamlines were started, following the computed diffusion directions from voxel to voxel until one of the stopping criteria was reached (being FA<0.1, sharp turn of 45 degrees or more, or exceeding brain tissue). This procedure resulted in a collection of reconstructable white matter tracts, from which fiber tracts of interest could be selected.

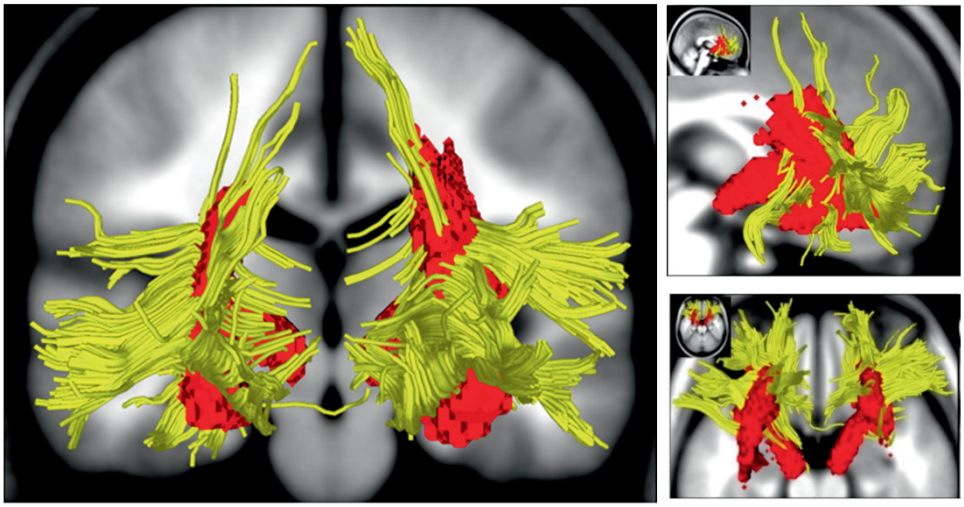


Figure 1. *The frontostriatal WM tract within an individual subject is displayed in yellow, with the striatum and PFC as inclusion ROIs. Red regions display the VOI. The VOI was created across the whole sample; a voxel was included when it had a frontostriatal fiber running through in at least 50% of the total sample.*

Frontostriatal volume of interest

We used a 'volume of interest' (VOI) to measure fronto-striatal white matter tracts as described by Peper *et al.* (2013). The VOI requires that the fiber tracts that are reconstructed for each subject in native space, are put into model space in order to create the VOI (for a detailed description, see Peper *et al.* (2013)). In short, tracts were required to run through both the striatum and PFC to be included as fronto-striatal white matter. Inclusion regions-of-interest (ROIs) were based on the automatic anatomical labeling (AAL) template (Tzourio-Mazoyer *et al.*, 2002), including the caudate, putamen, and pallidum (AAL regions 71–76), as well as the dorsolateral, ventrolateral, and ventromedial prefrontal cortices (AAL regions 5–10; 13– 16; 25–28). The ROIs were dilated with 2 voxels in all directions to ensure that they penetrate the white matter. Exclusion ROIs were the genu of the corpus

callosum (manually delineated on the midsagittal slice), the uncinate fasciculus, and the longitudinal fascicules (manually delineated by a plane through the temporal lobes where the amygdala was located). For fiber selection, all ROIs had to be defined only once, on the model brain. For an individual example of fronto-striatal fiber tracts, see Figure 1. All voxels within the selected fronto-striatal tracts were flagged, resulting in individual binary maps of fronto-striatal tracts (in model space) for each participant of the sample on both time-points T1 and T2. Subsequently, the VOI was created for fronto-striatal tracts of the sample: Every voxel within the fronto-striatal tract should have a fiber running through in at least 50% of the sample (i.e. thresholded at 50%; Figure 1). Then this particular voxel was flagged and added to the VOI. The left and right hemisphere were combined to ensure comparability with earlier reports (Liston et al., 2006; de Zeeuw et al., 2012; Peper et al., 2013; van den Bos et al., 2015) that did not report hemispheric differences in relation to impulsive behavior. Within the VOI of the fronto-striatal tract, DTI metrics (FA and MD) were calculated for each individual subject of the whole sample.

Global white matter

As a control measure of global white matter development and to test for specificity of the contribution of fronto-striatal white matter tracts to delay discounting behavior, white matter tracts of the whole brain –excluding fronto-striatal tracts- were examined as well.

Statistical analyses

Statistical analyses were conducted with Statistical Package for Social Sciences (SPSS), version 21 and in R, version 3.1.1. The contribution of gender and intelligence to delay of gratification skills (AUC normalized) were explored using independent sample T-tests and Pearson's correlation in SPSS. Pearson's correlation in SPSS were also used to investigate the stability of delay of gratification skills (AUC normalized) and white matter integrity (FA and MD) over time. Furthermore, mediation analyses were performed to test whether the relation between age and delay discounting was mediated by fronto-striatal white matter integrity, measured by FA and MD. For correct comparison between FA and MD we used z-values in the mediation analyses. The present study used a bootstrapping approach to mediation as implemented in the SPSS macros of Preacher and Hayes (Preacher and Hayes, 2008). Confidence intervals (95%) were estimated using the bias-corrected bootstrap method (number of resamples = 10000) implemented in the macros.

Mixed models were used to investigate age-related change (linear, quadratic or cubic) in delay of gratification skills (AUC normalized) and fronto-striatal white matter integrity (FA and MD). Analyses were performed with the nlme package in R (Pinheiro *et al.*, 2013). Mixed models are particularly useful in

longitudinal studies, since these datasets have time points within participants and the mixed model approach can recognize this type of data dependency. In order to test for developmental effects, we followed a formal model-fitting procedure (for a similar approach, see Braams *et al.* (2015)). We started by using a null model that only included a fixed and a random intercept, to allow for individual differences in starting points and to account for the repeated nature of the data. We fitted three polynomial age-models with increasing complexity that tested the grand mean trajectory of age: i.e., a linear, quadratic and cubic age-trend. Akaike Information Criterion (AIC; Akaike (1974)) and Bayesian Information Criterion (BIC; Schwarz (1978)), both standardized model-fit metrics were used to compare the different models. Lower AIC and BIC values indicates a better model fit. Log likelihood ratio tests were used between nested models, to test which age-trend best described the data. Reported p-values for the mixed models are based on log likelihood ratio tests. All models were fit with full information maximum likelihood estimates.

Ultimately, linear regression models in SPSS were used to test longitudinal prediction models. In specific, we tested whether fronto-striatal white matter integrity (FA and MD) at T1 could predict delay of gratification skills at T2, while taking into account delay of gratification performance at baseline.

Results

Age effects on delay discounting

Cross sectional data showed that advanced age was related to a larger AUC (normalized), meaning less steep discounting of delayed rewards with age, at both T1 (r=.207, p=.004) and at T2 (r=.204, p=.004). Delay of gratification skills at T1 were positively correlated with delay of gratification skills at T2 (r=.543, p<.001).

The longitudinal analyses, testing for linear, quadratic, and cubic changes in delay discounting, showed that age-related change in delay of gratification skills (AUC normalized) was best described by a quadratic age-model (age^1: β=.1.269, p<.001; age^2: β=-0.568, p=.040) see Table 2. This model indicates a 'peak' in AUC, during late adolescence/early adulthood (see Figure 2a). We also performed the analyses without the relative smaller group of young adults (N=21). However, age-related change in delay of gratification skills (AUC normalized) was –conform the analysis on the total sample- best described by a quadratic age-model (age^1: β=.1.274, p<.001; age^2: β=-0.509, p=.033). Finally, with respect to behavioral performance, we tested potential gender differences. In the current data set, there were no significant gender or gender x age interaction effects in delay of gratification.

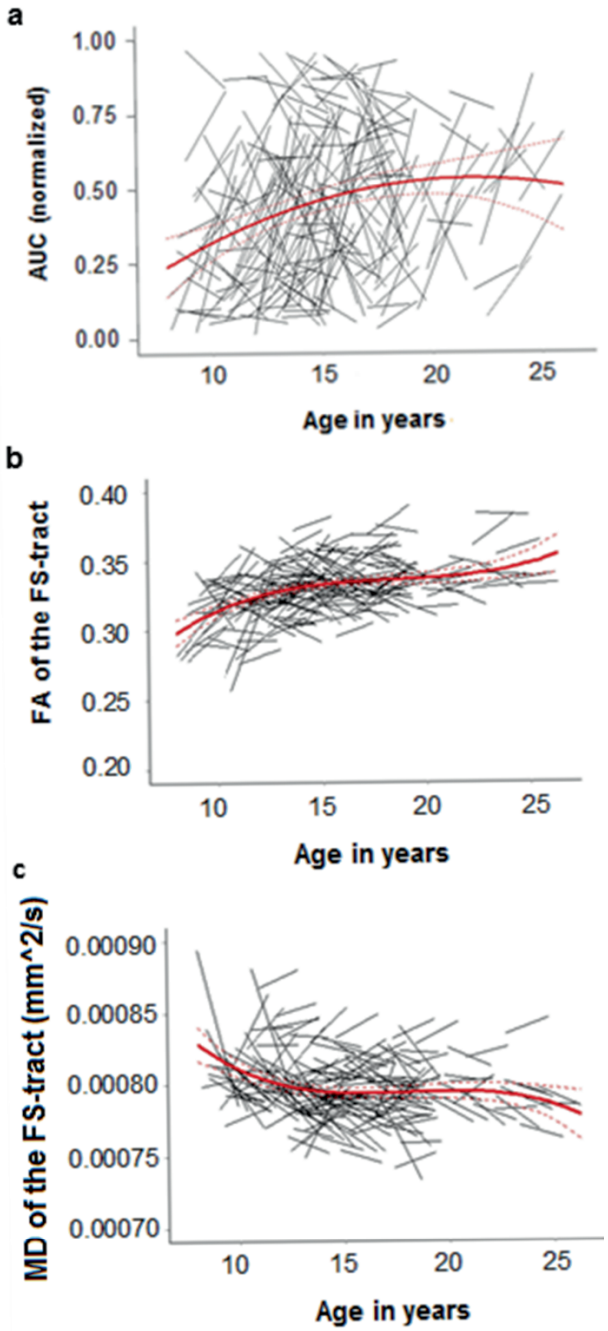


Figure 2. *Individual variability over time for AUC normalized (a), FA (b), and MD (c). Every line represents one individual, with AUC/FA/MD at T1 at the left side of the line and AUC/FA/MD at T2 at the right side of the line. The solid lines display the predicted value of the best-fitting age model. Dotted lines represent the 95% CI.*

Age effects on the frontostriatal tract

Cross-sectional data at T1 and T2 showed that white matter integrity of the fronto-striatal tract increased with age. Age was significantly positively correlated with FA at T1 (r=.440, p<.001) and at T2 (r=.351, p<.001), and significantly negatively correlated with MD at T1 (r=-.220, p=.002), but not at T2 (r=-.089, p=.089). Moreover, white
matter integrity measures were positively correlated between T1 and T2 (FA: r=.611, p<.001; MD: r=.583, p<.001).

Longitudinal analyses revealed that age-related change in white matter integrity (FA and MD) was best explained by a cubic age-model (FA: age¹: β=0.152, p<.001; age²: β=-0.050, p=.006; age3: β=0.047, p=.004; MD: age¹: β=-0.00010, p<.001; age²: β=0.00005, p=.018; age3: β=-0.00007, p=.001) see Table 2. More specifically, our data indicate that FA mostly increased during childhood and early adulthood. The reversed pattern of FA-changes was observed for MD (see Figure 2b and 2c). Analyses only including 8-18 year old participants revealed that age-related change in white matter integrity was best explained by a quadratic age-model (FA: age¹: β=0.137, p<.001; age²: β=-0.048, p=.005; age3: β=0.022, p=.1220; MD: age¹: β=-0.00011, p<.001; age²: β=0.00005, p=.015; age3: β=-0.00003, p=.131). Additional analyses showed that there were no significant gender or gender x age interaction effects in white matter integrity (nor in FA or in MD).

Mediation analyses

To investigate the relation between age and white matter integrity in explaining variance in delay of gratification skills, we performed mediation analyses using the Preacher and Hayes method (Preacher and Hayes, 2008). At T1, the effect of age on delay of gratification (path c: B=.016, p=.004) was fully mediated by FA (path a: B=.123, p<.001; path b: B= .067, p= .0019; path c': B=.008, p=.195; mediation effect a*b: 95% confidence interval (CI) .0034 - .0140; p=.004), see **Figure 3a.** Furthermore, the effect of age on delay of gratification skills (path c: B=.016, p=.004) was significantly mediated by MD (path a: B=-.0614, p=.002; path b: B=-.059, p=.003; Path c': B=.012, p=.026; mediation effect a*b: 95% CI .0012 - .0076; p=.030).

Partly overlapping results were found at T2: FA was a significant mediator of the association between age and delay of gratification skills (path c: B=.014, p=.005; path a: B=.097, p<.001 ; path b: B=.038, p=.047; Path c': B=.011, p=.046; mediation effect a*b: 95% CI .0004 - .0081; p=.061), see Figure 3b. However, MD within the fronto-striatal-tract did not mediate the association between age and delay of gratification skills (path c: B=.014, p=.005; path a: B=-.035, p= .083; path b: B=.012, p=0.488; path c': B=.015, p=.004; mediation effect a*b: 95% CI= -.0028 - .0006; p=.517). Thus, the relation between age and delay of

gratification performance was mediated by white matter integrity within the fronto-striatal tract at both time points.

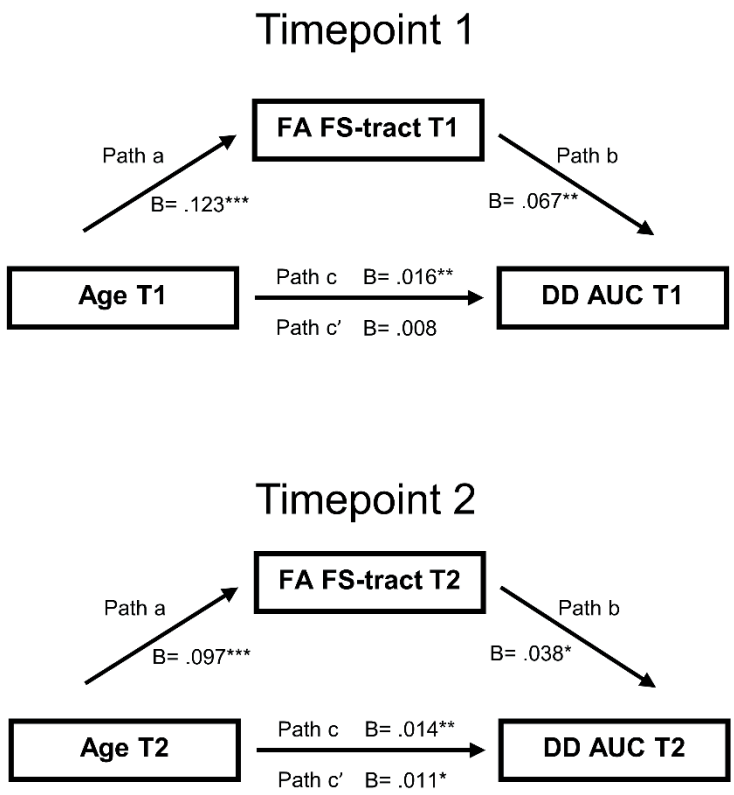


Figure 3. *Mediation models. The relation between age and delay of gratification skills is partly mediated by FA at timepoint 1 and at timepoint 2. Values are standardized regression coefficients and asterisks indicate significance coefficients (*p<0.05; **p<0.01; ***p<0.001).*

Longitudinal prediction

To test whether white matter integrity of the fronto-striatal tract could predict future discounting behavior we performed a linear regression analysis with delay of gratification skills (AUC normalized), age, FA and MD at T1 as predictors for delay of gratification skills at T2. The results showed that in addition to delay of gratification skills at T1 (β=.504, p<.001), FA was a significant predictor (β=.158, p=.034) for delay of gratification skills at T2 (R^2 *total model*=.321, R^2 *FA =.017*),

see Table 3 and Figure 4. Age at T1 and MD did not significantly predict future discounting behavior. The same analyses were performed with non-linear age changes (age² and age³). On top of delay of gratification skills and FA at T1, age² and age³ did not significantly predict future discounting behavior. Thus, while accounting for behavioral performance at baseline, FA within the fronto-striatal tract explains unique variance in future delay of gratification skills.

We also investigated whether delay of gratification skills at T1 was predictive of fronto-striatal white matter integrity at T2. We entered FA at T2 as dependent variables and FA, Age and delay of gratification skills (AUC normalized) at T1 as predictor. The same analyses were conducted with MD. Linear regression analyses showed that both FA (β=-.018, p=.763) and MD (β=-.008, p=.895) at T2 were not significantly predicted by delay of gratification skills at T1.

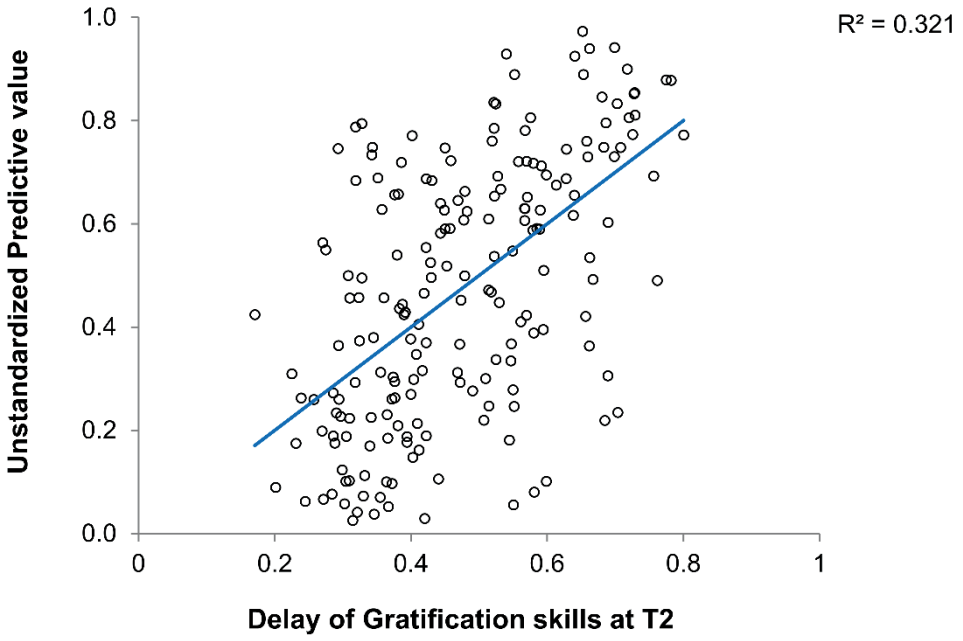


Figure 4. *Delay of gratification skills (AUC normalized) at T2 was predicted by delay of gratification skills (AUC normalized) at T1 and FA of the frontostriatal tract at T1. The y-axis displays the unstandardized predictive value of the regression model with AUC (normalized), age, FA of the frontostriatal tract, and MD of the frontostriatal tract at T1 as predictors.*

Table 2. AIC and BIC values for null, linear, quadratic, and cubic age models fitted separately for delay of gratification skills (AUC normalized), FA of the frontostriatal (FS) tract, and MD of the FS-tract.

	Null		Linear		Quadratic		Cubic	
Measure	AIC	BIC	AIC	BIC	AIC	BIC	AIC	BIC
AUC (normalized)	19.19	31.04	2.57	18.37	0.36	20.12	0.29	23.99
FA of the FS-tract	-2000.71	-1988.86	-2050.19	-2034.39	-2055.72	-2035.97	-2062.04	-2038.34
MD of the FS-tract	-7168.88	-7157.02	-7183.25	-7167.45	-7186.82	-7167.07	-7195.07	-7171.36

Global white matter effects

In order to test for the specificity of the fronto-striatal tract in predicting discounting behavior, we performed a similar analysis with global FA and MD (i.e., all white matter connections excluding the connections marked as fronto-striatal tract). Longitudinal analyses revealed that age-related change in global white matter integrity (FA and MD) was also best explained by a cubic age-model (FA: age^1: β=0.225, p<.001; age^2: β=-0.095, p<.001; age3: β=0.047, p=.004; MD: age^1: β=-0.00010, p<.001; age^2: β=0.00005, p=.018; age3: β=-0.00007, p=.001). Age-related change between 8 and 18 years only was –similar to the fronto-striatal tracts- best explained by a quadratic age-model (FA: age^1: β=0.227, p<.001; age^2: β=-0.041, p<.001; age3: β=0.017, p=.073; MD: age^1: β=0.00005, p=.063; age^2: β=0.00009, p<.001; age3: β=-0.00002, p=.123). Importantly, the linear regression analysis showed that global FA (β=.059, p=.539) and MD (β=.060, p=.802) did not predict future discounting behavior.

Table 3. Linear regression predicting delay of gratification skills at T2 using delay of gratification skills (AUC normalized), age, FA, and MD at T1.

	B	SE	β	p
Constant	-.996	.772		.199
T1 AUC (normalized)	.463	.059	.504	.000
T1 Age	.003	.005	.048	.473
T1 FA of the FS-tract	1.970	.922	.158	.034
T1 MD of the FS-tract	726.143	766.871	.064	.345

Discussion

Development in risk-taking tendencies and impulsive control have been attributed to an imbalance between subcortical and cortical brain regions (Somerville *et al.*, 2010), but very few studies examined the anatomical connections between these areas in relation to impulsive choice. One important dimension of impulsivity is the ability to delay gratification (Whelan *et al.*, 2012). Next to examining developmental patterns in impulsive choice and fronto-striatal white matter integrity, the current study aimed to test if the integrity of fronto-striatal white matter connections *mediated and predicted* the ability to delay gratification across development. We were able to demonstrate that age-related increases in the preference for delayed rewards (i.e. less impulsive choice) was significantly dependent on a better quality of connections between the PFC and striatum. Moreover, the longitudinal analysis revealed that stronger connectivity between striatum and PFC predicted less impulsive choices two years later.

The first question addressed in this study was to test age related change in the ability to delay gratification between childhood and young adulthood. From our results it appears that delay of gratification is largest around late adolescence followed by a slight decline in young adults. This finding fits well with a recent study on age-related changes in discounting of real rewards (Scheres *et al.*, 2006). It appears that there is a gradual increase in delay of gratification skills between childhood and late-adolescence, reaching a plateau in late adolescence/ early adulthood. Prior studies also suggested most reward oriented behavior in mid-adolescence and a steep increase in late-adolescence in self-control (Steinberg *et al.*, 2008; Olson *et al.*, 2009; de Water *et al.*, 2014). A possible explanation that follows from these findings is that adolescents — more than children — flexibly apply self-control for the purpose of reward maximization, which levels off in early adulthood.

Next to developmental change, there was also evidence for consistency in behavior across sessions within individuals. That is to say, we found correlations between delay of gratification skills at T1 and T2, showing that participants who were better able to delay gratification at T1 were also better able to delay gratification at T2 which is consistent with prior studies (Audrain-McGovern *et al.*, 2009; Anokhin *et al.*, 2011). These results indicate a substantial level of trait-like, individual stability in delay of gratification skills in adolescence (Casey *et al.*, 2011). These findings set the stage for examining the hypothesis in this study: how individual variation in behavior is mediated and predicted by striatum-prefrontal cortex connectivity.

In a set of longitudinal analyses we investigated the age-related change in fronto-striatal white matter connections. Results indicated that the integrity of fronto-striatal white matter increases with age, and seems to do so in a cubic fashion: the most pronounced increases in white matter integrity appear to take place in pre-adolescence and young adulthood, with — on average — a relatively

stable period in between. This finding corresponds to previous longitudinal studies demonstrating protracted maturation of large association fiber bundles (Bava *et al.*, 2011; Lebel and Beaulieu, 2011). Studies testing for non-linear relations in white matter tracts are scarce (Olson *et al.* (2009) and reported similar cubic relations in white matter, with the strongest changes in FA and MD during pre-adolescence and young adulthood. Importantly, in a longitudinal study, Simmonds *et al.* (2014) recently reported -in white matter tracts connected to the PFC-, a period of rapid growth in childhood, followed by a slowdown of growth in mid-adolescence and acceleration of growth again in late adolescence/early adulthood. Our longitudinal results also suggest a 'plateau' in white matter development during mid-adolescence, but this seems to be the result of larger variation in white matter development during this period; some children show increases in white matter integrity, while others remain stable or even show decreases. Our results add to increasing evidence obtained from several neuroimaging modalities, showing large variability in brain activity, morphology and connectivity during mid-adolescence (Scherf *et al.*, 2012) pointing towards a unique period of vulnerabilities and opportunities (Crone and Dahl, 2012). It must be noted however, that due to a relative smaller number of participants early adulthood (N=21), the increase in white matter integrity in this period must be interpreted with caution (Mills and Tamnes, 2014). Indeed, the analyses without these young adults hint towards highest values of white matter integrity during late adolescence, leveling off thereafter. Thus, replication of these results in a larger number of adults is warranted to typify the exact nature of fronto-striatal white matter development after adolescence.

Next, we tested whether white matter integrity of fronto-striatal connections was related to individual differences in the ability to delay gratification in adolescents, similar as to what has previously been reported in adults (Peper *et al.*, 2013; van den Bos *et al.*, 2014). Our results showed that white matter integrity of the fronto-striatal tract (specifically FA) mediated the relation between age and delay discounting, consistent with findings of a recent study on the relation between fronto-striatal connectivity and adolescent delay discounting (van den Bos *et al.*, 2015). However, it is not clear whether the relationship between age and delay discounting is eliminated, or merely diminished, when connectivity is taken into account (Steinberg and Chein, 2015). Our results on T1 show a full mediation (the direct effect is no longer significant), while our results on T2 show a partly mediation.

Finally, we for the first time tested whether white matter frontostriatal connectivity *predicted* change in delay discounting across development. Predicting change is important for potential early identification of adolescents who are prone to impulsive choice (see also Ullman *et al.* (2014). The results showed that fronto-striatal white matter integrity was a significant predictor of the ability to delay gratification two years later, while taking into account delay of gratification performance at baseline. These findings indicate that brain

structure is an important underlying mechanism for predicting change in behavior, whereas a reversed claim (i.e., behavior being a predictor for brain change) cannot be made based on the current study. Taken together, change in delay of gratification is partly driven by a more mature white matter connectivity path between striatum and PFC.

It has to be noted that our results are based on a hypothetical delay-discounting task. According to the economic literature not actually paying the participant for the choices on the delay discounting task could possibly undermine the participants behavior in how seriously they take the choices. Although our earlier reported results of hypothetical discounting in adults (Peper *et al.*, 2013) were consistent with results of real discounting in adults (van den Bos *et al.*, 2014) and several studies have shown that choices on hypothetical- and real tasks significantly correlate in adults (Bickel *et al.*, 2009; Scheres *et al.*, 2010), it might be possible that specifically adolescents are influenced by the hypothetical aspect of our task. However, a recent study with a real-discounting task in a larger age range (8-25; van den Bos *et al.* (2015)) revealed similar modulating relations between structural connectivity and delay discounting, suggesting that the use of a hypothetical task might not influence the findings significantly.

Conclusion

In conclusion, the current study provides crucial links for our understanding of the neural mechanisms underlying delay of gratification skills. The ability to delay gratification improves between childhood and early adulthood and this is predicted by the integrity of fronto-striatal white matter connections. This study adds to a descriptive relation between white matter integrity and delay of gratification skills by showing that maturation of fronto-striatal connectivity predicts improvements in delay of gratification skills over a two-year period. These findings have implications for studies examining deviances in impulse control in adolescence, such as in cases of substance abuse or crime, by showing that the developmental path between striatum and PFC may be an important predictor for when development goes astray.

Acknowledgments

This work was supported by a VENI grant from the Dutch Science Foundation (NWO) awarded to J.S.P (VENI 451-10-007) and a European Research Council (ERC) starting grant awarded to E.A.C. (ERC-2010-StG-263234).

CHAPTER NINE

General discussion

Summary

The is thesis had the goal to provide a better understanding of why some children are more sensitive to social evaluation than others, a question that is currently more urgent than ever, given that young individuals connect not only through personal interactions but also through online communication. This thesis examined this question from a neurocognitive development perspective and incorporated both behavioral genetic modeling as well as longitudinal analyses. Neurodevelopmental models suggest that social emotional regulation can be partly explained by protracted development of subcortical and prefrontal cortex regions, as well as their connections (Nelson *et al.*, 2005; Casey *et al.*, 2008; Casey, 2015; Nelson *et al.*, 2016). These models focus mostly on adolescence, the transition period between childhood and adulthood, whereas childhood is a relatively unexplored phase in experimental neuroimaging research. Nevertheless, during childhood rapid changes in executive functioning occur (Luna *et al.*, 2004; Zelazo and Carlson, 2012; Peters *et al.*, 2016) and the first long lasting friendships emerge during this time (Berndt, 2004).

Social emotion regulation is an important factor in developing and maintaining these social relations. Social emotion regulation consists of processing social information (such as peer feedback) and regulating subsequent emotions and behaviors (such as aggression). A broad range of literature has shown that social rejection can result in behavioral aggression (Twenge *et al.*, 2001; Dodge *et al.*, 2003; Leary *et al.*, 2006; Nesdale and Lambert, 2007; Nesdale and Duffy, 2011; Chester *et al.*, 2014), but little is known about the underlying mechanisms of social rejection related aggression. This thesis aimed to fill this gap by investigating the nature, nurture, and neural mechanisms underlying social emotion regulation in childhood.

Testing the Social Network Aggression Task

In order to gain a better understanding of the underlying mechanisms of responses to social acceptance and rejection, I co-designed a novel experimental paradigm that is suitable to combine with neuroimaging. In the Social Network Aggression Task (SNAT) participants view pictures of peers that provide positive, neutral or negative feedback to the participant's profile. In addition to neural activation related to social acceptance and rejection, this paradigm enables studying regions that signal for general social salience, by contrasting both positive and negative feedback to a neutral social feedback condition. To study individual differences in behavioral responses towards social evaluation, we included a retaliation component to the SNAT. After viewing the social feedback, participants could blast a loud noise towards the peer, which was used as an index of aggression.

A crucial first step in understanding social evaluation processing in childhood is to detect robust behavioral patterns and neural signals that are related to processing social feedback. Therefore, in chapter 2 I used a meta-analytic approach to examine behavioral and neural correlates of social evaluation processing in seven-to-eleven-year-old children. I used three different samples: a pilot sample (n=19), a test sample (n=28), and a replication sample (n=27). The results showed that the SNAT revealed robust and reliable behavioral results with negative social feedback resulting in the highest levels of behavioral aggression. Moreover, meta-analyses on predefined brain regions of interest (ROIs) revealed that negative social feedback resulted in more neural activation in the amygdala (compared to positive feedback), the anterior insula (AI) and the anterior cingulate cortex gyrus (ACCg) (compared to neutral feedback). Exploratory whole brain analyses demonstrated heightened activation in the medial prefrontal cortex (MPFC) after negative relative to neutral social feedback. These findings show that the SNAT is a reliable paradigm for the investigation of social evaluation processing and aggression in children, and indicate that this paradigm is feasible for use in larger and longitudinal developmental studies.

Next, in chapter 3, I investigated the neural processes of social evaluation in adults. The aims of this study were three-fold: (1) to disentangle neural signals of positive and negative social feedback, (2) to examine aggressive responses toward the person signaling negative social feedback and (3) to test whether dorsolateral prefrontal cortex (DLPFC) activity was related to aggression regulation after experiencing negative social feedback, based on prior studies with comparable paradigms (Riva *et al.*, 2015). The DLPFC is a region often found implicated in behavioral control (Casey, 2015; Crone and Steinbeis, 2017). In line with the meta-analytical results of chapter 2, I found that negative social feedback was related to applying a longer noise blast toward the peer. At the neural level, conjunction analyses showed that both negative and positive social feedback resulted in increased activity in the ACCg and the bilateral AI, suggesting that these two regions generally respond to socially salient feedback, with no significant differentiation between negative and positive feedback. Neural activation that was specific for positive feedback was located in the striatum and the ventral MPFC, whereas there was no specific significant activation after negative (versus positive) social feedback. Brain-behavioral analyses, however, showed that increased DLPFC activity after negative social feedback was related to more aggression regulation. These results imply that individuals who show stronger activation in the DLPFC after negative social feedback may be better able to regulate social emotions and behavioral impulses.

Social emotion regulation in childhood

After verifying the experimental paradigm in children and adults, the next step was to examine to what extent individual variation in social evaluation was

explained by genetic and environmental factors. Some children might be more sensitive to social evaluation due to genetic predisposition, but likewise, children might be more prone to retaliation due to environmental influences such as violent video games (Konijn *et al.*, 2007). Unraveling these contributions is important as little is known about the genetic and environmental influences on brain responses to social feedback and regulatory responses. Behavioral genetic modeling can estimate the proportion of variance that is explained by additive genetics (A), common environment (C) and unique environment and measurement error (E).

In chapter 4, I used behavioral genetic modeling to investigate the heritability of social feedback processing and subsequent aggression in middle childhood (ages 7-9-years). Behavioral genetic modeling revealed that aggression following negative feedback was influenced by genetic as well as shared and unique environmental influences. Experimental neuroimaging analyses of a large childhood sample (N=512) showed again that the AI and ACCg responded to both positive and negative feedback (see also chapter 2 and 3), showing this social salience network is already present in childhood. Similar to what was observed in the pilot-test-replication study (chapter 2); positive feedback resulted in increased activation in caudate, supplementary motor cortex (SMA), as well as in the DLPFC. In this study I further observed that the MPFC and inferior frontal gyrus (IFG) were more strongly activated after negative feedback. To test relations with behavior in more detail, post-hoc analyses were performed using the significant whole brain clusters as ROIs. These analyses demonstrated that decreased SMA and DLPFC activation after negative feedback (relative to positive) was associated with more aggressive behavior after negative feedback. Thus, similar to what was observed in adults in chapter 3, in children the DLPFC was an important region for aggression regulation. Moreover, genetic modeling showed that 13%–14% of the variance in DLPFC activity was explained by genetics. These results suggest that the processing of social feedback is partly explained by genetic factors. Moreover, whereas the social salience network seemed to be in place already in middle childhood, the aggression regulation mechanism was less pronounced in middle childhood than in adults, which might suggest that this network is still developing during childhood. A final intriguing finding in chapter 4 was that the behavioral response to aggression (i.e., noise blast) was influenced by shared environment factors. Together, these findings set the stage to examine how brain responses (influenced by genetic factors) and behavior (influenced by shared environment factors) change over time.

Chapter 5 set out to test exactly this question, that is, to test developmental changes in aggression regulation and the underlying neural mechanisms using a longitudinal design. In this chapter I examined how changes in neural activity across childhood were related to change in behavioral development. For this purpose 492 same-sex twins (246 families of the original 256 families) underwent two fMRI sessions across the transition from middle

childhood (7-9 years) to late childhood (9-11 years). Results showed that behavioral aggression after social evaluation decreased over time, and this decrease was most pronounced for aggression after positive and neutral social feedback. Confirmatory ROI analyses showed that neural activity in the AI, MPFC and DLPFC increased across childhood, whereas activity in the IFG did not show developmental change. Moreover, increased activity in AI was correlated with more aggression, whereas increased activity in DLPFC was correlated with less aggression. Whole brain-behavior analyses confirmed that bilateral DLPFC activity was correlated with less subsequent aggression following negative social feedback. Finally, longitudinal comparisons revealed that a larger increase in DLPFC activity across childhood was related to a larger decrease in behavioral aggression after negative social feedback over time. These results provide insights on how the developing brain processes social feedback and suggest that the DLPFC serves as an emotion regulation mechanism when dealing with negative social feedback. The results provide a window for understanding individual differences in these developmental trajectories, showing that some children develop stronger regulation skills already in childhood.

Functional architecture of the childhood brain

Previous neurodevelopmental studies and theoretical frameworks have suggested that social emotion regulation might rely on a network of integrated connections between limbic/subcortical and cortical brain regions (Casey, 2015). Most prior studies focused on adolescence or included small samples of children and therefore little is known about functional brain connectivity in childhood. To overcome this gap in knowledge, in chapter 6 I investigated the robustness of findings regarding subcortical-PFC functional brain connectivity in childhood, and the heritability of these connections in 7-to-9-year-old twins. I specifically focused on two key subcortical structures: the ventral striatum (VS) and the amygdala. Reassuringly, I observed strongly replicable brain connectivity patterns over two genetically independent samples of 7- to-9-year-old children, both in the whole brain seed-based analyses and in the post-hoc ROI analyses. Behavioral genetic analyses revealed that VS and amygdala connectivity showed distinct influences of genetics and the environment. VS-PFC connections were best described by genetic and unique environmental factors, whereas amygdala-PFC connectivity was mainly explained by environmental influences (both shared and unique). Similarities were also found: connectivity between the ventral ACC and both subcortical regions showed influences of shared environment, while connectivity with the orbitofrontal cortex (OFC) showed stronger evidence for heritability. Together, this study provides the first evidence for a comprehensive analysis of genetic and environmental effects on subcortical-prefrontal cortex interactions in childhood. The findings demonstrate the need to understand not

only the development of these networks, but also how the environment shapes the maturation of these connections.

Neuroimaging in childhood: Pitfalls and possibilities

With the emergence of functional neuroimaging only two decades ago, the field of developmental cognitive neuroscience can still be considered relatively young and acquisition methods and analysis techniques are rapidly improving. Several prior developmental neuroimaging findings have been called into question after studies showed that these findings were largely influenced by age-related differences in head motion (Satterthwaite *et al.*, 2013), highlighting the need for an in-depth investigation of factors that can influence scan quality in children. In chapter 7 I therefore provide an overview of MRI scan quantity and quality in a large developmental twin sample and investigated the genetic and environmental influences on head motion. Overall, scan quantity was high (88% of participants completed all runs), while scan quality decreased with increasing session length. Scanner related distress was negatively associated with scan quantity, but not with scan quality. In line with previous studies, behavioral genetic analyses showed that genetics explained part of the variation in head motion, with heritability estimates of 29-65%. Additionally, the results revealed that subtle head motion - after exclusion of excessive head motion- showed lower heritability estimates (0–14%), indicating that findings of motion-corrected and quality-controlled MRI data are less confounded by genetic factors. Moreover, shared environmental influences played a larger role (15–33%) in the variation in quality-controlled head motion, suggesting that head motion can be influenced by participant instruction and age-appropriate scanner adjustments. This is specifically important for neuroimaging studies across different age-ranges, as this can minimize the confounding factor of age-related differences in head motion on findings regarding brain development.

Brain connectivity as predictor of emotion regulation

As was explained in the section on neurocognitive development models, the ability to regulate emotions and control impulses increases considerably during adolescence, the transition phase between childhood and adulthood. In chapter 8 I tested the hypothesis that this form of emotion regulation is driven by increased maturation of frontostriatal circuitry using a fiber-tracking approach combined with longitudinal imaging. Given the novelty of this approach, here I made use of a classic and often used paradigm to study impulse control; the delay discounting paradigm (Peper *et al.*, 2013). The delay discounting task estimates the preference to choose for a direct small reward over a delayed larger reward. In total, 192 healthy volunteers between 8 and 26 years underwent diffusion tensor imaging scanning and completed the delay discounting task twice,

separated by a 2-year interval. This sample was part of the 3-wave longitudinal Braintime study (van Duijvenvoorde *et al.*, 2016b). First, I examined linear and non-linear development of both brain connectivity and behavior. The development of delay of gratification showed a quadratic trajectory, with a steep increase during late childhood and the peak in late adolescence. Structural brain connectivity showed cubic relations across development, with the most pronounced changes during late childhood and early adolescence. Moreover, age related increases in the preference for delayed rewards (i.e., less impulsive choice) were significantly dependent on a better quality of connections between the PFC and striatum. The longitudinal analysis revealed that stronger connectivity between striatum and PFC predicted less impulsive choices 2 years later, indicating that brain maturation precedes emotion regulation and behavioral outcomes. These findings fit well with neurocognitive models suggesting that striatum-prefrontal cortex maturation is an important factor contributing to the development of emotion regulation (Casey, 2015; Nelson *et al.*, 2016).

Discussion

Taken together, the studies described in this thesis revealed several important findings. First, using the Social Network Aggression Task I was able to disentangle between neural activation that was specific for social rejection and social acceptance, and activity that was related to general social salience. Second, by including a retaliation component to the paradigm, I showed how individual differences in aggression regulation were related to differences in neural activation of the DLPFC. Third, by combining findings of task-based functional MRI with both functional and structural connectivity analyses, I gathered knowledge on the development of social emotion regulation and shed light on the important neural development that takes place during childhood. These three main outcomes are discussed in detail below and suggestions for a novel theoretical framework are provided.

Social pain, social gain and general social signaling

Prior studies on social evaluation processing have suggested that the ACC and AI might signal for social pain, as these regions showed increased neural activation after social rejection (Eisenberger and Lieberman, 2004; Kross *et al.*, 2011; Rotge *et al.*, 2015). However, several researchers have questioned this hypothesis as they reported increased activation of the ACC also in relation to expectancy violation (Somerville *et al.*, 2006; Cheng *et al.*, 2019), indicating these regions might signal for social salience in general (Dalgleish *et al.*, 2017). The Social

Network Aggression Task is the first social evaluation paradigm to experimentally disentangle neural activation for social rejection and social salience, by contrasting positive and negative social feedback to a neutral condition. In order to provide a comprehensive overview of the findings from the SNAT paradigm, I conducted a meta-analysis on the neural activation after general social salience (positive and negative feedback vs. neutral feedback), social rejection (negative vs. positive feedback) and social acceptance (positive vs. negative feedback). For this analyses I used GingerALE (Eickhoff *et al.*, 2009; Eickhoff *et al.*, 2012; Turkeltaub *et al.*, 2012), a Brainmap application that is based on activation likelihood estimation, with p<.005 and a minimal volume threshold of 300 mm2. Meta-analytical results are based on the findings of adults (chapter 3, table S1 and S3), middle childhood (chapter 4, table 3) and late childhood (chapter 5, table S6) and show distinct neural activation for social rejection and social acceptance, and additionally reveal a network of brain regions that are sensitive to general social salience, see **Table 1** and **Figure 1**.

Social rejection resulted in increased neural activation in the bilateral IFG, the MPFC, and visual regions in the occipital lobe, including the cuneus (**Table 1**, **Figure 1**). Previous studies often failed to find significant neural activation after negative social feedback (Gunther Moor *et al.*, 2010b; Guyer *et al.*, 2012) which could be related to low statistical power, as these studies often used small sample sizes (Mumford and Nichols, 2008; Button *et al.*, 2013). In chapter 3 of this thesis I also did not report significant activation after social rejection using a smaller sample size (n=30) in an adult sample. However, in the studies with large samples and strong statistical power (chapter 4 and 5) I consistently report strong activation in the IFG and MPFC in childhood. The MPFC has shown to play an important role in social cognition and behavior (Blakemore, 2008; Adolphs, 2009) and is specifically implicated when thinking about others (Apps *et al.*, 2016; Lee and Seo, 2016). Receiving negative social feedback may leave the children wondering what the other might have thought about them (Gallagher and Frith, 2003). Indeed, the social information processing network (SIPN) suggests that the MPFC is part of the "cognitive-regulatory node" were the mental states of others are perceived before inhibition of pre-potent responses are regulated by the lateral PFC (Nelson *et al.*, 2005; Nelson *et al.*, 2016). This corresponds to the MPFC specifically being activated after social rejection, as this might result in a stronger need for social emotion regulation than feedback leading to social acceptance.

Meta-analytical results showed that social acceptance specifically activated regions in the DLPFC, the SMA, and visual regions in the occipital lobe (**Table 1**), consistent with prior studies on social evaluation processing (Gunther Moor *et al.*, 2010b; Guyer *et al.*, 2012). The chosen GingerALE setting of clusters > 300 mm2 limits the possibility of finding meta-analytical activation in small regions such as the striatum, however, I did report significant activation in the caudate in both adults (chapter 3) and children (chapter 4). The SMA and DLPFC

have been related to motor planning and behavioral control (Casey, 2015; Riva *et al.*, 2015) and neural activation in these regions might be related to the retaliation component of the SNAT paradigm. That is, participants might like the peers that provided positive feedback and therefore be intrinsically motivated to release the button as soon as possible, resulting in increased activation in the SMA and DLPFC. Indeed, the behavioral results showed that participants liked social acceptance the most and the rewarding value of positive feedback was also depicted in increased striatum activation (Sescousse *et al.*, 2013). Increased striatal activation after positive feedback has been reported by previous social evaluation studies (Davey *et al.*, 2010; Gunther Moor *et al.*, 2010b; Guyer *et al.*, 2012) and fits well with the SIPN model that highlights the importance of the "affective node" (including striatal regions) in the processing of social stimuli (Nelson *et al.*, 2005; Nelson *et al.*, 2016).

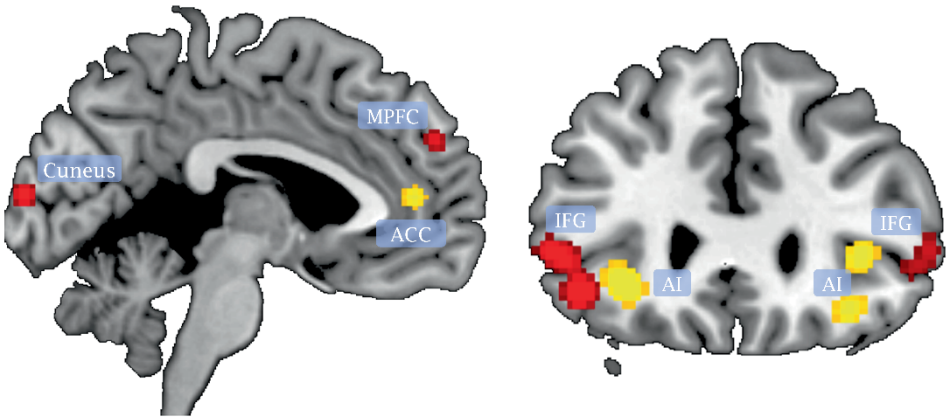


Figure 1. *Meta-analytic activation maps for Social Network Aggression Task studies of chapters 3, 4 and 5. Neural activation for social rejection (negative > positive feedback) depicted in red. Neural activation for general social salience (positive and negative > neutral feedback) depicted in yellow. Meta-analyses were conducted using GingerALE with p<.005 and volume > 300 mm2.*

Using the SNAT, I experimentally showed that there is a neural network sensitive for general social salience, irrespective of its valence. Both positive and negative social feedback resulted in increased neural activation in the ACCg, bilateral AI, medial frontal gyrus and visual regions in the occipital lobe (**Figure 1**, **Table 1**). These findings fit with the literature suggesting that the ACC and AI signal for social salience in general (Somerville *et al.*, 2006; Dalgleish *et al.*, 2017; Cheng *et al.*, 2019). These findings add to previous theoretical models of social information processing which indicated the fusiform face area as an important social detection mechanism (Nelson *et al.*, 2005; Nelson *et al.*, 2016), by showing

that the ACC and AI are also important in the detection and signaling of social relevant information. Moreover, the social salience networks reported in adults (chapter 3), middle childhood (chapter 4) and late childhood (chapter 5) show remarkable resemblances, indicating this might be a core social motivational mechanism in humans. This highlights the importance of incorporating childhood neurodevelopmental changes into theoretical frameworks, as social processing networks are already active during childhood. Moreover, chapter 5 describes how activation in the AI was related to behavioral aggression, and future studies should further explore whether individual differences in neural activation of the social salience network are related to individual differences in sensitivity to social evaluation. By taking real-life social interactions into account, future studies might be able to examine whether individual differences in sensitivity to social evaluations are a cause or an effect of individual differences in social (offline or online) interactions.

Aggression regulation following social feedback

Previous theoretical models of social emotion regulation have suggested that the lateral PFC is important for top down control over affective-motivational subcortical regions (Nelson *et al.*, 2005; Casey *et al.*, 2008; Casey, 2015; Nelson *et al.*, 2016). By including a retaliation component to the Social Network Aggression Task, I was able to directly test how individual differences in social emotion regulation were related to neural activation in the DLPFC. Consistent with prior experimental studies (Riva *et al.*, 2015), chapter 3 revealed that increased activation in the DLPFC after social rejection was related to less subsequent aggression in adults, suggesting that these individuals were more successful at regulating their behavioral aggression. Region of interest analyses of the DLPFC in a middle childhood sample (chapter 4) provided some indications of an aggression regulation network, but this was not strong enough to be depicted using whole brain-behavior analyses. When examining these same children two years later - now during late childhood - there was a significant association between brain and behavior. Similarly to adults, increased neural activation in the DLPFC was related to less behavioral aggression after negative social feedback. Importantly, the children who displayed the largest developmental increases in DLPFC activity across childhood also displayed the largest changes in social emotion regulation. These findings add to previous studies that suggested that the DLPFC is an important region for cool (non-emotional) cognitive control (Luna *et al.*, 2004; Luna *et al.*, 2010; Crone and Steinbeis, 2017) by showing that the DLPFC is also important in controlling hot emotional control (Zelazo and Carlson, 2012; Welsh and Peterson, 2014). Moreover, the results provide evidence for developmental models of social emotion regulation (Nelson *et al.*, 2005; Casey *et al.*, 2008; Casey, 2015; Nelson *et al.*, 2016) in such a way that they confirm that the DLPFC serves as a regulatory

mechanism and is related to behavioral outcomes. However, these models specifically focused on adolescent brain development, whereas the findings of this thesis show that important changes in this neural network occur during childhood. Theoretical perspectives based on behavioral studies have suggested that the development of emotion regulation is closely related to the development of cognitive control (Diamond, 2013) and experimental studies have shown that cognitive control development accelerates during childhood (Luna *et al.*, 2004; Zelazo and Carlson, 2012; Peters *et al.*, 2016). The current thesis provides direct links between maturation of cognitive control (DLPFC) regions and individual differences in social emotion regulation. This was shown in a specific age range (7-9-year old to 9-11-year old), to provide a detailed analysis of changes in childhood. The results provide a window for understanding individual differences in these developmental trajectories, showing that some children develop better regulation skills already in childhood. Future research should examine developmental changes in a longer time window by including more measurement points, which allows disentangling general developmental patterns from individual differences in growth trajectories.

Childhood: A window of opportunity

As children grow older and move towards adolescents, they generally receive more autonomy and are less often under adult supervision (Steinberg *et al.*, 1989). In some individuals this results in increased risk taking and sensation seeking, which can have negative consequences such as physical and psychological injury (Steinberg, 2008). To understand individual differences in these behaviors, several neurodevelopmental models have been proposed (see Casey (2015) for an overview), all of which focus on adolescent brain development. The longitudinal analyses across children, adolescents and adults in this thesis (chapter 8), however, showed that structural connectivity between the striatum and the PFC was predictive of behavioral control two years later, providing evidence that brain maturation can forecast future behavioral control. Knowing that brain development precedes behavior (Gabrieli *et al.*, 2015); the foundation for adolescent behavior is thus laid during childhood. The studies in this thesis highlight the importance of incorporating childhood brain development in neuroscientific models by showing that the steepest increases in both behavioral control and subcortical-PFC structural connectivity take place during childhood.

Both empirical studies as well as theoretical models have mostly focused on developmental peaks in brain maturation (Casey *et al.*, 2008; Galvan, 2010; Braams *et al.*, 2015; Peters and Crone, 2017). Although this can be illuminating, I argue that the road towards this peak is more informative when it comes to development. The developmental phase that marks the steep increase preceding the peak is the time in which actual change is taking place. This could possibly

reflect a moment where it is relatively easy to intervene in development. Metaphorically, if a rock is quickly rolling down a hill, one can easily change its course by gently tapping the rock. The faster the stone is rolling, the larger the impact of this small interference will be. However, when the stone has reached the end of the hill, the small tap will no longer have a big impact. As a broad range of studies - including chapters of this thesis- have shown that childhood marks pronounced changes in emotional reactivity (chapter 5; Silvers *et al.* (2012)), cognitive control (Luna *et al.*, 2004; Peters *et al.*, 2016) and structural brain connectivity (chapter 8; Wierenga *et al.* (2018b)). These accelerated changes in brain development could provide a window of opportunity for interventions that can change the course of development with smaller interference compared to later interventions (**Figure 2**).

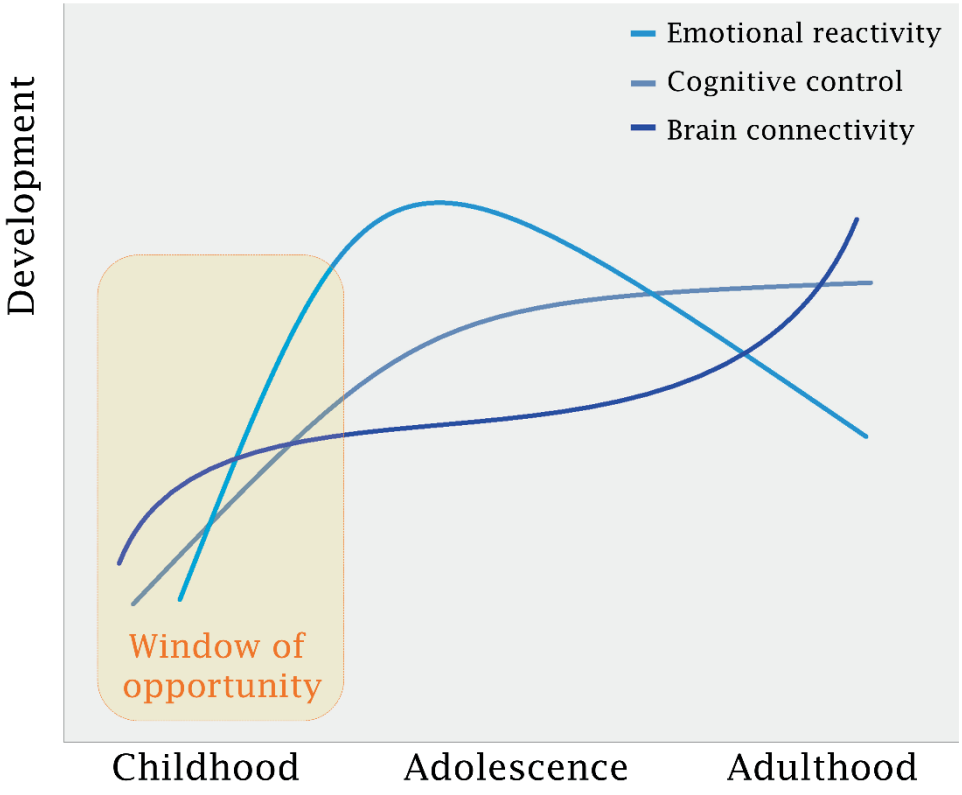


Figure 2. *Childhood as window of opportunity. The steepest increase in emotional reactivity, cognitive control and (structural) brain connectivity are in late childhood, which may reflect a unique window of opportunity in terms of development. Note: data of developmental trajectories are illustrative.*

Methodological Considerations

The studies discussed in this thesis make an important contribution to the literature on the development of social emotion regulation and point to childhood as a possible window of opportunity. Apart from these theoretical implications, there are four methodological considerations that arise from these studies, which are reviewed below.

Two of a kind: Generalizability of twins to singletons

The classical twin design is sometimes referred to as "the perfect natural experiment", as it provides the unique opportunity to tease apart genetic components from environmental influences. Using a twin design can provide important insights in the underlying mechanisms of a psychological construct. An important assumption of these studies is that findings can be generalized to the general (non-twin) population (Moilanen *et al.*, 1999). Although several studies have shown that this is true when it comes to general physical characteristics (i.e., blood pressure or height, (Andrew *et al.*, 2001)), twin-singleton comparisons on psychological constructs are limited. A large longitudinal study in middle and late childhood showed no significant differences between the developmental trajectories of externalizing problems of twins and singletons (Robbers *et al.*, 2010), suggesting that twin findings on behavioral control or emotion regulation might be generalizable. However, when investigating *social* emotion regulation, it is important to keep in mind the unique social buffer that twin-hood might provide (Branje *et al.*, 2004). It has been hypothesized that twins may have a favorable social environment due to interactions with, and social support of the co-twin (Pulkkinen *et al.*, 2003). In order to test whether the findings of this thesis are generalizable to non-twin children, it is important to compare the results on aggression regulation following social evaluation with a sample of non-twins. Recently, several other research facilities have started to use the Social Network Aggression Task, and combining these samples will enable such direct comparisons.

Multiple samples *vs.* Massive samples

A twin study provides the additional possibility to test a specific psychological construct in two similar samples (one co-twin in each), thereby replicating findings within a study. Replication designs are very useful for testing the robustness and reproducibility of results (Schmidt, 2009; Open Science, 2015). Examples of multiple samples within one study are provided in this thesis in chapter 2 (pilot- test- replication design), chapter 5 (ROI selection in independent sample) and chapter 7 (functional connectivity in two independent samples). The findings of thesis also showed that high statistical power is needed to detect

subtle brain-behavior associations, specifically in children. That is, using multiple smaller samples (n<30) in chapter 2 did not reveal the social rejection specific neural activity that was found using a larger sample (n>300) in chapter 4. Moreover, the independent sample for ROI selection (n=41) in chapter 5 had too little statistical power to reveal the whole brain-behavior associations that were reported with the exploratory analyses (n>300). An important methodological objective that follows from this thesis is that multiple samples are not necessarily better than large samples (or vice versa), but that they serve different purposes. Replicability is extremely important for confirming findings (Ioannidis, 2005; Schmidt, 2009), but for explorative discoveries we need a lot of statistical power and therefore large samples (Mumford and Nichols, 2008; Button *et al.*, 2013). This is especially true for developmental neuroscientific studies, as the attrition rate in children often is high (O'Shaughnessy *et al.*, 2008; Raschle *et al.*, 2012; Fassbender *et al.*, 2017a).

Control your head motion: Attrition biases

Children are more prone to head motion during the MRI scan than adolescents and adults (O'Shaughnessy *et al.*, 2008; Raschle *et al.*, 2012; Fassbender *et al.*, 2017a). To limit the confounding effect of head motion on MRI findings, it is important to exclude participants that exceed a specific threshold of head motion (Power *et al.*, 2015). This often results in an underrepresentation of children in cohort-sequential longitudinal studies, an issue that can be overcome by oversampling children during data acquisition. However, excluding participants who display excessive head motion might induce an additional bias: it is likely that participants who have difficulty regulating their head motion also experience difficulty regulating their emotions and behaviors. Indeed, studies showed a significant association between head motion and motor control (Zeng *et al.*, 2014; Ekhtiari *et al.*, 2019). This indicates that participants with the most behavioral control problems are the first to be excluded in MRI research (Kong *et al.*, 2014). This bias is almost insurmountable, but must be kept in mind when interpreting neuroscientific studies on emotion regulation and behavioral control. More and more methods to deal with head motion during MRI scan acquisition are being developed, for example by using real-time monitoring of head motion (Dosenbach *et al.*, 2017) or customized head molds (Power *et al.*, 2019), which might enable future studies to exclude less participants and thereby minimize attrition bias.

fMRI: State of mind or state of mess?

The reliability of functional MRI, specifically experimental (task-based) fMRI has been heavily debated in recent years (Nord *et al.*, 2017; Elliott *et al.*, 2019b; Frohner *et al.*, 2019). The variability observed in fMRI blood oxygen level dependent (BOLD) signal and the poor test-retest reliability in developing populations is a big concern for the field of developmental neuroscience (Herting

et al., 2018). Test-retest reliability is the extent to which a measure produces stable outcomes across different time points under comparable conditions (Dubois and Adolphs, 2016). Prior longitudinal developmental studies, including chapter 5 of this thesis, reported low intra-subject stability across different scan session (for an overview see Herting *et al.* (2018)). These could either reflect individual variability over time or might reflect unaccounted-for noise in the fMRI measurement (Dubois and Adolphs, 2016). The behavioral genetic analyses on fMRI in chapter 4, 5 and 6 showed that a large proportion of variance was explained by the E-factor, which includes both unique environmental influences and measurement error. An important objective for future research is to disentangle between the influence of unique environment and measurement error, for example by accounting for intra-subject fluctuations using repeated measures (Ge *et al.*, 2017). Using such a repeated measures approach, one can tease apart the stable effects (which are due to unique environment) from the transient effects (which might arise from measurement error) (Ge *et al.*, 2017).

Heritability estimates for fMRI are often lower than for structural MRI (sMRI) (Jansen *et al.*, 2015). Similar to the difference between questionnaire data and experimental data, sMRI can be seen as a trait-like measure of the brain, whereas fMRI provides a state-like measure (Greene *et al.*, 2018a). Indeed, questionnaire data often shows higher heritability and test-retest stability than experimental studies (Tuvblad and Baker, 2011), that are aimed to induce a specific state. A state can be defined as *"the particular condition that someone is in at a specific time",* and by this definition it seems reasonable that there is more intra-individual variability across time for experimental (fMRI) studies. An important benefit of the state-inducing ability of fMRI is that it can isolate specific aspects of complex behaviors. A broad range of literature - including chapter 3, 4 and 5 of this thesis- have shown that experimental fMRI is meaningful in relation to behavior and can provide valuable information about the underlying mechanisms of specific behaviors. It should be noted that the field of developmental neuroscience, and specifically the use of longitudinal experimental fMRI studies, is still young (Crone and Elzinga, 2015; Herting *et al.*, 2018). Perhaps the strength of fMRI lies in the combination of different MRI modalities (Dubois and Adolphs, 2016). That is, experimental fMRI might be used to detect meaningful associations between behavior and brain regions, which can be further examined by studying the stability or heritability within this region using additional MRI metrics (Greene *et al.*, 2018a; Elliott *et al.*, 2019a). This would provide an in-depth examination of both trait-like and state-dependent features of brain-behavior relations.

Future directions

Based on the main scientific outcomes of this thesis, and taking into account the methodological considerations that arose from the different studies, I have formulated three objectives that are important for future research.

Combined forces: Multimodal brain imaging

In order to use experimental neuroimaging to its full potential, while taking into account the limitations that it entails, it is important to combine different MRI metrics. Aggressive behavior and emotion regulation have been studied using different MRI methodologies, such as structural anatomy (Bos *et al.*, 2018), experimental fMRI (Ochsner *et al.*, 2012), functional connectivity (Fulwiler *et al.*, 2012) and structural connectivity (Olson *et al.*, 2009; Peper *et al.*, 2015), but the number of studies that combined different metrics is limited. Nevertheless, most theoretical frameworks suggest that behaviors and emotions are regulated through communication between specific brain regions that are part of a large and complex brain network (Casey, 2015). To empirically examine the complex features of the developing brain and its association with behavioral outcomes, a multimodal brain imaging approach is needed.

Individual differences in developmental trajectories

The single time-point studies in this thesis (chapters 2, 3, 4, 6, 7) provide starting points for understanding social emotion regulation in the childhood brain. To understand the developmental trajectories of social emotion regulation, however, we need longitudinal studies (Crone and Elzinga, 2015; Telzer *et al.*, 2018). Although I made a start with this approach in chapter 5 and 8, it should be noted that two measures are only slightly better than one. Three or more measures are needed to capture complex developmental trajectories, as this allows investigating both linear and non-linear individual growth trajectories (Madhyastha *et al.*, 2018). Both behavioral outcomes (such as reward sensitivity or emotional reactivity) and brain development have shown non-linear development across childhood, adolescence and adulthood (Galvan, 2010; Silvers *et al.*, 2012; Wierenga *et al.*, 2018a). Most of these studies had an underrepresentation of children, resulting in more uncertainty (larger confidence intervals) in developmental trajectories across childhood. The L-CID sample consists of a unique twin sample that will be followed for a total of six years (Euser *et al.*, 2016), including three MRI measures. This will allow for examination of individual differences in developmental trajectories across childhood and emerging adolescence. Additionally, due to the large sample size and therefore excellent statistical power, we can examine how childhood brain development

can predict adolescent behavior and further explore childhood as a window of opportunity.

Social communication of digital natives

Today's children are the first generation to grow up with unlimited internet access, enabling to be constantly connected to a complex and intense (digital) social network. Despite the fact that social media is everywhere around us and used by almost everyone on a daily basis, very little scientific research has been conducted on the effects of social media on the developing brain (Crone and Konijn, 2018). The studies in this thesis provide a starting point by unraveling the neural mechanisms of social evaluation in childhood. An important question for future research is whether individual differences in sensitivity to social evaluation are related to individual differences in real-life (digital) social interactions. Numerous studies have used real-life social media monitoring (for example see Montag *et al.* (2014)), mostly in combination with questionnaire data. Although this can provide insight on behavioral correlates, the covert neural mechanisms involved in social media remain unknown. The novel approach of bringing together both real-life social media monitoring, as well as innovative developmental neuroimaging will result in cutting edge research and can provide insights through a neuro-mechanistic approach.

Conclusion

This thesis provides a comprehensive overview of the underlying mechanisms of social emotion regulation in childhood. The studies show that our brain is prone to signal for socially relevant information, irrespective of its valence. This network of social saliency is already present in childhood, indicating this might be a core social mechanism. The thesis additionally shows that social rejection is often followed by behavioral aggression, and regulation of these retaliation emotions is related to control mechanisms of the DLPFC. The results are in line with previous neurodevelopmental models, which highlight the importance of top-down control of prefrontal regions over bottom-up processing subcortical-affective regions. As complement to these models, the results show that the vast architecture of functional subcortical-PFC brain connectivity is already in place in middle childhood and suggest fine tuning of (social evaluation) brain networks across childhood, highlighting the need to incorporate childhood into developmental models of social emotion regulation. Neuroimaging research, specifically neuroimaging in children is prone to challenges and several methodological considerations need to be taken into account when studying the childhood brain. In spite of these difficulties, studying childhood brain development has the potential to provide important insights into a unique developmental window of opportunity.

Table 1. Meta-analytical activation for social salience, social rejection and social acceptance. Results are based on 3 studies using the Social Network Aggression Task (chapter 3, 4, and 5). Note that there was no significant activation reported for the social rejection contrast in chapter 3. Meta-analytical results were obtained with GingerALE, using p<.001 and volume > 300 mm^2.

Anatomical Region	x	y	z	ALE	Z	p
Social Salience (positive and negative > neutral social feedback)						
Insula (left)	-32	26	-6	0.02	5.54	<.001
Insula (left)	-30	12	-16	0.02	4.83	<.001
Insula (left)	-44	16	-4	0.02	4.74	<.001
Insula (left)	-38	22	-16	0.01	3.51	<.001
Insula (left)	-30	18	0	0.01	3.17	0.001
Insula (right)	36	24	-12	0.02	4.74	<.001
Insula (right)	38	30	4	0.01	4.18	<.001
Medial frontal gyrus (right)	12	48	13	0.01	3.62	<.001
ACC gyrus	0	46	10	0.02	5.11	<.001
ACC gyrus	0	38	16	0.01	3.36	<.001
ACC gyrus	2	56	12	0.01	3.17	0.001
Occipital lobe (left)	-48	-76	-2	0.02	5.85	<.001
Occipital lobe (right)	48	-72	-4	0.02	5.03	<.001
Occipital lobe (right)	50	-62	-2	0.01	3.35	<.001
Occipital lobe (right)	50	-78	6	0.01	3.1	0.001
Social Rejection (negative > positive social feedback)						
IFG (right)	57	32	4		4.48	<.001
IFG (left)	-45	26	-8		5.69	<.001
IFG (left)	-52	28	4		4.22	<.001
Insula (left)	-38	-16	26		4.22	<.001
MPFC	-12	60	25		4.32	<.001
MPFC	-6	54	30		4.05	<.001
Cuneus (left)	-8	-97	12		4.83	<.001
Cuneus (right)	26	-91	16		5.11	<.001
Social Acceptance (positive > negative social feedback)						
DLPFC (right)	39	34	40		4.19	<.001
SMA (right)	26	6	56		4.4	<.001
Culum of cerebellum (right)	4	-74	-2		5.23	<.001
Occipital lobe (left)	-18	-85	-6		4.34	<.001

SUMMARY IN DUTCH

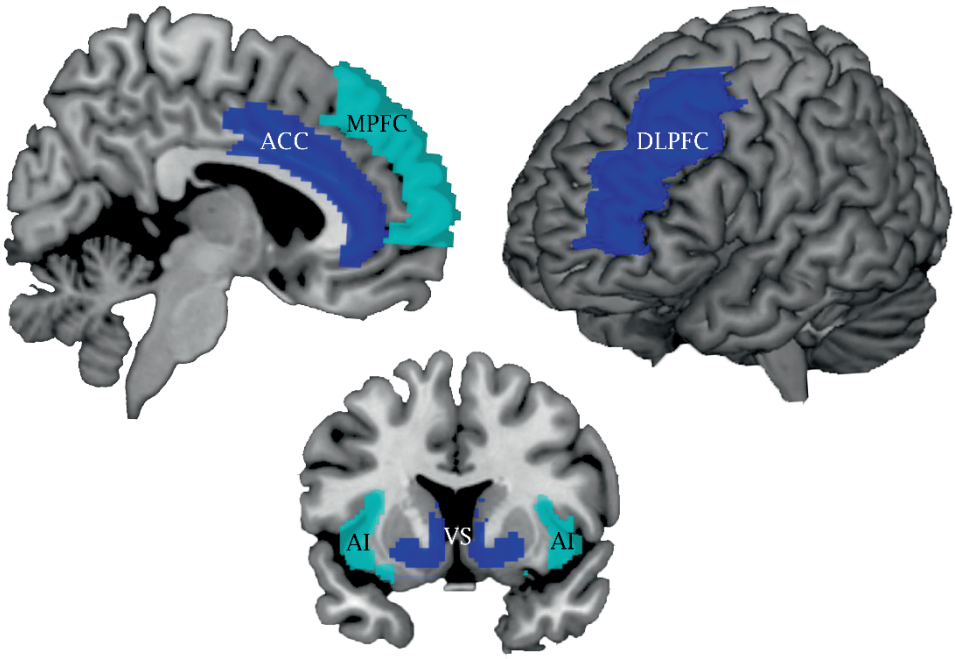
Nederlandse samenvatting

We wurmen ons letterlijk in bochten om de perfecte vakantiefoto te maken, bedenken er een inspirerende tekst bij, zetten het online en dan... wachten op de likes! Waarom doen we zoveel moeite om geaccepteerd te worden door anderen? En hoe komt het dat sociale afwijzing ons kan laten stampvoeten van woede? Wat zijn de onderliggende brein mechanismes van dit soort emoties en gedrag? En hoe ontwikkelen deze mechanismes zich tijdens de kindertijd? Deze vragen tracht ik te beantwoorden in dit proefschrift, om zo meer inzicht te krijgen in de onderliggende processen van sociale emotie regulatie in de kindertijd.

De huidige generatie van kinderen is de eerste die vanaf hun geboorte opgroeit met smartphones en tablets. Deze kinderen zijn constant verbonden met elkaar door middel van multiplayer video games en social media. Uit een onderzoek uit 2015 onder meer dan 1200 acht-tot-twaalf-jarige bleek dat kinderen in deze leeftijd gemiddeld zes uur per dag besteden aan (social) media (Common Sense Media Inc., 2015). Deze cijfers laten zien dat kinderen tegenwoordig al vanaf jongs af aan te maken hebben met social media en sociale verbondenheid. Sommige krantenartikelen beweren dat deze nieuwe vorm van media kinderen verandert in sociale junkies die altijd maar op zoek zijn naar sociale bevestiging. Maar hoe nieuw is deze sterke behoefte om geaccepteerd te worden, om "erbij te horen"? Eigenlijk is het helemaal niet nieuw. Sociale bevestiging is altijd al een belangrijk onderdeel van ons leven geweest. Als je heel vroeger bij een groep hoorde dan vergrootte dat de kans om te overleven. Voor onze voorouders was sociale bevestiging letterlijk van levensbelang.

Sociale acceptatie en afwijzing kan worden onderzocht door middel van wetenschappelijke experimenten waarbij feedback van leeftijdsgenoten op bijvoorbeeld het persoonlijk profiel van de deelnemers wordt gesimuleerd (Somerville et al., 2006, Gunther Moor et al., 2010b, Dalgleish et al., 2017). Deze experimenten kunnen ook worden gedaan in combinatie met een hersenscan, doormiddel van functionele magnetic resonance imaging (fMRI). Experimentele fMRI studies naar sociale acceptatie en afwijzing hebben laten zien dat het belang van sociale signalen niet alleen heel oud is, maar dat het ook diepgeworteld in ons brein zit. Sociale acceptatie is bijvoorbeeld gerelateerd aan verhoogde brein activiteit in het ventrale striatum (VS, figuur 1) (Guyer et al., 2009; Davey et al., 2009; Gunther Moor et al., 2010b; Sherman et al., 2018b). Dit gebied staat bekend als het beloningsgebied en wordt ook actiever als je geld wint (Secousse et al., 2013). Sociale afwijzing is gerelateerd aan verhoogde activatie in de dorsale en subgenuale anterieure cingulate cortex (ACC) en mediale prefrontale cortex (MPFC), zie figuur 1. Van de dorsale ACC en de anterieure insula (AI, figuur 1) werd in eerdere onderzoeken gezegd dat ze signaleren voor sociale pijn, aangezien deze gebieden ook actief worden bij het ervaren van fysieke pijn (Eisenberger and Liberman, 2004; Kross et al., 2011; Roge et al., 2015). Echter, andere onderzoekers vonden verhoogde activatie in de ACC en AI bij onverwachte

gebeurtenissen (Somerville et al., 2006, Cheng et al., 2019) en deze studies suggereren dat de gebieden wellicht belangrijk zijn bij het evalueren van sociale feedback in het algemeen, los van of dat deze positief of negatief is (Dalgleish et al., 2017).



Figuur 1. *Brein gebieden die belangrijk zijn bij het verwerken van sociale feedback en het reguleren van (sociale) emoties. ACC - Anterieure cingulate cortex, MPFC - mediale prefrontale cortex, DLPFC - dorsolaterale prefrontale cortex, AI - anterieure insula, VS - ventrale striatum.*

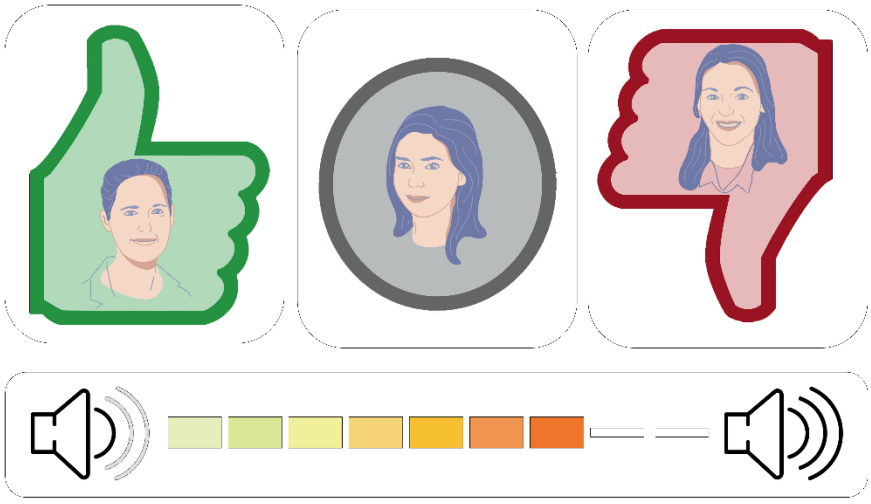
Eerdere studies hebben dus laten zien dat er verschillende neurale processen te onderscheiden zijn voor sociale acceptatie en afwijzing, maar er blijven nog veel open vragen. Om daadwerkelijk de neurale mechanismes bloot te leggen is er een nieuw experimenteel paradigma nodig, die onderscheid kan maken tussen breingebieden die van belang zijn bij sociale feedback in het algemeen of specifiek sociale acceptatie en afwijzing. Om dit goed te onderzoeken heb ik een nieuw experimenteel paradigma ontwikkeld, de Social Network Aggression Task (SNAT), zie figuur 2. Voorafgaand aan het bezoek vullen de deelnemers een persoonlijk profiel in, waarin ze vragen beantwoorden zoals *"Wat is je favoriete film?"* of *"Wat is je grootste wens"*. Tijdens de MRI-scan zien ze vervolgens feedback van onbekende leeftijdsgenoten op dat persoonlijk profiel. Naast positieve en negatieve feedback bevat de SNAT ook een neutrale feedback conditie. Dit vernieuwende aspect zorgt ervoor dat ik specifiek kon onderzoeken

welke gebieden er meer actief waren na positieve feedback (positief versus negatief), welke gebieden meer actief waren na negatieve feedback (negatief versus positief) en welke gebieden zowel bij positieve en negatieve feedback actief waren (positief en negatief versus neutrale feedback). Het is erg belangrijk om dit onderscheid te kunnen maken, zodat we meer inzicht kunnen krijgen in de brein processen die specifiek zijn voor bijvoorbeeld negatieve sociale feedback of buitensluiting. Buitensluiting wordt namelijk vaak gerelateerd aan negatieve gevolgen zoals depressie of agressie.

Afwijzing en Agressie

Bij sommige mensen leidt negatieve feedback of buitensluiting tot boosheid en frustratie, wat kan resulteren in reactieve agressie (ofwel *"wraak nemen")* (Twenge et al., 2001, Dodge et al., 2003; Leary et al., 2006; Nesdale and Lambert, 2007, Nesdale and Duffy, 2011; Chester et al., 2014). Reactieve agressie na sociale afwijzing is experimenteel onderzocht door deelnemers de mogelijkheid te geven om een hard geluid te blazen in de oren van de leeftijdgenoot die zojuist feedback had gegeven (Bushman and Baumeister, 1998; Twenge et al., 2001; Reijntjes et al., 2010). De deelnemers mogen daarbij zelf de intensiteit en duur van de geluidsexplosie bepalen. Dit soort studies hebben aangetoond dat deelnemers die werden buitengesloten of afgewezen aanzienlijk agressiever reageren dan deelnemers die werden geaccepteerd (Twenge et al., 2001; Leary et al., 2006; Reintjes et al., 2010; DeWall and Bushman, 2011; Chester et al., 2014; Riva et al., 2015).

Dat sociale afwijzing kan leiden tot agressief gedrag is waarschijnlijk gerelateerd aan een gebrek aan impulscontrole of inadequate emotie regulatie (Chester et al., 2014; Riva et al., 2015). Wetenschappelijk onderzoek met volwassen deelnemers heeft bijvoorbeeld aangetoond dat de mate van agressie na sociale afwijzing te maken had met de executieve functies van deelnemers. Onder executieve functies worden de hogere controlefuncties van de hersenen verstaan. Ze besturen het handelen en gedrag, helpen bij het stellen van doelen en het verwerkelijken daarvan. Deelnemers met betere executieve functies bleken hun agressie beter te kunnen beheersen dan deelnemers met minder goede executieve functies (Chester et al., 2014). Deze vorm van zelfcontrole is mogelijk afhankelijk van top-down controle van de dorsolaterale prefrontale cortex (DLPFC, zie Figuur 1) over subcorticale-limbische hersengebieden (zoals de VS) (Casey, 2015). Verschillende studies in volwassenen lieten inderdaad een relatie zien tussen brein activatie in de DLPFC en agressie regulatie (Riva et al., 2015, Chester and DeWall, 2016; Peper et al., 2015).



Figuur 2. *Social network aggression task (SNAT), een nieuw ontwikkeld experimenteel paradigma om sociale feedback verwerking te onderzoeken. Deelnemers ontvangen positieve, neutrale, of negatieve feedback van onbekende leeftijdgenoten. Vervolgens krijgt de deelnemer de mogelijkheid om een hard geluid in het oor van de leeftijdgenoot te blazen, als een index van reactieve agressie. De gezichten in dit figuur zijn getekende benaderingen van de foto stimuli uit Achterberg et al., 2016.*

Deze studies suggereren dat de DLPFC wellicht dient als regulatiemechanisme voor agressie ten gevolge van sociale afwijzing. Er zijn echter maar weinig studies die agressie na sociale afwijzing hebben onderzocht in kinderen, ondanks dat kinderen al vanaf jongs af aan te maken hebben met sociale acceptatie en afwijzing. Aangezien de prefrontale cortex en executief functioneren nog volop in ontwikkeling zijn tijdens de kindertijd zijn kinderen wellicht nog vatbaarder om agressief te reageren na sociale afwijzing, aangezien het voor deze leeftijdsgroep extra moeilijk is om sociale emoties te reguleren. Om agressie regulatie na sociale afwijzing goed te kunnen onderzoeken in kinderen is er een gedragscomponent toegevoegd aan het SNAT-paradigma (figuur 2). Nadat de deelnemers de sociale feedback van leeftijdgenoten zagen kregen zij de mogelijkheid om de deelnemer een hard geluid in de oren te blazen. De mate van deze geluidsexplosie heb ik vervolgens gebruikt als mate van reactieve agressie. Door het bestuderen van individuele verschillen in agressieregulatie kunnen we meer inzicht krijgen in waarom sommige kinderen gevoeliger zijn voor sociale afwijzing dan andere kinderen. Doordat we het innovatieve paradigma combineren met fMRI kunnen we daarnaast ook inzichten vergaren in de brein mechanisme die ten grondslag liggen aan sociale emotie regulatie.

Het sociale brein in ontwikkeling

Eerdere fMRI studies naar de verwerking van sociale feedback in volwassenen en adolescenten hebben aangetoond dat een netwerk van ACC-AI, samen met subcorticale hersengebieden zoals de VS betrokken zijn bij de directe effecten van sociale acceptatie en sociale afwijzing. Wat betreft het beheersen van sociale afwijzing gerelateerde agressie lijkt de DLPFC een belangrijke rol te spelen. Juist deze netwerken staan centraal in neurologische modellen van sociale emotie regulatie, zoals het *"Sociaal Informatie Verwerkingsnetwerk"* (SIPN - Social information processing network, Nelson et al., 2016; Nelson et al., 2005) en het *"Disbalans model"* (Imbalance model, Casey et al., 2008; Somerville et al., 2010). Het SIPN-model stelt dat doelgericht gedrag afhankelijk is van interacties tussen verschillende gebieden binnen de prefrontale cortex, die sociaal-emotionele informatie uit de subcorticale hersengebieden verwerken (Nelson et al., 2005). Aanvullend beschrijft het disbalans-model (Casey et al., 2008; Somerville et al., 2010) de mis match in ontwikkelingstrajecten van subcorticale hersengebieden en de prefrontale cortex. De relatief snelle ontwikkeling van affectieve subcorticale hersengebieden en de langzamere geleidelijke ontwikkelende controlegebieden in de prefrontale cortex zorgen voor een disbalans die het grootst is gedurende adolescentie.

Eerdere studies en theoretische modellen hebben daarnaast aangetoond dat sociale emotieregulatie niet alleen afhankelijk is van geïsoleerde hersengebieden, maar afhankelijk is van een netwerk van geïntegreerde verbindingen tussen subcorticale en corticale (prefrontale) hersengebieden (Chester et al., 2014; de Water, Cillessen, & Scheres, 2014; Olson et al., 2009; Peper et al., 2015; Silvers et al., 2016; van Duijvenvoorde, Achterberg, Braams, Peters, & Crone, 2016). De meeste van deze onderzoeken waren echter gericht op de adolescentie. Sommige van deze studies omvatten ook kinderen jonger dan tien jaar, maar de steekproefgroottes waren vaak erg klein. Het blijft daarom de vraag of deze geïntegreerde subcorticale-corticale hersennetwerken al aanwezig zijn tijdens de kindertijd. Weinig MRI studies hebben de ontwikkeling van sociale emotie regulatie tijdens de kindertijd onderzocht, ondanks wetenschappelijk studies die aantonen dat in de kindertijd de snelste veranderingen in executieve functies plaatsvinden (Luna, Garver, Urban, Lazar, & Sweeney, 2004; Peters, Van Duijvenvoorde , Koolschijn, & Crone, 2016; Zelazo & Carlson, 2012).

Een mogelijke oorzaak voor het kleine aantal experimentele MRI-studies in de kindertijd is dat het scannen van kinderen een grote uitdaging kan zijn: de MRI-scanner is behoorlijk imposant en kan spanning veroorzaken bij kinderen (Durston et al., 2009; Tyc, Fairclough, Fletcher, Leigh, & Mulhern, 1995). Door dergelijke spanning is het minder waarschijnlijk dat kinderen een MRI-scan succesvol afronden, wat resulteert in een lagere scankwantiteit en kwaliteit bij

kinderen in vergelijking met oudere deelnemers (Poldrack, Pare-Blagoev, & Grant, 2002; Satterthwaite et al., 2013). Om individuele verschillen te onderzoeken (waarom zijn sommige kinderen gevoeliger voor sociale evaluatie dan anderen), zijn grote aantallen proefpersonen nodig. We hebben niet alleen grote aantallen proefpersonen nodig om interpersoonlijke (tussen personen) verschillen in sociaal gedrag te onderzoeken, er zijn meerdere metingen van diezelfde grote steekproef nodig om intra-individuele (binnen personen) verschillen in ontwikkeling vast te leggen (Telzer et al., 2018). Dat wil zeggen, om echt ontwikkeling vast te leggen, hebben we longitudinaal onderzoek nodig (Pfeifer et al., 2018).

Samen Uniek Tweelingonderzoek

Met al deze factoren is rekening gehouden bij het opzetten van de longitudinale tweelingstudie *"Samen Uniek"*, onderdeel van het Leids Consortium on Individual Development (L-CID). De L-CID-studie bestaat uit twee cohorten (vroege kindertijd en late kindertijd) die gedurende zes constructieve jaren worden gevolgd, met jaarlijkse bezoeken aan huis of aan de universiteit (Euser et al., 2016). Dit longitudinale onderzoek geeft dus de mogelijkheid om individuele verschillen tussen personen en binnen personen te onderzoeken. Een ander bijzonder aspect van het *"Samen Uniek"* onderzoek is dat alle deelnemers tweeling zijn. Dit geeft ons de mogelijkheid om niet alleen de brein processen te onderzoeken, maar ook de erfelijkheid van deze processen. Zowel eeneiige als twee-eiige tweelingen groeien op in dezelfde omgeving (dezelfde ouders, hetzelfde huis, zelfs dezelfde verjaardag). Eeneiige tweelingen hebben daarnaast ook hetzelfde erfelijke materiaal, ze zijn als het ware genetische kopieën. Twee-eiige tweelingen daarentegen lijken genetisch gezien net zoveel op elkaar als gewone broers en zussen. Stel dat brein activatie tussen eeneiige tweelingen meer op elkaar lijkt dan tussen twee-eiige tweelingen, dan duidt dat op een erfelijke component. Dit soort gedrag-genetische analyses heb ik in verschillende hoofdstukken van mijn proefschrift toegepast.

Het merendeel van de onderzoeken in het huidige proefschrift zijn gebaseerd op data uit het late kindertijd cohort. Dit cohort omvatte 512 kinderen (256 gezinnen) tussen de leeftijd van 7 en 9 op tijdstip 1 (gemiddelde leeftijd: 7,94 ± 0,67; 49% jongens, 55% eeneiige tweeling). Deze grote steekproefomvang biedt voldoende statistische zekerheid om de ontwikkeling van de hersenen bij kinderen te onderzoeken, rekening houdend met het feit dat het percentage kwalitatieve MRI data lager ligt in kinderen dan in volwassenen (O'Shaughnessy, Berl, Moore, & Gaillard, 2008).

Studies binnen dit proefschrift

Binnen dit proefschrift bespreek ik de resultaten van zeven empirische MRI-studies. In **hoofdstuk 2** testte ik het SNAT-paradigma in drie afzonderlijke steekproeven van 7-11-jarige kinderen en vervolgens combineerde ik de resultaten door middel van een meta-analyse. In alle drie de groepen resulteerde negatieve sociale feedback in de hardste geluidsexplosie, dus de meeste agressie. De brein analyses in de losse groepen lieten geen duidelijke effecten zien, mogelijk omdat de groepen te klein waren (<30 proefpersonen). Een meta-analyse over verschillende breingebieden liet echter zien dat negatieve feedback resulteerde in meer brein activatie in de amygdala, AI en MPFC/ACC. Deze resultaten lieten zien dat sociale motivaties al van groot belang zijn bij 7-9 jaar oude kinderen en dat het SNAT-paradigma een valide paradigma is om sociale emotie regulatie te onderzoeken bij kinderen. Vervolgens heb ik in **hoofdstuk 3** de brein processen van sociale feedback verwerking bij volwassenen onderzocht. Ook hier vond ik dat negatieve feedback resulteerde in de hoogste mate van agressie. Brein analyses lieten zien dat de AI en MPFC/ACC meer actief werden na zowel positieve en negatieve sociale feedback, wat suggereert dat ze belangrijk zijn voor sociale feedback in het algemeen en niet specifiek voor sociale afwijzing. Daarnaast rapporteerde ik een link tussen brein activatie en gedrag: meer activatie in de DLPFC was gerelateerd aan minder agressie na sociale afwijzing. Dit wijst erop dat de DLPFC als een emotie regulatiemechanisme werkt in het brein.

Na validering van het experimentele paradigma bij kinderen en volwassenen, was de volgende stap om te onderzoeken in hoeverre individuele variatie in sociale evaluatie werd verklaard door genetica en omgevingsinvloeden. Om dit te onderzoeken heb ik in **hoofdstuk 4** gedrags-genetische analyses uitgevoerd op brein activatie tijdens sociale feedback verwerking. Hieruit bleek dat agressie na sociale afwijzing werd beïnvloed door zowel genetische- als omgevingsinvloeden. In het brein vonden we vergelijkbare resultaten als bij de volwassenen, mogelijk omdat we in deze studie veel meer kinderen includeerde (meer dan 350) dan in de studie in hoofdstuk 2. De gedrags-genetische analyses op hersenactivatie lieten zien dat ongeveer 15% van de variatie in brein activatie in de DLPFC verklaard werd door genetica (de activatie was tussen eeneiige tweelingen meer vergelijkbaar dan tussen twee-eiige tweelingen). Deze resultaten laten zien dat het verwerken van sociale feedback en het reguleren van emoties in de kindertijd wordt beïnvloed door zowel genetica als de omgeving.

Een belangrijke vervolgvraag is dan natuurlijk: *hoe ontwikkelen deze breinprocessen zich gedurende de kindertijd*? In **hoofdstuk 5** heb ik daarom individuele verschillen in longitudinale veranderingen van agressie regulatie in de kindertijd onderzocht. Daarbij vond ik dat agressie na sociale feedback

afneemt tussen de midden-kindertijd (7-8 jaar) en late kindertijd (9-11 jaar). Brein activatie in de AI, IFG, MPFC en DLPFC nam gedurende deze tijd juist toe. Daarnaast rapporteerde ik een link tussen brein activatie en gedrag die vergelijkbaar was met wat we eerder vonden in volwassenen. Meer brein activatie in de DLPFC tijdens de late kindertijd was gerelateerd aan minder agressie na sociale afwijzing. Dit verband was minder duidelijk in de midden kindertijd, wat duidt op een belangrijke ontwikkeling tijdens deze tijdsspanne. Dat juist de groei in DLPFC-activatie belangrijk was bleek ook uit de longitudinale analyse, waarin de toename in DLPFC-activatie gerelateerd was aan de afname in agressie. Met andere woorden, kinderen waarbij de DLPFC sneller ontwikkelde lieten ook een snellere ontwikkeling in sociale emotie regulatie zien.

De eerste vier studies binnen dit proefschrift richten zich op brein activatie in verschillende gebieden en hoe deze gerelateerd zijn aan sociale emotie regulatie. Echter werkt het brein niet als losse eilandjes, maar als een groot aaneengesloten netwerk. Aangezien eerdere onderzoeken vaak oudere deelnemers gebruikten of slechts een klein aantal kinderen bevatten is het tot op heden de vraag of functionele connecties tussen subcorticale en corticale hersengebieden al tijdens de kindertijd ontwikkelen of pas gedurende de adolescentie. Aangezien L-CID een groot en statistisch sterke steekproef omvat was ik in staat om functionele hersenconnectiviteit te onderzoeken in de kindertijd. In **hoofdstuk 6** heb ik de erfelijkheid van functionele hersenconnecties tussen subcorticale gebieden de prefrontale cortex onderzocht. Uit de analyses bleek dat er robuuste en repliceerbare hersenconnectiviteit was tussen de prefrontale cortex en de VS en amygdala. Over het algemeen lieten de connecties tussen de PFC-VS en PFC – amygdala verschillende genetische invloeden zien: VS-connecties werden vooral beïnvloed door genetica, maar amygdala connecties vooral door omgeving. Er waren ook wat overeenkomsten: zowel connecties van de VS als de amygdala en de ventrale ACC werden voornamelijk beïnvloed door gedeelde omgeving, terwijl connecties tussen de VS, amygdala en OFC voornamelijk erfelijk waren. Deze bevindingen kunnen inzicht bieden bij het opzetten van interventies naar sociale emotie regulatie, door te laten zien dat zowel genetische invloeden als omgeving (bijvoorbeeld opvoeding) van belang zijn bij de ontwikkeling van functionele hersenconnectiviteit.

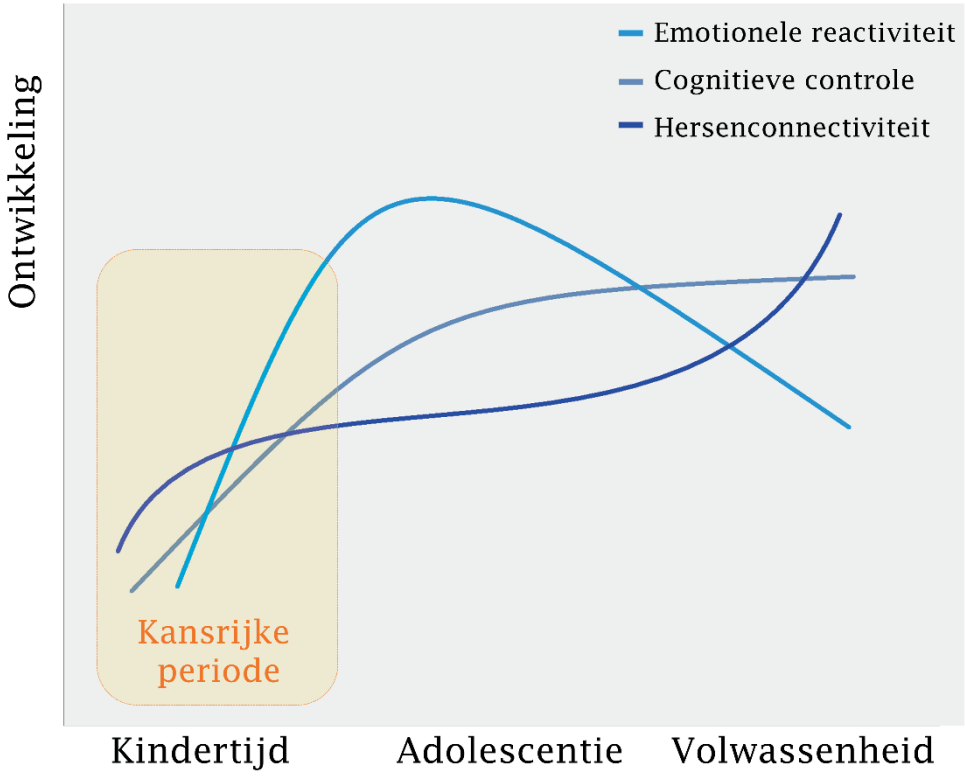
De resultaten uit hoofdstuk 2, 4, 5 en 6 gaven niet alleen inzicht in de breinprocessen bij kinderen, ze brachten me ook veel kennis en ervaring bij het doen van MRI-onderzoek bij kinderen. In **hoofdstuk 7** geef ik een uitgebreid overzicht van valkuilen en mogelijkheden van MRI-onderzoek bij jonge kinderen. Hierbij heb ik gekeken naar de relatie tussen spanning of angst voor de MRI-scan en de uiteindelijke kwantiteit en kwaliteit van de scan. We vroegen op 3 momenten gedurende het lab bezoek hoeveel spanning de kinderen ervaarden. Gedurende het bezoek nam de spanning steeds meer af en gaven kinderen aan het steeds leuker te vinden. Verder bleek dat de hoeveelheid spanning die door

de kinderen wordt ervaren samenhangt met hoeveel scans ze voltooien, maar niet met de kwaliteit van die scans. De gedrags-genetische analyses lieten verder zien dat de hoofdbeweging tijdens de scans (de hoofdreden van verminderde kwaliteit in scans) sterk genetisch bepaald was. Echter, als we controleerde voor extreme hoofdbeweging en alleen naar subtiele beweging keken verdween dit effect. Buitenproportionele hoofdbeweging is dus erfelijk, maar goed-gecontroleerde hoofdbeweging binnen MRI-scans wordt niet beïnvloed door genetische factoren. Deze bevindingen zijn zeer relevant voor de ontwikkelingsneurowetenschap, omdat we hiermee beter onderzoek kunnen doen naar hersenontwikkeling bij (jonge) kinderen.

Het uiteindelijke doel van de ontwikkelingsneurowetenschappen is om de ontwikkeling van de hersenen vanaf de kindertijd tot de volwassen leeftijd te onderzoeken en neurale ontwikkeling te relateren aan gedragsuitkomsten. In **hoofdstuk 8** heb ik de ontwikkeling van structurele subcorticale PFC-connectiviteit onderzocht in kinderen, adolescenten en volwassenen. Daarbij heb ik specifiek gekeken of de groei van deze connecties gedurende de ontwikkeling voorspellend was voor gedragscontrole. Allereerst vonden we dat kinderen naarmate ze ouder werden steeds beter hun gedrag konden controleren en het geduldigst waren in de late adolescentie. Structurele hersenconnectiviteit tussen de striatum en de PFC liet de sterkste groei zien tijdens de late kindertijd en vroege adolescentie. De sterkte van deze connecties was daarnaast voorspellend voor gedragscontrole. Dit duidt erop dat hersenontwikkeling voorafgaat aan gedragsuitkomsten en dat subcorticale- prefrontale connecties belangrijk zijn in de ontwikkeling van gedragscontrole.

De kansrijke kindertijd

De studies die in dit proefschrift worden beschreven hebben verschillende belangrijke bevindingen opgeleverd. Ten eerste kon ik met behulp van de Social Network Agrgression Task onderscheid maken tussen brein activatie die specifiek was voor sociale afwijzing en sociale acceptatie, en activiteit die gerelateerd was aan algemene sociale signalen. Ten tweede heb ik laten zien hoe individuele verschillen in agressie regulatie gerelateerd zijn aan verschillen in brein activatie in de DLPFC. Ten derde heb ik, door bevindingen van het fMRI paradigma te combineren met functionele en structurele hersenconnectiviteit, kennis weten te verzamelen over de ontwikkeling van sociale emotie regulatie tijdens de kindertijd en daarbij laten zien dat de kindertijd een kansrijke periode is (zie figuur 3).



Figuur 3. *De kansrijke kindertijd. De grootste toename in emotionele reactiviteit, cognitieve controle en (structurele) hersenconnectiviteit vinden plaats in de late kindertijd, wat mogelijk een kansrijke periode reflecteert in termen van ontwikkeling. NB: de data verbanden in dit figuur zijn illustratief.*

Naarmate kinderen ouder worden en naar adolescenten gaan, krijgen ze over het algemeen meer autonomie en staan ze minder vaak onder toezicht van volwassenen (Steinberg, Elmen, & Mounts, 1989). Bij sommige personen leidt dit tot verhoogde risico's en het zoeken naar sensaties, wat negatieve gevolgen kan hebben, zoals lichamelijke en psychische schade (Steinberg, 2008). Om individuele verschillen in dit gedrag te begrijpen, zijn verschillende neurologische ontwikkelingsmodellen voorgesteld (voor een overzicht, zie Casey, 2015), die allemaal gericht zijn op de ontwikkeling van de hersenen van adolescenten. De longitudinale analyses bij kinderen, adolescenten en volwassenen in dit proefschrift toonden echter aan dat structurele connectiviteit tussen het striatum en de PFC voorspellend was voor gedragscontrole, wat het bewijs levert dat hersenontwikkeling toekomstige gedragscontrole kan voorspellen. Wetende dat hersenontwikkeling voorafgaat aan gedrag (Gabrieli,

Ghosh, & Whitfield-Gabrieli, 2015); wil dus eigenlijk zeggen dat de basis voor gedrag in de adolescentie gelegd wordt tijdens de kindertijd. De studies in dit proefschrift benadrukken het belang van het integreren van hersenontwikkeling bij kinderen in neurowetenschappelijke modellen door aan te tonen dat de sterkste toename in zowel gedragscontrole als subcorticale-PFC structurele connectiviteit plaatsvindt tijdens de kindertijd.

Zowel empirische studies als theoretische modellen zijn vooral gericht op een piek in hersenontwikkeling, dus waar het traject het hoogste punt behaald (Braams, van Duijvenvoorde, Peper, & Crone, 2015; Casey et al., 2008; Galvan, 2010; Peters & Crone, 2017). Hoewel dit verhelderend kan zijn, pleit ik dat de weg naar deze piek informatiever is als het gaat om ontwikkeling. De ontwikkelingsfase die de sterke toename laat zien is immers de tijd waarin de feitelijke verandering plaatsvindt. Deze fase weerspiegelt mogelijk een moment waarop het relatief eenvoudig is om in te grijpen in ontwikkeling. Metaforisch gezien, als een steentje snel van een heuvel afrolt kun je gemakkelijk de route veranderen door zachtjes tegen de steen te tikken. Hoe sneller de steen rolt, hoe groter de impact van deze kleine handeling. Wanneer de steen het einde van de heuvel heeft bereikt, heeft het tikje op de steen echter geen grote impact meer. Uit een breed scala aan onderzoeken - inclusief hoofdstukken van dit proefschrift - is gebleken dat gedurende de (late) kindertijd de grootste veranderingen plaatsvinden in emotionele reactiviteit (hoofdstuk 5; Silvers et al. (2012)), cognitieve controle (Luna et al., 2004; Peters et al., 2016) en structurele hersenconnectiviteit (hoofdstuk 8; Wierenga, van den Heuvel, et al. (2018)). Deze versnelde veranderingen in de ontwikkeling van de hersenen kunnen een kans bieden voor interventies die de loop van de ontwikkeling kunnen veranderen met relatief kleine handelingen (**figuur 3**).

Conclusie

Dit proefschrift geeft een uitgebreid overzicht van de onderliggende mechanismen van sociale emotieregulatie in de kindertijd. De studies tonen aan dat onze hersenen geneigd zijn om te signaleren voor sociaal-relevante informatie, ongeacht de valentie. Dit netwerk van "sociaal signaleren" is al in de kindertijd aanwezig, wat aangeeft dat dit een belangrijk sociaal kern mechanisme kan zijn. De resultaten in dit proefschrift laten bovendien zien dat sociale afwijzing vaak wordt gevolgd door reactieve agressie en dat het beheersen van deze emoties verband houdt met controlemechanismen van de DLPFC. De resultaten zijn in lijn met eerdere neurologische modellen, die het belang benadrukken van top-down controle van prefrontale hersengebieden over bottom-up verwerking van subcorticale hersengebieden. Als aanvulling op deze modellen tonen mijn resultaten aan dat de basis voor de functionele en structurele architectuur van subcorticale prefrontale hersenconnectiviteit al zichtbaar is tijdens de kindertijd en dat ontwikkeling binnen deze netwerken belangrijk is voor sociale emotieregulatie. Neurowetenschappelijk onderzoek bij (jonge) kinderen brengt uitdagingen met zich mee en er moet dan ook rekening worden gehouden met verschillende methodologische overwegingen bij het bestuderen van de hersenen van kinderen. Ondanks deze moeilijkheden kan het bestuderen van de hersenontwikkeling bij kinderen belangrijke inzichten bieden in een unieke en kansrijke ontwikkelingsperiode.

ACKNOWLEDGMENTS

Dankwoord

Dit proefschrift had niet tot stand kunnen komen zonder de steun van vele mensen. De waardevolle contributies van mijn **coauteurs** staan genoemd op pagina 23. Tevens wil ik mijn (huidige en voorgaande) **collega's** van het Brain and Development Research Center bedanken voor de inspirerende en gezellige momenten.

Ik ben bijzonder dankbaar voor de enthousiaste inzet van alle **deelnemende gezinnen** binnen het Samen Uniek tweelingonderzoek. Het verzamelen van al deze data zou onmogelijk zijn zonder de buitenproportionele inzet van het (huidige en voorgaande) **L-CID onderzoeksteam**, hulde en bedankt!

Daarnaast is er een aantal mensen die ik in het bijzonder wil bedanken:

Allereerst **Mara**, wat was het fijn om alles met jou te kunnen delen. Ik bewonder je als wetenschapper en vriendin en heb respect voor jouw doorzettingsvermogen.

Anna, bedankt voor al je adviezen, zowel wetenschappelijk als persoonlijk. Je weet mij altijd enorm te inspireren.

Eveline, ik beschouw het als een voorrecht om met jou te mogen werken. Keer op keer weet je mij te motiveren om mijn passie te volgen. Ik kan mij geen betere mentor wensen en ben dankbaar voor alle kansen die je mij geeft.

Nim, thank you for your hospitality in welcoming me to your lab at Columbia University. My stay in New York City has taught me lots about developmental neuroscience and international collaborations.

Bianca, **Saskia**, en **Lara**, bedankt voor jullie steun en geduld. Ik ben trots en blij dat we een doorstart hebben gemaakt met het onderzoek en kijk uit naar de komende jaren van samenwerking.

Jorien, bedankt voor je opbeurende woorden, waardering en fijne koffie momenten.

Mijn beste vriendinnetjes **Marloes**, **Marcella, Yvonne** en **Miranda**: Bedankt voor jullie decennialange vriendschap. Het gevoel van trots dat jullie uitstralen is er één die alleen mijn eigen moeder zou kunnen evenaren.

Mijn lieve familie - in het bijzonder **Kevin**, **papa**, **Jacques** en **Anky** - bedankt voor jullie steun, interesse en onvoorwaardelijke liefde.

Oma, **Trix**, **Hanneke** en wooncentrum **de Wulverhorst**: jullie liefdevolle zorg voor mama geeft mij de ruimte om mijn dromen te volgen, zeer veel dank daarvoor.

Liefste **Arjen**, tranen van geluk, ellende en frustratie: Ze vielen allemaal op jouw schouders. Bedankt voor je grenzeloze liefde en je onuitputtelijke geduld. Jij bent mijn rots, mijn haven, mijn thuis: Ik hou van je.

Tien jaar ontwikkelingspsychologie valt in het niet met wat ik elke dag van mijn zoon leer, bedankt lieve **Dex**. Voor jouw liefde leef ik.

REFERENCES

Referenties

A

Achterberg, M., Bakermans-Kranenburg, M. J., van Ijzendoorn, M. H., van der Meulen, M., Tottenham, N. & Crone, E. A. (2018a) 'Distinctive heritability patterns of subcortical-prefrontal cortex resting state connectivity in childhood: A twin study', Neuroimage.

Achterberg, M., Peper, J. S., van Duijvenvoorde, A. C., Mandl, R. C. & Crone, E. A. (2016a) 'Frontostriatal White Matter Integrity Predicts Development of Delay of Gratification: A Longitudinal Study', J Neurosci, 36(6), pp. 1954-1961.

Achterberg, M. & van der Meulen, M. (2019) 'Genetic and environmental influences on MRI scan quantity and quality', Dev Cogn Neurosci, 38, p. 100667.

Achterberg, M., van Duijvenvoorde, A. C., Bakermans-Kranenburg, M. J. & Crone, E. A. (2016b) 'Control your anger! The neural basis of aggression regulation in response to negative social feedback', Soc Cogn Affect Neurosci, 11(5), pp. 712-720.

Achterberg, M., van Duijvenvoorde, A. C. K., van der Meulen, M., Bakermans-Kranenburg, M. J. & Crone, E. A. (2018b) 'Heritability of aggression following social evaluation in middle childhood: An fMRI study', Hum Brain Mapp, 39(7), pp. 2828-2841.

Achterberg, M., van Duijvenvoorde, A. C. K., van der Meulen, M., Euser, S., Bakermans-Kranenburg, M. J. & Crone, E. A. (2017) 'The neural and behavioral correlates of social evaluation in childhood', Dev Cogn Neurosci, 24, pp. 107-117.

Adolphs, R. (2009) 'The social brain: neural basis of social knowledge', Annu Rev Psychol, 60, pp. 693-716.

Akaike, H. (1974) 'New Look at Statistical-Model Identification', Ieee Transactions on Automatic Control, Ac19(6), pp. 716-723.

Andersson, J. L. & Skare, S. (2002) 'A model-based method for retrospective correction of geometric distortions in diffusion-weighted EPI', Neuroimage, 16(1), pp. 177-199.

Andersson, J. L., Skare, S. & Ashburner, J. (2003) 'How to correct susceptibility distortions in spin-echo echo-planar images: application to diffusion tensor imaging', Neuroimage, 20(2), pp. 870-888.

Andrew, T., Hart, D. J., Snieder, H., de Lange, M., Spector, T. D. & MacGregor, A. J. (2001) 'Are twins and singletons comparable? A study of disease-related and lifestyle characteristics in adult women', Twin Res, 4(6), pp. 464-477.

Anokhin, A. P., Golosheykin, S., Grant, J. D. & Heath, A. C. (2011) 'Heritability of delay discounting in adolescence: a longitudinal twin study', Behav Genet, 41(2), pp. 175-183.

Apps, M. A., Rushworth, M. F. & Chang, S. W. (2016) 'The Anterior Cingulate Gyrus and Social Cognition: Tracking the Motivation of Others', Neuron, 90(4), pp. 692-707.

Audrain-McGovern, J., Rodriguez, D., Epstein, L. H., Cuevas, J., Rodgers, K. & Wileyto, E. P. (2009) 'Does delay discounting play an etiological role in smoking or is it a consequence of smoking?', Drug Alcohol Depend, 103(3), pp. 99-106.

B

Bakermans-Kranenburg, M. J. & van Ijzendoorn, M. H. (2007) 'Research Review: genetic vulnerability or differential susceptibility in child development: the case of attachment', J Child Psychol Psychiatry, 48(12), pp. 1160-1173.

Bakermans-Kranenburg, M. J., Van, I. M. H., Pijlman, F. T., Mesman, J. & Juffer, F. (2008) 'Experimental evidence for differential susceptibility: dopamine D4 receptor polymorphism (DRD4 VNTR) moderates intervention effects on toddlers' externalizing behavior in a randomized controlled trial', Dev Psychol, 44(1), pp. 293-300.

Ball, T., Rahm, B., Eickhoff, S. B., Schulze-Bonhage, A., Speck, O. & Mutschler, I. (2007) 'Response Properties of Human Amygdala Subregions: Evidence Based on Functional MRI Combined with Probabilistic Anatomical Maps', PLoS One, 2(3).

Barch, D., Pagliaccio, D., Belden, A., Harms, M. P., Gaffrey, M., Sylvester, C. M., Tillman, R. & Luby, J. (2016) 'Effect of Hippocampal and Amygdala Connectivity on the Relationship Between Preschool Poverty and School-Age Depression', American Journal of Psychiatry, 173(6), pp. 625-634.

Barnes, K. A., Cohen, A. L., Power, J. D., Nelson, S. M., Dosenbach, Y. B., Miezin, F. M., Petersen, S. E. & Schlaggar, B. L. (2010) 'Identifying Basal Ganglia divisions in individuals using resting-state functional connectivity MRI', Front Syst Neurosci, 4, p. 18.

Basser, P. J. & Pierpaoli, C. (1996) 'Microstructural and physiological features of tissues elucidated by quantitative-diffusion-tensor MRI', J Magn Reson B, 111(3), pp. 209-219.

Bates, D., Machler, M., Bolker, B. M. & Walker, S. C. (2015) 'Fitting Linear Mixed-Effects Models Using lme4', Journal of Statistical Software, 67(1), pp. 1-48.

Baumeister, R. F. & Leary, M. R. (1995) 'The need to belong: desire for interpersonal attachments as a fundamental human motivation', Psychol Bull, 117(3), pp. 497-529.

Bava, S., Boucquey, V., Goldenberg, D., Thayer, R. E., Ward, M., Jacobus, J. & Tapert, S. F. (2011) 'Sex differences in adolescent white matter architecture', Brain Res, 1375, pp. 41-48.

Bava, S., Thayer, R., Jacobus, J., Ward, M., Jernigan, T. L. & Tapert, S. F. (2010) 'Longitudinal characterization of white matter maturation during adolescence', Brain Res, 1327, pp. 38-46.

Berndt, T. J. (2004) 'Children's friendships: Shifts over a half-century in perspectives on their development and their effects', Merrill-Palmer Quarterly-Journal of Developmental Psychology, 50(3), pp. 206-223.

Bickel, W. K., Pitcock, J. A., Yi, R. & Angtuaco, E. J. (2009) 'Congruence of BOLD response across intertemporal choice conditions: fictive and real money gains and losses', J Neurosci, 29(27), pp. 8839-8846.

Birn, R. M., Diamond, J. B., Smith, M. A. & Bandettini, P. A. (2006) 'Separating respiratory-variation-related neuronal-activity-related fluctuations in fluctuations from fMRI', Neuroimage, 31(4), pp. 1536-1548.

Blackwell, D., Leaman, C., Tramposch, R., Osborne, C. & Liss, M. (2017) 'Extraversion, neuroticism, attachment style and fear of missing out as predictors of social media use and addiction', Pers Individ Dif, 116, pp. 69-72.

Blakemore, S. J. (2008) 'The social brain in adolescence', Nat Rev Neurosci, 9(4), pp. 267-277.

Blokland, G. A., McMahon, K. L., Thompson, P. M., Martin, N. G., de Zubicaray, G. I. & Wright, M. J. (2011) 'Heritability of working memory brain activation', J Neurosci, 31(30), pp. 10882-10890.

Boecker, R., Holz, N. E., Buchmann, A. F., Blomeyer, D., Plichta, M. M., Wolf, I., Baumeister, S., Meyer-Lindenberg, A., Banaschewski, T., Brandeis, D. & Laucht, M. (2014) 'Impact of early life adversity on reward processing in young adults: EEG-fMRI results from a prospective study over 25 years', PLoS One, 9(8), p. e104185.

Borenstein, M., Rothstein, D. & Cohen, J. (2005) Comprehensive meta-analysis: A computer program for research synthesis, NJ: Biostat.

Bos, M. G. N., Wierenga, L. M., Blankenstein, N. E., Schreuders, E., Tamnes, C. K. & Crone, E. A. (2018) 'Longitudinal structural brain development and externalizing behavior in adolescence', J Child Psychol Psychiatry, 59(10), pp. 1061-1072.

Bouchard, T. J., Jr. & McGue, M. (2003) 'Genetic and environmental influences on human psychological differences', J Neurobiol, 54(1), pp. 4-45.

Braams, B. R., Guroglu, B., de Water, E., Meuwese, R., Koolschijn, P. C., Peper, J. S. & Crone, E. A. (2014a) 'Reward-related neural responses are dependent on the beneficiary', Soc Cogn Affect Neurosci, 9(7), pp. 1030-1037.

Braams, B. R., Peters, S., Peper, J. S., Guroglu, B. & Crone, E. A. (2014b) 'Gambling for self, friends, and antagonists: differential contributions of affective and social brain regions on adolescent reward processing', Neuroimage, 100, pp. 281-289.

Braams, B. R., van Duijvenvoorde, A. C., Peper, J. S. & Crone, E. A. (2015) 'Longitudinal changes in adolescent risk-taking: a comprehensive study of neural responses to rewards, pubertal development, and risk-taking behavior', J Neurosci, 35(18), pp. 7226-7238.

Branje, S. J. T., van Lieshout, C. F. M., van Aken, M. A. G. & Haselager, G. J. T. (2004) 'Perceived support in sibling relationships and adolescent adjustment', Journal of Child Psychology and Psychiatry, 45(8), pp. 1385-1396.

Brett, M., Anton, J. L., Valabregue, R. & Poline, J. B. (2002) 'Region of interest analysis using an SPM toolbox [abstract] Presented at the 8th International Conference on Functional Mapping of the Human Brain, June 2-6', Available on CD-ROM in NeuroImage, 16(2).

Brothers, L. (1990) 'The social brain: a project for integrating primate behavior and neurophysiology in a new domain. ', Concepts Neurosci., 1,, pp. 27–51.

Buckner, R. L., Krienen, F. M., Castellanos, A., Diaz, J. C. & Yeo, B. T. (2011) 'The organization of the human cerebellum estimated by intrinsic functional connectivity', J Neurophysiol, 106(5), pp. 2322-2345.

Bunge, S. A. & Zelazo, P. D. (2006) 'A brain-based account of the development of rule use in childhood', Current Directions in Psychological Science, 15(3), pp. 118-121.

Bushman, B. J. (2002) 'Does venting anger feed or extinguish the flame? Catharsis, rumination, distraction, anger, and aggressive responding', Personality and Social Psychology Bulletin, 28(6), pp. 724-731.

Bushman, B. J. & Baumeister, R. F. (1998) 'Threatened egotism, narcissism, self-esteem, and direct and displaced aggression: does self-love or self-hate lead to violence?', J Pers Soc Psychol, 75(1), pp. 219-229.

Button, K. S., Ioannidis, J. P., Mokrysz, C., Nosek, B. A., Flint, J., Robinson, E. S. & Munafo, M. R. (2013) 'Power failure: why small sample size undermines the reliability of neuroscience', Nat Rev Neurosci, 14(5), pp. 365-376.

C

Caballero-Gaudes, C. & Reynolds, R. C. (2017) 'Methods for cleaning the BOLD fMRI signal', Neuroimage, 154, pp. 128-149.

Cacioppo, S., Frum, C., Asp, E., Weiss, R. M., Lewis, J. W. & Cacioppo, J. T. (2013) 'A Quantitative Meta-Analysis of Functional Imaging Studies of Social Rejection', Sci Rep, 3.

Casement, M. D., Guyer, A. E., Hipwell, A. E., McAloon, R. L., Hoffmann, A. M., Keenan, K. E. & Forbes, E. E. (2014) 'Girls' challenging social experiences in early adolescence predict neural response to rewards and depressive symptoms', Dev Cogn Neurosci, 8, pp. 18-27.

Casey, B. J. (2015) 'Beyond Simple Models of Self-Control to Circuit-Based Accounts of Adolescent Behavior', Annual Review of Psychology, Vol 66, 66, pp. 295-319.

Casey, B. J., Jones, R. M. & Hare, T. A. (2008) 'The adolescent brain', Ann N Y Acad Sci, 1124, pp. 111-126.

Casey, B. J., Somerville, L. H., Gotlib, I. H., Ayduk, O., Franklin, N. T., Askren, M. K., Jonides, J., Berman, M. G., Wilson, N. L., Teslovich, T., Glover, G., Zayas, V., Mischel, W. & Shoda, Y. (2011) 'Behavioral and neural correlates of delay of gratification 40 years later', Proc Natl Acad Sci U S A, 108(36), pp. 14998-15003.

Centeno, M., Tierney, T. M., Perani, S., Shamshiri, E. A., StPier, K., Wilkinson, C., Konn, D., Banks, T., Vulliemoz, S., Lemieux, L., Pressler, R. M., Clark, C. A., Cross, J. H. & Carmichael, D. W. (2016) 'Optimising EEG-fMRI for Localisation of Focal Epilepsy in Children', PLoS One, 11(2), p. e0149048.

Chai, X. Q. J., Ofen, N., Gabrieli, J. D. E. & Whitfield-Gabrieli, S. (2014) 'Selective Development of Anticorrelated Networks in the Intrinsic Functional Organization of the Human Brain', J Cogn Neurosci, 26(3), pp. 501-513.

Chang, L. C., Jones, D. K. & Pierpaoli, C. (2005) 'RESTORE: robust estimation of tensors by outlier rejection', Magn Reson Med, 53(5), pp. 1088-1095.

Chang, L. C., Walker, L. & Pierpaoli, C. (2012) 'Informed RESTORE: A method for robust estimation of diffusion tensor from low redundancy datasets in the presence of physiological noise artifacts', Magn Reson Med, 68(5), pp. 1654-1663.

Cheng, T. W., Vijayakumar, N., Flournoy, J. C., Op de Macks, Z., Peake, S. J., Flannery, J. E., Mobasser, A., Alberti, S. L., Fisher, P. A. & Pfeifer, J. H. (2019) 'Feeling left out or just surprised? Neural correlates of social exclusion and over-inclusion in adolescence', bioRxiv, p. 524934.

Chester, D. S. & DeWall, C. N. (2016) 'The pleasure of revenge: retaliatory aggression arises from a neural imbalance toward reward', Soc Cogn Affect Neurosci, 11(7), pp. 1173-1182.

Chester, D. S., Eisenberger, N. I., Pond, R. S., Jr., Richman, S. B., Bushman, B. J. & Dewall, C. N. (2014) 'The interactive effect of social pain and executive functioning on aggression: an fMRI experiment', Soc Cogn Affect Neurosci, 9(5), pp. 699-704.

Choi, E. Y., Yeo, B. T. T. & Buckner, R. L. (2012) 'The organization of the human striatum estimated by intrinsic functional connectivity', J Neurophysiol, 108(8), pp. 2242-2263.

Christakou, C., Economou, F., Livadas, S., Piperi, C., Adamopoulos, C., Marinakis, E. & Jdiamanti-Kandarakis, E. (2011) 'Strong and positive association of endothelin-1 with AGEs in PCOS: a causal relationship or a bystander?', Hormones (Athens), 10(4), pp. 292-297.

Cicchetti, D. V. (1994) 'Guidelines, criteria, and rules of thumb for evaluating normed and standardized assessment instruments in psychology', Psychological Assessment, 6(4), pp. 284-290.

Colclough, G. L., Smith, S. M., Nichols, T. E., Winkler, A. M., Sotiropoulos, S. N., Glasser, M. F., Van Essen, D. C. & Woolrich, M. W. (2017) 'The heritability of multi-modal connectivity in human brain activity', Elife, 6.

Common Sense Media Incorporation (2015) The common sense census: Media use by tweens and teens.

Couvy-Duchesne, B., Blokland, G. A., Hickie, I. B., Thompson, P. M., Martin, N. G., de Zubicaray, G. I., McMahon, K. L. & Wright, M. J. (2014) 'Heritability of head motion during resting state functional MRI in 462 healthy twins', Neuroimage, 102 Pt 2, pp. 424-434.

Critchfield, T. S. & Kollins, S. H. (2001) 'Temporal discounting: basic research and the analysis of socially important behavior', J Appl Behav Anal, 34(1), pp. 101-122.

Crone, E. A. & Elzinga, B. M. (2015) 'Changing brains: how longitudinal functional magnetic resonance imaging studies can inform us about cognitive and social-affective growth trajectories', Wiley Interdiscip Rev Cogn Sci, 6(1), pp. 53-63.

Crone, E. A. & Konijn, E. A. (2018) 'Media use and brain development during adolescence', Nat Commun, 9(1), p. 588.

Crone, E. A. & Steinbeis, N. (2017) 'Neural Perspectives on Cognitive Control Development during Childhood and Adolescence', Trends Cogn Sci, 21(3), pp. 205-215.

D

Dale, A. M. (1999) 'Optimal experimental design for event-related fMRI', Hum Brain Mapp, 8(2-3), pp. 109-114.

Dale, A. M., Fischl, B. & Sereno, M. I. (1999) 'Cortical surface-based analysis. I. Segmentation and surface reconstruction', Neuroimage, 9(2), pp. 179-194.

Dalgleish, T., Walsh, N. D., Mobbs, D., Schweizer, S., van Harmelen, A. L., Dunn, B., Dunn, V., Goodyer, I. & Stretton, J. (2017) 'Social pain and social gain in the adolescent brain: A common neural circuitry underlying both positive and negative social evaluation', Sci Rep, 7, p. 42010.

Damoiseaux, J. S., Rombouts, S. A., Barkhof, F., Scheltens, P., Stam, C. J., Smith, S. M. & Beckmann, C. F. (2006) 'Consistent resting-state networks across healthy subjects', Proc Natl Acad Sci U S A, 103(37), pp. 13848-13853.

Davey, C. G., Allen, N. B., Harrison, B. J., Dwyer, D. B. & Yucel, M. (2010) 'Being liked activates primary reward and midline self-related brain regions', Hum Brain Mapp, 31(4), pp. 660-668.

de Water, E., Cillessen, A. H. & Scheres, A. (2014) 'Distinct age-related differences in temporal discounting and risk taking in adolescents and young adults', Child Dev, 85(5), pp. 1881-1897.

Deadwyler, S. A., Hayashizaki, S., Cheer, J. & Hampson, R. E. (2004) 'Reward, memory and substance abuse: functional neuronal circuits in the nucleus accumbens', Neurosci Biobehav Rev, 27(8), pp. 703-711.

Demetriou, L., Kowalczyk, O. S., Tyson, G., Bello, T., Newbould, R. D. & Wall, M. B. (2018) 'A comprehensive evaluation of increasing temporal resolution with multiband-accelerated protocols and effects on statistical outcome measures in fMRI', Neuroimage, 176, pp. 404-416.

Desikan, R. S., Segonne, F., Fischl, B., Quinn, B. T., Dickerson, B. C., Blacker, D., Buckner, R. L., Dale, A. M., Maguire, R. P., Hyman, B. T., Albert, M. S. & Killiany, R. J. (2006) 'An automated labeling system for subdividing the human cerebral cortex on MRI scans into gyral based regions of interest', Neuroimage, 31(3), pp. 968-980.

DeWall, C. N. & Bushman, B. J. (2011) 'Social Acceptance and Rejection: The Sweet and the Bitter', Current Directions in Psychological Science, 20(4), pp. 256-260.

DeWall, C. N., Deckman, T., Pond, R. S., Jr. & Bonser, I. (2011) 'Belongingness as a core personality trait: how social exclusion influences social functioning and personality expression', J Pers, 79(6), pp. 1281-1314.

Di Martino, A., Scheres, A., Margulies, D. S., Kelly, A. M., Uddin, L. Q., Shehzad, Z., Biswal, B., Walters, J. R., Castellanos, F. X. & Milham, M. P. (2008) 'Functional connectivity of human striatum: a resting state FMRI study', Cereb Cortex, 18(12), pp. 2735-2747.

Diamond, A. (2013) 'Executive functions', Annu Rev Psychol, 64, pp. 135-168.

Dodge, K. A., Lansford, J. E., Burks, V. S., Bates, J. E., Pettit, G. S., Fontaine, R. & Price, J. M. (2003) 'Peer rejection and social information-processing factors in the development of aggressive behavior problems in children', Child Dev, 74(2), pp. 374-393.

Dosenbach, N. U. F., Koller, J. M., Earl, E. A., Miranda-Dominguez, O., Klein, R. L., Van, A. N., Snyder, A. Z., Nagel, B. J., Nigg, J. T., Nguyen, A. L., Wesevich, V., Greene, D. J. & Fair, D. A. (2017) 'Real-time motion analytics during brain MRI improve data quality and reduce costs', Neuroimage, 161, pp. 80-93.

Du, W. J., Green, L. & Myerson, J. (2002) 'Cross-cultural comparisons of discounting delayed and probabilistic rewards', Psychological Record, 52(4), pp. 479-492.

Dubois, J. & Adolphs, R. (2016) 'Building a Science of Individual Differences from fMRI', Trends Cogn Sci, 20(6), pp. 425-443.

Durston, S., Nederveen, H., van Dijk, S., van Belle, J., de Zeeuw, P., Langen, M. & van Dijk, A. (2009) 'Magnetic resonance simulation is effective in reducing anxiety related to magnetic resonance scanning in children', J Am Acad Child Adolesc Psychiatry, 48(2), pp. 206-207.

E

Eickhoff, S. B., Bzdok, D., Laird, A. R., Kurth, F. & Fox, P. T. (2012) 'Activation likelihood estimation meta-analysis revisited', Neuroimage, 59(3), pp. 2349-2361.

Eickhoff, S. B., Laird, A. R., Grefkes, C., Wang, L. E., Zilles, K. & Fox, P. T. (2009) 'Coordinate-based activation likelihood estimation meta-analysis of neuroimaging data: a random-effects approach based on empirical estimates of spatial uncertainty', Hum Brain Mapp, 30(9), pp. 2907-2926.

Eigsti, I. M., Zayas, V., Mischel, W., Shoda, Y., Ayduk, O., Dadlani, M. B., Davidson, M. C., Lawrence Aber, J. & Casey, B. J. (2006) 'Predicting cognitive control from preschool to late adolescence and young adulthood', Psychol Sci, 17(6), pp. 478-484.

Eisenberger, N. I. & Lieberman, M. D. (2004) 'Why rejection hurts: a common neural alarm system for physical and social pain', Trends Cogn Sci, 8(7), pp. 294-300.

Eisenberger, N. I., Lieberman, M. D. & Williams, K. D. (2003) 'Does rejection hurt? An FMRI study of social exclusion', Science, 302(5643), pp. 290-292.

Ekhtiari, H., Kuplicki, R., Yeh, H. W. & Paulus, M. P. (2019) 'Physical characteristics not psychological state or trait characteristics predict motion during resting state fMRI', Sci Rep, 9.

Eklund, A., Nichols, T. E. & Knutsson, H. (2016) 'Cluster failure: Why fMRI inferences for spatial extent have inflated false-positive rates', Proc Natl Acad Sci U S A, 113(28), pp. 7900-7905.

Elliott, M. L., Knodt, A. R., Cooke, M., Kim, M. J., Melzer, T. R., Keenan, R., Ireland, D., Ramrakha, S., Poulton, R., Caspi, A., Moffitt, T. E. & Hariri, A. R. (2019a) 'General functional connectivity: Shared features of resting-state and task fMRI drive reliable and heritable individual differences in functional brain networks', Neuroimage, 189, pp. 516-532.

Elliott, M. L., Knodt, A. R., Ireland, D., Morris, M. L., Poulton, R., Ramrakha, S., Sison, M. L., Moffitt, T. E., Caspi, A. & Hariri, A. R. (2019b) 'Poor test-retest reliability of task-fMRI: New empirical evidence and a meta-analysis', bioRxiv.

Ellis, B. J., Boyce, W. T., Belsky, J., Bakermans-Kranenburg, M. J. & van Ijzendoorn, M. H. (2011) 'Differential susceptibility to the environment: An evolutionary-neurodevelopmental theory', Dev Psychopathol, 23(1), pp. 7-28.

Engelhardt, L. E., Roe, M. A., Juranek, J., DeMaster, D., Harden, K. P., Tucker-Drob, E. M. & Church, J. A. (2017) 'Children's head motion during fMRI tasks is heritable and stable over time', Dev Cogn Neurosci, 25, pp. 58-68.

Ernst, M. (2014) 'The triadic model perspective for the study of adolescent motivated behavior', Brain Cogn, 89, pp. 104-111.

Euser, S., Bakermans-Kranenburg, M. J., van den Bulk, B. G., Linting, M., Damsteegt, R. C., Vrijhof, C. I., van Wijk, I. C., Crone, E. A. & van, I. M. H. (2016) 'Efficacy of the Video-feedback Intervention to promote Positive Parenting and Sensitive Discipline in Twin Families (VIPP-Twins): Study protocol for a randomized controlled trial', BMC Psychol, 4(1), p. 33.

Evans, S. C., Fite, P. J., Hendrickson, M. L., Rubens, S. L. & Mages, A. K. (2015) 'The Role of Reactive Aggression in the Link Between Hyperactive-Impulsive Behaviors and Peer Rejection in Adolescents', Child Psychiatry Hum Dev.

F

Fair, D. A., Cohen, A. L., Power, J. D., Dosenbach, N. U., Church, J. A., Miezin, F. M., Schlaggar, B. L. & Petersen, S. E. (2009) 'Functional brain networks develop from a "local to distributed" organization', PLoS Comput Biol, 5(5), p. e1000381.

Fareri, D. S., Gabard-Durnam, L., Goff, B., Flannery, J., Gee, D. G., Lumian, D. S., Caldera, C. & Tottenham, N. (2015) 'Normative development of ventral striatal resting state connectivity in humans', Neuroimage, 118, pp. 422-437.

Fassbender, C., Mukherjee, P. & Schweitzer, J. B. (2017a) 'Minimizing noise in pediatric task-based functional MRI; Adolescents with developmental disabilities and typical development', Neuroimage, 149, pp. 338-347.

Fassbender, C., Mukherjee, P. & Schweitzer, J. B. (2017b) 'Reprint of: Minimizing noise in pediatric task-based functional MRI; Adolescents with developmental disabilities and typical development', Neuroimage, 154, pp. 230-239.

Feinberg, D. A. & Yacoub, E. (2012) 'The rapid development of high speed, resolution and precision in fMRI', Neuroimage, 62(2), pp. 720-725.

Ferguson, C. J. (2010) 'Genetic Contributions to Antisocial Personality and Behavior: A Meta-Analytic Review From an Evolutionary Perspective', Journal of Social Psychology, 150(2), pp. 160-180.

Figner, B., Knoch, D., Johnson, E. J., Krosch, A. R., Lisanby, S. H., Fehr, E. & Weber, E. U. (2010) 'Lateral prefrontal cortex and self-control in intertemporal choice', Nat Neurosci, 13(5), pp. 538-539.

Fischl, B., Sereno, M. I. & Dale, A. M. (1999) 'Cortical surface-based analysis. II: Inflation, flattening, and a surface-based coordinate system', Neuroimage, 9(2), pp. 195-207.

Flagan, T. & Beer, J. S. (2013) 'Three ways in which midline regions contribute to self-evaluation', Front Hum Neurosci, 7, p. 450.

Flint, J. & Kendler, K. S. (2014) 'The Genetics of Major Depression', Neuron, 81(3), pp. 484-503.

Fox, M. D. & Raichle, M. E. (2007) 'Spontaneous fluctuations in brain activity observed with functional magnetic resonance imaging', Nature Reviews Neuroscience, 8(9), pp. 700-711.

Franco, A., Malhotra, N. & Simonovits, G. (2014) 'Publication bias in the social sciences: Unlocking the file drawer', Science, 345(6203), pp. 1502-1505.

Frohner, J. H., Teckentrup, V., Smolka, M. N. & Kroemer, N. B. (2019) 'Addressing the reliability fallacy in fMRI: Similar group effects may arise from unreliable individual effects', Neuroimage, 195, pp. 174-189.

Fulwiler, C. E., King, J. A. & Zhang, N. (2012) 'Amygdala-orbitofrontal resting-state functional connectivity is associated with trait anger', Neuroreport, 23(10), pp. 606-610.

G

Gabard-Durnam, L. J., Flannery, J., Goff, B., Gee, D. G., Humphreys, K. L., Telzer, E., Hare, T. & Tottenham, N. (2014) 'The development of human amygdala functional connectivity at rest from 4 to 23 years: A cross-sectional study', Neuroimage, 95, pp. 193-207.

Gabrieli, J. D. E., Ghosh, S. S. & Whitfield-Gabrieli, S. (2015) 'Prediction as a Humanitarian and Pragmatic Contribution from Human Cognitive Neuroscience', Neuron, 85(1), pp. 11-26.

Gallagher, H. L. & Frith, C. D. (2003) 'Functional imaging of 'theory of mind'', Trends Cogn Sci, 7(2), pp. 77-83.

Galvan, A. (2010) 'Adolescent development of the reward system', Front Hum Neurosci, 4, p. 6.

Galvan, A., Van Leijenhorst, L. & McGlennen, K. M. (2012) 'Considerations for imaging the adolescent brain', Dev Cogn Neurosci, 2(3), pp. 293-302.

Garrett, A. S., Carrion, V., Kletter, H., Karchemskiy, A., Weems, C. F. & Reiss, A. (2012) 'Brain activation to facial expressions in youth with PTSD symptoms', Depress Anxiety, 29(5), pp. 449-459.

Ge, T., Holmes, A. J., Buckner, R. L., Smoller, J. W. & Sabuncu, M. R. (2017) 'Heritability analysis with repeat measurements and its application to resting-state functional connectivity', Proc Natl Acad Sci U S A, 114(21), pp. 5521-5526.

Gee, D. G., Gabard-Durnam, L., Telzer, E. H., Humphreys, K. L., Goff, B., Shapiro, M., Flannery, J., Lumian, D. S., Fareri, D. S., Caldera, C. & Tottenham, N. (2014) 'Maternal Buffering of Human Amygdala-Prefrontal Circuitry During Childhood but Not During Adolescence', Psychol Sci, 25(11), pp. 2067-2078.

Giglietto, F., Rossi, L. & Bennato, D. (2012) 'The Open Laboratory: Limits and Possibilities of Using Facebook, Twitter, and YouTube as a Research Data Source', Journal of Technology in Human Services, 30(3-4), pp. 145-159.

Gilmore, J. H., Knickmeyer, R. C. & Gao, W. (2018) 'Imaging structural and functional brain development in early childhood', Nat Rev Neurosci, 19(3), pp. 123-137.

Glahn, D. C., Winkler, A. M., Kochunov, P., Almasy, L., Duggirala, R., Carless, M. A., Curran, J. C., Olvera, R. L., Laird, A. R., Smith, S. M., Beckmann, C. F., Fox, P. T. & Blangero, J. (2010) 'Genetic control over the resting brain', Proc Natl Acad Sci U S A, 107(3), pp. 1223-1228.

Glover, G. H. (2011) 'Overview of functional magnetic resonance imaging', Neurosurg Clin N Am, 22(2), pp. 133-139, vii.

Goff, B., Gee, D. G., Telzer, E. H., Humphreys, K. L., Gabard-Durnam, L., Flannery, J. & Tottenham, N. (2013) 'Reduced nucleus accumbens reactivity and adolescent depression following early-life stress', Neuroscience, 249, pp. 129-138.

Gogtay, N., Giedd, J. N., Lusk, L., Hayashi, K. M., Greenstein, D., Vaituzis, A. C., Nugent, T. F., Herman, D. H., Clasen, L. S., Toga, A. W., Rapoport, J. L. & Thompson, P. M. (2004) 'Dynamic mapping of human cortical development during childhood through early adulthood', Proc Natl Acad Sci U S A, 101(21), pp. 8174-8179.

Green, L., Fristoe, N. & Myerson, J. (1994) 'Temporal discounting and preference reversals in choice between delayed outcomes', Psychon Bull Rev, 1(3), pp. 383-389.

Greene, A. S., Gao, S., Scheinost, D. & Constable, R. T. (2018a) 'Task-induced brain state manipulation improves prediction of individual traits', Nat Commun, 9(1), p. 2807.

Greene, D. J., Koller, J. M., Hampton, J. M., Wesevich, V., Van, A. N., Nguyen, A. L., Hoyt, C. R., McIntyre, L., Earl, E. A., Klein, R. L., Shimony, J. S., Petersen, S. E., Schlaggar, B. L., Fair, D. A. & Dosenbach, N. U. F. (2018b) 'Behavioral interventions for reducing head motion during MRI scans in children', Neuroimage, 171, pp. 234-245.

Greve, D. N. & Fischl, B. (2009) 'Accurate and robust brain image alignment using boundary-based registration', Neuroimage, 48(1), pp. 63-72.

Gunther Moor, B., Bos, M. G., Crone, E. A. & van der Molen, M. W. (2014) 'Peer rejection cues induce cardiac slowing after transition into adolescence', Dev Psychol, 50(3), pp. 947-955.

Gunther Moor, B., Crone, E. A. & van der Molen, M. W. (2010a) 'The heartbrake of social rejection: heart rate deceleration in response to unexpected peer rejection', Psychol Sci, 21(9), pp. 1326-1333.

Gunther Moor, B., van Leijenhorst, L., Rombouts, S. A., Crone, E. A. & Van der Molen, M. W. (2010b) 'Do you like me? Neural correlates of social evaluation and developmental trajectories', Soc Neurosci, 5(5-6), pp. 461-482.

Guroglu, B., van den Bos, W. & Crone, E. A. (2014) 'Sharing and giving across adolescence: an experimental study examining the development of prosocial behavior', Front Psychol, 5.

Guroglu, B., van den Bos, W., Rombouts, S. A. & Crone, E. A. (2010) 'Unfair? It depends: neural correlates of fairness in social context', Soc Cogn Affect Neurosci, 5(4), pp. 414-423.

Guyer, A. E., Caouette, J. D., Lee, C. C. & Ruiz, S. K. (2014) 'Will they like me? Adolescents' emotional responses to peer evaluation', Int J Behav Dev, 38(2), pp. 155-163.

Guyer, A. E., Choate, V. R., Pine, D. S. & Nelson, E. E. (2012) 'Neural circuitry underlying affective response to peer feedback in adolescence', Soc Cogn Affect Neurosci, 7(1), pp. 81-92.

Guyer, A. E., Lau, J. Y., McClure-Tone, E. B., Parrish, J., Shiffrin, N. D., Reynolds, R. C., Chen, G., Blair, R. J., Leibenluft, E., Fox, N. A., Ernst, M., Pine, D. S. & Nelson, E. E. (2008) 'Amygdala and ventrolateral prefrontal cortex function during anticipated peer evaluation in pediatric social anxiety', Arch Gen Psychiatry, 65(11), pp. 1303-1312.

Guyer, A. E., McClure-Tone, E. B., Shiffrin, N. D., Pine, D. S. & Nelson, E. E. (2009) 'Probing the neural correlates of anticipated peer evaluation in adolescence', Child Dev, 80(4), pp. 1000-1015.

Guyer, A. E., Silk, J. S. & Nelson, E. E. (2016) 'The neurobiology of the emotional adolescent: From the inside out', Neurosci Biobehav Rev, 70, pp. 74-85.

H

Haber, S. N. & Knutson, B. (2010) 'The Reward Circuit: Linking Primate Anatomy and Human Imaging', Neuropsychopharmacology, 35(1), pp. 4-26.

Hallowell, L. M., Stewart, S. E., de Amorim, E. S. C. T. & Ditchfield, M. R. (2008) 'Reviewing the process of preparing children for MRI', Pediatr Radiol, 38(3), pp. 271-279.

Hanson, J. L., Albert, D., Iselin, A. M. R., Carre, J. M., Dodge, K. A. & Hariri, A. R. (2016) 'Cumulative stress in childhood is associated with blunted reward-related brain activity in adulthood', Soc Cogn Affect Neurosci, 11(3), pp. 405-412.

Hayes, A. F. & Cai, L. (2007) 'Using heteroskedasticity-consistent standard error estimators in OLS regression: an introduction and software implementation', Behav Res Methods, 39(4), pp. 709-722.

Heller, R., Stanley, D., Yekutieli, D., Rubin, N. & Benjamini, Y. (2006) 'Cluster-based analysis of FMRI data', Neuroimage, 33(2), pp. 599-608.

Herting, M. M., Gautam, P., Chen, Z., Mezher, A. & Vetter, N. C. (2018) 'Test-retest reliability of longitudinal task-based fMRI: Implications for developmental studies', Dev Cogn Neurosci, 33, pp. 17-26.

Hughes, B. L. & Beer, J. S. (2013) 'Protecting the self: the effect of social-evaluative threat on neural representations of self', J Cogn Neurosci, 25(4), pp. 613-622.

Huijbers, W., Van Dijk, K. R. A., Boenniger, M. M., Stirnberg, R. & Breteler, M. M. B. (2017) 'Less head motion during MRI under task than resting-state conditions', Neuroimage, 147, pp. 111-120.

Hyman, S. E. (2000) 'The genetics of mental illness: implications for practice', Bull World Health Organ, 78(4), pp. 455-463.

I

Ioannidis, J. P. A. (2005) 'Why most published research findings are false', Plos Medicine, 2(8), pp. 696-701.

J

Jalbrzikowski, M., Larsen, B., Hallquist, M. N., Foran, W., Calabro, F. & Luna, B. (2017) 'Development of White Matter Microstructure and Intrinsic Functional Connectivity Between the Amygdala and Ventromedial Prefrontal Cortex: Associations With Anxiety and Depression', Biol Psychiatry.

Jansen, A. G., Mous, S. E., White, T., Posthuma, D. & Polderman, T. J. (2015) 'What twin studies tell us about the heritability of brain development, morphology, and function: a review', Neuropsychol Rev, 25(1), pp. 27-46.

Jarcho, J. M., Fox, N. A., Pine, D. S., Etkin, A., Leibenluft, E., Shechner, T. & Ernst, M. (2013) 'The neural correlates of emotion-based cognitive control in adults with early childhood behavioral inhibition', Biol Psychol, 92(2), pp. 306-314.

Jenkinson, M., Bannister, P., Brady, M. & Smith, S. (2002) 'Improved optimization for the robust and accurate linear registration and motion correction of brain images', Neuroimage, 17(2), pp. 825-841.

Jenkinson, M. & Smith, S. (2001) 'A global optimisation method for robust affine registration of brain images', Med Image Anal, 5(2), pp. 143-156.

Jolles, D. D., van Buchem, M. A., Crone, E. A. & Rombouts, S. A. (2011) 'A comprehensive study of whole-brain functional connectivity in children and young adults', Cereb Cortex, 21(2), pp. 385-391.

Jones, D. K. (2008) 'Studying connections in the living human brain with diffusion MRI', Cortex, 44(8), pp. 936-952.

Juffer, F. & Bakermans-Kranenburg, M. J. (2018) 'Working with Video-feedback Intervention to promote Positive Parenting and Sensitive Discipline (VIPP-SD): A case study', Journal of Clinical Psychology, 74(8), pp. 1346-1357.

Juffer, F., Bakermans-Kranenburg, M. J. & van IJzendoorn, M. H. (2017a) 'Pairing attachment theory and social learning theory in video-feedback intervention to promote positive parenting', Current Opinion in Psychology, 15, pp. 189-194.

Juffer, F., Bakermans-Kranenburg, M. J. & van Ijzendoorn, M. H. (2017b) 'Video Feedback Intervention to Promote Positive Parenting and Sensitive Discipline (VIPP-SD): Development and meta-analytic evidence of its effectiveness. ', in H. Steele & M. Steele (eds), Handbook of attachment-based interventions, New York, Guilford Publications.

K

Klapwijk, E. T., van de Kamp, F., van der Meulen, M., Peters, S. & Wierenga, L. M. (2019) 'Qoala-T: A supervised-learning tool for quality control of FreeSurfer segmented MRI data', Neuroimage, 189, pp. 116-129.

Kong, X. Z., Zhen, Z., Li, X., Lu, H. H., Wang, R., Liu, L., He, Y., Zang, Y. & Liu, J. (2014) 'Individual differences in impulsivity predict head motion during magnetic resonance imaging', PLoS One, 9(8), p. e104989.

Konijn, E. A., Bijvank, M. N. & Bushman, B. J. (2007) 'I wish I were a warrior: the role of wishful identification in the effects of violent video games on aggression in adolescent boys', Dev Psychol, 43(4), pp. 1038-1044.

Kotsoni, E., Byrd, D. & Casey, B. J. (2006) 'Special considerations for functional magnetic resonance imaging of pediatric populations', J Magn Reson Imaging, 23(6), pp. 877-886.

Kross, E., Berman, M. G., Mischel, W., Smith, E. E. & Wager, T. D. (2011) 'Social rejection shares somatosensory representations with physical pain', Proc Natl Acad Sci U S A, 108(15), pp. 6270-6275.

L

Lansford, J. E., Malone, P. S., Dodge, K. A., Pettit, G. S. & Bates, J. E. (2010) 'Developmental cascades of peer rejection, social information processing biases, and aggression during middle childhood', Dev Psychopathol, 22(3), pp. 593-602.

Leary, M. R. & Baumeister, R. F. (2000) 'The nature and function of self-esteem: Sociometer theory', Advances in Experimental Social Psychology, Vol 32, 32, pp. 1-62.

Leary, M. R., Kowalski, R. M., Smith, L. & Phillips, S. (2003) 'Teasing, rejection, and violence: Case studies of the school shootings', Aggressive Behavior, 29(3), pp. 202-214.

Leary, M. R., Twenge, J. M. & Quinlivan, E. (2006) 'Interpersonal rejection as a determinant of anger and aggression', Pers Soc Psychol Rev, 10(2), pp. 111-132.

Lebel, C. & Beaulieu, C. (2011) 'Longitudinal development of human brain wiring continues from childhood into adulthood', J Neurosci, 31(30), pp. 10937-10947.

Lee, D. & Seo, H. (2016) 'Neural Basis of Strategic Decision Making', Trends Neurosci, 39(1), pp. 40-48.

Lenroot, R. K. & Giedd, J. N. (2006) 'Brain development in children and adolescents: insights from anatomical magnetic resonance imaging', Neurosci Biobehav Rev, 30(6), pp. 718-729.

Lenroot, R. K. & Giedd, J. N. (2011) 'Annual Research Review: Developmental considerations of gene by environment interactions', J Child Psychol Psychiatry, 52(4), pp. 429-441.

Lenroot, R. K., Schmitt, J. E., Ordaz, S. J., Wallace, G. L., Neale, M. C., Lerch, J. P., Kendler, K. S., Evans, A. C. & Giedd, J. N. (2009) 'Differences in Genetic and Environmental Influences on the Human Cerebral Cortex Associated With Development During Childhood and Adolescence', Hum Brain Mapp, 30(1), pp. 163-174.

Lieberman, M. D. & Eisenberger, N. I. (2009) 'Neuroscience. Pains and pleasures of social life', Science, 323(5916), pp. 890-891.

Liu, T. T. (2017) 'Reprint of 'Noise contributions to the fMRI signal: An Overview'', Neuroimage, 154, pp. 4-14.

Long, J. S. & Ervin, L. H. (2000) 'Using heteroscedasticity consistent standard errors in the linear regression model', American Statistician, 54(3), pp. 217-224.

Luna, B., Garver, K. E., Urban, T. A., Lazar, N. A. & Sweeney, J. A. (2004) 'Maturation of cognitive processes from late childhood to adulthood', Child Dev, 75(5), pp. 1357-1372.

Luna, B., Padmanabhan, A. & O'Hearn, K. (2010) 'What has fMRI told us about the development of cognitive control through adolescence?', Brain Cogn, 72(1), pp. 101-113.

Lupien, S. J., McEwen, B. S., Gunnar, M. R. & Heim, C. (2009) 'Effects of stress throughout the lifespan on the brain, behaviour and cognition', Nat Rev Neurosci, 10(6), pp. 434-445.

M

Madhyastha, T., Peverill, M., Koh, N., McCabe, C., Flournoy, J., Mills, K., King, K., Pfeifer, J. & McLaughlin, K. A. (2018) 'Current methods and limitations for longitudinal fMRI analysis across development', Dev Cogn Neurosci, 33, pp. 118-128.

Masten, C. L., Eisenberger, N. I., Borofsky, L. A., Pfeifer, J. H., McNealy, K., Mazziotta, J. C. & Dapretto, M. (2009) 'Neural correlates of social exclusion during adolescence: understanding the distress of peer rejection', Soc Cogn Affect Neurosci, 4(2), pp. 143-157.

Mazaika, P. K., Hoeft, F., Glover, G. H. & Reiss, A. L. (2009) 'Methods and Software for fMRI analyses for Clinical Subjects.', Human Brain Mapping Conference, San Francisco, CA. .

McClure, S. M., Laibson, D. I., Loewenstein, G. & Cohen, J. D. (2004) 'Separate neural systems value immediate and delayed monetary rewards', Science, 306(5695), pp. 503-507.

Menon, V. (2013) 'Developmental pathways to functional brain networks: emerging principles', Trends Cogn Sci, 17(12), pp. 627-640.

Mezulis, A. H., Abramson, L. Y., Hyde, J. S. & Hankin, B. L. (2004) 'Is there a universal positivity bias in attributions? A meta-analytic review of individual, developmental, and cultural differences in the self-serving attributional bias', Psychol Bull, 130(5), pp. 711-747.

Miles, D. R. & Carey, G. (1997) 'Genetic and environmental architecture of human aggression', J Pers Soc Psychol, 72(1), pp. 207-217.

Mischel, W., Shoda, Y. & Rodriguez, M. I. (1989) 'Delay of gratification in children', Science, 244(4907), pp. 933-938.

Misic, B. & Sporns, O. (2016) 'From regions to connections and networks: new bridges between brain and behavior', Curr Opin Neurobiol, 40, pp. 1-7.

Moilanen, I., Linna, S. L., Ebeling, H., Kumpulainen, K., Tamminen, T., Piha, J. & Almqvist, F. (1999) 'Are twins' behavioural/emotional problems different from singletons'?', Eur Child Adolesc Psychiatry, 8 Suppl 4, pp. 62-67.

Montag, C., Blaszkiewicz, K., Lachmann, B., Andone, I., Sariyska, R., Trendafilov, B., Reuter, M. & Markowetz, A. (2014) 'Correlating Personality and Actual Phone Usage Evidence From Psychoinformatics', Journal of Individual Differences, 35(3), pp. 158-165.

Montag, C., Markowetz, A., Blaszkiewicz, K., Andone, I., Lachmann, B., Sariyska, R., Trendafilov, B., Eibes, M., Kolb, J., Reuter, M., Weber, B. & Markett, S. (2017) 'Facebook usage on smartphones and gray matter volume of the nucleus accumbens', Behav Brain Res, 329, pp. 221-228.

Mori, S., Crain, B. J., Chacko, V. P. & van Zijl, P. C. (1999) 'Three-dimensional tracking of axonal projections in the brain by magnetic resonance imaging', Ann Neurol, 45(2), pp. 265-269.

Mumford, J. A. & Nichols, T. E. (2008) 'Power calculation for group fMRI studies accounting for arbitrary design and temporal autocorrelation', Neuroimage, 39(1), pp. 261-268.

Murphy, K., Birn, R. M., Handwerker, D. A., Jones, T. B. & Bandettini, P. A. (2009) 'The impact of global signal regression on resting state correlations: are anti-correlated networks introduced?', Neuroimage, 44(3), pp. 893-905.

Myerson, J., Green, L. & Warusawitharana, M. (2001) 'Area under the curve as a measure of discounting', J Exp Anal Behav, 76(2), pp. 235-243.

N

Neale, M. C., Hunter, M. D., Pritikin, J. N., Zahery, M., Brick, T. R., Kirkpatrick, R. M., Estabrook, R., Bates, T. C., Maes, H. H. & Boker, S. M. (2016) 'OpenMx 2.0: Extended Structural Equation and Statistical Modeling', Psychometrika, 81(2), pp. 535-549.

Nelson, E. E., Jarcho, J. M. & Guyer, A. E. (2016) 'Social re-orientation and brain development: An expanded and updated view', Dev Cogn Neurosci, 17, pp. 118-127.

Nelson, E. E., Leibenluft, E., McClure, E. B. & Pine, D. S. (2005) 'The social re-orientation of adolescence: a neuroscience perspective on the process and its relation to psychopathology', Psychol Med, 35(2), pp. 163-174.

Nesdale, D. & Duffy, A. (2011) 'Social identity, peer group rejection, and young children's reactive, displaced, and proactive aggression', Br J Dev Psychol, 29(Pt 4), pp. 823-841.

Nesdale, D. & Lambert, A. (2007) 'Effects of experimentally manipulated peer rejection on children's negative affect, self-esteem, and maladaptive social behavior', International Journal of Behavioral Development, 31(2), pp. 115-122.

Nichols, T., Brett, M., Andersson, J., Wager, T. & Poline, J. B. (2005) 'Valid conjunction inference with the minimum statistic', Neuroimage, 25(3), pp. 653-660.

Nolan, S. A., Flynn, C. & Garber, J. (2003) 'Prospective relations between rejection and depression in young adolescents', J Pers Soc Psychol, 85(4), pp. 745-755.

Nord, C. L., Gray, A., Charpentier, C. J., Robinson, O. J. & Roiser, J. P. (2017) 'Unreliability of putative fMRI biomarkers during emotional face processing', Neuroimage, 156, pp. 119-127.

Novin, S., Bos, M. G. N., Stevenson, C. E. & Rieffe, C. (2018) 'Adolescents' responses to online peer conflict: How self-evaluation and ethnicity matter', Infant and Child Development, 27(2), p. e2067.

O

O'Shaughnessy, E. S., Berl, M. M., Moore, E. N. & Gaillard, W. D. (2008) 'Pediatric functional magnetic resonance imaging (fMRI): Issues and applications', J Child Neurol, 23(7), pp. 791-801.

Ochsner, K. N., Silvers, J. A. & Buhle, J. T. (2012) 'Functional imaging studies of emotion regulation: a synthetic review and evolving model of the cognitive control of emotion', Year in Cognitive Neuroscience, 1251, pp. E1-E24.

Olson, E. A., Collins, P. F., Hooper, C. J., Muetzel, R., Lim, K. O. & Luciana, M. (2009) 'White matter integrity predicts delay discounting behavior in 9- to 23-year-olds: a diffusion tensor imaging study', J Cogn Neurosci, 21(7), pp. 1406-1421.

Olson, E. A., Hooper, C. J., Collins, P. & Luciana, M. (2007) 'Adolescents' performance on delay and probability discounting tasks: contributions of age, intelligence, executive functioning, and self-reported externalizing behavior', Pers Individ Dif, 43(7), pp. 1886-1897.

Open Science, C. (2015) 'PSYCHOLOGY. Estimating the reproducibility of psychological science', Science, 349(6251), p. aac4716.

P

Park, A. T., Leonard, J. A., Saxler, P., Cyr, A. B., Gabrieli, J. D. E. & Mackey, A. P. (in press) 'Amygdala-medial prefrontal connectivity relates to stress and mental health in early childhood', Soc Cogn Affect Neurosci.

Peper, J. S., de Reus, M. A., van den Heuvel, M. P. & Schutter, D. J. (2015) 'Short fused? associations between white matter connections, sex steroids, and aggression across adolescence', Hum Brain Mapp, 36(3), pp. 1043-1052.

Peper, J. S., Mandl, R. C., Braams, B. R., de Water, E., Heijboer, A. C., Koolschijn, P. C. & Crone, E. A. (2013) 'Delay discounting and frontostriatal fiber tracts: a combined DTI and MTR study on impulsive choices in healthy young adults', Cereb Cortex, 23(7), pp. 1695-1702.

Peters, J. & Buchel, C. (2011) 'The neural mechanisms of inter-temporal decision-making: understanding variability', Trends Cogn Sci, 15(5), pp. 227-239.

Peters, S., Braams, B. R., Raijmakers, M. E., Koolschijn, P. C. & Crone, E. A. (2014a) 'The neural coding of feedback learning across child and adolescent development', J Cogn Neurosci, 26(8), pp. 1705-1720.

Peters, S. & Crone, E. A. (2017) 'Increased striatal activity in adolescence benefits learning', Nat Commun, 8(1), p. 1983.

Peters, S., Koolschijn, P. C., Crone, E. A., Van Duijvenvoorde, A. C. K. & Raijmakers, M. E. (2014b) 'Strategies influence neural activity for feedback learning across child and adolescent development', Neuropsychologia, 62, pp. 365-374.

Peters, S., Van Duijvenvoorde, A. C., Koolschijn, P. C. & Crone, E. A. (2016) 'Longitudinal development of frontoparietal activity during feedback learning: Contributions of age, performance, working memory and cortical thickness', Dev Cogn Neurosci, 19, pp. 211-222.

Pfeifer, J. H. & Allen, N. B. (2016) 'The audacity of specificity: Moving adolescent developmental neuroscience towards more powerful scientific paradigms and translatable models', Dev Cogn Neurosci, 17, pp. 131-137.

Pfeifer, J. H., Allen, N. B., Byrne, M. L. & Mills, K. L. (2018) 'Modeling Developmental Change: Contemporary Approaches to Key Methodological Challenges in Developmental Neuroimaging', Dev Cogn Neurosci, 33, pp. 1-4.

Phelps, E. A. (2004) 'Human emotion and memory: interactions of the amygdala and hippocampal complex', Curr Opin Neurobiol, 14(2), pp. 198-202.

Pinheiro, J., Bates, D., DebRoy, S. & Sarkar, D. (2013) 'the R Development Core Team: nlme: Linear and Nonlinear Mixed Effects Models.', R package version 3.1-104. In.

Polderman, T. J., Benyamin, B., de Leeuw, C. A., Sullivan, P. F., van Bochoven, A., Visscher, P. M. & Posthuma, D. (2015) 'Meta-analysis of the heritability of human traits based on fifty years of twin studies', Nat Genet, 47(7), pp. 702-709.

Poldrack, R. A. (2007) 'Region of interest analysis for fMRI', Soc Cogn Affect Neurosci, 2(1), pp. 67-70.

Poldrack, R. A., Pare-Blagoev, E. J. & Grant, P. E. (2002) 'Pediatric functional magnetic resonance imaging: progress and challenges', Top Magn Reson Imaging, 13(1), pp. 61-70.

Porsch, R. M., Middeldorp, C. M., Cherny, S. S., Krapohl, E., van Beijsterveldt, C. E. M., Loukola, A., Korhonen, T., Pulkkinen, L., Corley, R., Rhee, S., Kaprio, J., Rose, R. R., Hewitt, J. K., Sham, P., Plomin, R., Boomsma, D. I. & Bartels, M. (2016) 'Longitudinal Heritability of Childhood Aggression', American Journal of Medical Genetics Part B-Neuropsychiatric Genetics, 171(5), pp. 697-707.

Porter, J. N., Roy, A. K., Benson, B., Carlisi, C., Collins, P. F., Leibenluft, E., Pine, D. S., Luciana, M. & Ernst, M. (2015) 'Age-related changes in the intrinsic functional connectivity of the human ventral vs. dorsal striatum from childhood to middle age', Dev Cogn Neurosci, 11, pp. 83-95.

Power, J. D. (2017) 'A simple but useful way to assess fMRI scan qualities', Neuroimage, 154, pp. 150-158.

Power, J. D., Barnes, K. A., Snyder, A. Z., Schlaggar, B. L. & Petersen, S. E. (2012) 'Spurious but systematic correlations in functional connectivity MRI networks arise from subject motion', Neuroimage, 59(3), pp. 2142-2154.

Power, J. D., Fair, D. A., Schlaggar, B. L. & Petersen, S. E. (2010) 'The development of human functional brain networks', Neuron, 67(5), pp. 735-748.

Power, J. D., Mitra, A., Laumann, T. O., Snyder, A. Z., Schlaggar, B. L. & Petersen, S. E. (2014) 'Methods to detect, characterize, and remove motion artifact in resting state fMRI', Neuroimage, 84, pp. 320-341.

Power, J. D., Schlaggar, B. L. & Petersen, S. E. (2015) 'Recent progress and outstanding issues in motion correction in resting state fMRI', Neuroimage, 105, pp. 536-551.

Power, J. D., Silver, B. M., Silverman, M. R., Ajodan, E. L., Bos, D. J. & Jones, R. M. (2019) 'Customized head molds reduce motion during resting state fMRI scans', Neuroimage, 189, pp. 141-149.

Preacher, K. J. & Hayes, A. F. (2008) 'Asymptotic and resampling strategies for assessing and comparing indirect effects in multiple mediator models', Behav Res Methods, 40(3), pp. 879-891.

Prinstein, M. J. & La Greca, A. M. (2004) 'Childhood peer rejection and aggression as predictors of adolescent girls' externalizing and health risk behaviors: a 6-year longitudinal study', J Consult Clin Psychol, 72(1), pp. 103-112.

Pulkkinen, L., Vaalamo, I., Hietala, R., Kaprio, J. & Rose, R. J. (2003) 'Peer reports of adaptive behavior in twins and singletons: is twinship a risk or an advantage?', Twin Res, 6(2), pp. 106-118.

R

R Core Team (2015) R: A language and environment for statistical computing, Vienna, Austria, R Foundation for Statistical Computing.

Raschle, N., Zuk, J., Ortiz-Mantilla, S., Sliva, D. D., Franceschi, A., Grant, P. E., Benasich, A. A. & Gaab, N. (2012) 'Pediatric neuroimaging in early childhood and infancy: challenges and practical guidelines', Ann N Y Acad Sci, 1252, pp. 43-50.

Reijntjes, A., Thomaes, S., Bushman, B. J., Boelen, P. A., de Castro, B. O. & Telch, M. J. (2010) 'The outcast-lash-out effect in youth: alienation increases aggression following peer rejection', Psychol Sci, 21(10), pp. 1394-1398.

Reijntjes, A., Thomaes, S., Kamphuis, J. H., Bushman, B. J., de Castro, B. O. & Telch, M. J. (2011) 'Explaining the Paradoxical Rejection-Aggression Link: The Mediating Effects of Hostile Intent Attributions, Anger, and Decreases in State Self-Esteem on Peer Rejection-Induced Aggression in Youth', Personality and Social Psychology Bulletin, 37(7), pp. 955-963.

Rhee, S. H. & Waldman, I. D. (2002) 'Genetic and environmental influences on antisocial behavior: A meta-analysis of twin and adoption studies', Psychol Bull, 128(3), pp. 490-529.

Richards, J. B., Zhang, L., Mitchell, S. H. & de Wit, H. (1999) 'Delay or probability discounting in a model of impulsive behavior: effect of alcohol', J Exp Anal Behav, 71(2), pp. 121-143.

Richmond, S., Johnson, K. A., Seal, M. L., Allen, N. B. & Whittle, S. (2016) 'Development of brain networks and relevance of environmental and genetic factors: A systematic review', Neurosci Biobehav Rev, 71, pp. 215-239.

Riva, P., Romero Lauro, L. J., DeWall, C. N., Chester, D. S. & Bushman, B. J. (2015) 'Reducing aggressive responses to social exclusion using transcranial direct current stimulation', Soc Cogn Affect Neurosci, 10(3), pp. 352-356.

Robbers, S. C., Bartels, M., van Oort, F. V., van Beijsterveldt, C. E., van der Ende, J., Verhulst, F. C., Boomsma, D. I. & Huizink, A. C. (2010) 'A twin-singleton comparison of developmental trajectories of externalizing and internalizing problems in 6- to 12-year-old children', Twin Res Hum Genet, 13(1), pp. 79-87.

Rodman, A. M., Powers, K. E. & Somerville, L. H. (2017) 'Development of self-protective biases in response to social evaluative feedback', Proc Natl Acad Sci U S A, 114(50), pp. 13158-13163.

Rosenberg, D. R., Sweeney, J. A., Gillen, J. S., Kim, J., Varanelli, M. J., O'Hearn, K. M., Erb, P. A., Davis, D. & Thulborn, K. R. (1997) 'Magnetic resonance imaging of children without sedation: preparation with simulation', J Am Acad Child Adolesc Psychiatry, 36(6), pp. 853-859.

Rotge, J. Y., Lemogne, C., Hinfray, S., Huguet, P., Grynszpan, O., Tartour, E., George, N. & Fossati, P. (2015) 'A meta-analysis of the anterior cingulate contribution to social pain', Soc Cogn Affect Neurosci, 10(1), pp. 19-27.

Roy, A. K., Shehzad, Z., Margulies, D. S., Kelly, A. M., Uddin, L. Q., Gotimer, K., Biswal, B. B., Castellanos, F. X. & Milham, M. P. (2009) 'Functional connectivity of the human amygdala using resting state fMRI', Neuroimage, 45(2), pp. 614-626.

Rubia, K. (2013) 'Functional brain imaging across development', Eur Child Adolesc Psychiatry, 22(12), pp. 719-731.

Russo, S. J. & Nestler, E. J. (2013) 'The brain reward circuitry in mood disorders', Nat Rev Neurosci, 14(9), pp. 609-625.

S

Satterthwaite, T. D., Wolf, D. H., Ruparel, K., Erus, G., Elliott, M. A., Eickhoff, S. B., Gennatas, E. D., Jackson, C., Prabhakaran, K., Smith, A., Hakonarson, H., Verna, R., Davatzikos, C., Gur, R. E. & Gur, R. C. (2013) 'Heterogeneous impact of motion on fundamental patterns of developmental changes in functional connectivity during youth', Neuroimage, 83, pp. 45-57.

Savalia, N. K., Agres, P. F., Chan, M. Y., Feczko, E. J., Kennedy, K. M. & Wig, G. S. (2017) 'Motion-related artifacts in structural brain images revealed with independent estimates of in-scanner head motion', Hum Brain Mapp, 38(1), pp. 472-492.

Scheibehenne, B., Jamil, T. & Wagenmakers, E. J. (2016) 'Bayesian Evidence Synthesis Can Reconcile Seemingly Inconsistent Results: The Case of Hotel Towel Reuse', Psychol Sci, 27(7), pp. 1043-1046.

Scheres, A., Dijkstra, M., Ainslie, E., Balkan, J., Reynolds, B., Sonuga-Barke, E. & Castellanos, F. X. (2006) 'Temporal and probabilistic discounting of rewards in children and adolescents: effects of age and ADHD symptoms', Neuropsychologia, 44(11), pp. 2092-2103.

Scheres, A., Sumiya, M. & Thoeny, A. L. (2010) 'Studying the relation between temporal reward discounting tasks used in populations with ADHD: a factor analysis', Int J Methods Psychiatr Res, 19(3), pp. 167-176.

Scheres, A., Tontsch, C., Thoeny, A. L. & Sumiya, M. (2014) 'Temporal reward discounting in children, adolescents, and emerging adults during an experiential task', Front Psychol, 5, p. 711.

Scherf, K. S., Behrmann, M. & Dahl, R. E. (2012) 'Facing changes and changing faces in adolescence: a new model for investigating adolescent-specific interactions between pubertal, brain and behavioral development', Dev Cogn Neurosci, 2(2), pp. 199-219.

Schmidt, S. (2009) 'Shall We Really Do It Again? The Powerful Concept of Replication Is Neglected in the Social Sciences', Review of General Psychology, 13(2), pp. 90-100.

Schmithorst, V. J. & Yuan, W. (2010) 'White matter development during adolescence as shown by diffusion MRI', Brain Cogn, 72(1), pp. 16-25.

Schwarz, G. (1978) 'Estimating Dimension of a Model', Annals of Statistics, 6(2), pp. 461-464.

Sektnan, M., McClelland, M. M., Acock, A. & Morrison, F. J. (2010) 'Relations between early family risk, children's behavioral regulation, and academic achievement', Early Childhood Research Quarterly, 25(4), pp. 464-479.

Sescousse, G., Caldu, X., Segura, B. & Dreher, J. C. (2013) 'Processing of primary and secondary rewards: a quantitative meta-analysis and review of human functional neuroimaging studies', Neurosci Biobehav Rev, 37(4), pp. 681-696.

Sherman, L. E., Greenfield, P. M., Hernandez, L. M. & Dapretto, M. (2018a) 'Peer Influence Via Instagram: Effects on Brain and Behavior in Adolescence and Young Adulthood', Child Dev, 89(1), pp. 37-47.

Sherman, L. E., Hernandez, L. M., Greenfield, P. M. & Dapretto, M. (2018b) 'What the brain 'Likes': neural correlates of providing feedback on social media', Soc Cogn Affect Neurosci, 13(7), pp. 699-707.

Siegle, G. J., Steinhauer, S. R., Carter, C. S., Ramel, W. & Thase, M. E. (2003) 'Do the seconds turn into hours? Relationships between sustained pupil dilation in response to emotional information and self-reported rumination', Cognitive Therapy and Research, 27(3), pp. 365-382.

Silk, J. S., Siegle, G. J., Lee, K. H., Nelson, E. E., Stroud, L. R. & Dahl, R. E. (2014) 'Increased neural response to peer rejection associated with adolescent depression and pubertal development', Soc Cogn Affect Neurosci, 9(11), pp. 1798-1807.

Silk, J. S., Stroud, L. R., Siegle, G. J., Dahl, R. E., Lee, K. H. & Nelson, E. E. (2012) 'Peer acceptance and rejection through the eyes of youth: pupillary, eyetracking and ecological data from the Chatroom Interact task', Soc Cogn Affect Neurosci, 7(1), pp. 93-105.

Silvers, J. A., Insel, C., Powers, A., Franz, P., Helion, C., Martin, R., Weber, J., Mischel, W., Casey, B. J. & Ochsner, K. N. (2016a) 'The transition from childhood to adolescence is marked by a general decrease in amygdala reactivity and an affect-specific ventral-to-dorsal shift in medial prefrontal recruitment', Dev Cogn Neurosci.

Silvers, J. A., Insel, C., Powers, A., Franz, P., Helion, C., Martin, R. E., Weber, J., Mischel, W., Casey, B. J. & Ochsner, K. N. (2016b) 'vlPFC-vmPFC-Amygdala Interactions Underlie Age-Related Differences in Cognitive Regulation of Emotion', Cereb Cortex.

Silvers, J. A., McRae, K., Gabrieli, J. D., Gross, J. J., Remy, K. A. & Ochsner, K. N. (2012) 'Age-related differences in emotional reactivity, regulation, and rejection sensitivity in adolescence', Emotion, 12(6), pp. 1235-1247.

Simmonds, D. J., Hallquist, M. N., Asato, M. & Luna, B. (2014) 'Developmental stages and sex differences of white matter and behavioral development through adolescence: a longitudinal diffusion tensor imaging (DTI) study', Neuroimage, 92, pp. 356-368.

Singmann, H. (2013) 'afex: analysis of Factorial Experiments. R package version 0.7-90', http://CRAN.R-project.org/package afex.

Smith, S. M. (2002) 'Fast robust automated brain extraction', Hum Brain Mapp, 17(3), pp. 143-155.

Smith, S. M., Jenkinson, M., Woolrich, M. W., Beckmann, C. F., Behrens, T. E., Johansen-Berg, H., Bannister, P. R., De Luca, M., Drobnjak, I., Flitney, D. E., Niazy, R. K., Saunders, J., Vickers, J., Zhang, Y., De Stefano, N., Brady, J. M. & Matthews, P. M. (2004) 'Advances in functional and structural MR image analysis and implementation as FSL', Neuroimage, 23 Suppl 1, pp. S208-219.

Smith, S. M. & Nichols, T. E. (2009) 'Threshold-free cluster enhancement: addressing problems of smoothing, threshold dependence and localisation in cluster inference', Neuroimage, 44(1), pp. 83-98.

Somerville, L. H., Heatherton, T. F. & Kelley, W. M. (2006) 'Anterior cingulate cortex responds differentially to expectancy violation and social rejection', Nat Neurosci, 9(8), pp. 1007-1008.

Somerville, L. H., Jones, R. M. & Casey, B. J. (2010) 'A time of change: behavioral and neural correlates of adolescent sensitivity to appetitive and aversive environmental cues', Brain Cogn, 72(1), pp. 124-133.

Sowell, E. R., Delis, D., Stiles, J. & Jernigan, T. L. (2001) 'Improved memory functioning and frontal lobe maturation between childhood and adolescence: a structural MRI study', J Int Neuropsychol Soc, 7(3), pp. 312-322.

Stein, J. L., Wiedholz, L. M., Bassett, D. S., Weinberger, D. R., Zink, C. F., Mattay, V. S. & Meyer-Lindenberg, A. (2007) 'A validated network of effective amygdala connectivity', Neuroimage, 36(3), pp. 736-745.

Steinberg, L. (2008) 'A Social Neuroscience Perspective on Adolescent Risk-Taking', Dev Rev, 28(1), pp. 78-106.

Steinberg, L., Albert, D., Cauffman, E., Banich, M., Graham, S. & Woolard, J. (2008) 'Age differences in sensation seeking and impulsivity as indexed by behavior and self-report: evidence for a dual systems model', Dev Psychol, 44(6), pp. 1764-1778.

Steinberg, L. & Chein, J. M. (2015) 'Multiple accounts of adolescent impulsivity', Proc Natl Acad Sci U S A, 112(29), pp. 8807-8808.

Steinberg, L., Elmen, J. D. & Mounts, N. S. (1989) 'Authoritative Parenting, Psychosocial Maturity, and Academic-Success among Adolescents', Child Dev, 60(6), pp. 1424-1436.

T

Tabachnick, B. & Fidell, S. (2013) Using Multivariate Statistics, 6th edition, Boston, Pearson.

Telzer, E. H., McCormick, E. M., Peters, S., Cosme, D., Pfeifer, J. H. & van Duijvenvoorde, A. C. K. (2018) 'Methodological considerations for developmental longitudinal fMRI research', Dev Cogn Neurosci.

Thomaes, S., Stegge, H., Olthof, T., Bushman, B. J. & Nezlek, J. B. (2011) 'Turning Shame Inside-Out: "Humiliated Fury" in Young Adolescents', Emotion, 11(4), pp. 786-793.

Thomason, M. E. (2009) 'Children in Non-Clinical Functional Magnetic Resonance Imaging (fMRI) Studies Give the Scan Experience a "Thumbs Up"', American Journal of Bioethics, 9(1), pp. 25-27.

Thomason, M. E., Dennis, E. L., Joshi, A. A., Joshi, S. H., Dinov, I. D., Chang, C., Henry, M. L., Johnson, R. F., Thompson, P. M., Toga, A. W., Glover, G. H., Van Horn, J. D. & Gotlib, I. H. (2011) 'Resting-state fMRI can reliably map neural networks in children', Neuroimage, 55(1), pp. 165-175.

Tottenham, N. & Galvan, A. (2016) 'Stress and the adolescent brain: Amygdala-prefrontal cortex circuitry and ventral striatum as developmental targets', Neurosci Biobehav Rev, 70, pp. 217-227.

Tottenham, N., Hare, T. A., Millner, A., Gilhooly, T., Zevin, J. D. & Casey, B. J. (2011) 'Elevated amygdala response to faces following early deprivation', Dev Sci, 14(2), pp. 190-204.

Tottenham, N. & Sheridan, M. A. (2009) 'A review of adversity, the amygdala and the hippocampus: a consideration of developmental timing', Front Hum Neurosci, 3, p. 68.

Turkeltaub, P. E., Eickhoff, S. B., Laird, A. R., Fox, M., Wiener, M. & Fox, P. (2012) 'Minimizing within-experiment and within-group effects in Activation Likelihood Estimation meta-analyses', Hum Brain Mapp, 33(1), pp. 1-13.

Tuvblad, C. & Baker, L. A. (2011) 'Human aggression across the lifespan: genetic propensities and environmental moderators', Adv Genet, 75, pp. 171-214.

Tuvblad, C., Raine, A., Zheng, M. & Baker, L. A. (2009) 'Genetic and environmental stability differs in reactive and proactive aggression', Aggress Behav, 35(6), pp. 437-452.

Twenge, J. M., Baumeister, R. F., Tice, D. M. & Stucke, T. S. (2001) 'If you can't join them, beat them: effects of social exclusion on aggressive behavior', J Pers Soc Psychol, 81(6), pp. 1058-1069.

Tyc, V. L., Fairclough, D., Fletcher, B., Leigh, L. & Mulhern, R. K. (1995) 'Childrens Distress during Magnetic-Resonance-Imaging Procedures', Childrens Health Care, 24(1), pp. 5-19.

Tziortzi, A. C., Haber, S. N., Searle, G. E., Tsoumpas, C., Long, C. J., Shotbolt, P., Douaud, G., Jbabdi, S., Behrens, T. E. J., Rabiner, E. A., Jenkinson, M. & Gunn, R. N. (2014) 'Connectivity-Based Functional Analysis of Dopamine Release in the Striatum Using Diffusion-Weighted MRI and Positron Emission Tomography', Cereb Cortex, 24(5), pp. 1165-1177.

Tzourio-Mazoyer, N., Landeau, B., Papathanassiou, D., Crivello, F., Etard, O., Delcroix, N., Mazoyer, B. & Joliot, M. (2002) 'Automated anatomical labeling of activations in SPM using a macroscopic anatomical parcellation of the MNI MRI single-subject brain', Neuroimage, 15(1), pp. 273-289.

U

Ullman, H., Almeida, R. & Klingberg, T. (2014) 'Structural maturation and brain activity predict future working memory capacity during childhood development', J Neurosci, 34(5), pp. 1592-1598.

V

van den Bos, W., Rodriguez, C. A., Schweitzer, J. B. & McClure, S. M. (2014) 'Connectivity strength of dissociable striatal tracts predict individual differences in temporal discounting', J Neurosci, 34(31), pp. 10298-10310.

van den Bos, W., Rodriguez, C. A., Schweitzer, J. B. & McClure, S. M. (2015) 'Adolescent impatience decreases with increased frontostriatal connectivity', Proc Natl Acad Sci U S A, 112(29), pp. E3765-3774.

van den Bos, W., van Dijk, E., Westenberg, M., Rombouts, S. A. & Crone, E. A. (2011) 'Changing brains, changing perspectives: the neurocognitive development of reciprocity', Psychol Sci, 22(1), pp. 60-70.

van den Bulk, B. G., Koolschijn, P. C., Meens, P. H., van Lang, N. D., van der Wee, N. J., Rombouts, S. A., Vermeiren, R. R. & Crone, E. A. (2013) 'How stable is activation in the amygdala and prefrontal cortex in adolescence? A study of emotional face processing across three measurements', Dev Cogn Neurosci, 4, pp. 65-76.

van den Heuvel, M. P., van Soelen, I. L., Stam, C. J., Kahn, R. S., Boomsma, D. I. & Hulshoff Pol, H. E. (2013) 'Genetic control of functional brain network efficiency in children', Eur Neuropsychopharmacol, 23(1), pp. 19-23.

van der Meulen, M., Steinbeis, N., Achterberg, M., van, I. M. H. & Crone, E. A. (2018) 'Heritability of neural reactions to social exclusion and prosocial compensation in middle childhood', Dev Cogn Neurosci, 34, pp. 42-52.

van Dijk, K. R., Hedden, T., Venkataraman, A., Evans, K. C., Lazar, S. W. & Buckner, R. L. (2010) 'Intrinsic functional connectivity as a tool for human connectomics: theory, properties, and optimization', J Neurophysiol, 103(1), pp. 297-321.

van Dijk, K. R., Sabuncu, M. R. & Buckner, R. L. (2012) 'The influence of head motion on intrinsic functional connectivity MRI', Neuroimage, 59(1), pp. 431-438.

van Duijvenvoorde, A. C., Achterberg, M., Braams, B. R., Peters, S. & Crone, E. A. (2016a) 'Testing a dual-systems model of adolescent brain development using resting-state connectivity analyses', Neuroimage, 124(Pt A), pp. 409-420.

van Duijvenvoorde, A. C., Peters, S., Braams, B. R. & Crone, E. A. (2016b) 'What motivates adolescents? Neural responses to rewards and their influence on adolescents' risk taking, learning, and cognitive control', Neurosci Biobehav Rev, 70, pp. 135-147.

van Horn, J. D. & Pelphrey, K. A. (2015) 'Neuroimaging of the developing brain', Brain Imaging Behav, 9(1), pp. 1-4.

van IJzendoorn, M. H. (1994) 'Process model of replication studies: on the relations between different types of replication. ', in R. van der Veer, M. H. Van IJzendoorn & J. Valsiner (eds), On reconstructing the mind. Replicability in research on human development, NJ.: Ablex, Norwood.

van Zeijl, J., Mesman, J., Van, I. M. H., Bakermans-Kranenburg, M. J., Juffer, F., Stolk, M. N., Koot, H. M. & Alink, L. R. (2006) 'Attachment-based intervention for enhancing sensitive discipline in mothers of 1- to 3-year-old children at risk for externalizing behavior problems: a randomized controlled trial', J Consult Clin Psychol, 74(6), pp. 994-1005.

Verhulst, B. (2017) 'A Power Calculator for the Classical Twin Design', Behav Genet, 47(2), pp. 255-261.

Vijayakumar, N., Cheng, T. W. & Pfeifer, J. H. (2017) 'Neural correlates of social exclusion across ages: A coordinate-based meta-analysis of functional MRI studies', Neuroimage, 153, pp. 359-368.

Visscher, P. M. (2004) 'Power of the classical twin design revisited', Twin Res, 7(5), pp. 505-512.

Vogel, A. C., Power, J. D., Petersen, S. E. & Schlaggar, B. L. (2010) 'Development of the Brain's Functional Network Architecture', Neuropsychol Rev, 20(4), pp. 362-375.

Vrijhof, C. I., van der Voort, A., van IJzendoorn, M. H. & Euser, S. (2018) 'Stressful Family Environments and Children's Behavioral Control: A Multimethod Test and Replication Study With Twins', Journal of Family Psychology, 32(1), pp. 49-59.

W

Watts, T. W., Duncan, G. J. & Quan, H. (2018) 'Revisiting the Marshmallow Test: A Conceptual Replication Investigating Links Between Early Delay of Gratification and Later Outcomes', Psychol Sci, 29(7), pp. 1159-1177.

Wechsler, D. (1991) The Wechsler intelligence scale for children—third edition. , San Antonio, TX, The Psychological Corporation.

Wechsler, D. (1997) WAIS-III, wechsler adult intelligence scale: Administration and scoring manual., Psychological Corporation. .

Welsh, M. & Peterson, E. (2014) 'Issues in the Conceptualization and Assessment of Hot Executive Functions in Childhood', Journal of the International Neuropsychological Society, 20(2), pp. 152-156.

Whelan, R., Conrod, P. J., Poline, J. B., Lourdusamy, A., Banaschewski, T., Barker, G. J., Bellgrove, M. A., Buchel, C., Byrne, M., Cummins, T. D., Fauth-Buhler, M., Flor, H., Gallinat, J., Heinz, A., Ittermann, B., Mann, K., Martinot, J. L., Lalor, E. C., Lathrop, M., Loth, E., Nees, F., Paus, T., Rietschel, M., Smolka, M. N., Spanagel, R., Stephens, D. N., Struve, M., Thyreau, B., Vollstaedt-Klein, S., Robbins, T. W., Schumann, G., Garavan, H. & Consortium, I. (2012) 'Adolescent impulsivity phenotypes characterized by distinct brain networks', Nat Neurosci, 15(6), pp. 920-925.

Whittle, S., Lichter, R., Dennison, M., Vijayakumar, N., Schwartz, O., Byrne, M. L., Simmons, J. G., Yucel, M., Pantelis, C., McGorry, P. & Allen, N. B. (2014) 'Structural brain development and depression onset during adolescence: a prospective longitudinal study', Am J Psychiatry, 171(5), pp. 564-571.

Wierenga, L. M., Bos, M. G. N., Schreuders, E., Vd Kamp, F., Peper, J. S., Tamnes, C. K. & Crone, E. A. (2018a) 'Unraveling age, puberty and testosterone effects on subcortical brain development across adolescence', Psychoneuroendocrinology, 91, pp. 105-114.

Wierenga, L. M., van den Heuvel, M. P., Oranje, B., Giedd, J. N., Durston, S., Peper, J. S., Brown, T. T., Crone, E. A., The Pediatric Longitudinal Imaging, N. & Genetics, S. (2018b) 'A multisample study of longitudinal changes in brain network architecture in 4-13-year-old children', Hum Brain Mapp, 39(1), pp. 157-170.

Williams, K. D. (2007) 'Ostracism', Annu Rev Psychol, 58, pp. 425-452.

Williams, K. D., Cheung, C. K. & Choi, W. (2000) 'Cyberostracism: effects of being ignored over the Internet', J Pers Soc Psychol, 79(5), pp. 748-762.

Woo, C. W., Krishnan, A. & Wager, T. D. (2014) 'Cluster-extent based thresholding in fMRI analyses: Pitfalls and recommendations', Neuroimage, 91, pp. 412-419.

Y

Yang, Z., Zuo, X. N., McMahon, K. L., Craddock, R. C., Kelly, C., de Zubicaray, G. I., Hickie, I., Bandettini, P. A., Castellanos, F. X., Milham, M. P. & Wright, M. J. (2016) 'Genetic and Environmental Contributions to Functional Connectivity Architecture of the Human Brain', Cereb Cortex, 26(5), pp. 2341-2352.

Yeo, B. T., Krienen, F. M., Sepulcre, J., Sabuncu, M. R., Lashkari, D., Hollinshead, M., Roffman, J. L., Smoller, J. W., Zollei, L., Polimeni, J. R., Fischl, B., Liu, H. & Buckner, R. L. (2011) 'The organization of the human cerebral cortex estimated by intrinsic functional connectivity', J Neurophysiol, 106(3), pp. 1125-1165.

Z

Zelazo, P. D. & Carlson, S. M. (2012) 'Hot and Cool Executive Function in Childhood and Adolescence: Development and Plasticity', Child Development Perspectives, 6(4), pp. 354-360.

Zeng, L. L., Wang, D., Fox, M. D., Sabuncu, M., Hu, D., Ge, M., Buckner, R. L. & Liu, H. (2014) 'Neurobiological basis of head motion in brain imaging', Proc Natl Acad Sci U S A, 111(16), pp. 6058-6062.

Zhang, Y. Y., Brady, M. & Smith, S. (2001) 'Segmentation of brain MR images through a hidden Markov random field model and the expectation-maximization algorithm', IEEE Trans Med Imaging, 20(1), pp. 45-57.

LIST OF PUBLICATIONS

Publicatielijst

Published:

Achterberg, M. & van der Meulen, M. (2019) Genetic and environmental influences on MRI scan quantity and quality. *Developmental Cognitive Neuroscience,* 38, pp. 100667.

Achterberg, M., Bakermans-Kranenburg, M. J., van IJzendoorn, M. H., van der Meulen, M., Tottenham, N. & Crone, E. A. (2018) Distinctive heritability patterns of subcortical-prefrontal cortex resting state connectivity in childhood: A twin study. *Neuroimage,* 175, pp. 138-149.

Achterberg, M., van Duijvenvoorde, A. C. K., van der Meulen, M., Bakermans-Kranenburg, M. J. & Crone, E. A. (2018) Heritability of aggression following social evaluation in middle childhood: An fMRI study. *Human Brain Mapping,* 39, pp. 2828-2841.

van der Meulen, M., Steinbeis, N., **Achterberg, M.**, van IJzendoorn, M. H., & Crone, E. A. (2018). Heritability of neural reactions to social exclusion and prosocial compensation in middle childhood. *Developmental Cognitive Neuroscience,* 34, 42-52.

Achterberg, M., van Duijvenvoorde, A. C. K., van der Meulen, M., Euser, S., Bakermans-Kranenburg, M. J. & Crone, E. A. (2017) The neural and behavioral correlates of social evaluation in childhood. *Developmental Cognitive Neuroscience*, 24, pp. 107-117.

Bos, D.J., Oranje, B., **Achterberg, M.**, Vlaskamp, C., Ambrosino, S., de Reus, M. A., van der Heuvel, M. P. & Rombouts, S. A. R. B. (2017). Structural and functional connectivity in children and adolescents with Attention Deficit/Hyperactivity Disorder. *Journal of Child Psychology and Psychiatry,* 58, pp. 810-818.

van der Meulen, M., Steinbeis, N., **Achterberg, M.**, Bilo, E., van den Bulk, B. G., van IJzendoorn, M. H., & Crone, E. A. (2017). The neural correlates of dealing with social exclusion in childhood. *Neuropsychologia*, 103, 27-39.

Achterberg, M.*, Peper, J. S*., van Duijvenvoorde, A. C., Mandl, R. C. & Crone, E. A. (2016) Frontostriatal White Matter Integrity Predicts Development of Delay of Gratification: A Longitudinal Study, *Journal of Neuroscience*, 36, pp. 1954-1961. **shared first author*

Achterberg, M., van Duijvenvoorde, A. C., Bakermans-Kranenburg, M. J. & Crone, E. A. (2016) Control your anger! The neural basis of aggression regulation in response to negative social feedback. *Social Cognitive and Affective Neuroscience,* 11, pp. 712-720.

Van Duijvenvoorde, A. C. K., **Achterberg, M.**, Braams, B. R., Peters, S., & Crone, E. A. (2016). Testing a dual-systems model of adolescent brain development using resting-state connectivity analyses. Neuroimage, 1, 409-420.

In revision:

Achterberg, M., van Duijvenvoorde, A. C. K., van IJzendoorn, M. H., Bakermans-Kranenburg, M. J. & Crone, E. A. Longitudinal changes in DLPFC activation during childhood are related to decreased aggression following social rejection.

Crone, E.A., **Achterberg, M.**, Dobbelaar, S., Euser, S., van den Bulk, B. G., van der Meulen, M., van Druunen, L., Wierenga, L.M., Bakermans-Kranenburg, M. J & van IJzendoorn, M.H. Social acceptance and inclusion from early to middle childhood: The Leiden consortium on Individual Development on neurocognitive development and social enrichment.

Konijn, E.A., & **Achterberg, M.** Neuropsychological Underpinnings of Emotional Responsiveness to Media. In J. van den Bulck (Ed.), The International Encyclopedia of Media Psychology. John Wiley & Sons.

Overgaauw, S., **Achterberg, M.**, Bakermans-Kranenburg, M.J. Aggression after social evaluations in typically and atypically developing adolescents.

Van der Meulen, M., Wierenga, L. M., **Achterberg, M.**, Drenth, N., van IJzendoorn, M.H. & Crone, E. A. Shared genetic and environmental influences on structure of the social brain in children.

ABOUT THE AUTHOR

Curriculum vitae

Curriculum Vitae

Michelle Achterberg was born on May 28th 1991 in Gouda, the Netherlands. After graduating from secondary school (De Goudse Waarden, Gouda) in 2009, she went to Utrecht University to study psychology and neuroscience. Michelle obtained her Bachelor's degree in Psychology in 2012 and her Research Master's degree in Neuroscience and Cognition in 2014. During her masters, Michelle worked as a research intern at the department of (child) psychiatry, University Medical Center Utrecht, were she gained her first experience with neuroimaging in children. During the second year of her studies she joined the Brian and Development Research Center as a research assistant. Following her passion for developmental neuroscience, Michelle started her PhD project in 2014 as part of the Leiden Consortium on Individual Development at Leiden University under supervision of Prof. dr. Eveline Crone, Prof. dr. Marian Bakermans- Kranenburg and Dr. Anna van Duijvenvoorde. In her project, she focused on the underlying neural mechanisms of social emotion regulation in childhood using a large, longitudinal, twin-design. Michelle will continue her work on developmental neuroscience as a post-doctoral researcher at Erasmus University Rotterdam.

Michelle Achterberg werd op 28 mei 1991 geboren te Gouda. Na het behalen van haar vwo-diploma (De Goudse Waarden, Gouda) in 2009 ging ze naar de Universiteit Utrecht om psychologie en neurowetenschappen te studeren. Michelle behaalde haar bachelor diploma Psychologie in 2012 en haar masterdiploma in Neurowetenschap en Cognitie in 2014. Tijdens haar masteropleiding werkte Michelle als onderzoek stagiaire bij de afdeling (kinder) psychiatrie van het Universitair Medisch Centrum Utrecht, waar ze haar eerste ervaringen opdeed met hersenonderzoek bij kinderen. Tijdens het tweede jaar van haar masterstudie begon Michelle als onderzoeksassistent bij het Breinlab in Leiden. Michelle volgde haar passie voor neurowetenschappelijk onderzoek en begon in 2014 haar promotieonderzoek binnen het Samen Uniek tweelingonderzoek onder begeleiding van Prof. dr. Eveline Crone, Prof. dr. Marian Bakermans-Kranenburg en Dr. Anna van Duijvenvoorde. Tijdens haar promotie heeft Michelle onderzoek gedaan naar de neurale mechanisme van sociale emotie regulatie in kinderen door middel van een groot, longitudinaal tweelingonderzoek. Michelle zal haar onderzoek naar hersenontwikkeling voortzetten als postdoctoraal onderzoeker aan de Erasmus Universiteit Rotterdam.

Michelle Achterberg is a developmental neuroscientist with an interest in social emotional development. In her thesis, Michelle provides a comprehensive overview of the underlying mechanisms of social emotion regulation in childhood. Her studies show that the brain is prone to signal for socially relevant information. She revealed that the network of social saliency is already present in childhood, indicating that this might be a core social mechanism.

The thesis additionally shows that social rejection is often followed by behavioral aggression, and regulation of these retaliation emotions is related to control mechanisms of the dorsolateral prefrontal cortex. Moreover, the results show that the vast architecture of functional subcortical-prefrontal brain connectivity is already in place in middle childhood and suggest fine tuning of (social evaluation) brain networks across childhood. These findings highlighting the need to incorporate childhood into developmental models of social emotion regulation.

Neuroimaging research, specifically neuroimaging in children, is prone to challenges and several methodological considerations need to be taken into account when studying the childhood brain. In spite of these difficulties, studying childhood brain development has the potential to provide important insights into a unique developmental window of opportunity.



ISBN: 978-94-6332-584-4